frontiers | Research Topics

Sulforaphane and isothiocyanates in health

Edited by
Paul Licciardi, Francesco Grassi, Tom C. Karagiannis, Diego A. Moreno and Jed William Fahey

Coordinated by
Nadia Mazarakis

Published in
Frontiers in Nutrition

ISSN 1664-8714
ISBN 978-2-8325-6083-9
DOI 10.3389/978-2-8325-6083-9

About Frontiers

Frontiers is more than just an open access publisher of scholarly articles: it is a pioneering approach to the world of academia, radically improving the way scholarly research is managed. The grand vision of Frontiers is a world where all people have an equal opportunity to seek, share and generate knowledge. Frontiers provides immediate and permanent online open access to all its publications, but this alone is not enough to realize our grand goals.

Frontiers journal series

The Frontiers journal series is a multi-tier and interdisciplinary set of open-access, online journals, promising a paradigm shift from the current review, selection and dissemination processes in academic publishing. All Frontiers journals are driven by researchers for researchers; therefore, they constitute a service to the scholarly community. At the same time, the *Frontiers journal series* operates on a revolutionary invention, the tiered publishing system, initially addressing specific communities of scholars, and gradually climbing up to broader public understanding, thus serving the interests of the lay society, too.

Dedication to quality

Each Frontiers article is a landmark of the highest quality, thanks to genuinely collaborative interactions between authors and review editors, who include some of the world's best academicians. Research must be certified by peers before entering a stream of knowledge that may eventually reach the public - and shape society; therefore, Frontiers only applies the most rigorous and unbiased reviews. Frontiers revolutionizes research publishing by freely delivering the most outstanding research, evaluated with no bias from both the academic and social point of view. By applying the most advanced information technologies, Frontiers is catapulting scholarly publishing into a new generation.

What are Frontiers Research Topics?

Frontiers Research Topics are very popular trademarks of the *Frontiers journals series*: they are collections of at least ten articles, all centered on a particular subject. With their unique mix of varied contributions from Original Research to Review Articles, Frontiers Research Topics unify the most influential researchers, the latest key findings and historical advances in a hot research area.

Find out more on how to host your own Frontiers Research Topic or contribute to one as an author by contacting the Frontiers editorial office: frontiersin.org/about/contact

Sulforaphane and isothiocyanates in health

Topic editors

Paul Licciardi — Murdoch Childrens Research Institute, Royal Children's Hospital, Australia

Francesco Grassi — Rizzoli Orthopedic Institute (IRCCS), Italy

Tom C. Karagiannis — The University of Melbourne, Australia

Diego A. Moreno — Center for Edaphology and Applied Biology of Segura, Spanish National Research Council (CSIC), Spain

Jed William Fahey — Johns Hopkins University, United States

Topic coordinator

Nadia Mazarakis — Murdoch Childrens Research Institute, Royal Children's Hospital, Australia

Citation

Licciardi, P., Grassi, F., Karagiannis, T. C., Moreno, D. A., Fahey, J. W., Mazarakis, N., eds. (2025). *Sulforaphane and isothiocyanates in health*. Lausanne: Frontiers Media SA. doi: 10.3389/978-2-8325-6083-9

Table of contents

04 Editorial: Sulforaphane and isothiocyanates in health
Jed W. Fahey, Diego A. Moreno, Paul Licciardi, Francesco Grassi, Tom C. Karagiannis and Nadia Mazarakis

07 The beneficial effect of sulforaphane on platelet responsiveness during caloric load: a single-intake, double-blind, placebo-controlled, crossover trial in healthy participants
Hidde P. van Steenwijk, Evi Winter, Edward Knaven, Jos F. Brouwers, Myrthe van Baardwijk, Jasper B. van Dalum, Teus J. C. Luijendijk, Frits H. M. van Osch, Freddy J. Troost, Aalt Bast, Khrystyna O. Semen and Alie de Boer

21 Therapeutic efficacy of sulforaphane in autism spectrum disorders and its association with gut microbiota: animal model and human longitudinal studies
Jiexian Yang, Li He, Si Dai, Huihui Zheng, Xilong Cui, Jianjun Ou and Xiaojie Zhang

36 Prospective cohort study of broccoli consumption frequency and all-cause and cause-specific mortality risks
Xiangliang Liu, Yu Chang, Yuguang Li, Xinwei Zhang, Fangqi Li, Jia Song, Hanping Shi, Xiao Chen and Jiuwei Cui

48 Effect of allyl-isothiocyanate on survival and antimicrobial peptide expression following oral bacterial infections in *Drosophila melanogaster*
Christian Zimmermann, Sonja Dähn and Anika E. Wagner

62 Dietary isothiocyanates and anticancer agents: exploring synergism for improved cancer management
Qi Wang, Dan Li, Lihua Liu, Yujuan Shan and Yongping Bao

77 The role of isothiocyanate-rich plants and supplements in neuropsychiatric disorders: a review and update
Monica Ramakrishnan, Jed W. Fahey, Andrew W. Zimmerman, Xinyi Zhou and Anita A. Panjwani

94 The effect of sulforaphane on markers of inflammation and metabolism in virally suppressed HIV patients
Jose Giron, Lauren Smiarowski and Johannah Katz

102 Sulforaphane acutely activates multiple starvation response pathways
Kendra S. Plafker, Constantin Georgescu, Nathan Pezant, Atul Pranay and Scott M. Plafker

frontiers | Frontiers in Nutrition

TYPE Editorial
PUBLISHED 11 February 2025
DOI 10.3389/fnut.2025.1558025

OPEN ACCESS

EDITED AND REVIEWED BY
Mario Allegra,
University of Palermo, Italy

*CORRESPONDENCE
Jed W. Fahey
✉ jfahey@jhmi.edu

RECEIVED 09 January 2025
ACCEPTED 15 January 2025
PUBLISHED 11 February 2025

CITATION
Fahey JW, Moreno DA, Licciardi P, Grassi F, Karagiannis TC and Mazarakis N (2025) Editorial: Sulforaphane and isothiocyanates in health. *Front. Nutr.* 12:1558025. doi: 10.3389/fnut.2025.1558025

Editorial: Sulforaphane and isothiocyanates in health

Jed W. Fahey[1,2]*, Diego A. Moreno[3], Paul Licciardi[4,5], Francesco Grassi[6], Tom C. Karagiannis[7] and Nadia Mazarakis[4,5]

[1]Departments of Medicine, Pharmacology and Molecular Sciences, Psychiatry and Behavioral Sciences, and iMIND Institute, School of Medicine, Johns Hopkins University, Baltimore, MD, United States, [2]Institute of Medicine, University of Maine, Orono, ME, United States, [3]Phytochemistry and Healthy Food Lab (LabFAS), CSIC, CEBAS, Campus Universitario de Espinardo, Murcia, Spain, [4]Murdoch Children's Research Institute, Royal Children's Hospital, Melbourne, VIC, Australia, [5]Department of Paediatrics, The University of Melbourne, Parkville, VIC, Australia, [6]SSD Lab RAMSES, IRCCS Rizzoli Orthopaedic Institute, Bologna, Italy, [7]The University of Melbourne, Parkville, VIC, Australia

KEYWORDS

glucosinolate, myrosinase, clinical, epidemiologic, chronic disease, antimicrobial, food, phytochemical

Editorial on the Research Topic
Sulforaphane and isothiocyanates in health

The capacity of isothiocyanates (ITC) such as sulforaphane (SF; 4-methylsulfinylbutyl-ITC) to be of clinical utility in preventing and treating chronic disease is clear. The health-promoting, preventive, protective, and therapeutic applications of SF are well established, having been the subject of thousands of studies including more than 125 clinical trials. This, despite the fact that as a natural compound present in food, SF cannot and should not be positioned as a drug, nor is it within the province of the pharmaceutical industry. The many mechanisms of action of SF in mammalian systems have been extensively documented. It is the most potent naturally occurring inducer of the Keap1-Nrf2 pathway, which is best-known for its upregulation of antioxidant and detoxification mechanisms as well as its anti-inflammatory potency.

The establishment of health claims *per se* is problematic from a regulatory perspective since SF and other plant-sourced phytochemicals (a.k.a. phytonutrients or bioactives) are omnipresent in non-ultraprocessed plant foods. SF or its biogenic precursor, glucoraphanin can also be delivered in standardized and/or enriched supplement form. As becomes clear in the contributions for this Research Topic, research interest in ITCs has continued to grow (Figure 1) since the discovery of SF's biological activity the early 1990s (2). More and more applications to a wide variety of diseases continue to be investigated despite lack of regulatory clarity and in the absence of the massive pharmaceutical funding which drives so many other clinical investigations.

Although much of the research on SF and other ITCs is associated with its ability to activate the Keap1-Nrf2 pathway, it exhibits a range of other important biological effects (e.g., inflammation modulation through NF-κB downregulation, infection control, immune system support, selective antibiosis, and cell cycle control), in preclinical and clinical interventions. The dose-response data span disease states and tissue types and indicate that biologically relevant quantities of SF and other isothiocyanates can be provided with practical food- or supplement-based delivery systems. Other aspects of their bioavailability, including potential synergistic, additive, or antagonistic effects coming

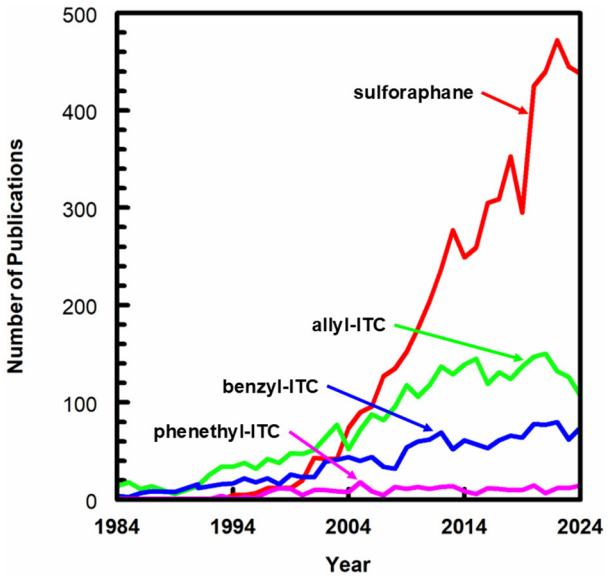

FIGURE 1
Annual number of peer-reviewed papers on SF, allyl-, benzyl-, and phenethyl- ITC over the last 40 years. Data for graph derived from a Boolean search of Scopus® on Jan 3, 2025.

from combined treatments or food matrix effects are not yet as well understood at the clinical level.

This Research Topic brings together new ideas and provide an updated consensus on the bioactive SF, and other structurally-related and biologically active ITCs. We have thus brought together two reviews (Ramakrishnan et al. and Wang et al.), one epidemiologic study (Liu et al.), two mechanistic studies (Plafker et al., Zimmerman et al.), two clinical studies (Giron et al. and Steenwijk et al.), and a hybrid study in which both animal models and a human longitudinal study are combined (Yang et al.).

Giron et al. conducted the first ever study of the effects of SF on human beings living with HIV. In their 16-week pilot study of 14 virally suppressed HIV patients, given 225 μmol SF daily, a reduction in C-reactive protein was demonstrated. This should encourage more clinical work to examine the efficacy of ITCs not just on people living with HIV, but with other chronic conditions and diseases. The review by Wang et al. is therefore extremely timely in that they evaluated synergisms between dietary ITC and anticancer agents. The word "synergy" has been greatly misused in both the scientific and popular literature. Applying the classic definition of synergy (1), SF is truly synergistic with a lengthy list of drugs and other natural products and the mechanism(s) of those synergies are actually becoming well understood. The review in this Research Topic nicely explains some of these synergies and their mechanisms as they pertain to cancer therapeutic drugs.

The effects of broccoli consumption on a variety of outcomes, primarily cancer-related, have been examined in a number of prospective cohort studies over the years. To our knowledge however, Liu et al. are the first to assess the effects of the frequency of broccoli consumption on all-cause (and cause-specific) mortality. Their findings, based on National Health and Nutrition Examination Survey (NHANES) data from 12,486 adults, confirmed that broccoli consumption 1–2 times per week was associated with a 32–43% lower all-cause mortality risk.

Neurodevelopmental and neurodegenerative conditions that are impacted by treatment with ITCs are extensively reviewed by Ramakrishnan et al. who give special scrutiny to the >80 preclinical studies and 16 clinical studies evaluating the effects of SF on autism spectrum disorder (ASD) and schizophrenia. ASD is also the focus of an exciting new animal model and human clinical study following 12 weeks of SF (equivalent to 30 μmol) supplementation (Yang et al.). Changes in abundance of specific microbial taxa were associated with improvements in ASD symptoms following SF treatment in both rats and humans.

In a 12-subject preliminary intervention, Steenwijk et al. showed that when a single oral intake of SF in the form of broccoli sprouts (16 g) was followed by a high-calorie challenge, platelet responsiveness and improved functionality. These improvements have important clinical promise for safe and efficacious platelet-targeting phytotherapeutics that could have dramatic implications in a variety of thrombotic and chronic inflammatory conditions.

Allyl-ITC, most abundantly found in mustards, white cabbage, radish, and wasabi, has already shown great promise experimentally against bladder cancer. It has long been known to have an array of direct *in-vitro* antimicrobial potencies, thus leading to great interest in its use in food packaging systems. Zimmerman et al. have now provided dramatic data on the antimicrobial properties of allyl-ITC in a *Drosophila* model system. This demonstration of concentration-dependent direct antimicrobial properties as well as its ability to modulate host production of antimicrobial peptides adds to the dossier of allyl-ITC functionality which may have broader applicability to the ITCs in general.

And finally, in a sophisticated model of human retinal pigment epithelial cells, Plafker et al. provide evidence that 25 μM SF elicits cellular responses consistent with its being a fasting/caloric restriction mimetic. Increased mitochondrial mass, reduced glucose uptake, and suppression of insulin signaling are among the modes of action identified, pointing to new plausible mechanisms for SF effect under conditions of metabolic stress (i.e., hyperglycemia, mitochondrial dysfunction) and calling for this theory to be tested promptly in animal models.

Overall, the extensive scope of this Research Topic on SF and other ITCs emphasizes their potential utility in preventing and managing a wide range of human pathologies. While certain mechanisms of action, particularly induction of the Keap1-Nrf2 pathway, are well established, further exploration of molecular mechanisms is required. In this context, there is accumulating evidence indicating epigenetic mechanisms, including DNA methylation and histone modification, associated with SF. Further exploration of genetic and epigenetic modifications may enhance our understanding of the underlying mechanisms accounting for the broad beneficial health effects of SF and other ITCs, as highlighted in this Research Topic.

Author contributions

JWF: Writing – original draft, Writing – review & editing. DAM: Writing – original draft, Writing – review & editing. PL: Writing – original draft, Writing – review & editing. FG: Writing – original draft, Writing – review & editing. TCK: Writing – original draft, Writing – review & editing. NM: Writing – original draft, Writing – review & editing.

Conflict of interest

The authors declare that the research was conducted in the absence of any commercial or financial relationships that could be construed as a potential conflict of interest.

The author(s) declared that they were an editorial board member of Frontiers, at the time of submission. This had no impact on the peer review process and the final decision.

Publisher's note

References

1. Chou T-C, and Talalay P. Quantitative analysis of dose-effect relationships: the combined effects of multiple drugs or enzyme inhibitors. *Adv. Enzyme Regul.* (1984) 22:27–55. doi: 10.1016/0065-2571(84)90007-4

2. Zhang Y, Talalay P, Cho CG, Posner GH. A major inducer of anticarcinogenic protective enzymes from broccoli: isolation and elucidation of structure. *Proc Natl Acad Sci USA.* (1992) 89:2399–403. doi: 10.1073/pnas.89.6.2399

frontiers | Frontiers in Nutrition

TYPE Clinical Trial
PUBLISHED 06 July 2023
DOI 10.3389/fnut.2023.1204561

OPEN ACCESS

EDITED BY
Vijaya Juturu,
Independent Researcher,
Flemington, NJ, United States

REVIEWED BY
Susan Sergeant,
Wake Forest University, United States
Jed William Fahey,
Johns Hopkins University, United States

*CORRESPONDENCE
Hidde P. van Steenwijk
h.vansteenwijk@maastrichtuniversity.nl

RECEIVED 12 April 2023
ACCEPTED 15 June 2023
PUBLISHED 06 July 2023

CITATION
van Steenwijk HP, Winter E, Knaven E, Brouwers JF, van Baardwijk M, van Dalum JB, Luijendijk TJC, van Osch FHM, Troost FJ, Bast A, Semen KO and de Boer A (2023) The beneficial effect of sulforaphane on platelet responsiveness during caloric load: a single-intake, double-blind, placebo-controlled, crossover trial in healthy participants. *Front. Nutr.* 10:1204561. doi: 10.3389/fnut.2023.1204561

The beneficial effect of sulforaphane on platelet responsiveness during caloric load: a single-intake, double-blind, placebo-controlled, crossover trial in healthy participants

Hidde P. van Steenwijk[1]*, Evi Winter[1], Edward Knaven[2], Jos F. Brouwers[2], Myrthe van Baardwijk[3,4], Jasper B. van Dalum[3], Teus J. C. Luijendijk[5], Frits H. M. van Osch[6,7], Freddy J. Troost[8,9], Aalt Bast[10,11], Khrystyna O. Semen[10] and Alie de Boer[1]

[1]Food Claims Centre Venlo, Faculty of Science and Engineering, Maastricht University, Maastricht, Netherlands, [2]Research Group Analysis Techniques in the Life Sciences, Avans University of Applied Sciences, Breda, Netherlands, [3]Omnigen B.V., Delft, Netherlands, [4]Department of Pathology and Clinical Bioinformatics, Erasmus MC, University Medical Center Rotterdam, Rotterdam, Netherlands, [5]Stichting Control in Food and Flowers, Delfgauw, Netherlands, [6]Department of Clinical Epidemiology, VieCuri Medical Center, Venlo, Netherlands, [7]Department of Epidemiology, NUTRIM, Faculty of Health, Medicine and Life Sciences, Maastricht University, Maastricht, Netherlands, [8]Division of Gastroenterology-Hepatology, Department of Internal Medicine, School of Nutrition and Translational Research in Metabolism, Maastricht University Medical Center+, Maastricht, Netherlands, [9]Food Innovation and Health, Centre for Healthy Eating and Food Innovation, Maastricht University, Maastricht, Netherlands, [10]University College Venlo, Faculty of Science and Engineering, Maastricht University, Maastricht, Netherlands, [11]Department of Pharmacology and Toxicology, Faculty of Health, Medicine and Life Sciences, Maastricht University, Maastricht, Netherlands

Background and aims: As our understanding of platelet activation in response to infections and/or inflammatory conditions is growing, it is becoming clearer that safe, yet efficacious, platelet-targeted phytochemicals could improve public health beyond the field of cardiovascular diseases. The phytonutrient sulforaphane shows promise for clinical use due to its effect on inflammatory pathways, favorable pharmacokinetic profile, and high bioavailability. The potential of sulforaphane to improve platelet functionality in impaired metabolic processes has however hardly been studied in humans. This study investigated the effects of broccoli sprout consumption, as a source of sulforaphane, on urinary 11-dehydro-thromboxane B_2 (TXB_2), a stable thromboxane metabolite used to monitor eicosanoid biosynthesis and response to antithrombotic therapy, in healthy participants exposed to caloric overload.

Methods: In this double-blind, placebo-controlled, crossover trial 12 healthy participants were administered 16g of broccoli sprouts, or pea sprouts (placebo) followed by the standardized high-caloric drink PhenFlex given to challenge healthy homeostasis. Urine samples were collected during the study visits and analyzed for 11-dehydro-TXB_2, sulforaphane and its metabolites. Genotyping was performed using Illumina GSA v3.0 DTCBooster.

Results: Administration of broccoli sprouts before the caloric load reduced urinary 11-dehydro-TXB_2 levels by 50% (p=0.018). The amount of sulforaphane excreted

in the urine during the study visits correlated negatively with 11-dehydro-TXB_2 (r_s=−0.377, p=0.025). Participants carrying the polymorphic variant NAD(P)H dehydrogenase quinone 1 (NQO1*2) showed decreased excretion of sulforaphane (p=0.035).

Conclusion: Sulforaphane was shown to be effective in targeting platelet responsiveness after a single intake. Our results indicate an inverse causal relationship between sulforaphane and 11-dehydro-TXB_2, which is unaffected by the concomitant intake of the metabolic challenge. 11-Dehydro-TXB_2 shows promise as a non-invasive, sensitive, and suitable biomarker to investigate the effects of phytonutrients on platelet aggregation within hours.

Clinical trial registration: [https://clinicaltrials.gov/], identifier [NCT05146804].

KEYWORDS

immunothrombosis, inflammation, dietary antiplatelets, phytonutrients, thromboxanes, nutrition, non-communicable diseases

1. Introduction

Our understanding of platelet functionality has changed dramatically over the past decade. Platelets are no longer viewed simply as hemostasis regulators; they are now recognized as crucial in coordinating inflammatory and immune responses (1, 2). Impaired platelet function has been observed in several chronic inflammatory conditions, including thrombosis and thrombotic disorders (3), asthma (4), myocardial infarction (5), unstable angina pectoris (6), atherosclerosis (7), and type 2 diabetes (8, 9). Interestingly, also postprandial hyperglycemia has been shown to cause platelet activation (10) and promote inflammatory state in healthy individuals (11–13). In the clinical setting, administering caloric loads to humans has been used as a tool to pressurize adaptive mechanisms and trigger inflammation which may also be associated with an increase in platelet reactivity (14).

Thromboxanes are arachidonic acid metabolites with significant biological activity, including regulation of platelet functionality (15–17). Increased production of thromboxanes was recognized to contribute to vasculopathy by adversely affecting endothelial function and promoting vascular inflammation (18). By activating the thromboxane receptor, those metabolites cause significant alterations of platelet shape, inside-out activation of integrins, and degranulation (15–17), which might subsequently lead to increased platelet aggregation and thrombosis. On the other hand, increased production of thromboxane A and activation of platelets are recognized to be crucial modulators of the functionality of multiple inflammatory pathways involved in the progression of the cardiovascular diseases (19). 11-Dehydro-thromboxane B_2 (TXB_2) is produced from the breakdown of thromboxane A and can be measured in urine as a relevant marker of platelet reactivity, e.g., to monitor the response to aspirin (ASA) therapy when used to prevent heart disease (20, 21).

In fact, targeting thromboxane production via antiplatelet agents has become a cornerstone of cardiovascular disease treatment (1, 22). Antiplatelet drugs (i.e., ASA, clopidogrel, prasugrel and abciximab) typically irreversibly suppress a specific pathway of platelet aggregation (1, 22). Therefore, the main limitations of current antiplatelet agents include the risk of bleeding and prolonged duration of action that cannot be reversed if the need for hemostasis or emergency surgery arises (22, 23), which limits their use in many clinical situations, e.g., prophylaxis of cardiovascular events in high-risk groups (1). Phytonutrients have also been shown to affect platelet functionality with water-soluble tomato concentrate (WSTC) being the first to be recognized by the European Food Safety Agency (EFSA) as functional food that helps to maintain normal platelet aggregation, which contributes to healthy blood flow (24). Unlike drug therapy, the antiplatelet effect of most phytochemicals is reversible, making them potentially safe for use in a variety of clinical scenarios, including primary prevention of cardiovascular diseases (17.9 million deaths annually) in the general population (1, 25, 26). Therefore, it is paramount to search for novel nutritional strategies that support platelet functionality.

Of the various plant-derived bioactive nutrients, sulforaphane holds the most promise for clinical testing due to superior absorption and pharmacokinetic profile (27–46). Glucoraphanin, the biogenic precursor of sulforaphane, is present in large amounts in broccoli and to a lesser extent in other Brassica species (47, 48). Since glucoraphanin is biologically inert, factors controlling the biosynthesis of glucoraphanin and conversion to sulforaphane by the enzyme myrosinase are of great importance to the potential health effects of these vegetables (28, 39, 48). The antithrombotic properties of sulforaphane have been demonstrated in animals and *in vitro* studies (49, 50). Sulforaphane exerts antiplatelet activity which may initially activate adenylate cyclase/cAMP, followed by reversible inhibition of multiple intracellular signals such as the PI3-kinase/Akt and PLCγ2-PKC-p47 cascades (49, 50). Although promising, demonstrating an antithrombotic effect *in vivo* after oral administration of the compound has been scarcely explored in clinical trials, hence sulforaphane's ability to modulate platelet functionality in humans is still poorly studied (51).

These findings motivated us to investigate the effects of broccoli sprout consumption, as a source of sulforaphane, on urinary 11-dehydro-TXB_2 in healthy participants exposed to a standardized caloric load and to investigate interindividual genetic variability.

2. Methods

A randomized, placebo-controlled, double-blind study was conducted with a cross-over design. The study protocol (NL77272.068.21) was approved by the Medical Ethics Review Committee of Maastricht University Medical Centre+ (MUMC+) and Maastricht University, Maastricht, the Netherlands, and performed in full accordance with the declaration of Helsinki of 1975 as revised in 2013, Fortaleza, Brazil (52). The trial registration number within ClinicalTrials.gov is NCT05146804. All subjects provided written informed consent to participate.

2.1. Subjects

Healthy men and women were recruited by local and social media advertisements. Inclusion criteria were that participants were between 18 and 50 years old, had a body mass index (BMI) between 18.5 and 30 kg/m^2, with a stable weight (<5% body weight change) and constant eating habits over the past 3 months. Exclusion criteria were the previous diagnosis of an inflammatory condition or disease or a history of hypothyroidism, chronic kidney or/and liver disorders, coronary artery disease, malignant hypertension, seizures, involved in intensive sports activities more than four times a week or at top sport level, regular intake of medication that may affect inflammatory response including NSAIDs, psychotic, addictive, or other mental disorders, aversion, intolerance or allergy to cruciferous vegetables and/or palm olein, dextrose, protein supplement, vanilla aroma, the use of dietary supplements with potential effects on antioxidant or inflammatory status and/or viral or bacterial infections requiring the use of antibiotics, laxatives and anti-diarrheal drugs 4 weeks prior to inclusion, excessive alcohol consumption (≥28 consumptions, approx. 250 g alcohol per week), pregnancy and/or breastfeeding, reported slimming or medically prescribed diet, as well as adhering to a vegetarian or vegan lifestyle.

2.2. Study design and procedures

Commercially available broccoli sprouts BroccoCress®, a rich source of sulforaphane, were used as the experimental product. In total, 16 g of sprouts were used per serving. Sulforaphane (BroccoCress®) and placebo (Affilla Cress®) were administered to each participant in the randomized fashion on different testing days. The period between two visits was 7 ± 3 days. Information about demographics, alcohol consumption, and anthropometric data were assessed on the first visit. BMI, total body fat and visceral fat were measured using the Omron BF511R® monitor. The same testing scheme was applied during two visits (Figure 1), i.e., each participant received a single serving of intervention/placebo, which after 90 min was followed by oral administration of the PhenFlex challenge. Urine samples were collected throughout the day of the visit, preferably before the intervention/placebo, between intervention/placebo and the PhenFlex challenge, and after the PhenFlex administration. All participants were instructed to come fasted to each visit, to avoid consumption of broccoli or other cruciferous vegetables 2 days before each visit and to refrain from intense physical activity on the day of the visit. During the visit, participants remained in the testing location and were allowed to drink water *ad libitum*. No food intake was permitted during the visit.

2.3. Intervention and caloric challenge (PhenFlex)

Shortly (maximum of 3 min) before administration, the sprouts were cut approximately 1 cm below the leaves, weighed, and mashed with a small amount of tap water (approximately 13°C) in a kitchen blender for 30s at room temperature (Premium Impuls Blender Smoothiemaker; Impuls; 180 W). Subsequently, tap water (approximately 13°C) was added to a total amount of 250 mL and participants were instructed to drink the entire mixture. Commercially available pea sprouts (Affilla Cress®) were used as placebo in this study since pea sprouts do not contain glucoraphanin/sulforaphane. Affilla Cress (16 g) was prepared and administered in a similar fashion. Blinding of participants was ensured by the even appearance of both drinks and the use of nasal plugs during consumption of the investigational products. The placebo or intervention product was prepared by a researcher who was not involved in any other study procedures and data analysis. Ninety minutes after administration of the investigational products, participants were asked to drink a high-fat, high-glucose, high-caloric product (PhenFlex) (53). For the preparation of the PhenFlex (400 mL, 950 kcal) 60 g palm olein, 75 g

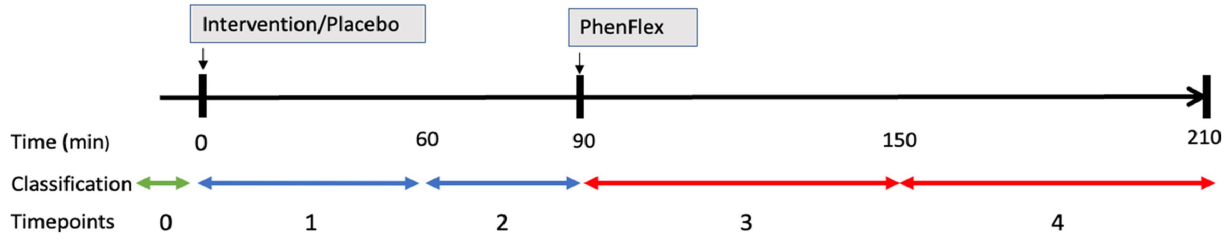

FIGURE 1
Schematic presentation of a study visit. Administration of intervention (sulforaphane/placebo) was followed in 90min by administration of standardized caloric challenge PhenFlex. Urine samples were classified into three groups: **(A)** (baseline, green line), **(B)** (after intervention or placebo, blue lines), and **(C)** (after PhenFlex challenge, red lines). In addition, samples were also divided into 5 timepoints: 0 (baseline), 1 (<60min after intervention or placebo), 2 (>60min after intervention or placebo), 3 (<60min after PhenFlex challenge), and 4 (>60min after PhenFlex challenge).

dextrose, 20 g protein, 0.5 g artificial vanilla aroma and 320 mL tap water were used (53). In all cases, PhenFlex mixtures were freshly prepared, and the participants were instructed to consume the drink within 5 min.

2.4. Urine sampling and assessment of 11-dehydro-TXB_2

Urine samples were collected throughout the days of the visits in pre-labeled containers. The total volume and time of collection of each sample was recorded. Samples were aliquoted and stored at ≤ −80°C until the day of analysis. Urine samples were analyzed for 11-dehydro-TXB_2 using an enzyme-linked immunoassay kit (UTxB2: assay #519510, Cayman Chemical, Ann Arbor, MI) following the manufacturer's instructions. The manufacturer recommended standardizing urinary 11-dehydro-TXB_2 values for creatinine levels using a colorimetric assay kit [Creatinine (urinary) Colorimetric Assay Kit: assay #500701, Cayman Chemical, Ann Arbor, MI]. 11-Dehydro-TXB_2 concentrations were normalized to urinary creatinine concentrations expressed as μg/mg Cr to account for inter-individual variability in urine dilution. Urine samples were classified into three groups for analysis: A (baseline), B (after intervention or placebo) and C (after PhenFlex challenge). In addition, samples were also divided into five timepoints: 0 (baseline), 1 (<60 min after intervention or placebo), 2 (>60 min after intervention or placebo), 3 (<60 min after PhenFlex challenge) and 4 (>60 min after PhenFlex challenge).

2.5. Measurement of urinary sulforaphane and metabolites

The determination of sulforaphane (SFN) and sulforaphane-glutathione (SFN-GSH), sulforaphane-cysteine (SFN-Cys), sulforaphane-cysteine-glycine (SFN-CG) and sulforaphane-N-acetylcysteine (SFN-NAC) in human urine was based on an HPLC–MS/MS method from Egner et al. (54).

2.6. Materials

Trc Canada deuterated stable Isotope solutions of sulforaphane-d8 and sulforaphane-d8-N-acetyl-L-cysteine were purchased from LGC standards (Wesel, Germany). J.T. Baker ethanol and Biosolve acetonitrile were purchased from Boom (Meppel, the Netherlands). Formic acid (FA) was purchased from VWR (Amsterdam, the Netherlands). Fresh water was obtained from an inhouse MilliQ Advantage A10 system containing a LC–MS filter pack (Millipore, Burlington, MA). All chemicals were of analytical quality or higher.

2.6.1. Internal standard preparation

The stock solutions of SFN-d8-NAC and SFN-d8 were diluted with ethanol containing 0.2% FA by a factor of 10 and 100, respectively. From both dilutions 40 μL was taken and combined in a new tube. The mixture was further diluted with ethanol containing 0.2% FA to give final concentrations of 2 μg/mL for SFN-d8-NAC and 0.2 μg/mL for SFN-d8 (IS mix). Stability of IS mix was verified by repeated analysis over a time period of several days.

2.6.2. Sample preparation

Urine samples were taken from the −80°C storage and thawed on ice. The samples were vortexed briefly and centrifuged at 21000 *g* and 4°C for 5 min. From the supernatant 20 μL was transferred to a HPLC vial with a 200 μL insert. IS mix (20 μL) was added and mixed with the urine sample. Thereafter, the samples (5 μL) were directly injected into the analytical system.

2.6.3. Instrumental and data processing

For chromatographic separation an ExionLC UHPLC system (AB Sciex Framingham, MA) equipped with a binary pump, a thermostated autosampler and a column oven was used to maintain a constant temperature (40°C) during the analytical run. For detection a X500R qToF MS system (AB Sciex Framingham, MA) was used. Data acquisition was performed using SciexOS V2.1.6.59781 (AB Sciex). Data processing and identification of sulforaphane and its metabolites was performed by MS-DIAL (version 4.92).

2.7. Genotyping

The participants were requested to take a DNA sample using cheek swabs. Subsequently, all samples were processed at the Human Genomics Facility (HuGe-F) of the Genetic Laboratory of the Department of Internal Medicine at Erasmus MC using the Illumina GSA v3.0 DTC array consisting of 703,320 unique Single Nucleotide Polymorphisms (SNPs). The HuGe-F applied genotyping using the GenomeStudio v2 software with in-house cluster files for reference genome GRCh37. The resulting genotype files are subjected to in-house quality control pipelines which includes correcting for missing data and removing SNPs violating Hardy–Weinberg Equilibrium (55). Finally, imputation is applied to the corrected and filtered SNPs with Beagle software (56) using a reference panel from the 1.000 Genomes project consisting of 2,141 samples (57). Seven gene regions were selected for the analysis based on literature review (36, 58–64). For these genes, their genomic location according to the GRCh37 reference genome was determined from the NCBI Gene database and can be viewed in Table 1 (72). The preprocessed SNPs were filtered on overlap with these gene regions. The resulting subset of potentially interesting SNPs was annotated with information from the NCBI dbSNP database (72).

2.8. Statistical analysis

All normally distributed data are presented as mean ± standard deviation (SD). The non-normally distributed data are shown as median (interquartile range). For categorical variables, frequency and/or percentages are presented. Differences between the groups were assessed by repeated measures ANOVA for normally distributed parameters, or Skillings-Mack tests for the data that was not normally distributed. In addition, paired sample *t*-tests and Wilcoxon rank-sum tests were performed as *post-hoc* tests for the normally distributed samples and the non-normally

TABLE 1 Selected genes based on sulforaphane (SFN) metabolism and effects.

Gene name	Chromosome	Start position (bp)	End position (bp)	Influence on sulforaphane metabolism and/or effects of sulforaphane in humans
GSTM1	1	110,230,439	110,236,367	GSTM1-null mutations may benefit more from SFN, due to decreased metabolism (58, 59, 65).
GSTP1	11	67,351,283	67,354,124	GSTP1Ile105Val genotypes may benefit more from SFN, due to decreased metabolism (66, 67).
GSTT1	22	24,376,133	24,384,311	GSTT1-null mutations may benefit more from SFN, due to decreased metabolism (58, 59, 65).
NQO1	16	69,743,304	69,760,463	NQO1 polymorphisms may indirectly affect SFN metabolism (58).
CYP1A2	15	75,041,186	75,048,948	CYP1A2 polymorphisms may influence the effects of SFN (59).
UGT1A1	2	234,668,916	234,681,946	UGT1A1 polymorphisms may influence the effects of SFN (62, 68–70).
NAT2	8	18,248,792	18,258,728	NAT2 polymorphisms may influence the effects of SFN (36, 71).

The genomic locations are listed according to the GRCh37 reference genome and the NCBI gene database.

TABLE 2 Characteristics of the study participants [mean (SD)].

Characteristics	Population (n=12)
Sex (n, %)	
Female	1 (8.3)
Male	11 (91.7)
Age (years)	26.9 (3.6)
BMI (kg/m^2)	23.1 (1.6)
Body Fat (%)	
Female	28.9 (n/a)
Male	21.4 (3.1)
All	22.0 (3.6)
Visceral fat level	5.17 (1.57)
Alcohol consumption, n (%)	
Moderate	0 (0)
Heavy	9 (75)
Very heavy	3 (25)
Smoking status, n (%)	
Smoker	5 (42)
Non-smoker	7 (58)

distributed samples, respectively. Mann–Whitney U tests were performed to compare the change in urinary 11-dehydro-TXB$_2$ within sample groups between subjects. To study the association between 11-dehydro-TXB$_2$ and sulforaphane (metabolites), Spearman correlation was performed. The tool Stargazer (73) was used for phenotyping the metabolizer type of the participants for the NAT1 and NAT2 pharmacogenes. Participants were subdivided into low versus high excretion of sulforaphane. An adaptation of Fisher's Exact test within the plink genomics software was applied on the groups to test for significantly different genotypes (74). Additionally, adaptive permutation testing within plink was executed to test the validity of the resulting p-values. All analyses were performed two-tailed with $p \leq 0.05$ considered statistically significant.

3. Results

3.1. Subject characteristics

Between November 2021 and January 2022, a total of 12 subjects were found to be eligible to participate in the present study and were randomly allocated to either initial administration of sulforaphane or placebo. Baseline characteristics of the study population (n = 12) are summarized in Table 2. All participants completed the study and were included in the data analysis for biochemical testing (Figure 2). A total of 54 urine samples were collected and assessed. Urine samples were classified into three groups: A (baseline), B (after intervention or placebo) and C (after PhenFlex challenge). In addition, samples were also divided into five timepoints: 0 (baseline), 1 (<60 min after intervention or placebo), 2 (>60 min after intervention or placebo), 3 (<60 min after PhenFlex challenge) and 4 (>60 min after PhenFlex challenge). Given the crossover design of the study, a pre-test was first performed to verify whether the time of the washout period was sufficient and to exclude any carry-over effects. The pre-test (Wilcoxon rank sum test) revealed no differences between treatment allocations for 11-dehydro-TXB$_2$ ($z < -4.47$, $p > 0.655$). A significant difference between the time of sampling in each sample group was checked by Kruskal-Wallis test H (5) = 63.647, $p < 0.001$.

3.2. The effect of sulforaphane on 11-dehydro-TXB$_2$

Differences between groups were assessed for uncorrected and creatinine-corrected 11-dehydro-TXB$_2$. For the uncorrected data, a significant difference was observed in urinary 11-dehydro-TXB$_2$ concentrations between all groups in the sulforaphane group ($X^2(2) = 11.60$, $p = 0.003$) and in the placebo group ($X^2(2) = 7.58$, $p = 0.023$). *Post hoc* analysis showed significant differences for the sulforaphane group between samples A and B, and between samples A and C ($p = 0.028$ and $p = 0.018$), and between samples A and B for placebo ($p = 0.028$; Figure 3). Analysis of the corrected data showed a significant difference in urinary 11-dehydro-TXB$_2$ concentration between all groups in the sulforaphane group ($X^2(2) = 9.27$, $p = 0.010$), no significant differences were observed in the placebo group

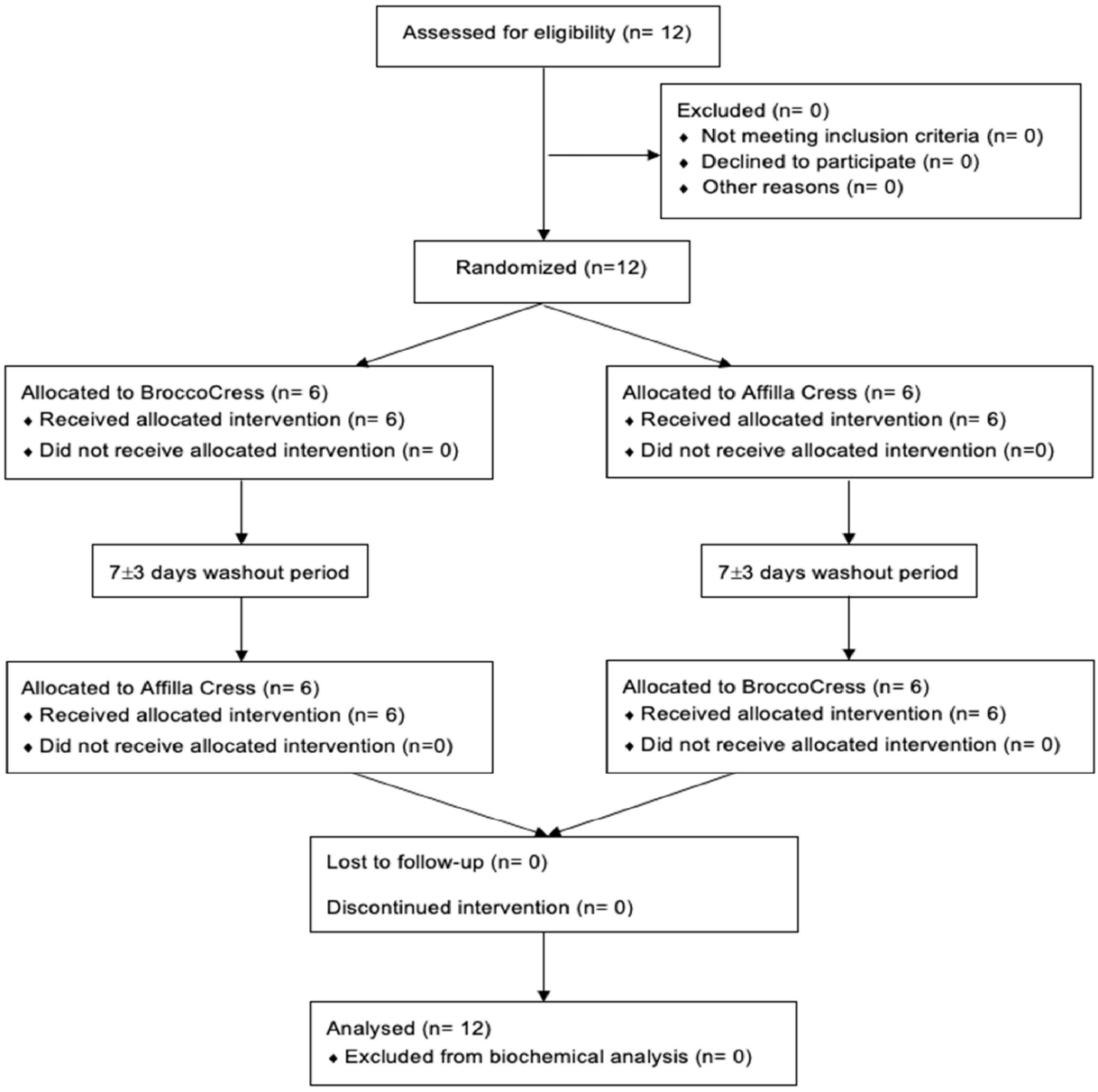

FIGURE 2
CONSORT flow diagram.

($X^2(2) = 3.53$, $p = 0.171$). *Post hoc* analysis showed a significant difference in the sulforaphane group between samples A and C for corrected data ($p = 0.018$; Figure 4). Analysis between treatment allocations within samples showed no significant results (Table 3).

3.3. Sulforaphane excretion

The presence of sulforaphane after consuming fresh broccoli sprouts, and absence after placebo, was determined in urine samples collected during the study visits, indicating an adequate period of abstinence (mean total amount of sulforaphane and metabolites: 8.2 vs. 0.4 μmol, $p < 0.001$). Sulforaphane, SFN-N-acetylcysteine (SFN-NAC), SFN-cysteine, and total amount of metabolites were determined in all urine samples. No detectable levels of SFN-glutathione and SFN-cysteine-glycine were quantified. In the intervention group, the amount of sulforaphane excreted in urine significantly increased 120 min after its administration ($p = 0.028$) and decreased during the subsequent hour ($p = 0.043$; Figure 5A). The amount of SFN-NAC excreted in urine significantly increased 120 min after the intervention ($p = 0.028$), and from the first 45 min to 1.5 h afterwards ($p = 0.028$) decreased during the subsequent hour ($p = 0.043$; Figure 5B). The amount of SFN-cysteine excreted in urine significantly increased 2 h after the intervention ($p = 0.028$; Figure 5C). The total amount of metabolites excreted in urine significantly increased 120 min after the intervention ($p = 0.028$) and from the first 45 min to an hour and a half afterwards ($p = 0.046$) and decreased during the subsequent hour ($p = 0.043$) (Figure 5D).

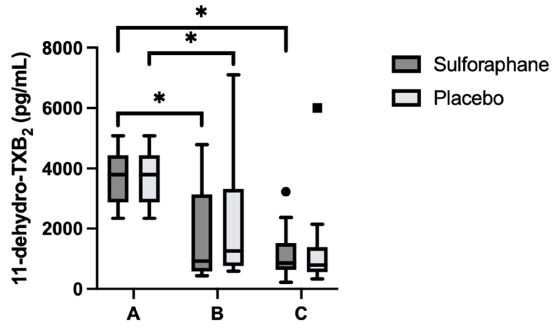

FIGURE 3
Changes in urinary 11-dehydro-TXB_2 concentration in sulforaphane and placebo groups. Uncorrected data are presented as boxplots [median, interquartile range, outliers (circles) and far outliers (squares)]. Urine samples were clustered into three timepoints: **(A)** (baseline), **(B)** (after intervention or placebo), and **(C)** (after PhenFlex challenge). *p<0.05.

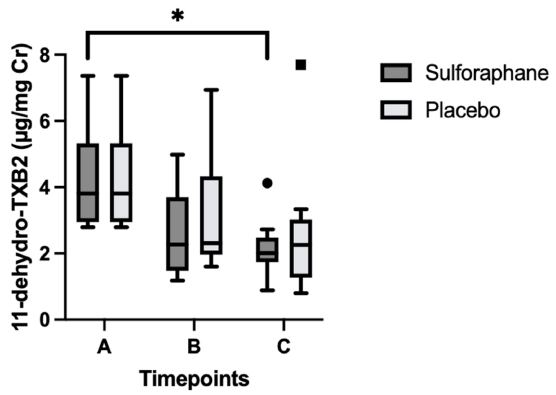

FIGURE 4
Changes in urinary 11-dehydro-TXB_2 concentration in sulforaphane and placebo groups corrected for creatinine. Data are presented as boxplots [median, interquartile range, outliers (circles) and far outliers (squares)]. Urine samples were clustered into three timepoints: **(A)** (baseline), **(B)** (after intervention or placebo), and **(C)** (after PhenFlex challenge). *p<0.05.

In addition, the amount of sulforaphane excreted in the urine during the study visits correlated negatively with 11-dehydro-TXB_2 ($r_s = -0.377$, $p = 0.025$). Moderate strength, inverse correlations between other metabolites SFN-NAC ($r_s = -0.210$, $p = 0.225$), SFN-Cys ($r_s = -0.131$, $p = 0.452$) and total metabolites ($r_s = -0.196$, $p = 0.258$) were observed.

3.4. The influence of single nucleotide polymorphisms on sulforaphane and 11-dehydro-TXB_2

The 703,320 SNPs were subjected to the quality control pipeline, after which 624,240 SNPs were left. The subsequent imputation with Beagle resulted in 24,232,949 SNPs available for downstream analysis. Seven genes were selected for further analysis based on previous literature. Filtering the imputed SNPs using the gene regions as defined in Table 1 resulted in 77 SNPs that were further annotated and tested. Based on dbSNP annotations these included seven missense, 63 intronic, three synonymous, three 3′ untranslated regions (UTR), and one 5′ prime UTR variants. Testing the 77 relevant SNPs using Plink's adoption of Fisher's Exact test resulted in six SNPs associated with sulforaphane excretion (Table 4). All SNPs were found in the NQO1 gene and all, but one were intronic variants, while the other SNP was a missense variant causing a change from proline to serine. Participants carrying this polymorphic variant NQO1*2, which is characterized by a C609T (rs1800566, Pro187Ser) polymorphism of the NQO1 gene, showed decreased excretion of sulforaphane during the study visits [6.2 (1.0) vs. 9.2 (1.6) µmol total metabolites, $p = 0.035$]. No influence of these SNPs on 11-dehydro-TXB_2 levels was observed. No influence of SNPs in GSTM1, GSTP1, GSTT1, CYP1A2, UGT1A1 and NAT2 genes, or type of NAT1 and NAT2 metabolizer on sulforaphane excretion and 11-dehydro-TXB_2 levels was observed (Supplementary Tables 1, 2).

4. Discussion

The aim of this work was to investigate the effects of sulforaphane on the arachidonic acid metabolite, as well as the relationship between 11-dehydro-TXB_2 and sulforaphane and its mercapturic conjugates in urine. Therefore, we assessed the effect of a single intake of fresh broccoli sprouts on urinary 11-dehydro-TXB_2 in healthy participants exposed to a standardized caloric load.

4.1. Sulforaphane decreased urinary 11-dehydro-TXB_2 in young healthy subjects exposed to caloric overload

This study showed that consumption of 16 g of broccoli sprouts before a caloric overload reduced the amount of urinary 11-dehydro-TXB_2 in healthy participants by 50%. These results are consistent with previous research examining the effects of sulforaphane on urinary biomarkers associated with inflammation. Medina et al. (51) showed that higher doses (30 g and 60 g) of broccoli sprouts significantly reduced urinary 11-dehydro-TXB_2 levels by 91 and 94%, respectively, within 12 h in healthy subjects. The higher reduction found by Medina et al. (51) is probably due to the combination of the higher amount of broccoli sprouts given, the lack of a caloric challenge, and the longer time of observation. These results, additionally, indicate that urinary 11-dehydro-TXB_2 shows promise as a sensitive and suitable biomarker to investigate the effects of phytonutrients on platelet aggregation, at least in young healthy participants who are metabolically challenged in a short period of time. For example, in this study, the amount of urinary inflammatory biomarker high-sensitivity C-reactive protein (hs-CRP) remained unchanged during the study visits and was only detectable in 33/54 samples (data not shown).

TABLE 3 Uncorrected and corrected urinary 11-dehydro-TXB_2 concentrations (mean±SD) per timepoint per treatment allocation.

		Population (n=12)				
Treatment	Timepoints^	0 (A)	1 (B)	2 (B)	3 (C)	4 (C)
Sulforaphane	Samples (n)	7	6	5	10	7
	Time of sampling (median (IQR))	n/a	45 (28)	75 (43)	120 (38)	180 (40)
	Sample volumes [median (IQR)]	90 (93)	383 (485)	240 (330)	418 (380)	380 (490)
	Uncorrected TXB_2 (pg/mL)	3671 ± 860	4115 ± 7247	2076 ± 1637	1131 ± 1132	1106 ± 843
	Corrected TXB_2 (μg/mg Cr)	4.21 ± 1.51	3.74 ± 4.38	3.21 ± 1.08	2.07 ± 1.07	2.12 ± 1.02
Placebo	Samples (n)	7	7	7	6	11
	Time of sampling [median (IQR)]	n/a	45 (20)	85 (30)	118 (16)	200 (35)
	Sample volumes [median (IQR)]	90 (93)	240 (320)	260 (310)	400 (278)	350 (150)
	Uncorrected TXB_2 (pg/mL)	3671 ± 860	2908 ± 2927	1839 ± 1540	618 ± 154	1357 ± 1558
	Corrected TXB_2 (μg/mg Cr)	4.21 ± 1.51	3.74 ± 2.44	2.78 ± 1.26	1.48 ± 0.55	2.67 ± 1.85

Cr – corrected for creatinine (mg/mL). ^ Timepoints clustered in three groups: 0 = A (baseline), 1 + 2 = B (after intervention or placebo) and 3 + 4 = C (after PhenFlex challenge).

4.2. The amount of sulforaphane and 11-dehydro TXB_2 excreted in the urine showed an inverse relationship during the caloric challenge

Our data on sulforaphane excretion and its relationship to urinary thromboxane metabolites shows a significant inverse correlation between sulforaphane and urinary 11-dehydro-TXB_2 ($r_s = -0.377$, $p = 0.025$) during the metabolic challenge. In contrast to previous studies, this inverse relationship was only significant for sulforaphane and not for other metabolites nor total metabolites, which may have been influenced by the co-ingestion of the caloric load and the shorter duration of urine collection (51). It is striking however, that from these results it can be concluded that the metabolic state apparently has no effect on the effect of sulforaphane on 11-dehydro-TXB_2 levels.

Previous research has shown that a single administration of a standardized caloric load, the PhenFlex challenge, impacts relevant metabolic processes involved in maintaining or regaining homeostasis of metabolic health in healthy volunteers (12). Contrary to our expectations, the caloric overload did not increase urinary 11-dehydro-TXB_2 measured 2 h after administration of placebo (pea sprouts). Although pea sprouts have a similar nutrient profile to broccoli sprouts, except presence of sulforaphane, the increased amount of retinol and beta-carotene may have counteracted the expected post-challenge increase in 11-dehydro-TXB_2. Retinol and beta-carotene are transformed to retinoic acid (RA) by retinaldehyde dehydrogenases via numerous conversions (75). RA is mediated by two nuclear receptor families, the retinoic acid receptors, and the retinoid X receptors (RXR) (76). These receptors interact with retinoic acid response elements on the promoter regions of target genes, resulting in the activation of nuclear transcription factors (77, 78). The main antithrombotic effect of retinol and beta-carotene is based on the interference of RXR with the NF-κB pathway (79, 80). Inhibition of NF-κB disrupts platelet function by reducing its thrombogenic potential and shows promise when compounds that block NF-κB activation, such as sulforaphane and RA, are considered for prophylaxis of various thrombo-inflammatory diseases (80).

4.3. The NQO1*2 polymorphism may decrease sulforaphane excretion

Previous reports have shown that genetic predisposition may influence the bioavailability and excretion rate of sulforaphane, however results are incongruent (48, 58, 59, 61, 64, 81–87). Partially consistent with Boddupalli et al. (58), we found lower excretion of sulforaphane in participants carrying the polymorphic variant NQO1*2, but no effect of SNPs in other phase II detoxification enzyme genes.

When cruciferous vegetables are damaged, such as when preparing or chewing, myrosinase is released. This enzyme is normally stored separately from glucosinolates, such as glucoraphanin, in different cells or in different intracellular compartments, depending on the plant species (44). Myrosinase catalyzes the hydrolysis of glucoraphanin to liberate the glucose group, resulting in an unstable aglucone that spontaneously rearranges to give rise to a range of products, of which sulforaphane is the most reactive (Figure 6) (44). Cooking cruciferous vegetables inactivates myrosinase, resulting in less sulforaphane formation (44). Bacterial populations of the gut microbiota are also able to converse glucoraphanin to sulforaphane; however, it is estimated to be approximately six-fold less effective than plant myrosinase (88). After this critical first step, sulforaphane is conjugated with glutathione (GSH) upon entry into the mammalian cell, catalyzed by glutathione S-transferases (GSTs), in the liver, entering the mercapturic acid pathway (89). The glutathione conjugate is subjected to a series of sequential conversions, resulting in the *N*-acetylcysteine conjugate (mercapturic acid) as the main metabolite, which is excreted in the urine (Figure 6) (44). Consistent with other studies, this study found the *N*-acetylcysteine conjugate as the primary metabolite in the urine samples (44, 48). However, compared to studies that examined timed urine samples over a longer period of time (8 h and longer), we found lower ratios of SFN-cysteine/total metabolites and no detectable levels of SFN-glutathione and SFN-cysteine-glycine (44, 48). We hypothesize that the longer period of observation and timed collection of urine samples could explain the differences in ratios. The results of Medina et al. (51), which showed that the SFN-cysteine/total metabolites ratio was twice as high in the first 12 h as in the subsequent 12 h, are in line with this hypothesis.

10.3389/fnut.2023.1204561

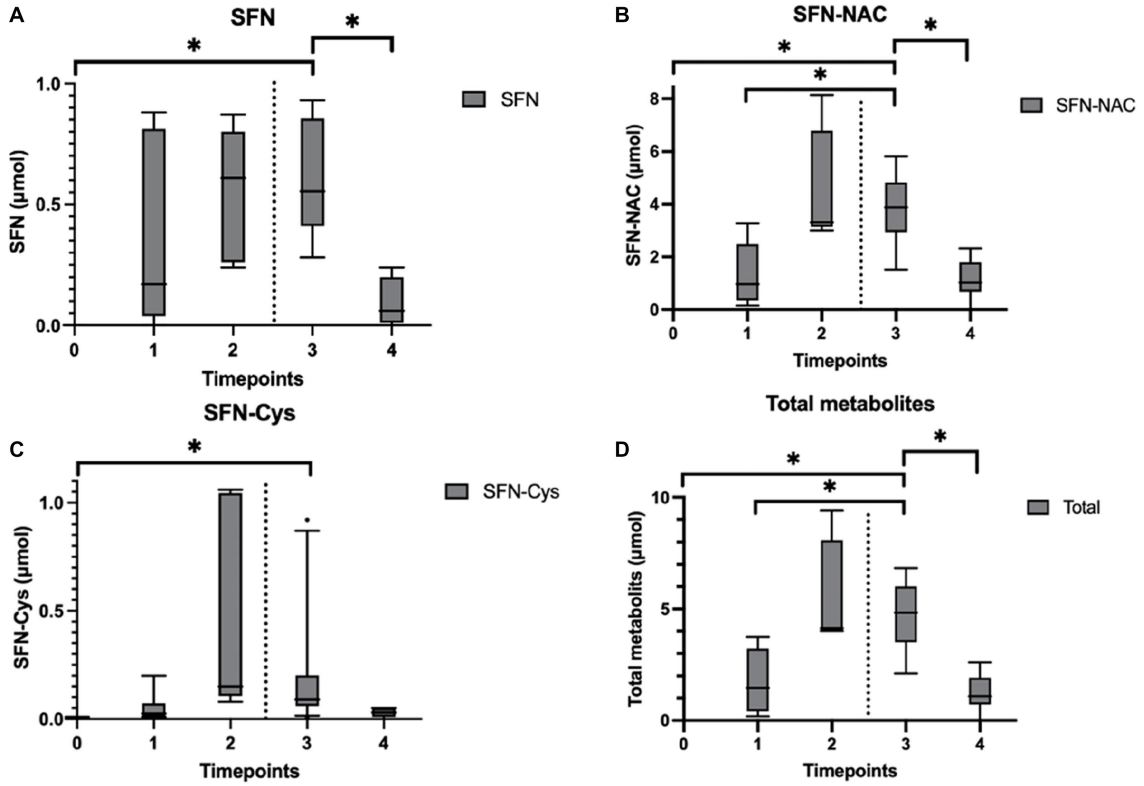

FIGURE 5
Urinary sulforaphane (SFN), sulforaphane-cysteine (SFN-Cys), sulforaphane-N-acetylcysteine (SFN-NAC), and total metabolites excretion after participants consumed a single intake (16g) of broccoli sprouts. Data are presented as boxplots [median, interquartile range, and outliers (circles)]. The dashed lines indicate when the PhenFlex challenge was administered. Urine samples were clustered into five timepoints: 0 (baseline), 1 (<60min after intervention), 2 (>60min after intervention), 3 (<60min after PhenFlex challenge), and 4 (>60min after PhenFlex challenge). The amount of SFN **(A)** excreted in the urine correlated negatively with 11-dehydro-TXB_2 (r_s=−0.377, p=0.025). Moderate strength, inverse correlations between other metabolites were observed, i.e., SFN-NAC **(B)** (r_s=−0.210, p=0.225), SFN-Cys **(C)** (r_s=−0.131, p=0.452) and total metabolites **(D)** (r_s=−0.196, p=0.258). *p<0.05.

TABLE 4 Single nucleotide polymorphisms (SNPs) associated with sulforaphane excretion.

Gene name	Reference SNP ID (RsID)	Chromosome	Base pair (bp) position	Type	Consequence (missense only)	Fisher's exact test p-value	Permutation p-value
NQO1	rs1800566	16	69,745,145	Missense	Proline→Serine	0.087	0.035
NQO1	rs57964521	16	69,750,092	Intron	–	0.087	0.035
NQO1	rs7186002	16	69,751,065	Intron	–	0.087	0.035
NQO1	rs1437135	16	69,757,828	Intron	–	0.087	0.035
NQO1	rs2196574	16	69,758,076	Intron	–	0.087	0.035
NQO1	rs2361839	16	69,758,395	Intron	–	0.087	0.035

The genomic locations are listed according to the GRCh37 reference genome and the NCBI gene database.

Future research into the relationship between different metabolite ratios and time differences could provide an explanation for these inconsistencies.

Polymorphisms in phase II enzymes involved in the mercapturic acid pathway may help explain the individual outcomes of sulforaphane interventions (Table 1; Figure 6) (58, 59). In the current study, we found that not the enzymes directly involved, but an antioxidant enzyme, NQO1, indirectly involved in this metabolic route influenced sulforaphane secretion. Previous studies showed that the null NQO1*2 polymorphism results in a lack of functional NQO1 protein due to reduced stability, the ability to bind flavin adenine dinucleotide, and a dramatically reduced half-life due to rapid polyubiquitination and proteasomal degradation (83, 90). The lack of functional NQO1 would then in turn reduce the pool of other enzymes that catalyze detoxification of electrophiles, e.g., GSTs (91, 92). We hypothesize that because sulforaphane is metabolized by GSTs, the reduced glutathione pool will result in longer half-lives of circulating sulforaphane and potentially greater systemic effects of cruciferous vegetables. Paradoxically, the increased activation of Nrf2/ARE-dependent genes by sulforaphane, including GSTs, thioredoxin and heme oxygenase 1, would also result in more non-functional NQO1 in individuals with the NQO1*2 polymorphism (41). This

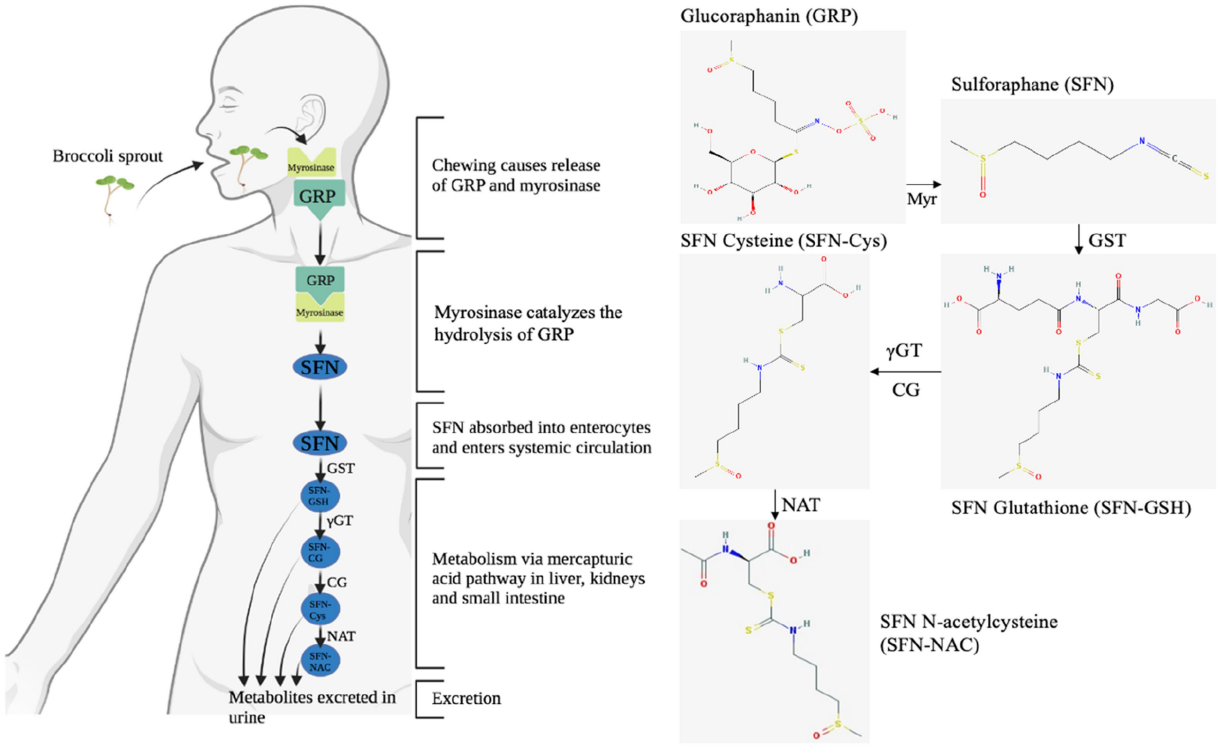

FIGURE 6
The enzymatic conversion of glucoraphanin (GRP) to sulforaphane (SFN) by myrosinase (Myr), followed by the absorption, distribution, metabolism, and excretion of SFN via the mercapturic acid pathway. The enzymatic conversion of GRP to SFN is considered to be the rate-limiting step affecting bioavailability within this cascade, as the efficiency of conversion of SFN to metabolites in humans is very high (70–90%) (48). GRP, glucoraphanin; GST, glutathione S-transferase; Myr, myrosinase; γGT, γ-glutamyl transferase; CG, cysteinylglycinase; NAT, N-acetyl transferase; SFN-Cys, sulforaphane-cysteine; SFN-NAC, sulforaphane-N-acetylcysteine; SFN-GSH, sulforaphane glutathione conjugate.

positive feedback loop could explain the lower excretion of sulforaphane in participants carrying the polymorphic variant NQO1*2, while no initial differences in antithrombotic effect were observed after a single administration of broccoli sprouts. Repeated-dose studies could reveal whether individuals with genetic polymorphisms that reduce the activity of detoxification enzymes could benefit even more from consumption of cruciferous vegetables. Further clarification of the interactions between polymorphisms and the downstream effectors of sulforaphane are promising new lines of research to elucidate the relationship between the consumption of cruciferous vegetables and human health and well-being (58).

4.4. Food-derived sulforaphane has implications for functional food innovation

Overall, only a limited number of food-derived compounds have been clinically investigated for their antiplatelet effects. Some success has been achieved in developing antiplatelet nutraceuticals, with WSTC to date being the only functional food proven to function as a natural cardio-protective functional ingredient, as assessed by the EFSA (25). Therefore, Fruitflow®, the trademarked name of WSTC, is authorized by the European Commission to use the health claim (new function claims, Art. 13.5): "water-soluble tomato concentrate (WSTC) I and II helps maintain normal platelet aggregation, which contributes to healthy blood flow" (93, 94). To provide stakeholders with greater clarity on which effects related to cardiovascular health could be studied to support health claims, in 2018, a guidance was published by EFSA's Panel on Dietetic Products, Nutrition and Allergies (NDA Panel). This guidance document provides more detailed guidelines for the evaluation of Articles 13.1, 13.5, and 14 health claims in this area (95). According to the Panel, a reduction in platelet aggregation [i.e., the percentage of inhibition of platelet aggregation using light transmission aggregometry (LTA) according to well-accepted and standardized protocols] in subjects with platelet activation during sustained exposure to the food/constituent (at least 4 weeks) is a beneficial physiological effect. Other outcome variables, such as thromboxane A_2 (TXA_2) or plasma soluble P-selectin, are not considered established markers of platelet aggregation, but can be used as supporting evidence for the scientific substantiation of these claims (95, 96).

Although LTA has been considered the gold standard to assess platelet function for over 40 years, poor standardization and the required manipulation by a skilled technician limit its use to specialized laboratories (20, 97–100). Numerous platelet function tests are currently available; however, their methodologies are diverse, and little is known about the comparability or interchangeability of these tests (20, 97). O'Kennedy et al. examined TXA_2 levels (via thromboxane B_2, the stable metabolite of TXA_2) after a single dose of Fruitflow® (65 mg tomato total active fraction), or 75 mg aspirin (ASA) and found a reduction of approximately 25% at 3 h and 37% at 5 h for WSTC and 66% for ASA after 5 h (26, 94). Our results indicate that sulforaphane seems more effective in reducing overall platelet

aggregation at lower doses. In addition, the correlations between sulforaphane and thromboxane demonstrate causation, which is the last criterion in the evaluation of a scientific health claim dossier by EFSA (51, 101, 102). A logical next step for future research would therefore be to investigate the effects of sulforaphane on inhibition of platelet aggregation using LTA in subjects with platelet activation.

4.5. Limitations and future directions

This study is the first to demonstrate that urinary 11-dehydro-TXB_2 is a sensitive, easy-to-use, and suitable biomarker to investigate the effects of phytonutrients on platelet aggregation in young healthy participants who are metabolically challenged in a short period of time. This study is not without limitations. First, the glucoraphanin content of the active sprout material and placebo may have differed from product labels and may have been adversely affected by cultivation conditions, batch-to-batch variation, and preparation methods. Second, it is challenging to find an impeccable placebo in nutritional intervention studies, especially for whole foods in a double-blinded setting. In current study, the placebo had to match the broccoli sprouts in terms of nutrient value, except for sulforaphane content. Despite our efforts, the increased amount of β-carotene and some vitamins in the pea sprouts may have counteracted the expected post-challenge increase in 11-dehydro-TXB_2 (79, 80). In addition, follow-up studies with a larger sample size will shed more light on the effects of interindividual genetic variability with respect to cruciferous vegetable consumption. Nevertheless, this study has increased our understanding of the antithrombotic effects of sulforaphane and can be used as supporting evidence for the scientific substantiation of claims on the reduction of platelet aggregation (95, 96). When follow-up studies on the effects of sulforaphane using LTA yield positive results, fresh broccoli sprouts or other produce containing enough sulforaphane per serving, could apply for the same authorized claim as WSTC.

5. Conclusion

This study demonstrated that a single administration of broccoli sprouts reduced urinary 11-dehydro-TXB_2 levels by clinically relevant amounts in healthy participants exposed to a standardized caloric load. In addition, the correlations between sulforaphane and thromboxane indicate a causal relationship, which is not influenced by the co-ingestion of the metabolic challenge. 11-Dehydro-TXB_2 shows promise as a non-invasive, sensitive, and suitable biomarker to investigate the acute effects of phytonutrients on platelet aggregation within hours. Genetic predisposition may influence the health effects of cruciferous vegetable consumption, but more research is needed to ultimately provide personalized dietary advice for consumers. This study forms the basis for a scientific substantiation of claims on the reduction of platelet aggregation for fresh produce containing sulforaphane in the future.

Data availability statement

The data presented in the study are deposited in the European Variation Archive (EVA) at EMBL-EBI repository under accession number PRJEB63376.

Ethics statement

The study protocol (NL77272.068.21) was approved by the Medical Ethics Review Committee of Maastricht University Medical Centre+ (MUMC+) and Maastricht University, Maastricht, the Netherlands. The patients/participants provided their written informed consent to participate in this study.

Author contributions

HS: conceptualization, investigation, formal analysis, visualization, and writing—original draft. EW, EK, MB, and JD: investigation and formal analysis. JB: investigation, formal analysis, and writing—review and editing. TL and FT: writing—review and editing. FO: methodology and writing—review and editing. ABa: conceptualization, writing—review and editing, and supervision. KS: conceptualization, data curation, methodology, visualization, and writing—review and editing. ABo: conceptualization, writing—review and editing, funding acquisition, and supervision. All authors contributed to the article and approved the submitted version.

Funding

This research was funded by the Dutch Topsector Tuinbouw & Uitgangsmaterialen, grant number TU1118.

Acknowledgments

The authors thank Diede Nijmeijer and Ardi Cengo for their contributions.

Conflict of interest

MB and JD were employed by Omnigen B.V.

The remaining authors declare that the research was conducted in the absence of any commercial or financial relationships that could be construed as a potential conflict of interest.

Publisher's note

Supplementary material

The Supplementary material for this article can be found online at: https://www.frontiersin.org/articles/10.3389/fnut.2023.1204561/full#supplementary-material

References

1. O'Kennedy N, Duss R, Duttaroy AK. Dietary antiplatelets: a new perspective on the health benefits of the water-soluble tomato concentrate Fruitflow(®). *Nutrients*. (2021) 13:2184. doi: 10.3390/nu13072184

2. von Hundelshausen P, Weber C. Platelets as immune cells: bridging inflammation and cardiovascular disease. *Circ Res*. (2007) 100:27–40. doi: 10.1161/01.RES.0000252802.25497.b7

3. Saldeen P, Nilsson IM, Saldeen T. Increased synthesis of thromboxane B2 and 6-keto-PGF1 alpha in hand veins from patients with deep venous thrombosis. *Thromb Res*. (1983) 32:461–7. doi: 10.1016/0049-3848(83)90256-6

4. Dogné J-M, de Leval X, Benoit P, Delarge J, Masereel B. Thromboxane A2 inhibition: therapeutic potential in bronchial asthma. *Am J Respir Med Drugs Devices Other Interv*. (2002) 1:11–7. doi: 10.1007/BF03257158

5. Eikelboom JW, Hirsh J, Weitz JI, Johnston M, Yi Q, Yusuf S. Aspirin-resistant thromboxane biosynthesis and the risk of myocardial infarction, stroke, or cardiovascular death in patients at high risk for cardiovascular events. *Circulation*. (2002) 105:1650–5. doi: 10.1161/01.cir.0000013777.21160.07

6. Hamm CW, Lorenz RL, Bleifeld W, Kupper W, Wober W, Weber PC. Biochemical evidence of platelet activation in patients with persistent unstable angina. *J Am Coll Cardiol*. (1987) 10:998–1004. doi: 10.1016/s0735-1097(87)80336-4

7. Mehta JL, Lawson D, Mehta P, Saldeen T. Increased prostacyclin and thromboxane A2 biosynthesis in atherosclerosis. *Proc Natl Acad Sci U S A*. (1988) 85:4511–5. doi: 10.1073/pnas.85.12.4511

8. Hishinuma T, Tsukamoto H, Suzuki K, Mizugaki M. Relationship between thromboxane/prostacyclin ratio and diabetic vascular complications. *Prostaglandins Leukot Essent Fatty Acids*. (2001) 65:191–6. doi: 10.1054/plef.2001.0310

9. Chen SY, Yu BJ, Liang YQ, Lin WD. Platelet aggregation, platelet cAMP levels and thromboxane B2 synthesis in patients with diabetes mellitus. *Chin Med J*. (1990) 103:312–8.

10. Santilli F, Formoso G, Sbraccia P, Averna M, Miccoli R, Di Fulvio P, et al. Postprandial hyperglycemia is a determinant of platelet activation in early type 2 diabetes mellitus. *J Thromb Haemost*. (2010) 8:828–37. doi: 10.1111/j.1538-7836.2010.03742.x

11. Stroeve JHM, van Wietmarschen H, Kremer BHA, van Ommen B, Wopereis S. Phenotypic flexibility as a measure of health: the optimal nutritional stress response test. *Genes Nutr*. (2015) 10:13. doi: 10.1007/s12263-015-0459-1

12. Wopereis S, Stroeve JHM, Stafleu A, Bakker GCM, Burggraaf J, van Erk MJ, et al. Multi-parameter comparison of a standardized mixed meal tolerance test in healthy and type 2 diabetic subjects: the PhenFlex challenge. *Genes Nutr*. (2017) 12:21. doi: 10.1186/s12263-017-0570-6

13. van den Broek TJ, Bakker GCM, Rubingh CM, Bijlsma S, Stroeve JHM, van Ommen B, et al. Ranges of phenotypic flexibility in healthy subjects. *Genes Nutr*. (2017) 12:32. doi: 10.1186/s12263-017-0589-8

14. Hoevenaars F, van der Kamp J-W, van den Brink W, Wopereis S. Next generation health claims based on resilience: the example of whole-grain wheat. *Nutr*. (2020) 12:12. doi: 10.3390/nu12102945

15. Ally AI, Horrobin DF. Thromboxane A2 in blood vessel walls and its physiological significance: relevance to thrombosis and hypertension. *Prostaglandins Med*. (1980) 4:431–8. doi: 10.1016/0161-4630(80)90051-8

16. Ishizuka T, Taniguchi O, Yamamoto M, Kajita K, Nagashima T, Takeda N, et al. Thrombin-induced platelet aggregation, phosphoinositide metabolism and protein phosphorylation in NIDDM patients treated by diet, sulphonylurea or insulin. *Diabetologia*. (1994) 37:632–8. doi: 10.1007/BF00403384

17. Offermanns S. Activation of platelet function through G protein–coupled receptors. *Circ Res*. (2006) 99:1293–304. doi: 10.1161/01.RES.0000251742.71301.16

18. Capra V, Bäck M, Angiolillo DJ, Cattaneo M, Sakariassen KS. Impact of vascular thromboxane prostanoid receptor activation on hemostasis, thrombosis, oxidative stress, and inflammation. *J Thromb Haemost*. (2014) 12:126–37. doi: 10.1111/jth.12472

19. Lordan R, Tsoupras A, Zabetakis I. Platelet activation and prothrombotic mediators at the nexus of inflammation and atherosclerosis: potential role of antiplatelet agents. *Blood Rev*. (2021) 45:100694. doi: 10.1016/j.blre.2020.100694

20. Lordkipanidzé M, Pharand C, Schampaert E, Turgeon J, Palisaitis DA, Diodati JG. A comparison of six major platelet function tests to determine the prevalence of aspirin resistance in patients with stable coronary artery disease. *Eur Heart J*. (2007) 28:1702–8. doi: 10.1093/eurheartj/ehm226

21. Catella F, Healy D, Lawson JA, FitzGerald GA. 11-Dehydrothromboxane B2: a quantitative index of thromboxane A2 formation in the human circulation. *Proc Natl Acad Sci U S A*. (1986) 83:5861–5. doi: 10.1073/pnas.83.16.5861

22. Di Minno MND, Guida A, Camera M, Colli S, Di Minno G, Tremoli E. Overcoming limitations of current antiplatelet drugs: a concerted effort for more profitable strategies of intervention. *Ann Med*. (2011) 43:531–44. doi: 10.3109/07853890.2011.582137

23. Abbas H, Kumar Nayudu S, Ravi M, Saad M, Bathini K, Ravi P, et al. Does extended use of Clopidogrel-based dual anti-platelet therapy increase the risk of gastrointestinal bleeding? *Gastroenterol Res*. (2020) 13:146–9. doi: 10.14740/gr1285

24. Cámara M, Fernández-Ruiz V, Sánchez-Mata M-C, Cámara RM, Domínguez L, Sesso HD. Scientific evidence of the beneficial effects of tomato products on cardiovascular disease and platelet aggregation. *Front Nutr*. (2022) 9:849841. doi: 10.3389/fnut.2022.849841

25. Tsoupras A, Lordan R, Zabetakis I. Thrombosis and COVID-19: the potential role of nutrition. *Front Nutr*. (2020) 7:583080. doi: 10.3389/fnut.2020.583080

26. O'Kennedy N, Crosbie L, Song H-J, Zhang X, Horgan G, Duttaroy AK. A randomised controlled trial comparing a dietary antiplatelet, the water-soluble tomato extract Fruitflow, with 75 mg aspirin in healthy subjects. *Eur J Clin Nutr*. (2017) 71:723–30. doi: 10.1038/ejcn.2016.222

27. Mazarakis N, Snibson K, Licciardi PV, Karagiannis TC. The potential use of L-sulforaphane for the treatment of chronic inflammatory diseases: a review of the clinical evidence. *Clin Nutr*. (2020) 39:664–75. doi: 10.1016/j.clnu.2019.03.022

28. Fahey JW, Zhang Y, Talalay P. Broccoli sprouts: an exceptionally rich source of inducers of enzymes that protect against chemical carcinogens. *Proc Natl Acad Sci U S A*. (1997) 94:10367–72. doi: 10.1073/pnas.94.19.10367

29. Atwell LL, Hsu A, Wong CP, Stevens JF, Bella D, Yu T-W, et al. Absorption and chemopreventive targets of sulforaphane in humans following consumption of broccoli sprouts or a myrosinase-treated broccoli sprout extract. *Mol Nutr Food Res*. (2015) 59:424–33. doi: 10.1002/mnfr.201400674

30. Oliviero T, Verkerk R, Vermeulen M, Dekker M. In vivo formation and bioavailability of isothiocyanates from glucosinolates in broccoli as affected by processing conditions. *Mol Nutr Food Res*. (2014) 58:1447–56. doi: 10.1002/mnfr.201300894

31. Saha S, Hollands W, Teucher B, Needs PW, Narbad A, Ortori CA, et al. Isothiocyanate concentrations and interconversion of sulforaphane to erucin in human subjects after consumption of commercial frozen broccoli compared to fresh broccoli. *Mol Nutr Food Res*. (2012) 56:1906–16. doi: 10.1002/mnfr.201200225

32. Cramer JM, Teran-Garcia M, Jeffery EH. Enhancing sulforaphane absorption and excretion in healthy men through the combined consumption of fresh broccoli sprouts and a glucoraphanin-rich powder. *Br J Nutr*. (2012) 107:1333–8. doi: 10.1017/S0007114511004429

33. Hauder J, Winkler S, Bub A, Rüfer CE, Pignitter M, Somoza V. LC-MS/MS quantification of sulforaphane and indole-3-carbinol metabolites in human plasma and urine after dietary intake of selenium-fortified broccoli. *J Agric Food Chem*. (2011) 59:8047–57. doi: 10.1021/jf201501x

34. Egner PA, Chen JG, Wang JB, Wu Y, Sun Y, Lu JH, et al. Bioavailability of sulforaphane from two broccoli sprout beverages: results of a short-term, cross-over clinical trial in Qidong, China. *Cancer Prev Res*. (2011) 4:384–95. doi: 10.1158/1940-6207.CAPR-10-0296

35. Hanlon N, Coldham N, Gielbert A, Sauer MJ, Ioannides C. Repeated intake of broccoli does not lead to higher plasma levels of sulforaphane in human volunteers. *Cancer Lett*. (2009) 284:15–20. doi: 10.1016/j.canlet.2009.04.004

36. Vermeulen M, Klöpping-Ketelaars IWAA, Van Den Berg R, Vaes WHJ. Bioavailability and kinetics of sulforaphane in humans after consumption of cooked versus raw broccoli. *J Agric Food Chem*. (2008) 56:10505–9. doi: 10.1021/jf801989e

37. Rungapamestry V, Duncan AJ, Fuller Z, Ratcliffe B. Effect of meal composition and cooking duration on the fate of sulforaphane following consumption of broccoli by healthy human subjects. *Br J Nutr*. (2007) 97:644–52. doi: 10.1017/S0007114507381403

38. Conaway CC, Getahun SM, Liebes LL, Pusateri DJ, Topham DK, Botero-Omary M, et al. Disposition of glucosinolates and sulforaphane in humans after ingestion of steamed and fresh broccoli. *Nutr Cancer*. (2000) 38:168–78. doi: 10.1207/S15327914NC382_5

39. Posner GH, Cho CG, Green JV, Zhang Y, Talalay P. Design and synthesis of bifunctional isothiocyanate analogs of sulforaphane: correlation between structure and potency as inducers of anticarcinogenic detoxication enzymes. *J Med Chem*. (1994) 37:170–6. doi: 10.1021/jm00027a021

40. Valgimigli L, Iori R. Antioxidant and pro-oxidant capacities of ITCs. *Environ Mol Mutagen*. (2009) 50:222–37. doi: 10.1002/em.20468

41. Bryan HK, Olayanju A, Goldring CE, Park BK. The Nrf2 cell defence pathway: Keap1-dependent and -independent mechanisms of regulation. *Biochem Pharmacol*. (2013) 85:705–17. doi: 10.1016/j.bcp.2012.11.016

42. Dong Z, Shang H, Chen YQ, Pan LL, Bhatia M, Sun J. Sulforaphane protects pancreatic acinar cell injury by modulating Nrf2-mediated oxidative stress and NLRP3 inflammatory pathway. *Oxidative Med Cell Longev*. (2016) 2016:1–12. doi: 10.1155/2016/7864150

43. Traka MH, Saha S, Huseby S, Kopriva S, Walley PG, Barker GC, et al. Genetic regulation of glucoraphanin accumulation in Beneforté® broccoli. *New Phytol*. (2013) 198:1085–95. doi: 10.1111/nph.12232

44. Barba FJ, Nikmaram N, Roohinejad S, Khelfa A, Zhu Z, Koubaa M. Bioavailability of Glucosinolates and their breakdown products: impact of processing. *Front Nutr*. (2016) 3:24. doi: 10.3389/fnut.2016.00024

45. Okunade O, Niranjan K, Ghawi SK, Kuhnle G, Methven L. Supplementation of the diet by exogenous myrosinase via mustard seeds to increase the bioavailability of

sulforaphane in healthy human subjects after the consumption of cooked broccoli. *Mol Nutr Food Res*. (2018) 62:e1700980. doi: 10.1002/mnfr.201700980

46. Sivapalan T, Melchini A, Saha S, Needs PW, Traka MH, Tapp H, et al. Bioavailability of glucoraphanin and sulforaphane from high-glucoraphanin broccoli. *Mol Nutr Food Res*. (2018) 62:e1700911. doi: 10.1002/mnfr.201700911

47. Murillo G, Mehta RG. Cruciferous vegetables and cancer prevention. *Nutr Cancer*. (2001) 41:17–28. doi: 10.1080/01635581.2001.9680607

48. Fahey JW, Wehage SL, Holtzclaw WD, Kensler TW, Egner PA, Shapiro TA, et al. Protection of humans by plant glucosinolates: efficiency of conversion of glucosinolates to isothiocyanates by the gastrointestinal microflora. *Cancer Prev Res*. (2012) 5:603–11. doi: 10.1158/1940-6207.CAPR-11-0538

49. Chuang W-Y, Kung P-H, Kuo C-Y, Wu C-C. Sulforaphane prevents human platelet aggregation through inhibiting the phosphatidylinositol 3-kinase/Akt pathway. *Thromb Haemost*. (2013) 109:1120–30. doi: 10.1160/TH12-09-0636

50. Jayakumar T, Chen W-F, Lu W-J, Chou D-S, Hsiao G, Hsu C-Y, et al. A novel antithrombotic effect of sulforaphane via activation of platelet adenylate cyclase: ex vivo and in vivo studies. *J Nutr Biochem*. (2013) 24:1086–95. doi: 10.1016/j.jnutbio.2012.08.007

51. Medina S, Domínguez-Perles R, Moreno DA, García-Viguera C, Ferreres F, Gil JI, et al. The intake of broccoli sprouts modulates the inflammatory and vascular prostanoids but not the oxidative stress-related isoprostanes in healthy humans. *Food Chem*. (2015) 173:1187–94. doi: 10.1016/j.foodchem.2014.10.152

52. World Medical Association. World Medical Association declaration of Helsinki: ethical principles for medical research involving human subjects. *JAMA*. (2013) 310:2191–4. doi: 10.1001/jama.2013.281053

53. Hoevenaars FPM, Esser D, Schutte S, Priebe MG, Vonk RJ, Van Den Brink WJ, et al. Whole grain wheat consumption affects postprandial inflammatory response in a randomized controlled trial in overweight and obese adults with mild hypercholesterolemia in the graandioos study. *J Nutr*. (2019) 149:2133–44. doi: 10.1093/jn/nxz177

54. Egner PA, Kensler TW, Chen J-G, Gange SJ, Groopman JD, Friesen MD. Quantification of sulforaphane mercapturic acid pathway conjugates in human urine by high-performance liquid chromatography and isotope-dilution tandem mass spectrometry. *Chem Res Toxicol*. (2008) 21:1991–6. doi: 10.1021/tx800210k

55. Turner S, Armstrong LL, Bradford Y, Carlson CS, Crawford DC, Crenshaw AT, et al. Quality control procedures for genome-wide association studies. *Curr Protoc Hum Genet*. (2011) Chapter 1:Unit1.19. doi: 10.1002/0471142905.hg0119s68

56. Browning BL, Zhou Y, Browning SR. A one-penny imputed genome from next-generation reference panels. *Am J Hum Genet*. (2018) 103:338–48. doi: 10.1016/j.ajhg.2018.07.015

57. Auton A, Abecasis GR, Altshuler DM, Durbin RM, Abecasis GR, Bentley DR, et al. A global reference for human genetic variation. *Nature*. (2015) 526:68–74. doi: 10.1038/nature15393

58. Boddupalli S, Mein JR, Lakkanna S, James DR. Induction of phase 2 antioxidant enzymes by broccoli sulforaphane: perspectives in maintaining the antioxidant activity of vitamins A, C, and E. *Front Genet*. (2012) 3:7. doi: 10.3389/fgene.2012.00007

59. Lampe JW, Peterson S. Brassica, biotransformation and cancer risk: genetic polymorphisms alter the preventive effects of cruciferous vegetables. *J Nutr*. (2002) 132:2991–4. doi: 10.1093/jn/131.10.2991

60. Houghton CA. Sulforaphane: its "coming of age" as a clinically relevant nutraceutical in the prevention and treatment of chronic disease. *Oxidative Med Cell Longev*. (2019) 2019:1–27. doi: 10.1155/2019/2716870

61. Joseph MA, Moysich KB, Freudenheim JL, Shields PG, Bowman ED, Zhang Y, et al. Cruciferous vegetables, genetic polymorphisms in glutathione S-transferases M1 and T1, and prostate cancer risk. *Nutr Cancer*. (2004) 50:206–13. doi: 10.1207/s15327914nc5002_11

62. Ambrosone CB, Tang L. Cruciferous vegetable intake and cancer prevention: role of nutrigenetics. *Cancer Prev Res*. (2009) 2:298–300. doi: 10.1158/1940-6207.CAPR-09-0037

63. Traka M, Gasper AV, Melchini A, Bacon JR, Needs PW, Frost V, et al. Broccoli consumption interacts with GSTM1 to perturb oncogenic signalling pathways in the prostate. *PLoS One*. (2008) 3:e2568. doi: 10.1371/journal.pone.0002568

64. Gasper AV, Al-Janobi A, Smith JA, Bacon JR, Fortun P, Atherton C, et al. Glutathione S-transferase M1 polymorphism and metabolism of sulforaphane from standard and high-glucosinolate broccoli. *Am J Clin Nutr*. (2005) 82:1283–91. doi: 10.1093/ajcn/82.6.1283

65. Seow A, Vainio H, Yu MC. Effect of glutathione-S-transferase polymorphisms on the cancer preventive potential of isothiocyanates: an epidemiological perspective. *Mutat. Res.* (2005) 592:58–67. doi: 10.1016/j.mrfmmm.2005.06.004

66. Steck SE, Gammon MD, Hebert JR, Wall DE, Zeisel SH. GSTM1, GSTT1, GSTP1, and GSTA1 polymorphisms and urinary isothiocyanate metabolites following broccoli consumption in humans. *J. Nutr.* (2007) 137:904–9. doi: 10.1093/jn/137.4.904

67. Lin HJ, Johansson AS, Stenberg G, Materi AM, Park JM, Dai A, et al. Naturally occurring Phe151Leu substitution near a conserved folding module lowers stability of glutathione transferase P1-1. *Biochim. Biophys. Acta*. (2003) 1649:16–23. doi: 10.1016/s1570-9639(03)00149-3

68. Peterson S, Bigler J, Horner NK, Potter JD, Lampe JW. Cruciferae interact with the UGT1A1*28 polymorphism to determine serum bilirubin levels in humans. *J. Nutr.* (2005) 135:1051–5. doi: 10.1093/jn/135.5.1051

69. Chang J-L, Bigler J, Schwarz Y, Li SS, Li L, King IB, et al. UGT1A1 polymorphism is associated with serum bilirubin concentrations in a randomized, controlled, fruit and vegetable feeding trial. *J. Nutr.* (2007) 137:890–7. doi: 10.1093/jn/137.4.890

70. Navarro SL, Peterson S, Chen C, Makar KW, Schwarz Y, King IB, et al. Cruciferous vegetable feeding alters UGT1A1 activity: diet- and genotype-dependent changes in serum bilirubin in a controlled feeding trial. *Cancer Prev. Res.* (2009) 2:345–52. doi: 10.1158/1940-6207.CAPR-08-0178

71. Zhao H, Lin J, Grossman HB, Hernandez LM, Dinney CP, Wu X. Dietary isothiocyanates, GSTM1, GSTT1, NAT2 polymorphisms and bladder cancer risk. *Int. J. cancer*. (2007) 120:2208–13. doi: 10.1002/ijc.22549

72. Sayers EW, Bolton EE, Brister JR, Canese K, Chan J, Comeau DC, et al. Database resources of the national center for biotechnology information. *Nucleic Acids Res*. (2022) 50:D20–6. doi: 10.1093/nar/gkab1112

73. Lee S, Wheeler MM, Patterson K, McGee S, Dalton R, Woodahl EL, et al. Stargazer: a software tool for calling star alleles from next-generation sequencing data using CYP2D6 as a model. *Genet Med*. (2019) 21:361–72. doi: 10.1038/s41436-018-0054-0

74. Purcell S, Neale B, Todd-Brown K, Thomas L, Ferreira MAR, Bender D, et al. PLINK: a tool set for whole-genome association and population-based linkage analyses. *Am J Hum Genet*. (2007) 81:559–75. doi: 10.1086/519795

75. Blomhoff R, Blomhoff HK. Overview of retinoid metabolism and function. *J Neurobiol*. (2006) 66:606–30. doi: 10.1002/neu.20242

76. Dollé P, Fraulob V, Kastner P, Chambon P. Developmental expression of murine retinoid X receptor (RXR) genes. *Mech Dev*. (1994) 45:91–104. doi: 10.1016/0925-4773(94)90023-x

77. Giguere V, Ong ES, Segui P, Evans RM. Identification of a receptor for the morphogen retinoic acid. *Nature*. (1987) 330:624–9. doi: 10.1038/330624a0

78. Petkovich M, Brand NJ, Krust A, Chambon P. A human retinoic acid receptor which belongs to the family of nuclear receptors. *Nature*. (1987) 330:444–50. doi: 10.1038/330444a0

79. Na SY, Kang BY, Chung SW, Han SJ, Ma X, Trinchieri G, et al. Retinoids inhibit interleukin-12 production in macrophages through physical associations of retinoid X receptor and NFkappaB. *J Biol Chem*. (1999) 274:7674–80. doi: 10.1074/jbc.274.12.7674

80. Kojok K, El-Kadiry AE-H, Merhi Y. Role of NF-κB in platelet function. *Int J Mol Sci*. (2019) 20:4185. doi: 10.3390/ijms20174185

81. Edmands WMB, Beckonert OP, Stella C, Campbell A, Lake BG, Lindon JC, et al. Identification of human urinary biomarkers of cruciferous vegetable consumption by metabonomic profiling. *J Proteome Res*. (2011) 10:4513–21. doi: 10.1021/pr200326k

82. Clarke JD, Hsu A, Riedl K, Bella D, Schwartz SJ, Stevens JF, et al. Bioavailability and inter-conversion of sulforaphane and erucin in human subjects consuming broccoli sprouts or broccoli supplement in a cross-over study design. *Pharmacol Res*. (2011) 64:456–63. doi: 10.1016/j.phrs.2011.07.005

83. Ross D, Siegel D. NAD(P)H:quinone oxidoreductase 1 (NQO1, DT-diaphorase), functions and pharmacogenetics. *Methods Enzymol*. (2004) 382:115–44. doi: 10.1016/S0076-6879(04)82008-1

84. Kiyohara C, Yoshimasu K, Takayama K, Nakanishi Y. NQO1, MPO, and the risk of lung cancer: a HuGE review. *Genet Med Off J Am Coll Med Genet*. (2005) 7:463–78. doi: 10.1097/01.gim.0000177530.55043.c1

85. Fowke JH, Shu X-O, Dai Q, Shintani A, Conaway CC, Chung F-L, et al. Urinary isothiocyanate excretion, brassica consumption, and gene polymorphisms among women living in Shanghai, China. *Cancer Epidemiol Biomarkers Prev*. (2003) 12:1536–9.

86. Spitz MR, Duphorne CM, Detry MA, Pillow PC, Amos CI, Lei L, et al. Dietary intake of isothiocyanates: evidence of a joint effect with glutathione S-transferase polymorphisms in lung cancer risk. *Cancer Epidemiol. Biomarkers Prev*. (2000) 9:1017–20.

87. Wang LI, Giovannucci EL, Hunter D, Neuberg D, Su L, Christiani DC. Dietary intake of cruciferous vegetables, glutathione S-transferase (GST) polymorphisms and lung cancer risk in a Caucasian population. *Cancer Causes Control*. (2004) 15:977–85. doi: 10.1007/s10552-004-1093-1

88. Shapiro TA, Fahey JW, Wade KL, Stephenson KK, Talalay P. Chemoprotective glucosinolates and isothiocyanates of broccoli sprouts: metabolism and excretion in humans. *Cancer Epidemiol Biomark Prev*. (2001) 10:501–8.

89. Lampe JW. Interindividual differences in response to plant-based diets: implications for cancer risk. *Am J Clin Nutr*. (2009) 89:1553S–7S. doi: 10.3945/ajcn.2009.26736D

90. Ross D, Siegel D. The diverse functionality of NQO1 and its roles in redox control. *Redox Biol*. (2021) 41:101950. doi: 10.1016/j.redox.2021.101950

91. Dinkova-Kostova AT, Talalay P. NAD(P)H:quinone acceptor oxidoreductase 1 (NQO1), a multifunctional antioxidant enzyme and exceptionally versatile cytoprotector. *Arch Biochem Biophys*. (2010) 501:116–23. doi: 10.1016/j.abb.2010.03.019

92. Lushchak VI. Glutathione homeostasis and functions: potential targets for medical interventions. *J Amino Acids*. (2012) 2012:736837. doi: 10.1155/2012/736837

93. O'Kennedy N, Raederstorff D, Duttaroy AK. Fruitflow(®): the first European food safety authority-approved natural cardio-protective functional ingredient. *Eur J Nutr*. (2017) 56:461–82. doi: 10.1007/s00394-016-1265-2

94. European Food Safety Authority. Water-soluble tomato concentrate (WSTC I and II) and platelet aggregation. *EFSA J*. (2009) 7:1101. doi: 10.2903/j.efsa.2009.1101

95. EFSA Panel on Dietetic Products, Nutrition and Allergies (EFSA NDA Panel)Turck D, Bresson J-L, Burlingame B, Dean T, Fairweather-Tait S, et al. Guidance for the scientific requirements for health claims related to antioxidants, oxidative damage and cardiovascular health. *EFSA J*. (2018) 16:e05136. doi: 10.2903/j.efsa.2018.5136

96. Cattaneo M, Cerletti C, Harrison P, Hayward CPM, Kenny D, Nugent D, et al. Recommendations for the standardization of light transmission aggregometry: a consensus of the working party from the platelet physiology subcommittee of SSC/ISTH. *J Thromb Haemost*. (2013) 11:1183–9. doi: 10.1111/jth.12231

97. Michelson AD. Platelet function testing in cardiovascular diseases. *Circulation*. (2004) 110:e489–93. doi: 10.1161/01.CIR.0000147228.29325.F9

98. Harrison P. Progress in the assessment of platelet function. *Br J Haematol*. (2000) 111:733–44. doi: 10.1111/j.1365-2141.2000.02269.x

99. Nicholson NS, Panzer-Knodle SG, Haas NF, Taite BB, Szalony JA, Page JD, et al. Assessment of platelet function assays. *Am Heart J*. (1998) 135:S170–8. doi: 10.1016/s0002-8703(98)70245-5

100. Gum PA, Kottke-Marchant K, Welsh PA, White J, Topol EJ. A prospective, blinded determination of the natural history of aspirin resistance among stable patients with cardiovascular disease. *J Am Coll Cardiol*. (2003) 41:961–5. doi: 10.1016/s0735-1097(02)03014-0

101. The European Commission Commission Regulation (EU) No 432/2012. *Off J Eur Union*. (2012) 13:281–320.

frontiers | Frontiers in Nutrition

TYPE Original Research
PUBLISHED 08 January 2024
DOI 10.3389/fnut.2023.1294057

OPEN ACCESS

EDITED BY
Paul Licciardi,
Royal Children's Hospital, Australia

REVIEWED BY
Kiran Veer Sandhu,
University College Cork, Ireland
Milton Prabu,
Annamalai University, India
Phiwayinkosi V. Dludla,
South African Medical Research Council, South Africa

*CORRESPONDENCE
Jianjun Ou
✉ oujianjun@csu.edu.cn
Xiaojie Zhang
✉ xiaojiezhang2014@csu.edu.cn

†These authors have contributed equally to this work

RECEIVED 14 September 2023
ACCEPTED 11 December 2023
PUBLISHED 08 January 2024

CITATION
Yang J, He L, Dai S, Zheng H, Cui X, Ou J and Zhang X (2024) Therapeutic efficacy of sulforaphane in autism spectrum disorders and its association with gut microbiota: animal model and human longitudinal studies. *Front. Nutr.* 10:1294057. doi: 10.3389/fnut.2023.1294057

Therapeutic efficacy of sulforaphane in autism spectrum disorders and its association with gut microbiota: animal model and human longitudinal studies

Jiexian Yang†, Li He†, Si Dai, Huihui Zheng, Xilong Cui, Jianjun Ou* and Xiaojie Zhang*

Department of Psychiatry, National Clinical Research Center for Mental Disorders, and National Center for Mental Disorders, The Second Xiangya Hospital of Central South University, Changsha, Hunan, China

Introduction: Sulforaphane (SFN) has been found to alleviate complications linked with several diseases by regulating gut microbiota (GM), while the effect of GM on SFN for autism spectrum disorders (ASD) has not been studied. Therefore, this study aimed to investigate the relationship between the effects of SFN on childhood ASD and GM through animal model and human studies.

Methods: We evaluated the therapeutic effects of SFN on maternal immune activation (MIA) induced ASD-like rat model and pediatric autism patients using three-chamber social test and OSU Autism Rating Scale-DSM-IV (OARS-4), respectively, with parallel GM analysis using 16SrRNA sequencing.

Results: SFN significantly improved the sniffing times of ASD-like rats in the three-chamber test. For human participants, the average verbal or non-verbal communication (OSU-CO) scores of SFN group had changed significantly at the 12-wk endpoint. SFN was safe and no serious side effects after taking. GM changes were similar for both ASD-like rats and ASD patients, such as consistent changes in order *Bacillales*, family *Staphylococcaceae* and genus *Staphylococcus*. Although the gut microbiota composition was significantly altered in SFN-treated ASD-like rats, the alteration of GM was not evident in ASD patients after 12 weeks of SFN treatment. However, in the network analysis, we found 25 taxa correlated with rats' social behavior, 8 of which were associated with SFN treatment in ASD-like rats, For ASD patients, we found 35 GM abundance alterations correlated with improvements in ASD symptoms after SFN treatment. Moreover, family *Pasteurellaceae* and genus *Haemophilus* were found to be associated with SFN administration in the network analyses in both ASD-like rats and ASD patients.

Discussion: These findings suggest that SFN could provide a novel avenue for preventing and treating ASD, and its therapeutic effects might be related to gut microbiota.

KEYWORDS

sulforaphane, autism spectrum disorders, gut microbiota, animal model, clinical study

1 Introduction

Autism spectrum disorder (ASD) is a neurodevelopmental disorder characterized by verbal or non-verbal expression difficulties, social difficulties, abnormal narrow interests, and continuous repetitive movements. According to the Autism and Developmental Disabilities Monitoring Network, the prevalence of ASD was 2.3% among children aged

8 years in the US, with boys affected more frequently than girls, 3.7% (95% CI, 3.5–3.8) in boys and 0.9% (95% CI, 0.8–0.9) in girls (1). Currently, no medications have demonstrated efficacy for the core diagnostic symptoms of ASD (2), and behavioral interventions remain the primary means of treatment. Therefore, there is an urgent need to develop and research therapies that target core symptoms.

SFN, derived from broccoli, has gained attention for its health benefits, including its potential in treating cancer and cardiovascular disease (3). Recently, clinical studies have shown improvements in ASD patients treated with SFN. In a double-blind randomized trial with young men (aged 13–27) with ASD, SFN treatment led to significant behavioral improvements, with a 34% decline in Aberrant Behavior Checklist scores and a 17% decline in Social Responsiveness Scale scores (4). Similar positive effects were observed in children and young adults (aged 3–12) using a broccoli seed extract (5) and a randomized clinical trial ($N = 108$) in China (6). However, a study of children aged 3–7 with ASD showed inconsistent results, with no significant clinical improvement (7). Basic research studies about the mechanism of SFN in treating ASD were focused on redox metabolism (8), oxidative stress (9), mitochondrial dysfunction (10), immune dysregulation, neuroinflammation (11, 12), febrile illness (13), heat shock response (14), and synaptic dysfunction (15, 16). However, the exact therapeutic mechanism is still unclear.

Evidence suggested a bilateral influence between ASD and the gut microbiome (17). Individuals with ASD exhibit distinct gut bacterial communities, with a higher abundance of *Bacteroides*, *Parabacteroides*, *Clostridium*, *Faecalibacterium*, and *Phascolarctobacterium* and a lower abundance of *Coprococcus* and *Bifidobacterium*. (18). Some of them (*Bacteroides*, *Parabacteroides, Coprococcus,* and *Bifidobacterium*) have consistent changes in rat models of ASD (19–22). Furthermore, a recent study showed that autism-like behavior can be transferred to germ-free mice by transplanting fecal microbes from children with ASD (23). Additionally, interventions targeting the gut microbiome have shown promise in alleviating ASD symptoms. For example, oral vancomycin resulted in short-term benefits in a small group of children with ASD (24), and microbiota transfer therapy (MTT) altered the gut microbiome and improved GI and behavioral symptoms in children with ASD (25). Rat models of ASD have also demonstrated that *Bacteroides fragilis* (26) and *Lactobacillus reuteri* (27) could modulate gut microbiota and improve ASD-associated behaviors. All of this evidence suggests that gut microbes might play an important role in modulating brain function and behavior of ASD. Moreover, SFN has been shown to alleviate complications linked with several diseases in animal studies by modulating the gut microbiome. For example, SFN treatment increased the abundance of gut microbiome, such as *Butyricicoccus* in a mouse model of ulcerative colitis (28, 29), normalized dysbacteriosis bacteria in a bladder cancer mice model (30), and altered the relative abundance of disease-associated microbial species in a hyperuricemia rat model, particularly by increasing the abundance of *Saccharomyces*, Lactobacillaceae, and Clostridiaceae and decreasing the abundances of *Bacteroides*, *Parasutterella*, and *Alistipes* (31). SFN also reduced body weight, liver inflammation, and hepatic steatosis in high-fat diet mice by modulating the gut microbiota (32). These studies indicated the impact of SFN on the gut microbiome, but no studies have yet explored whether SFN can alleviate ASD symptoms by regulating the gut microbiome.

To investigate the therapeutic effect of SFN treatment on childhood ASD and its potential relationship with GM, we constructed a younger age ASD animal model using MIA-induced ASD-like rat model, evaluated the therapeutic effect of SFN, and investigated the potential role of GM by three-chamber social test and 16S rRNA sequencing, respectively. Meanwhile, we also conducted a longitudinal study to investigate the therapeutic effects of SFN on childhood ASD by recruiting patients aged 4–7 years with ASD and to explore the potential relationship between the therapeutic effects of SFN and GM. In summary, this study aims to reveal the role of SFN in the treatment of ASD in children and its potential relationship with GM through both clinical and animal studies and to provide new insights into the treatment and pathogenesis of ASD.

2 Materials and methods

2.1 Animal and ASD-like rat model

Sprague–Dawley rats were purchased from Hunan Silaike Jingda Laboratory Animal, China. Animals were housed in groups of five per cage under a regular 12-h light/dark cycle and with access to food and water *ad libitum*. The rats were fed by the same type of food and lived in the same environment. The maternal immune activation (MIA)-induced ASD-like rat model was employed as previously described (33, 34). Adult pregnant female Sprague-Dawley rats were randomly divided into two groups and were intraperitoneal injected with lipopolysaccharide (LPS; 200 μg/kg) in saline or saline vehicle (veh, 0.9% NaCl) on gestational days 12 and 15, respectively. On postnatal day 25, the newborn male rats were separated and on day 40 were subjected to the three-chamber test to confirm autistic-like features (LPS modeled group: $n = 38$; saline group: $n = 10$). Then, the LPS modeled group and the saline group were divided into two subgroups, which were intraperitoneal injected with SFN 20 ug/kg or vehicle control, respectively, for another 28 days: LPS modeled group treated by SFN (LPS-SFN): $n = 19$; LPS modeled group treated by saline (LPS-NS): $n = 19$; saline group treated by SFN (NS-SFN): $n = 5$; saline group treated by saline (NS-NS): $n = 5$. After the treatment, all four groups of rats were subjected to the three-chamber test. The Animal Users Care and Use Committee of Central South University approved our experimental protocol, and the ethics approval number is 20200006.

2.2 Three-chamber test

The three-chamber apparatus used in the experiment consisted of a non-transparent plexiglass box with two transparent partitions creating left, center, and right chambers (40 × 60 cm). Each partition had a square opening (10 × 10 cm) in the bottom center. A wire cage (18 cm diameter) was used as an inanimate object or to house a stranger rat, with a water-filled bottle placed on top to prevent the test rat from climbing. The unit and wire cups were cleaned with 70% ethanol between each trial. In the first

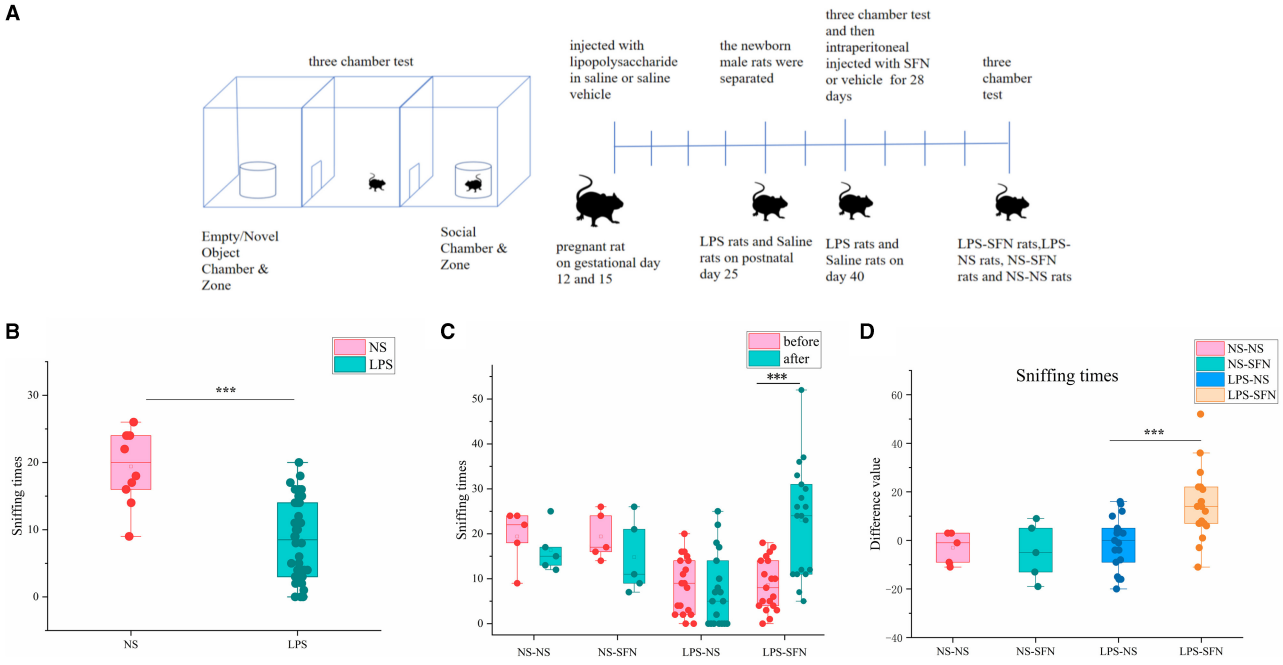

FIGURE 1
Behavioral assessment of MIA-induced ASD-like rat model before and after SFN treatment. **(A)** Flow diagram of experiment. **(B)** Sniffing time of MIA-induced ASD-like rats (LPS) vs. control rats (NS) in the three-chamber test before SFN or saline treatment. **(C)** The sniffing times of different groups of rats in the three-chamber test (before or after the administration of saline or SFN). **(D)** Difference value in sniffing times after-before the administration of saline or SFN (***$p < 0.001$, paired Students' *t*-test or unpaired Students' *t*-test). Difference value: rats' sniffing times after the administration of saline or SFN were subtracted from the same rat's sniffing times before the administration.

10-min session, the test rat explored the empty chambers. In the second 10-min session, a stranger rat was placed in one of the wire cages, and in the last 10-min session, a second stranger rat was placed in the other wire cage (Figure 1A). The movement of the rat was recorded by a USB webcam (LifeCam HD-6000, Microsoft) and PC-based video capture software (WinAVI Video Capture, ZJ Media Digital Technology). The recorded video file was further analyzed by offline video tracking software (EthoVision XT 7.0). The sniffing times to each wire cage were measured. We performed two three-chamber tests on rats, the first at 40 days postnatal and the second at 68 days postnatal, when rats were administered SFN or saline for 28 consecutive days.

2.3 Clinical trial design

The data and stool samples of ASD patients were obtained from previous clinical trials (6), and healthy controls were recruited by age-matched. Eleven healthy controls and six individuals with ASD were recruited by the Department of Psychiatry, Second Xiangya Hospital, which is affiliated with Central South University in Changsha, Hunan Province of China. There were no significant differences in age between the healthy control and ASD patients. All the recruited subjects were boys. In the present study, we included 4- to 7-year-old children with ASD diagnosed based on the following criteria: (1) 4- to 7-year-old only; (2) met Diagnostic and Statistical Manual of Mental Disorders, Fifth Edition (DSM-V) diagnostic criteria for ASD; (3) re-confirmed using Autism Diagnostic Interview-Revised (ADI-R) and Autism Diagnostic Observation Schedule (ADOS). The exclusion criteria were as follows: (1) severe physical diseases (i.e., thyroid disease and congenital heart disease); (2) known history of ASD-associating genetic syndromes (i.e., Fragile-X syndrome and Down's syndrome); (3) severe brain diseases (i.e., epilepsy and brain trauma); (4) absence of neurodevelopmental disorders and other psychiatric disorders as assessed by a child psychiatrist.

After screening, participants with ASD were treated by SFN for 12 weeks. We obtained fecal samples of both the healthy control group and the ASD group at baseline (ASD-Baseline) and the ASD group on the last day of week 12 (ASD-SFN). Guardians of all participants received information about the protocol and provided an informed consent form before enrollment. The study was approved by the ethics committee of Second Xiangya Hospital and was registered at ClinicalTrials.gov (NCT02879110).

2.4 Medication intervention, safety measures, and behavioral outcome measures

SFN was delivered as Avmacol® (Nutramax Laboratories, Inc., Edgewood, Maryland, USA) tablets which contain both glucoraphanin and active myrosinase enzyme and are formulated to support sulforaphane production from ≥30 μmol of glucoraphanin per tablet. Tablets were maintained at room temperature and checked periodically microbiologically. The dose

of SFN was based on weight. SFN was safe and no serious side effects after taking. Changes in the OSU Autism Rating Scale-DSM-IV (OARS-4) were the priority primary outcome measurement. OARS-4 consists of three domains, namely, social interaction (OSU-SO), verbal or non-verbal communication (OSU-CO), and repetitive or ritualistic behaviors (OSU-ST), and their average scores stand for the total behavioral outcome (OSU-total). The score of the ASD group was assessed at baseline and on the last day of week 12. Refer to our previous clinical studies for specific SFN usage, safety measures, and OARS-4 measures (6).

2.5 Fecal sample collection

Fecal samples from rats were collected uniformly after the three-chamber test was done, while fecal samples from clinical participants were collected before (baseline) and after 12 weeks of SFN treatment. All fecal samples were collected into sterile tubes and rapidly frozen with liquid nitrogen. It is stored in a refrigerator at −80°C until use.

2.6 DNA extraction, PCR amplification, and 16S rRNA gene sequencing

DNA was extracted from stool samples using the E.Z.N.A® DNA kit (Omega Bio-Tek, USA). The V3–V4 regions of the bacteria 16S rRNA gene were amplified by polymerase chain reaction (PCR) (98°C for 5 min, followed by 25 cycles consisting of denaturation at 98°C for 30 s, annealing at 53°C for 30 s, and extension at 72°C for 45 s, and a final extension at 72°C for 5 min). PCR amplicons were purified using Vazyme VAHTSTM DN A Clean Beads (Vazyme, N Nanjing, China China), quantified using the Quant-iT PicoGreen dsDNA Assay Kit (Invitrogen, Carlsbad, CA, USA), and sequenced using the Illumina MiSeq platform with MiSeq Reagent Kit v3 at Shanghai Personal Biotechnology Co., Ltd (Shanghai, China). Purified amplicons were pooled at equimolar concentrations and sequenced (2 × 300) on the MiSeq platform (San Diego, USA) according to the standard protocol of Mariobio Biomedical Technologies (Shanghai, China).

2.7 Processing of sequencing data

Quality filtering at QIIME (version 1.9.1) was followed by first demultiplexing, using the previously used set of validation criteria: (i) Quality fraction checks were performed with 300 bp reads at any site to obtain an average quality fraction <20 over a 50 bp sliding window; truncated reads <50 bp were discarded. (ii) Removal of exact barcode matches, two nucleotide mismatches in primer matches, and reads containing ambiguous characters. (iii) Sequence assembly, where only sequences with overlap lengths >10 bp are assembled based on the overlapping sequences. Reads that cannot be assembled will be discarded.

Operational taxonomic units (OTUs) were clustered using UPARSE (version 7.1) with a 97% cutoff threshold, 19 sequences were identified, and chimeric sequences were removed using UCHIME.20. For each 16S rRNA gene sequence, the SILVA (SSU123) 16S rRNA database was analyzed for classification using the RDP classifier21 with a 70% confidence threshold.

To improve downstream statistical analysis, we removed low-quality or uninformative features by low count filter and low variance filter. The cutoff threshold of low count filter was set at 10% prevalence filter which means at least 10% of its values should contain at least two counts and the low variance filter was measured by inter-quartile range (IQR).

2.8 Network analysis

Network analysis for the GM and sniffing times and SFN treatment or clinical ASD symptoms was performed using Spearman's rank correlations conducted by IBM SPSS Statistics 27.0.1 and network reconstruction and property measurements conducted by Gephi 0.9.7. We first computed the correlation between each node, and only statistically significant Spearman's rank correlations ($p < 0.05$) were defined as an edge of two nodes. We next constructed undirected network graphs to display the potential relationship between GM and social features in MIA-induced ASD-like rat models or ASD patients using Gephi 0.9.7.

2.9 Statistical analysis

Richness (ACE and Chao1) and diversity (Shannon and Simpson) were used to assess the α-diversity indexes. Principal coordinate analysis (PCoA) of weighted and unweighted UniFrac22 was used to visualize the clustering patterns between samples based on β-diversity distances via R language. ANOSIM test was performed to identify differences in β-diversity among groups. Identification of key gut microbiota responsible for the differentiation between taxa using the effective size of linear discriminant analysis (LDA), only LDA > 1.5 at a $p < 0.05$ were considered significantly enriched. Multiple group comparisons were performed using one-way analysis of variance (ANOVA) followed by LSD as a *post-hoc* test and two-tailed Student's *t*-test or Mann–Whitney *U*-test to determine the difference between the two groups. All correlations were calculated using Spearman's correlation. Statistical analyses were conducted using the software SPSS, R package, and plots were generated from R and GraphPad Prism version 8.0. A *p*-value of 0.05 is significant for the test above. All data were analyzed using two-way ANOVA with Bonferroni's *post-hoc* analysis and one-way ANOVA with Tukey's *post-hoc* analysis.

3 Results

3.1 SFN treatment rescued the social deficits of MIA-induced ASD-like rat model

We first employed the MIA-induced ASD-like rat model and validated it by a three-chamber test. In the third 10-min

test of the three-chamber test, sniffing times for novel rats in the LPS group were significantly less than that in the NS group (Figure 1B, p <0.001). The results showed that rats in the LPS group demonstrated social deficits, indicating the successful establishment of our MIA-induced ASD-like rat model. Then, the LPS group and the saline group were subgroup into two groups and treated by SFN or saline, respectively. SFN treatment markedly rescued the reduced-sniffing times (Figure 1C; $p < 0.001$) of the LPS modeled group toward the novel rats, suggesting the rescued impaired social ability of SFN treatment. Comparing the difference value in Sniffing times before and after saline administration in the LPS-NS group, the difference value in Sniffing times before and after the administration of SFN was higher in the LPS-SFN group. It suggested that SFN treatment significantly increased the Sniffing times in MIA-induced ASD-like rats (Figure 1D, $p < 0.001$). These results indicated that our LPS modeling was successful and that SFN could reverse the socially deficient behavior of LPS rats.

3.2 Diversity of gut microbiota significantly altered in ASD-like rat model

We used 16S rRNA sequencing to evaluate alpha and beta diversity to determine differences in gut microbiota diversity. The alpha diversity was based on the numbers of observed OTUs, richness (ACE and Chao1), and diversity (Shannon and Simpson) (Figure 2). Observed OTU, ACE, and Chao1 indicated less microbiota alpha diversity in the LPS-NS group compared to the NS-NS group ($p = 0.02$, $p = 0.03$, and $p = 0.03$, respectively, Figure 2), but SFN treatment did not increase in alpha diversity in LPS rats. To evaluate the β-diversity of gut microbiota across different groups, principal coordinate analysis (PCoA) based on the unweighted UniFrac distance matrixes was conducted. Beta diversity assessed by the ANOSIM tests found the four groups could not cluster into distinct groups.

3.3 Changes of gut microbiota taxonomic composition in ASD-like rats and after SFN treatment

We next investigated the dynamic changes of microbial composition in groups. At the phylum level, all groups showed a similar taxonomic composition, i.e., dominated by the phylum Firmicutes and Bacteroidetes, while the LPS-NS group had an increase in the mean Firmicutes/Bacteroidetes ratio (6.01 vs. 4.98) and a decrease in the abundance of Bacteroidetes compared to the NS-NS group. In the LPS-NS group, the abundance of Actinobacteria declined and SFN treatment ameliorated the reduction of Bacteroidetes and Actinobacteria (Figure 3A). Taxonomic compositions at the genus level were analyzed in the four groups (Figure 3B). The relative abundance of genus *Ruminococcaceae_UCG_005* enriched in the LPS-NS rats compared to the NS-NS rats. The relative abundance of genus *Lactobacillus* enriched in the LPS-SFN group (Figure 3B).

The LEfSe analysis, a method for identifying bacterial taxa as biomarkers using LDA with effect size measurements, was used to explore the significant differences at distinct microbial levels. The Fusobacteria (from the phylum to the genus *Fusobacterium*), Corynebacteriales (from the class to the genus *Corynebacterium 1*), Leptotrichiaceae (the family and the genus *Leptotrichia*), Neisseriaceae (the family and the genus *Neisseria*), Pasteurellales (the order and the family *Pasteurellaceae*), order Betaproteobacteriales, and genus *Haemophilus* enriched in NS-NS rats. Genus *Allobaculum*, *Anaerotruncus,* uncultured of Family_XIII, and unclassified_Micrococcaceaewere enriched in the NS-SFN group. Family uncultured and genus uncultured of order Coriobacteriales enriched in the LPS-NS group. Genus *Prevotella* displayed a relative enrichment in the LPS-SFN group ($p < 0.05$, Figures 3C, D).

To obtain deeper insight into microbiota alterations upon LPS or SFN administration, we analyze specific taxa in four groups by Venn diagram. As was shown in Figure 3E, three taxa were common in "LPS-NS vs. NS-NS" (Figure S1) and "LPS-NS vs. LPS-SFN" (Figure S1): phylum Fusobacteria, order Fusobacteriales, and class Fusobacteriia. Moreover, genus *Anaerotruncus* was common in "LPS-NS vs. NS-NS," "LPS-NS vs. LPS-SFN," and "NS-NS vs. NS-SFN" (Figure S1). These data suggested that SFN may exert a therapeutic effect by altering the abundance of some specific taxa.

3.4 Network analysis shows associations between GM and rats' social behavior

Figure 4 shows the network analysis in the MIA-induced ASD-like rat model, and it showed associations between GM and rats' social behavior or SFN treatment. At the genus level, the relative abundance of *Alloprevotella* ($r = 0.335$, $p = 0.04$), *Prevotella* ($r = 0.333$, $p = 0.041$), *Prevotellaceae_UCG-001* ($r = 0.387$, $p = 0.016$), *Peptostreptococcus* ($r = 0.346$, $p = 0.033$), *Cupriavidus* ($r = 0.421$, $p = 0.009$), *uncultured* ($r = 0.422$, $p = 0.08$), and *Oribacterium* ($r = 0.333$, $p = 0.041$) was positively correlated with sniffing times, while the relative abundance of *Corynebacterium* ($r = -0.359$, $p = 0.027$), *Sporosarcina* ($r = -0.322$, $p = 0.049$), *unclassified_Staphylococcaceae* ($r = -0.334$, $p = 0.04$), *Clostridium_sensu_stricto_1* ($r = -0.375$, $p = 0.02$), *Neisseria* ($r = -0.379$, $p = 0.019$), *unclassified_Enterobacteriaceae* ($r = -0.435$, $p = 0.006$), *Haemophilus* ($r = -0.421$, $p = 0.009$), *Moraxella* ($r = -0.333$, $p = 0.041$), and *Sphingomonas* ($r = -0.415$, $p = 0.001$) was negatively correlated with sniffing times. In addition, of the taxa which had a correlation with sniffing times, we found that the genus *Prevotella* ($r = 0.468$, $p = 0.003$), genus *Peptostreptococcus* ($r = 0.366$, $p = 0.024$), and genus *Oribacterium* ($r = 0.431$, $p = 0.007$) were positively correlated with SFN treatment, while order Pasteurellales ($r = -0.452$, $p = 0.004$), family Sphingomonadaceae ($r = -0.388$, $p = 0.016$), family Pasteurellaceae ($r = -0.452$, $p = 0.004$), *genus unclassified_Enterobacteriaceae* ($r = -0.342$, $p = 0.035$), and *genus Haemophilus* ($r = -0.501$, $p = 0.001$) were negatively correlated with SFN treatment. In addition, of the taxa associated with SFN treatment, we found order Pasteurellales, family Pasteurellaceae, and *genus Haemophilus* enriched in the NS-NS group and *genus Prevotella* enriched in the LPS-SFN group.

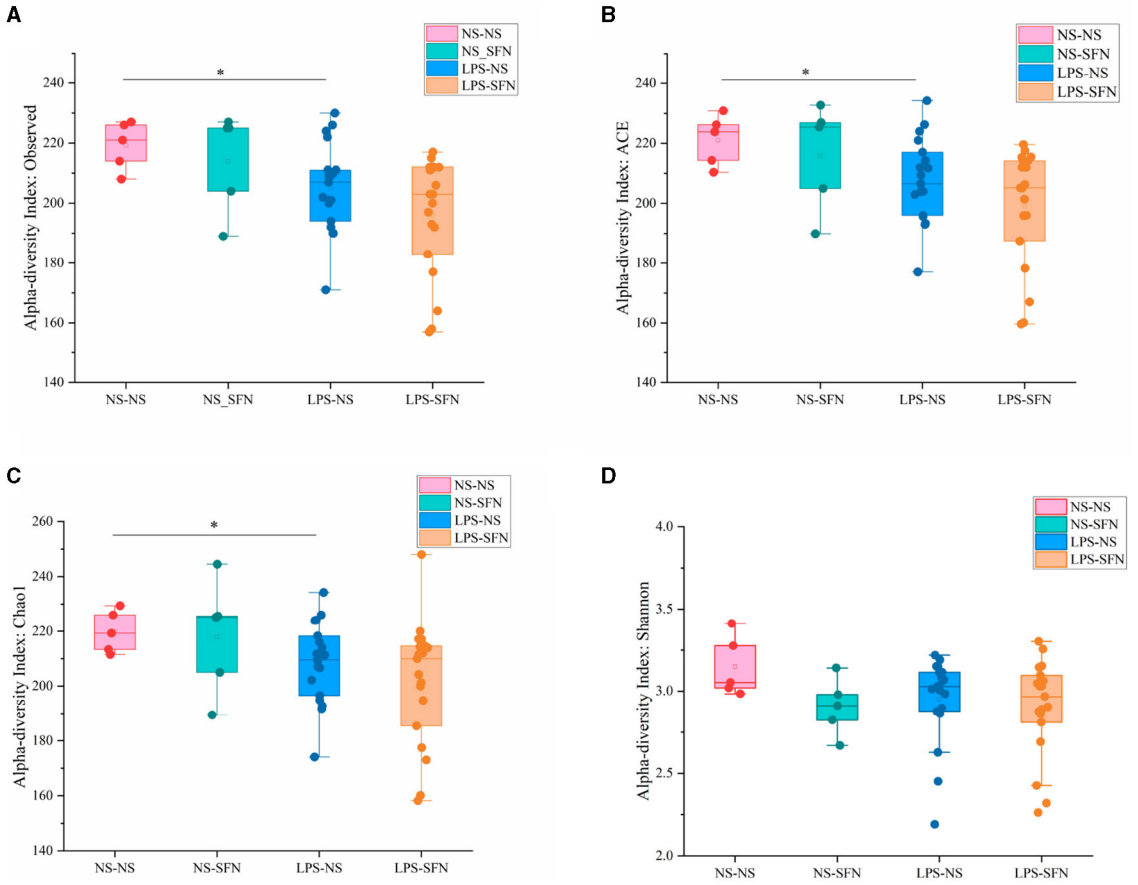

FIGURE 2
Diversity analysis of MIA-induced ASD-like rat model with or without SFN treatment. The observed operational taxonomic units (OTUs) **(A)**, ACE **(B)**, Chao1 **(C)**, and Shannon **(D)** used the Student's *t*-test (*$p < 0.05$).

3.5 Beneficial effect of SFN treatment in ASD patients

We also conducted a 12-week clinical study to explore whether the SFN altered gut microbiome in ASD patients and ameliorated ASD by alteration of gut microbiota. The mean behavioral subscores and total scores and their changes of OSU of the six SFN-treated recipients from enrollment to the 12-week end of treatment are shown in Figure 5. Half of the participants experiencing improvement to SFN and the average OSU-CO scores of the SFN group had changed significantly at the 12-week endpoint (Figure 5B).

3.6 Gut microbial diversity altered in ASD patients

The methods for assessing alpha and beta diversity were consistent with the animal part of this study. Figure 6 shows the alpha and beta diversity in ASD patients. In this study, gut microbial diversity estimated by the Shannon index, was greater in health controls (HCs) compared to untreated ASD patients ($p = 0.03$, Figure 6C). Beta diversity of ASD patients and HCs estimated by PCoA with weighted UniFrac showed that axis 1 accounted for 48.3% of the variation and axis 2 explained 25% of the variation. The fecal microbiota in untreated ASD and HCs could cluster separately ($p = 0.002$, Figure 6D). However, no diversity changes were associated with SFN treatment, which was estimated by paired Students' *t*-test between the ASD-Baseline group and the ASD-SFN group.

3.7 Changes of gut microbiota taxonomic composition in ASD patients

The analysis of the gut microbiota composition at the phylum and genus levels showed specific differences in groups (Figures 7A, B). In terms of bacterial composition at the phylum level, untreated ASD patients had an increase in the mean Firmicutes/Bacteroidetes ratio (3.02 vs. 1.25) and a decrease in the abundance of Bacteroidetes compared to the HCs. The phylum *Bacteroidetes* was higher in HCs, while Actinobacteria enriched in ASD patients (Figure 7A). In terms of the genus level, all groups exhibited similar taxonomic

10.3389/fnut.2023.1294057

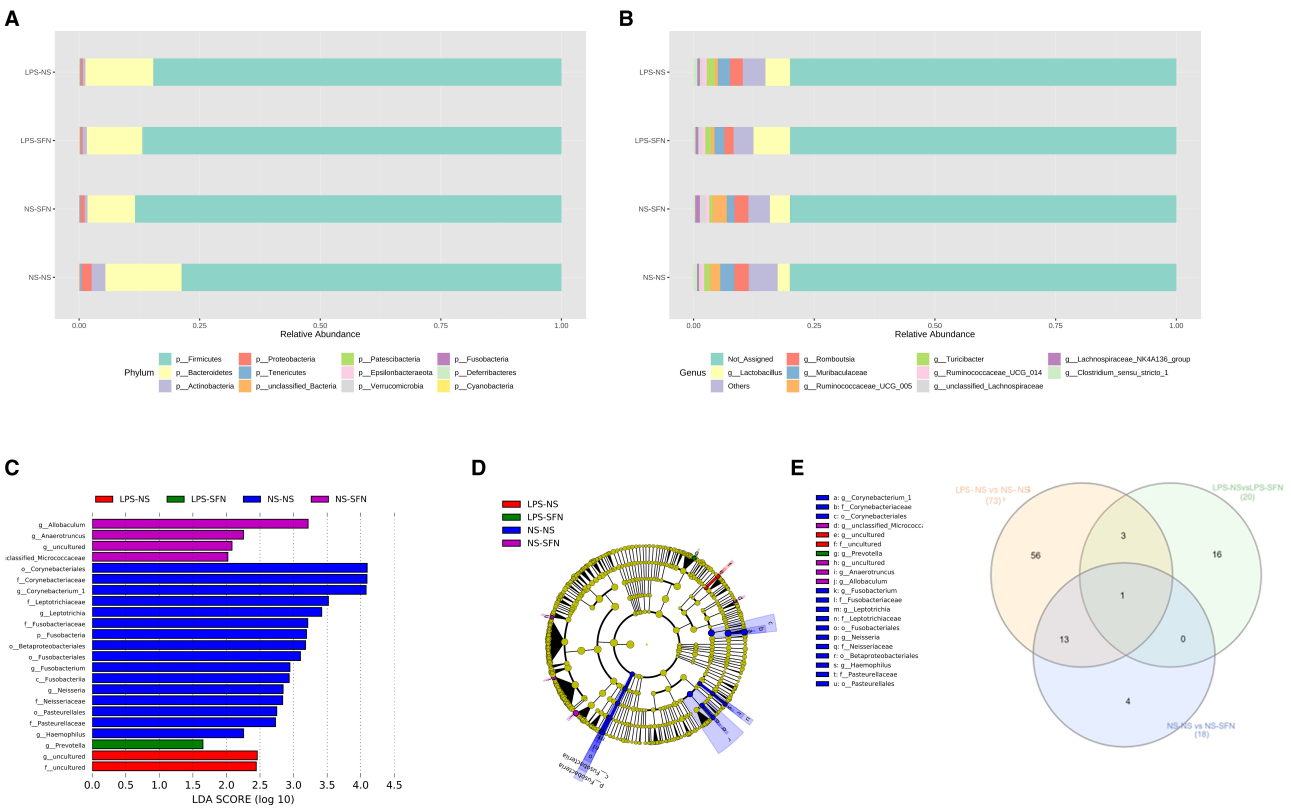

FIGURE 3
Relative abundance of differential taxa ASD-like rats and after SFN treatment. **(A)** Bar plots of the phylum taxonomic levels and genus taxonomic levels **(B)** among four groups (only the top 10 phylum bacteria are shown). **(C)** Histogram and cladogram **(D)** of the linear discriminant analysis (LDA) scores revealed distinct taxa in the gut microbiota among four groups. **(E)** Venn diagram showing the distribution of the OTUs among intergroup comparison.

communities, i.e., dominated by the genus *Faecalibacterium* and *Bacteroides*. The relative abundance of genus *Bacteroides* was significantly higher in the HCs compared to the ASD groups, while *Bifidobacterium* enriched in the ASD groups (Figure 7B).

The LEfSe analysis was used to explore the significant differences at distinct microbial levels among groups. We found that some gut microbiota had significant differences (Figures 7C, D). The Bacteroidetes (from the phylum to the genus *Bacteroides*), Prevotellaceae (the family and the genus *Prevotella*), Corynebacteriaceae (the family and the genus *Corynebacterium*), order Bacillales, and family Tissierellaceae enriched in HC group. The Erysipelotrichia (from the class to the family *Erysipelotrichaceae*), Coriobacteriia (from the class to the family *Coriobacteriaceae*), Xanthomonadales (from the order to the genus *unidentified Xanthomonadaceae*), Eubacteriaceae (the family and the genus *Eubacterium*), Peptococcaceae (the family and the genus *unidentified Peptococcaceae*), phylum Actinobacteria, class Gammaproteobacteria, and genus *Clostridium, Bulleidia, unclassified Gemellaceae, Chelativorans, and Bilophila* were found enriched in untreated patients. Bifidobacteriales (from the order to the genus *Bifidobacterium*), Halomonadaceae (the family and the genus *Halomonas*), Streptococcaceae (the family and the genus *Streptococcus*), class Actinobacteria and Bacilli, order Oceanospirillales and Lactobacillales, *and* genus *Dialister, Veillonella,* and *Devosia* enriched in the treated by SFN patients.

3.8 Network analysis of microbiome abundance alterations and improvements in ASD symptoms after SFN treatment

To elucidate the actual relationship between the alteration of the relative abundance of bacterial taxa on each taxonomical level and improvements in autistic symptoms after SFN treatment, we conducted a co-expression network analysis in ASD patients (Figure 8). At the genus level, the alteration of the relative abundance of *Atopobium* ($r = 0.845$, $p = 0.034$) and *unidentified_Xanthomonadaceae* ($r = 0.812$, $p = 0.05$) had a positive correlation with OSU_Change_Total, while *Actinomyces* ($r = -0.845$, $p = 0.034$), *unidentified_Coriobacteriaceae* ($r = -0.928$, $p = 0.008$), *unidentified_Erysipelotrichaceae* ($r = -0.899$, $p = 0.015$), *Chelativorans* ($r = -0.845$, $p = 0.034$), and *Haemophilus* ($r = -0.886$, $p = 0.019$) had a negative correlation with OSU_Change_Total. *unidentified_[Barnesiellaceae]* ($r = 0.857$, $p = 0.029$) *Coprococcus* ($r = 0.928$, $p = 0.008$) and *unidentified_Xanthomonadaceae* ($r = 0.897$, $p = 0.015$)

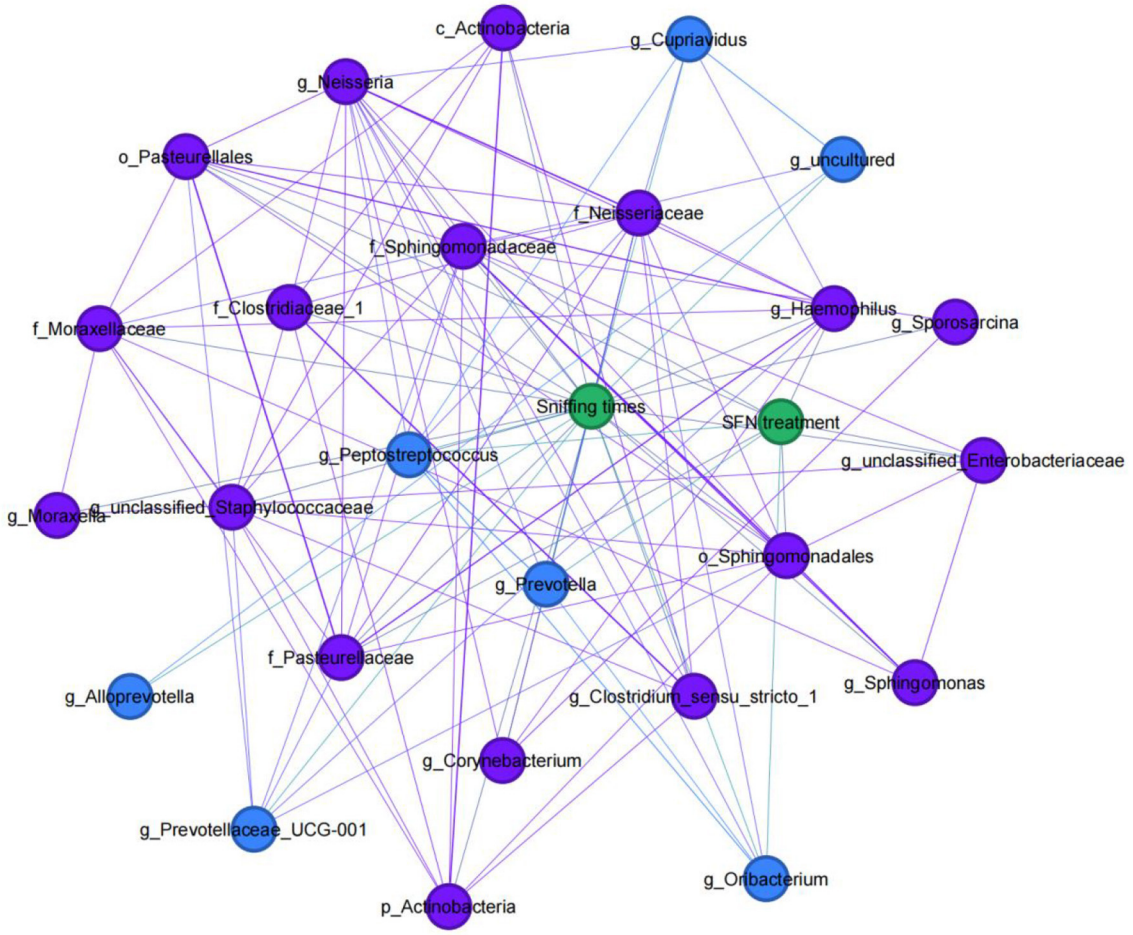

FIGURE 4
Social behavior-microbial network in MIA-induced ASD-like rat model. An undirected network from the microbiota to social behavior or SFN treatment of MIA-induced ASD-like rat model was built. Blue nodes indicate gut microbiota taxa that were positively correlated with sniffing times, and purple nodes indicate taxa that were negatively correlated with sniffing times.

were positively correlated with OSU_Change_SO, while *unidentified_Coriobacteriaceae* ($r = -0.824$, $p = 0.044$) and *unidentified_[Mogibacteriaceae]* ($r = -0.868$, $p = 0.025$) were negatively correlated with OSU_Change_SO. For OSU_Change_CO, *unclassified_Carnobacteriaceae* ($r = 0.876$, $p = 0.022$), and *unidentified_Peptococcaceae* ($r = 0.822$, $p = 0.045$) had a positive correlation with it, while *Devosia* ($r = -0.939$, $p = 0.005$) had a negative correlation with it. In addition, *Turicibacter* ($r = 0.971$, $p = 0.001$), *Oceanicaulis* ($r = 0.857$, $p = 0.029$), and *unclassified_Clostridiales* ($r = 0.841$, $p = 0.036$) were positively correlated with OSU_Change_ST, while *Chelativorans* ($r = -0.823$, $p = 0.044$) was negatively correlated with OSU_Change_ST.

Moreover, of the taxa which had co-association with ASD symptoms, we found phylum Bacteroidetes, class Bacteroidia, and order Bacteroidales were enriched in HC, family Peptococcaceae, family Xanthomonadaceae, genus *Chelativorans*, genus *unidentified_Peptococcaceae,* and genus *unidentified_Xanthomonadaceae* enriched in the ASD-Baseline group, and family Hyphomicrobiaceae and genus *Devosia* enriched in the ASD-SFN group. In addition, the family Pasteurellaceae and *the* genus *Haemophilus* were found in the network analysis in the rat model which was also associated with SFN treatment.

3.9 Commonly altered microbial taxa in both ASD-like rats and ASD patients

We next compared the gut microbiota which had significant differences between ASD-like rats and ASD patients and found three taxa had consistent changes in both "NS-NS vs. LPS-NS" (Figure S1) and "HC vs. ASD-Baseline" (Figure S2). The relative abundance of order Bacillales, family Staphylococcaceae, and genus *Staphylococcus* ($p < 0.0001$, 0.0002, and 0.0002, respectively, for the rats; $p = 0.0076$, 0.004, and 0.004, respectively, for the human) was lower in ASD-like rats and ASD patients (Figure 9). In our study, differences of the relative abundance of these several taxa were overlapped in different species, i.e., rat and human, but no overlap was found between species for SFN treatment-related differential microbiota.

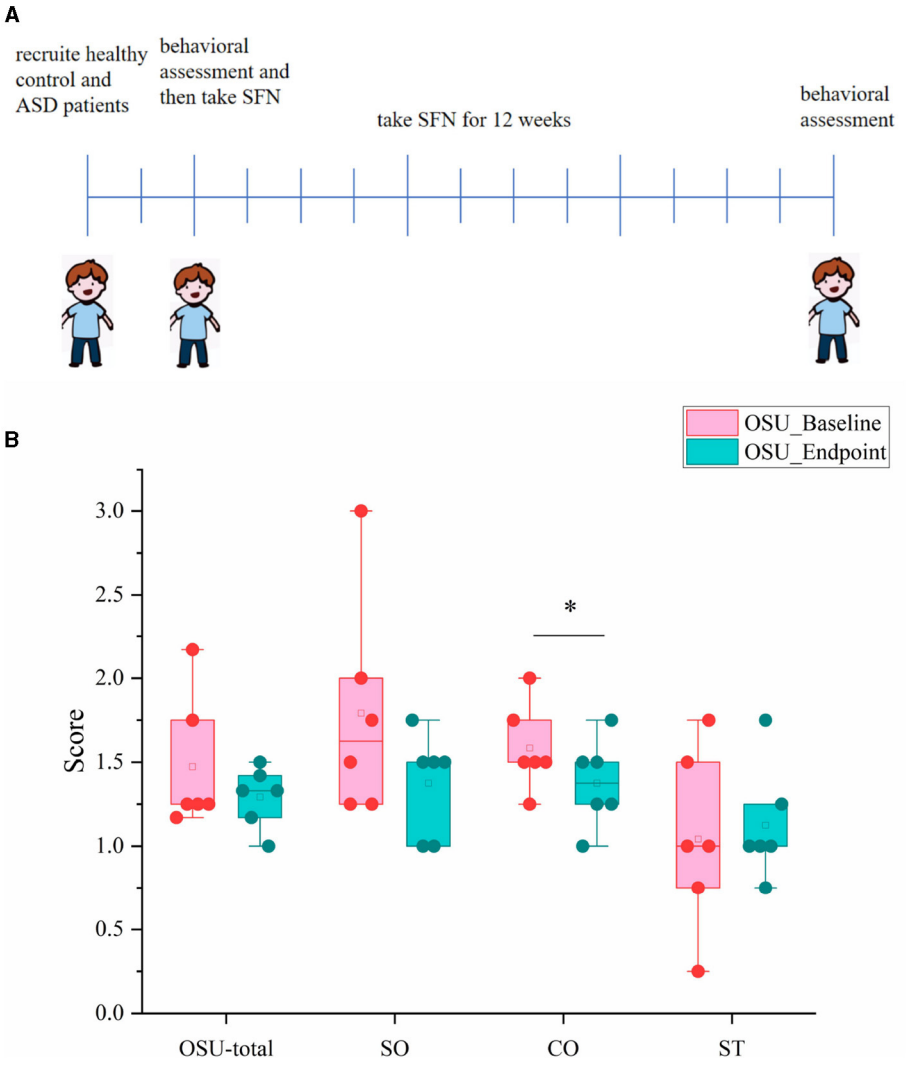

FIGURE 5
OSU scores and subscores of ASD patients at baseline and endpoint. **(A)** Schematic of experimental protocols. **(B)** OSU-total for total OSU behavioral scores, OSU-SO for social interactive OSU behavioral subscores, OSU-CO for non-verbal communicative OSU behavioral subscores, and OSU-ST for repetitive or ritualistic OSU behavioral subscores (*$p < 0.05$, paired Students' *t*-test).

4 Discussion

In the present study, we demonstrated that SFN treatment rescued the social deficits of ASD-like rats and ASD children. Additionally, SFN treatment-induced improvement in social deficits was associated with the relative abundance of gut microbial genera that differed significantly between groups in ASD-like rats. In addition, microbiome abundance alterations of gut microbes were associated with improvements in ASD symptoms of children with ASD after SFN treatment. Our study identified differences in the composition of the gut microbiota of ASD-like rats and ASD patients, which may contribute to autism-related behaviors, and these taxa are associated with improvements in symptoms of autism. These results suggested that the therapeutic effect of SFN may be related to gut microbiota.

We found that SFN treatment rescued the social deficits of MIA-induced ASD-like rats in the three-chambered test. Although current clinical studies suggest a role for SFN in the treatment of ASD, fewer studies have used animal models to explore its specific mechanisms, and only one study that used mice models of autism found the therapeutic effect of SFN (35). Using a MIA-induced ASD-like rat model and three-chamber social tests, we found the improvement effect of SFN on social behavior in ASD, and it may provide new ideas for future experimental animal studies. Furthermore, we explored the therapeutic effects of SFN on autism-related behaviors in children aged 4–7 years with ASD. Given our findings in animal models, we conducted a study with a small clinical sample with the aim of exploring the therapeutic effects of SFN in patients with ASD, focusing on the gut microbiota. Half of the participants had ASD symptom improvement after SFN administration, and there were significant changes in OSU-CO scores at the endpoint of 12 weeks in the SFN group. However, this is only a small sample of our attempts, and larger sample sizes

10.3389/fnut.2023.1294057

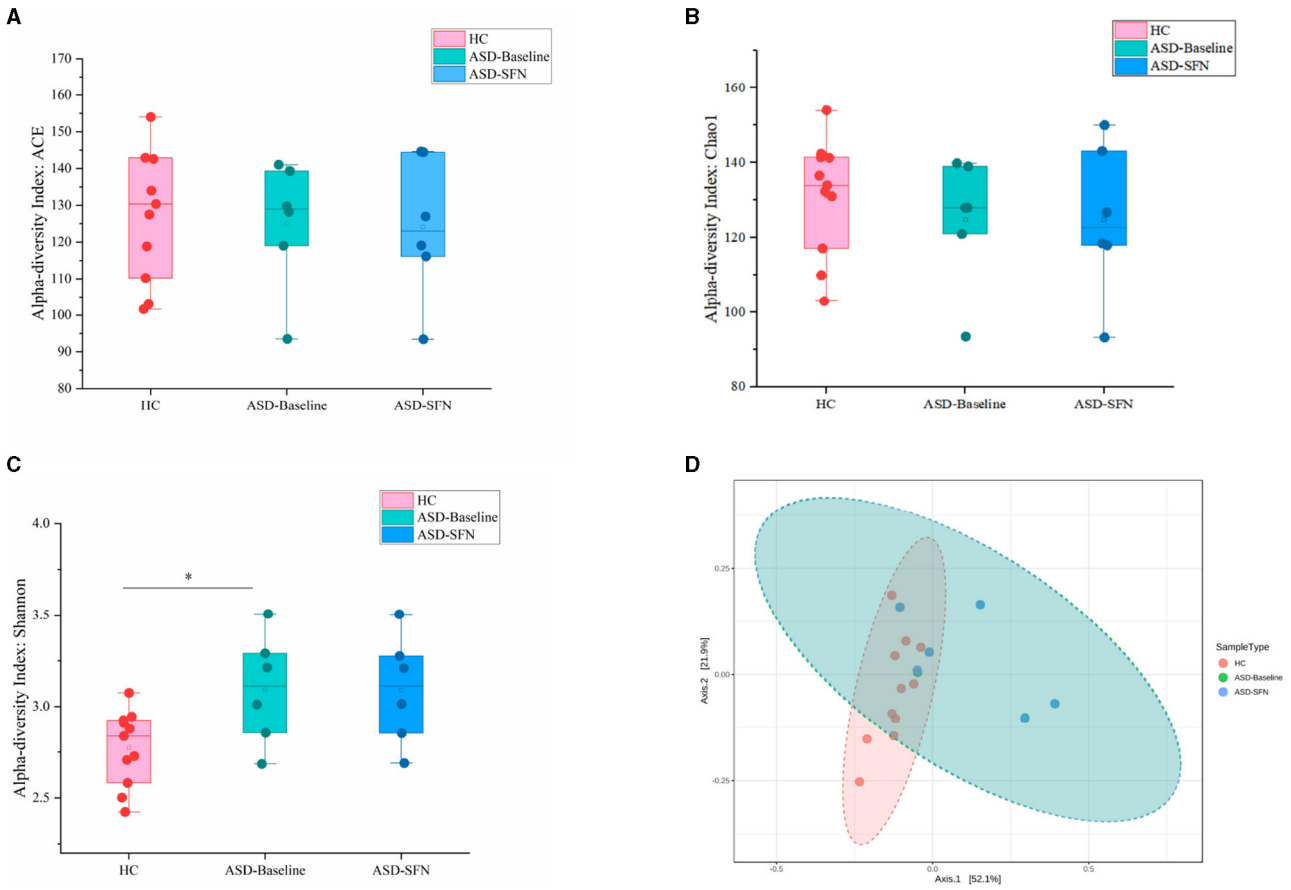

FIGURE 6
Diversity of the gut community altered in ASD patients. The ACE **(A)**, Chao1 **(B)**, and Shannon **(C)** used the Student's *t*-test and principal coordinates analysis (PCoA) of the samples with weighted UniFrac **(D)** (*$p < 0.05$).

will be needed in future to validate the therapeutic effects of SFN on ASD.

We found that the GM diversity of ASD-like rats and ASD patients was significantly different from that of the control group, which is consistent with previous studies (21, 22, 36–38), but we did not find that SFN had a significant effect on the GM diversity of the animals or clinical subjects. In addition, we found order Bacillales, family Staphylococcaceae, and genus *Staphylococcus* showed consistent alteration in both "NS-NS vs. LPS-NS" from the animal model and "HC vs. ASD-Baseline" from clinical samples. Their relative abundance was significantly lower in ASD-like rats and ASD patients and the alteration preserved cross-species, suggesting that these specific taxa may play an important role in the development of ASD and could potentially be biomarkers for identifying ASD. One previous study found a significantly higher abundance level of the genus *Staphylococcus* in the valproic acid rat model of the autism group than the control group, but this increase was observed only in females (39). It was different from our study, and this difference may be caused by gender. However, we did not find an overlap between taxa for SFN treatment-related differential microbiota in animal and human studies. This may be due to differences in the duration of SFN treatment (4 vs. 12 weeks), SFN administration patterns (intraperitoneal injection vs. oral), and the species itself.

Moreover, there were also some differences in the composition of the gut microbial community among ASD-like rats and ASD children. In a rat model, genus *Anaerotruncus* was found enriched in the LPS-NS group compared to the NS-NS group and the LPS-SFN group, but our study in ASD patients did not show an increased relative abundance of *Anaerotruncus*. Interestingly, we found beneficial bacteria, *Bifidobacterium* and *Lactobacillales*, enriched in ASD children treated by SFN. *Bifidobacterium* was found an increased abundance in children treated by microbiota transfer therapy which improved their gastrointestinal and autistic symptoms (40). In addition, the supplementation of *Lactobacillus reuteri*, which belongs to Lactobacillales, could alleviate ASD-like behaviors (27).

Of note, SFN administration caused an increase in the relative abundance of genus *Prevotella* in LPS-SFN rats. Although SFN treatment resulted in a significant increase in the abundance of *Prevotella* in rats, this result was not found in clinical samples, and previous studies have demonstrated that *Prevotella* had a decreased relative abundance in patients with ASD (41–43), as well as in the ASD mice model (44, 45), which was also demonstrated in our clinical samples. In children with ASD, microbiota transfer therapy

10.3389/fnut.2023.1294057

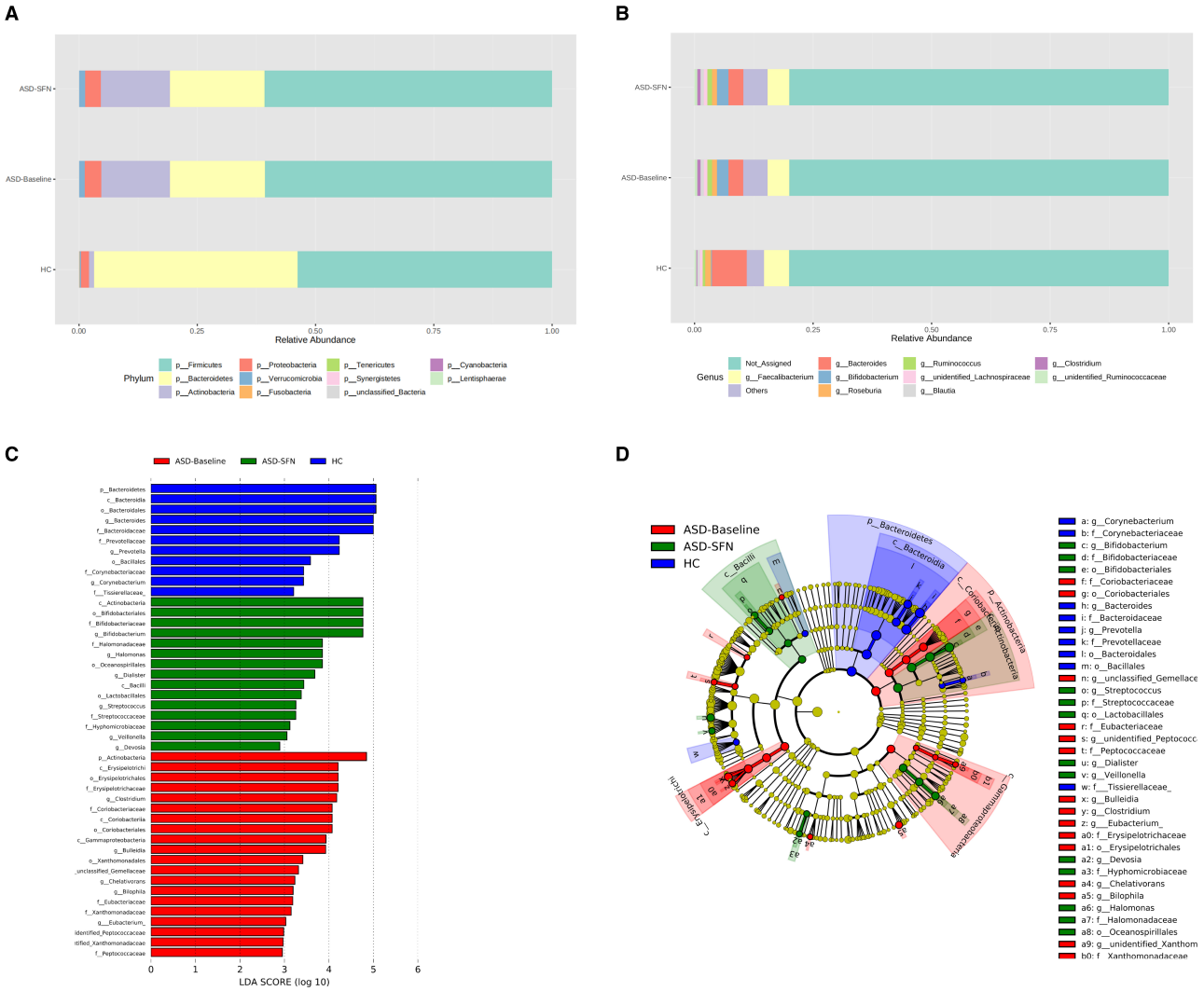

FIGURE 7
Differential taxa abundance in the gut microbiota. **(A)** Bar plots of the phylum taxonomic levels and genus taxonomic levels **(B)** among three groups (only the top 10 phylum bacteria are shown). **(C)** Histogram and cladogram **(D)** of the linear discriminant analysis (LDA) scores revealed distinct taxa in the gut microbiota among three groups.

altered the gut ecosystem, increasing overall bacterial diversity and the abundance of *Bifidobacterium*, *Prevotella*, and *Desulfovibrio* and improving gastrointestinal and autism symptoms (40). In the network analysis, we found a strongly positive association between genus *Prevotella* and the sniffing times of the three-chamber test in rats, suggesting increased *Prevotella* could rescue social deficits. All of these findings suggest that *Prevotella* plays an important role in the development and treatment of ASD.

Of note, family Pasteurellaceae and genus *Haemophilus* were found in the network analysis in both MIA-induced ASD-like rat models and ASD patients. Moreover, Pasteurellaceae was negatively correlated with SFN treatment in a rat model and had a positive correlation with OSU_Change_Total in ASD patients, which were consistent in both ASD-like rat models and ASD patients. Previous studies have demonstrated that Pasteurellaceae and *Haemophilus* had a decreased relative abundance in patients with ASD (46, 47). However, we did not find Pasteurellaceae, and *Haemophilus* had significant differences between ASD patients and HCs. It suggested that they may be related to the therapeutic efficacy of SFN and that future studies need to give them more attention.

Previous studies have shown that SFN could alleviate hyperuricemia by decreasing the relative abundance of the genus *Parasutterella* and increasing the relative abundance of the family Lactobacillaceae (31). It is worth noting that in our study, it was also found that SFN may alleviate the symptoms of ASD by regulating the relative abundance of these gut microbiota. Research has shown that compared to HCs, the abundance of genus *Parasutterella* was lower in patients with ASD (48, 49). We found that in a rat model, *Parasutterella* was enriched in the NS-SFN group compared to the LPS-SFN group (Figure S1), suggesting that SFN has the potential to ameliorate ASD symptoms by decreasing the relative abundance of *parasutterella*. It has been reported that order Lactobacillales, family Lactobacillaceae, and genus *Lactobacillus* have a lower relative abundance in the ASD

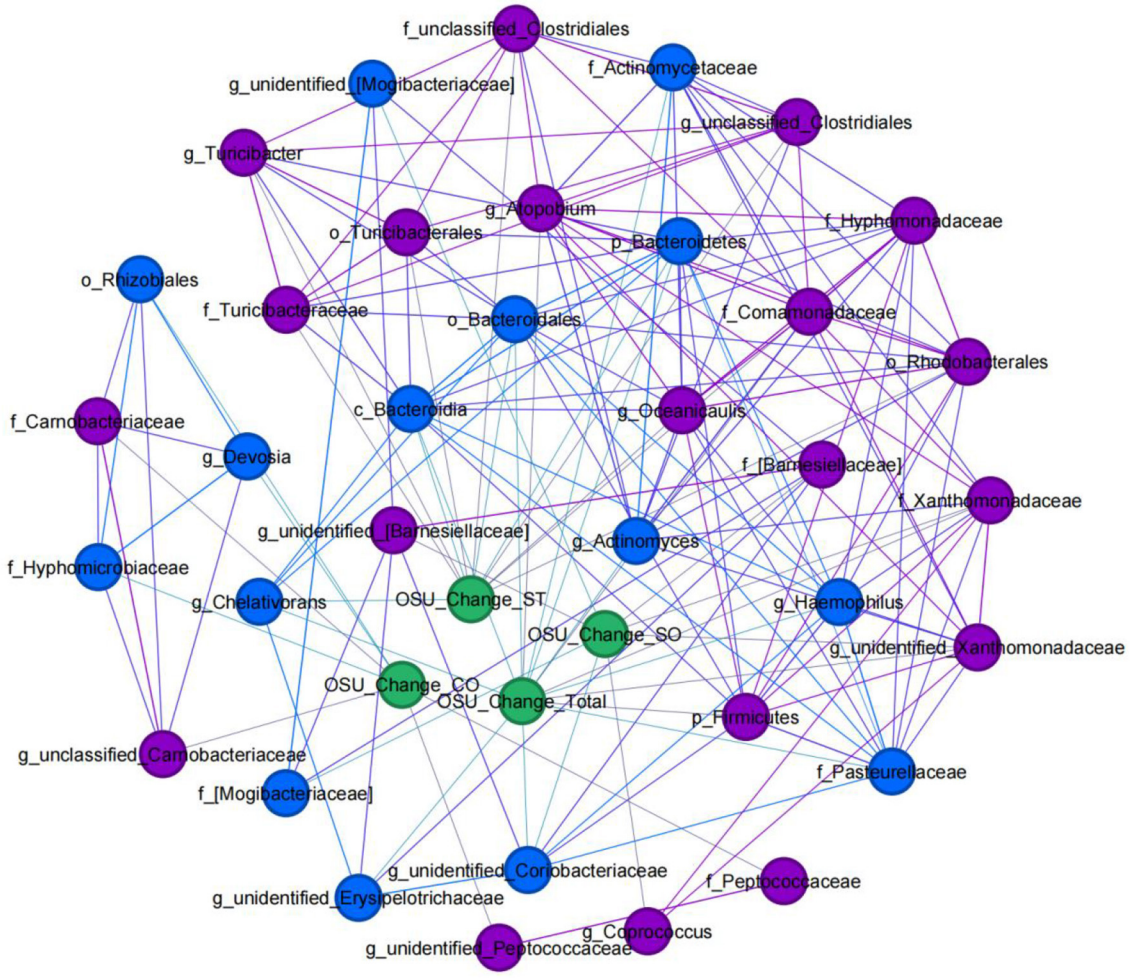

FIGURE 8
Clinical-microbial network in ASD patients with SFN treatment. An undirected network from microbiome abundance alterations to improvements in ASD symptoms after SFN treatment was built. Blue nodes indicate gut microbiota taxa that were positively correlated with OSU change, and purple nodes indicate taxa that were negatively correlated with OSU change. Alteration of the relative abundance of gut microbes: gut microbes' relative abundance at the endpoint was subtracted from the same gut microbes' relative abundance at time 0 ("Baseline"). OSU change: individuals' scores at endpoint were subtracted from the same individual's scores at time 0 ("Baseline").

mice model. Moreover, the administration of Lactobacillus reuteri, which belongs to Lactobacillaceae, could alleviate the symptoms of ASD (44). Interestingly, our study found that order Lactobacillales was enriched in the patients of the ASD-SFN group.

Taken together, our study was the first to investigate SFN's ability to ameliorate core ASD symptoms through modulation of the gut microbiota, and our study demonstrated that SFN treatment attenuates social deficits in rats and young children with ASD and some gut microbiota associated with the improvements in symptoms of ASD. These results suggested that SFN supplementation is a viable strategy for improving specific core symptoms of ASD and its therapeutic effects may be related to gut microbiota. It should be mentioned that there are some limitations in this study: First, studies were conducted in male rats and boys only; therefore, female rats and girls need to be included in future studies to determine whether gut microbiota and behavioral changes respond to SFN treatment in a sex-dependent manner; second, the sample size of our clinical study is relatively small and needs to be further expanded in future; finally, this study only uncovered a potential link between gut flora and the therapeutic effects of SFN on ASD, and the relationship between the mechanism of SFN and gut microbiota has not been systematically validated, the exact mechanisms of which need to be explored in further studies.

5 Conclusion

These data demonstrate that SFN treatment alleviates social deficits in MIA-induced ASD-like rats and ASD patients, and the improvements might be associated with gut microbiota. These data indicated that SFN, as a potential intervention targeting the gut microbiota, could provide a novel avenue for preventing and treating ASD. However, the mechanisms involved in the association of these microbiota with the therapeutic effects of SFN need to be further explored.

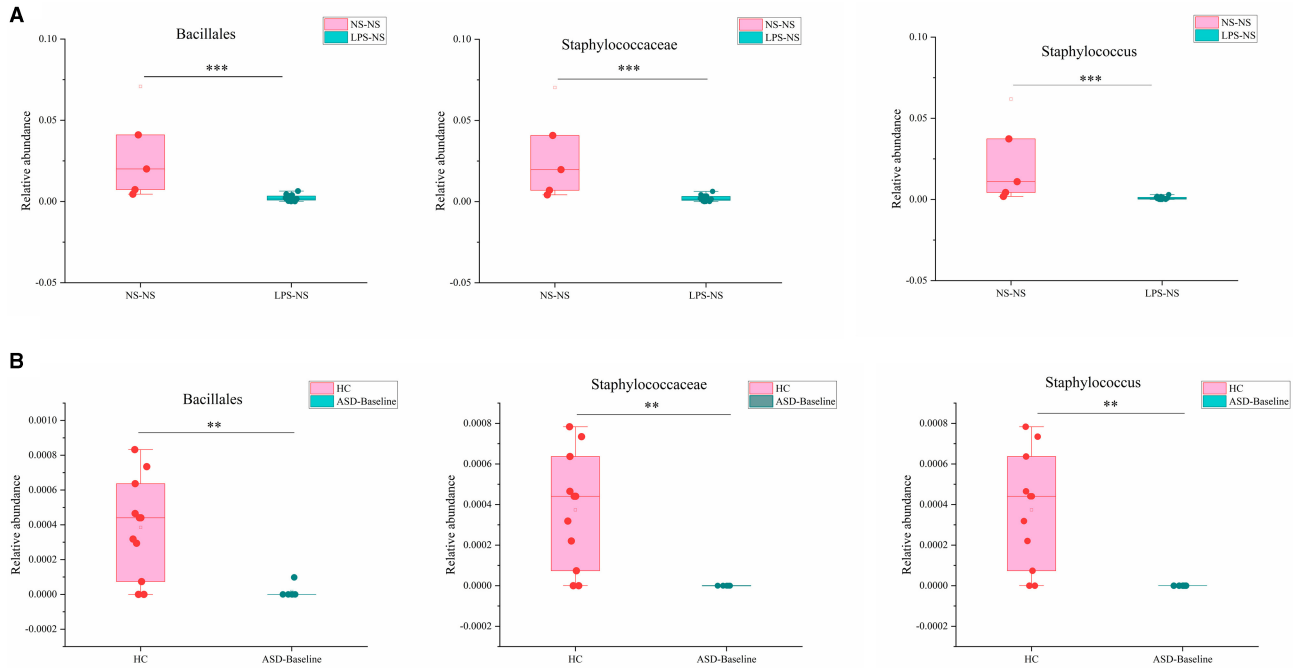

FIGURE 9
Overlapping altered microbial taxa in ASD-like rat models and ASD patient samples. **(A)** The overlap gut microbiota showed different relative abundances between the NS-NS group and the LPS-NS group. **(B)** The overlap gut microbiota showed different relative abundance between the HC group and the ASD-Baseline group (**$p < 0.01$ and ***$p < 0.001$, unpaired Students' *t*-test).

Data availability statement

The original contributions presented in the study are publicly available. This data can be found at: https://www.ncbi.nlm.nih.gov/sra. For rats 16S rRNA sequencing data—BioProject ID: PRJNA1018541. For human 16S rRNA sequencing data—BioProject ID: PRJNA1018910.

Ethics statement

The studies involving humans were approved by Ethics Committee of Second Xiangya Hospital. The studies were conducted in accordance with the local legislation and institutional requirements. Written informed consent for participation in this study was provided by the participants' legal guardians/next of kin. The animal study was approved by the Animal Users Care and Use Committee of Central South University. The study was conducted in accordance with the local legislation and institutional requirements.

Author contributions

JY: Data curation, Writing – original draft. LH: Data curation, Writing – original draft. SD: Writing – original draft. HZ: Writing – original draft. XC: Writing – original draft. JO: Writing – review & editing, Funding acquisition. XZ: Writing – review & editing, Funding acquisition.

Funding

The author(s) declare financial support was received for the research, authorship, and/or publication of this article. This study was supported by the National Natural Science Foundation of China (82271535 and 81974217), the Science and Technology Innovation Program of Hunan Province (2022RC1008 and 2021SK53516), Hunan Provincial Natural Science Foundation (2021JJ40894), and Scientific Research Project of Hunan Provincial Health Commission (202103090528).

Acknowledgments

The authors would like to thank the participating families, who graciously volunteered their time and energy to advance research.

Conflict of interest

The authors declare that the research was conducted in the absence of any commercial or financial relationships that could be construed as a potential conflict of interest.

Publisher's note

All claims expressed in this article are solely those of the authors and do not necessarily represent those of

their affiliated organizations, or those of the publisher, the editors and the reviewers. Any product that may be evaluated in this article, or claim that may be made by its manufacturer, is not guaranteed or endorsed by the publisher.

Supplementary material

The Supplementary Material for this article can be found online at: https://www.frontiersin.org/articles/10.3389/fnut.2023.1294057/full#supplementary-material

References

1. Maenner MJ, Shaw KA, Bakian AV, Bilder DA, Durkin MS, Esler A, et al. Prevalence and characteristics of autism spectrum disorder among children aged 8 years - autism and developmental disabilities monitoring network, 11 Sites, United States, 2018. *MMWR Surveill Summ.* (2021) 70:1–16. doi: 10.15585/mmwr.ss7011a1

2. Siafis S, Ciray O, Wu H, Schneider-Thoma J, Bighelli I, Krause M, et al. Pharmacological and dietary-supplement treatments for autism spectrum disorder: a systematic review and network meta-analysis. *Mol Autism.* (2022) 13:10. doi: 10.1186/s13229-022-00488-4

3. Vanduchova A, Anzenbacher P, Anzenbacherova E. Isothiocyanate from broccoli, sulforaphane, and its properties. *J Med Food.* (2019) 22:121–6. doi: 10.1089/jmf.2018.0024

4. Singh K, Connors SL, Macklin EA, Smith KD, Fahey JW, Talalay P, et al. Sulforaphane treatment of autism spectrum disorder (ASD). *Proc Natl Acad Sci U S A.* (2014) 111:15550–5. doi: 10.1073/pnas.1416940111

5. Bent S, Lawton B, Warren T, Widjaja F, Dang K, Fahey JW, et al. Identification of urinary metabolites that correlate with clinical improvements in children with autism treated with sulforaphane from broccoli. *Mol Autism.* (2018) 9:35. doi: 10.1186/s13229-018-0218-4

6. Ou J, Smith RC, Tobe RH, Lin J, Arriaza J, Fahey JW, et al. Efficacy of sulforaphane in treatment of children with autism spectrum disorder: a randomized double-blind placebo-controlled multi-center trial. *J Autism Dev Disord.* (2022). doi: 10.1007/s10803-022-05784-9

7. Magner M, Thorova K, Zupova V, Houska M, Svandova I, Novotna P, et al. Sulforaphane treatment in children with autism: a prospective randomized double-blind study. *Nutrients.* (2023) 15:718. doi: 10.3390/nu15030718

8. Schachtele SJ, Hu S, Lokensgard JR. Modulation of experimental herpes encephalitis-associated neurotoxicity through sulforaphane treatment. *PLoS ONE.* (2012) 7:e36216. doi: 10.1371/journal.pone.0036216

9. Li D, Shao R, Wang N, Zhou N, Du K, Shi J, et al. Sulforaphane activates a lysosome-dependent transcriptional program to mitigate oxidative stress. *Autophagy.* (2021) 17:872–87. doi: 10.1080/15548627.2020.1739442

10. Lei P, Tian S, Teng C, Huang L, Liu X, Wang J, et al. Sulforaphane improves lipid metabolism by enhancing mitochondrial function and biogenesis *in vivo* and *in vitro*. *Mol Nutr Food Res.* (2019) 63:e1800795. doi: 10.1002/mnfr.201800795

11. Huang C, Wu J, Chen D, Jin J, Wu Y, Chen Z. Effects of sulforaphane in the central nervous system. *Eur J Pharmacol.* (2019) 853:153–68. doi: 10.1016/j.ejphar.2019.03.010

12. Wang ZC, Chen Q, Wang J, Yu LS, Chen LW. Sulforaphane mitigates LPS-induced neuroinflammation through modulation of Cezanne/NF-kappaB signalling. *Life Sci.* (2020) 262:118519. doi: 10.1016/j.lfs.2020.118519

13. Singh K, Zimmerman AW. Sulforaphane treatment of young men with autism spectrum disorder. *CNS Neurol Disord-Drug Targets.* (2016) 15:597–601. doi: 10.2174/1871527315666160413122525

14. Gan N, Wu YC, Brunet M, Garrido C, Chung FL Dai C, et al. Sulforaphane activates heat shock response and enhances proteasome activity through up-regulation of Hsp27. *J Biol Chem.* (2010) 285:35528–36. doi: 10.1074/jbc.M110.152686

15. Liu H, Talalay P, Fahey JW. Biomarker-guided strategy for treatment of autism spectrum disorder (ASD). *CNS Neurol Disord-Drug Targets.* (2016) 15:602–13. doi: 10.2174/1871527315666160413120414

16. Deth R, Muratore C, Benzecry J, Power-Charnitsky V-A, Waly M. How environmental and genetic factors combine to cause autism: a redox/methylation hypothesis. *Neurotoxicology.* (2008) 29:190–201. doi: 10.1016/j.neuro.2007.09.010

17. Wong GC, Montgomery JM, Taylor MW. The gut-microbiota-brain axis in autism spectrum disorder. In: Grabrucker AM, editor. *Autism Spectrum Disorders.* Brisbane: Exon Publications (2021), p. 95–114. doi: 10.36255/exonpublications.autismspectrumdisorders.2021.gutmicrobiota

18. Iglesias-Vázquez L, Van Ginkel Riba G, Arija V, Canals J. Composition of gut microbiota in children with autism spectrum disorder: a systematic review and meta-analysis. *Nutrients.* (2020) 12:792. doi: 10.3390/nu12030792

19. Hosie S, Ellis M, Swaminathan M, Ramalhosa F, Seger GO, Balasuriya GK, et al. Gastrointestinal dysfunction in patients and mice expressing the autism-associated R451C mutation in neuroligin-3. *Autism Res.* (2019) 12:1043–56. doi: 10.1002/aur.2127

20. Sauer AK, Bockmann J, Steinestel K, Boeckers TM, Grabrucker AM. Altered intestinal morphology and microbiota composition in the autism spectrum disorders associated SHANK3 mouse model. *Int J Mol Sci.* (2019) 20:2134. doi: 10.3390/ijms20092134

21. Coretti L, Cristiano C, Florio E, Scala G, Lama A, Keller S, et al. Sex-related alterations of gut microbiota composition in the BTBR mouse model of autism spectrum disorder. *Sci Rep.* (2017) 7:45356. doi: 10.1038/srep45356

22. Golubeva AV, Joyce SA, Moloney G, Burokas A, Sherwin E, Arboleya S, et al. Microbiota-related changes in bile acid & tryptophan metabolism are associated with gastrointestinal dysfunction in a mouse model of autism. *EBioMedicine.* (2017) 24:166–78. doi: 10.1016/j.ebiom.2017.09.020

23. Sharon G, Cruz NJ, Kang DW, Gandal MJ, Wang B, Kim YM, et al. Human gut microbiota from autism spectrum disorder promote behavioral symptoms in mice. *Cell.* (2019) 177:1600–18.e17. doi: 10.1016/j.cell.2019.05.004

24. Sandler RH, Finegold SM, Bolte ER, Buchanan CP, Maxwell AP, Vaisanen ML, et al. Short-term benefit from oral vancomycin treatment of regressive-onset autism. *J Child Neurol.* (2000) 15:429–35. doi: 10.1177/088307380001500701

25. Kang DW, Adams JB, Coleman DM, Pollard EL, Maldonado J, McDonough-Means S, et al. Long-term benefit of microbiota transfer therapy on autism symptoms and gut microbiota. *Sci Rep.* (2019) 9:5821. doi: 10.1038/s41598-019-42183-0

26. Hsiao EY, McBride SW, Hsien S, Sharon G, Hyde ER, McCue T, et al. Microbiota modulate behavioral and physiological abnormalities associated with neurodevelopmental disorders. *Cell.* (2013) 155:1451–63. doi: 10.1016/j.cell.2013.11.024

27. Sgritta M, Dooling SW, Buffington SA, Momin EN, Francis MB, Britton RA, et al. Mechanisms underlying microbial-mediated changes in social behavior in mouse models of autism spectrum disorder. *Neuron.* (2019) 101:246–59.e6. doi: 10.1016/j.neuron.2018.11.018

28. Wu J, Guo W, Cui S, Tang X, Zhang Q, Lu W, et al. Broccoli seed extract rich in polysaccharides and glucoraphanin ameliorates DSS-induced colitis via intestinal barrier protection and gut microbiota modulation in mice. *J Sci Food Agric.* (2023) 103:1749–60. doi: 10.1002/jsfa.12382

29. Zhang Y, Tan L, Li C, Wu H, Ran D, Zhang Z. Sulforaphane alter the microbiota and mitigate colitis severity on mice ulcerative colitis induced by DSS. *AMB Express.* (2020) 10:119. doi: 10.1186/s13568-020-01053-z

30. He C, Huang L, Lei P, Liu X, Li B, Shan Y. Sulforaphane normalizes intestinal flora and enhances gut barrier in mice with BBN-induced bladder cancer. *Mol Nutr Food Res.* (2018) 62:e1800427. doi: 10.1002/mnfr.201800427

31. Wang R, Halimulati M, Huang X, Ma Y, Li L, Zhang Z. Sulforaphane-driven reprogramming of gut microbiome and metabolome ameliorates the progression of hyperuricemia. *J Adv Res.* (2022) 52:19–28. doi: 10.1016/j.jare.2022.11.003

32. Xu X, Sun S, Liang L, Lou C, He Q, Ran M, et al. Role of the Aryl hydrocarbon receptor and gut microbiota-derived metabolites indole-3-acetic acid in sulforaphane alleviates hepatic steatosis in mice. *Front Nutr.* (2021) 8:756565. doi: 10.3389/fnut.2021.756565

33. Vitor-Vieira F, Vilela FC, Giusti-Paiva A. Hyperactivation of the amygdala correlates with impaired social play behavior of prepubertal male rats in a maternal immune activation model. *Behav Brain Res.* (2021) 414:113503. doi: 10.1016/j.bbr.2021.113503

34. Oskvig DB, Elkahloun AG, Johnson KR, Phillips TM, Herkenham M. Maternal immune activation by LPS selectively alters specific gene expression profiles of interneuron migration and oxidative stress in the fetus without triggering a fetal immune response. *Brain Behav Immun.* (2012) 26:623–34. doi: 10.1016/j.bbi.2012.01.015

35. Nadeem A, Ahmad SF, Al-Harbi NO, Attia SM, Bakheet SA, Ibrahim KE, et al. Nrf2 activator, sulforaphane ameliorates autism-like symptoms through suppression of Th17 related signaling and rectification of oxidant-antioxidant imbalance in periphery and brain of BTBR T+tf/J mice. *Behav Brain Res.* (2019) 364:213–24. doi: 10.1016/j.bbr.2019.02.031

36. Septyaningtrias DE, Lin CW, Ouchida R, Nakai N, Suda W, Hattori M, et al. Altered microbiota composition reflects enhanced communication in 15q11-13 CNV mice. *Neurosci Res.* (2020) 161:59–67. doi: 10.1016/j.neures.2019.12.010

37. Chen K, Fu Y, Wang Y, Liao L, Xu H, Zhang A, et al. Therapeutic effects of the *in vitro* cultured human gut microbiota as transplants on altering gut microbiota and improving symptoms associated with autism spectrum disorder. *Microb Ecol.* (2020) 80:475–86. doi: 10.1007/s00248-020-01494-w

38. Liu S, Li E, Sun Z, Fu D, Duan G, Jiang M, et al. Altered gut microbiota and short chain fatty acids in Chinese children with autism spectrum disorder. *Sci Rep.* (2019) 9:287. doi: 10.1038/s41598-018-36430-z

39. Liu F, Horton-Sparks K, Hull V, Li RW, Martinez-Cerdeno V. The valproic acid rat model of autism presents with gut bacterial dysbiosis similar to that in human autism. *Mol Autism.* (2018) 9:61. doi: 10.1186/s13229-018-0251-3

40. Kang DW, Adams JB, Gregory AC, Borody T, Chittick L, Fasano A, et al. Microbiota transfer therapy alters gut ecosystem and improves gastrointestinal and autism symptoms: an open-label study. *Microbiome.* (2017) 5:10. doi: 10.1186/s40168-016-0225-7

41. Strati F, Cavalieri D, Albanese D, De Felice C, Donati C, Hayek J, et al. New evidences on the altered gut microbiota in autism spectrum disorders. *Microbiome.* (2017) 5:24. doi: 10.1186/s40168-017-0242-1

42. Kang DW, Park JG, Ilhan ZE, Wallstrom G, Labaer J, Adams JB, et al. Reduced incidence of prevotella and other fermenters in intestinal microflora of autistic children. *PLoS ONE.* (2013) 8:e68322. doi: 10.1371/journal.pone.0068322

43. Dan Z, Mao X, Liu Q, Guo M, Zhuang Y, Liu Z, et al. Altered gut microbial profile is associated with abnormal metabolism activity of autism spectrum disorder. *Gut Microbes.* (2020) 11:1246–67. doi: 10.1080/19490976.2020.1747329

44. Tabouy L, Getselter D, Ziv O, Karpuj M, Tabouy T, Lukic I, et al. Dysbiosis of microbiome and probiotic treatment in a genetic model of autism spectrum disorders. *Brain Behav Immun.* (2018) 73:310–9. doi: 10.1016/j.bbi.2018.05.015

45. Lim JS, Lim MY, Choi Y, Ko G. Modeling environmental risk factors of autism in mice induces IBD-related gut microbial dysbiosis and hyperserotonemia. *Mol Brain.* (2017) 10:14. doi: 10.1186/s13041-017-0292-0

46. Maigoro AY, Lee S. Gut microbiome-based analysis of lipid a biosynthesis in individuals with autism spectrum disorder: an *in silico* evaluation. *Nutrients*. (2021) 13:688. doi: 10.3390/nu13020688

47. Vernocchi P, Ristori MV, Guerrera S, Guarrasi V, Conte F, Russo A, et al. Gut microbiota ecology and inferred functions in children with ASD compared to neurotypical subjects. *Front Microbiol.* (2022) 13:871086. doi: 10.3389/fmicb.2022.871086

48. Chen Y-C, Lin H-Y, Chien Y, Tung Y-H, Ni Y-H, Gau SS-F. Altered gut microbiota correlates with behavioral problems but not gastrointestinal symptoms in individuals with autism. *Brain Behav Immun.* (2022) 106:161–78. doi: 10.1016/j.bbi.2022.08.015

49. Ding X, Xu Y, Zhang X, Zhang L, Duan G, Song C, et al. Gut microbiota changes in patients with autism spectrum disorders. *J Psychiatr Res.* (2020) 129:149–59. doi: 10.1016/j.jpsychires.2020.06.032

frontiers | Frontiers in Nutrition

TYPE Original Research
PUBLISHED 08 January 2024
DOI 10.3389/fnut.2023.1286658

OPEN ACCESS

EDITED BY
Tom C. Karagiannis,
The University of Melbourne, Australia

REVIEWED BY
Jed William Fahey,
Johns Hopkins University, United States
Yu An,
Capital Medical University, China

*CORRESPONDENCE
Xiao Chen
✉ chenxiao@jlu.edu.cn
Jiuwei Cui
✉ cuijw@jlu.edu.cn

†These authors share first authorship

RECEIVED 04 September 2023
ACCEPTED 12 December 2023
PUBLISHED 08 January 2024

CITATION
Liu X, Chang Y, Li Y, Zhang X, Li F, Song J, Shi H, Chen X and Cui J (2024) Prospective cohort study of broccoli consumption frequency and all-cause and cause-specific mortality risks.
Front. Nutr. 10:1286658.
doi: 10.3389/fnut.2023.1286658

Prospective cohort study of broccoli consumption frequency and all-cause and cause-specific mortality risks

Xiangliang Liu[1†], Yu Chang[1†], Yuguang Li[1†], Xinwei Zhang[1], Fangqi Li[1], Jia Song[1], Hanping Shi[2], Xiao Chen[1*] and Jiuwei Cui[1*]

[1]The First Hospital of Jilin University, Changchun, China, [2]Department of Gastrointestinal Surgery/Clinical Nutrition, Beijing Shijitan Hospital, Capital Medical University, The 9th Clinical College, Beijing, China

Background: Broccoli is rich in vitamins, minerals, and antioxidants with broad health benefits, but its intake frequency and dose–response relationship with mortality risk remain unclear.

Methods: Using data from the U.S. National Health and Nutrition Examination Survey 2003–2006, 12,486 adults were included. Broccoli intake frequency was evaluated by a food frequency questionnaire, and all-cause and cause-specific mortality risks were followed up. The relationship between broccoli intake and mortality risk was analyzed using Cox models.

Results: Compared with never consumption of broccoli, different frequencies of broccoli consumption were associated with significantly decreased risks of all-cause mortality (p for trend <0.001). Consuming broccoli 1–2 times per week was associated with a 32–43% lower mortality risk. More frequent broccoli consumption was negatively correlated with cardiovascular and cancer mortality risks ($p < 0.05$). Consuming broccoli 1–2 times per week for males and ≥ 3 times per week for females could significantly reduce all-cause mortality risk.

Conclusion: Moderate and frequent consumption of broccoli may reduce the risks of all-cause and cause-specific mortality. Optimal intake frequencies may differ by gender.

KEYWORDS

broccoli, mortality, risk factors, NHANES, diet

1 Introduction

With changes in lifestyle, the incidence and mortality of chronic non-communicable diseases such as cardiovascular disease and cancer continue to increase, posing a major threat to public health worldwide (1). Fruits and vegetables as natural health foods are nutritious and pharmacologically valuable in preventing many chronic diseases. In recent years, more and more epidemiological studies have begun to focus on the health benefits of single vegetables (2). Among them, broccoli from cruciferous vegetables has received much attention due to its unique nutritional composition and abundant bioactive components (3). Broccoli is not only rich in vitamins (vitamin C, carotenoids, etc.), minerals, and dietary fibers but also contains abundant sulfur-containing bioactive compounds (4). Numerous studies have shown that broccoli has

broad-spectrum pharmacological properties such as anti-inflammatory, antioxidant, anticancer, blood pressure lowering, hypoglycemic, and hypolipidemic effects and play an important role in preventing cardiovascular diseases, cancers, type 2 diabetes, and other diseases (5–8).

For example, broccoli is abundant in sulfur-containing organic compounds, among which the compound isothiocyanate sulforaphane has been found to have certain preventive effects on prostate cancer, pancreatic cancer, leukemia, and colon cancer (9–12). However, conclusions from different studies on the dose–response relationship between broccoli intake and the prevention of chronic diseases are inconsistent. Few prospective cohort studies have found that a higher intake of cruciferous vegetables is associated with a lower risk of overall mortality and cardiovascular disease mortality compared to a lower intake of cruciferous vegetables (13). However, the available data do not provide specific recommendations for broccoli consumption frequency. Therefore, it is of great significance to use large sample prospective study results to analyze the dose–response relationship between broccoli intake frequency and all-cause and cause-specific mortality, which can provide guidance for dietary adjustment in different populations, especially dietary interventions for patients with chronic diseases.

This study utilized the prospective cohort data of the National Health and Nutrition Examination Survey (NHANES) from 2003 to 2006 to assess the relationship between different frequencies of broccoli intake and all-cause mortality and cause-specific mortality from cardiovascular diseases, cancers, and other diseases in approximately 12,486 adult participants. The results can provide a basis for developing scientific dietary guidelines and guiding dietary adjustments for patients with chronic diseases.

2 Methods

2.1 Study population

NHANES is an important cross-sectional survey conducted by the National Center for Health Statistics (NCHS) using a stratified and probabilistic random sampling design, aiming to assess the health and nutritional status of the American population. NHANES primarily acquires data via face-to-face interviews, physical examinations, and laboratory tests administered by researchers. Within the database, we initially screened 12,486 patients and subsequently subjected them to inclusion and exclusion criteria. The inclusion criteria were as follows: (1) all participants aged 20 years or older who consistently participated in NHANES cycles from 2003 to 2006 and (2) participants who cooperated with follow-up assessments and provided informed consent. The exclusion criteria were as follows: (1) age below 20 years; (2) absence of dietary data at survey initiation; (3) unavailability of survival status; (4) the outcome event was death but the cause was missing; and (5) suffering from a certain non-communicable disease at the start of follow-up. As de-identified and publicly available data were utilized, institutional review board approval was not necessary.

2.2 Data collection

Dietary data on broccoli were obtained from the Food Frequency Questionnaire (FFQ) based on participants' responses to the questions: "Have you ever consumed broccoli? How frequently do you consume broccoli?," with responses recorded for never consuming broccoli and the frequency of broccoli consumption. Participants' responses were used to classify broccoli consumption into four categories: never ("never"), infrequently ("less than once a week"), occasionally ("1 to 2 times per week but less than 3 times per week"), and regularly ("3 or more times per week"). Furthermore, covariate information such as age, gender, race, education level, poverty income ratio (PIR), body mass index (BMI), smoking status, alcohol consumption status, and history of hypertension, dyslipidemia, and diabetes was collected through questionnaire surveys. Participants were stratified based on PIR as follows: PIR (low) ≤ 1, PIR (medium) > 1–<4, and PIR (high) ≥ 4 (14). BMI was determined as the ratio of weight (kg) to the square of height (m^2). Smoking status was categorized as follows: "Current" referred to individuals who reported smoking more than 100 cigarettes in their lifetime and currently smoked on all or some days; "Former" referred to individuals who reported smoking more than 100 cigarettes in their lifetime but currently did not smoke; and "Never" referred to individuals who reported smoking less than 100 cigarettes in their lifetime. In terms of alcohol consumption status, "Now" was defined as participants who consumed alcoholic beverages in the past year, "Former" was defined as participants who had consumed alcoholic beverages in the past year but had stopped drinking at the time of the survey, and "Never" was defined as participants who had not consumed any alcoholic beverages in the past year. If systolic blood pressure is $\geq$140 mmHg or diastolic blood pressure is $\geq$90 mmHg, with the use of antihypertensive medication, an individual can be diagnosed with hypertension. If triglyceride level is $\geq$150 mg/dL; high-density lipoprotein is $<$140 mg/dL; and low-density lipoprotein is $\geq$130 mg/dL, with the use of lipid-lowering medication, an individual can be diagnosed with dyslipidemia. If fasting blood glucose level is $\geq$7.0 mmol/L; 2-h postprandial blood glucose is $\geq$11.1 mmol/L; and glycated hemoglobin is $\geq$6.5%, with the use of hypoglycemic medication, an individual can be diagnosed with diabetes if they meet any of the above criteria.

Blood samples were collected at the start of follow-up to obtain values for monocytes, lymphocytes, platelets, and neutrophils. Based on these values, we calculated the following inflammation-related markers: lymphocyte-to-monocyte ratio (LMR) and systemic immune-inflammation index (SII), which is calculated as platelet $\times$ neutrophil count divided by lymphocyte count; and neutrophil-to-lymphocyte ratio (NLR) (15).

The National Death Index (NDI) database was utilized to associate the information of NHANES survey participants with their corresponding death records. This approach was confined to a designated range to ensure the attainment of precise mortality data for NHANES participants. The interval from the commencement of household interviews to either loss to follow-up or death was accounted for as the follow-up duration. The NDI database was employed to acquire the mortality status. Furthermore, the specific causes of death were ascertained as delineated by the International Classification of Diseases (ICD) 10.

2.3 Statistical analysis

In descriptive statistics, normal continuous variables were described using the mean (standard deviation, SD). Statistical differences were described using a t-test or analysis of variance.

Non-normal continuous variables were described using the median (interquartile range, IQR), and statistical differences were described using non-parametric tests. Categorical variables were described using frequency (represented as percentages), and statistical differences were described using the chi-square test. The Cox proportional hazards models were formulated to estimate hazard ratios (HRs) accompanied by 95% confidence intervals. Univariate and multivariate regression analyses were employed to evaluate the association between various determinants, notably broccoli intake frequency and the risks associated with all-cause and specific-cause mortality. A threshold of value of p of <0.05 was established for determining statistical significance. Data preprocessing and statistical evaluations were executed utilizing the intricate survey design module of the SPSS 25.0 (IBM) statistical software. Forest plots along with the correlation matrix were generated using R software version 4.2.3.

3 Results

3.1 Baseline characteristics

Our study ultimately encompassed 5,556 adults aged 20 years and older who provided valid responses to the broccoli diet query in the NHANES Food Frequency Questionnaire. The sample included 2,743 males and 2,813 females. Detailed specifics can be found in Figure 1. During the follow-up period that ended on 31 December 2019, the overall count of deaths from all causes reached 1,405, which represented 25.3% of the total sample population. The causes of these deaths, categorized according to the ICD-10, were primarily distributed across seven categories: cardiovascular diseases, pulmonary and chronic respiratory diseases, renal diseases, malignant tumors, diabetes, accidents, and miscellaneous causes. These categories also include the following distribution: Cardiovascular disease was responsible for 504 deaths, representing 35.9% of the total deaths; malignant tumors accounted for 292 deaths, representing 20.7% of the total deaths; 107 deaths were due to pulmonary and chronic respiratory diseases, representing 7.6% of the total deaths; diabetes resulted in 49 deaths, totaling 3.5% of all deaths; renal diseases led to 36 deaths, representing 2.6% of total deaths; 38 deaths were caused by accidents, accounting for 2.7% of all deaths; and 379 deaths were attributed to miscellaneous causes, representing 27% of all deaths.

As shown in Table 1, an observed disparity in the frequency of broccoli consumption between the genders indicated a more prevalent intake among females than males. A variance in broccoli consumption frequency was also detected across racial demographics, with the non-Hispanic white population reported to have more frequent consumption compared to other races. Discrepancies in broccoli consumption frequency were apparent among distinct PIR groups. Those falling within the medium-range PIR category (PIR > 1–<4) exhibited greater frequency compared to both the low (≤1) and high PIR groups (≥4). Frequent broccoli consumers demonstrated a decreased frequency of consumption in smokers compared to non-smokers. This implies that smoking habits could potentially impinge on regular broccoli consumption. Among habitual broccoli consumers, individuals who regularly consumed alcohol were observed to consume broccoli with greater frequency than those who had ceased alcohol consumption or abstained from it altogether, suggesting that alcohol consumption may be linked to an increased frequency of broccoli consumption.

3.2 Univariate and multivariate analyses of factors associated with all-cause and cause-specific mortality risks

In this cohort, we analyzed a range of variables, including age, gender, race, poverty income ratio (PIR), education level, smoking

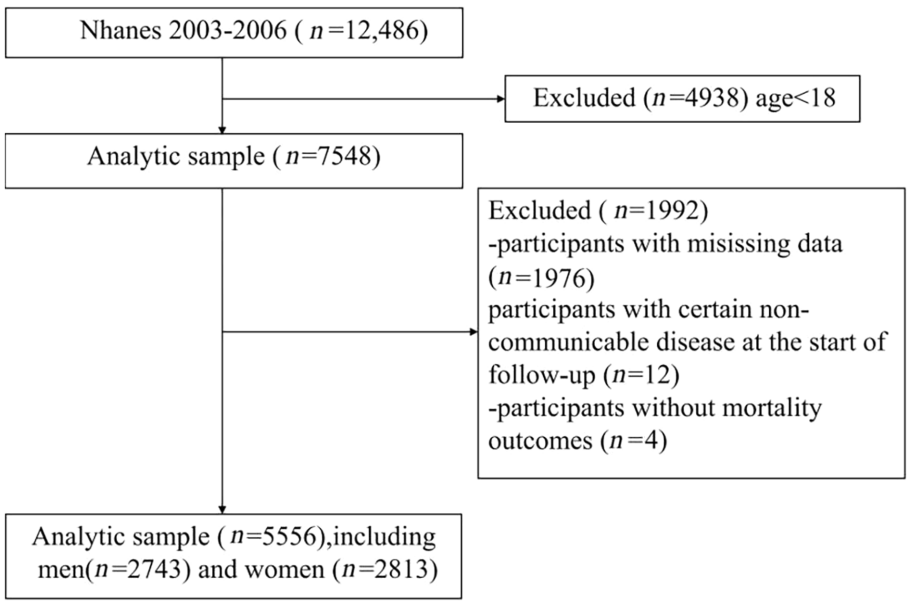

FIGURE 1
Flowchart of the study and participants excluded from the study.

10.3389/fnut.2023.1286658

TABLE 1 Baseline characteristic variables according to the broccoli consumption frequency.

Variable	Total (n = 5,556)	0 (n = 739)	1 (n = 3,181)	2 (n = 1,216)	3 (n = 420)	Statistic	p
Age, n (%)						$\chi^2 = 5.434$	0.143
<65	3,893 (70.07)	491 (66.44)	2,249 (70.70)	855 (70.31)	298 (70.95)		
≥65	1,663 (29.93)	248 (33.56)	932 (29.30)	361 (29.69)	122 (29.05)		
Gender, n (%)						$\chi^2 = 117.569$	<0.001
Male	2,743 (49.37)	486 (65.76)	1,567 (49.26)	531 (43.67)	159 (37.86)		
Female	2,813 (50.63)	253 (34.24)	1,614 (50.74)	685 (56.33)	261 (62.14)		
Race, n (%)						$\chi^2 = 47.293$	<0.001
Race (1)	3,149 (56.68)	410 (55.48)	1812 (56.96)	715 (58.80)	212 (50.48)		
Race (2)	1,067 (19.2)	150 (20.30)	625 (19.65)	184 (15.13)	108 (25.71)		
Race (3)	989 (17.8)	148 (20.03)	560 (17.60)	208 (17.11)	73 (17.38)		
Race (4)	351 (6.32)	31 (4.19)	184 (5.78)	109 (8.96)	27 (6.43)		
PIR, n (%)						$\chi^2 = 109.197$	<0.001
PIR (1)	860 (15.48)	158 (21.38)	467 (14.68)	162 (13.32)	73 (17.38)		
PIR (2)	3,125 (56.25)	469 (63.46)	1820 (57.21)	616 (50.66)	220 (52.38)		
PIR (3)	1,571 (28.28)	112 (15.16)	894 (28.10)	438 (36.02)	127 (30.24)		
Education level, n (%)						$\chi^2 = 169.380$	<0.001
Middle school or below	1,398 (25.16)	291 (39.38)	770 (24.21)	238 (19.57)	99 (23.57)		
High school	1,415 (25.47)	210 (28.42)	864 (27.16)	253 (20.81)	88 (20.95)		
College or above	2,743 (49.37)	238 (32.21)	1,547 (48.63)	725 (59.62)	233 (55.48)		
Diabetes, n (%)						$\chi^2 = 9.310$	0.157
No	4,363 (78.53)	554 (74.97)	2,511 (78.94)	963 (79.19)	335 (79.76)		
Prophase	347 (6.25)	46 (6.22)	203 (6.38)	71 (5.84)	27 (6.43)		
Yes	846 (15.23)	139 (18.81)	467 (14.68)	182 (14.97)	58 (13.81)		
Smoke History, n (%)						$\chi^2 = 69.519$	<0.001
Never	2,765 (49.77)	320 (43.30)	1,556 (48.92)	654 (53.78)	235 (55.95)		
Former	1,596 (28.73)	202 (27.33)	904 (28.42)	354 (29.11)	136 (32.38)		
Now	1,195 (21.51)	217 (29.36)	721 (22.67)	208 (17.11)	49 (11.67)		
Alcohol History, n (%)						$\chi^2 = 37.452$	<0.001
Never	750 (13.5)	112 (15.16)	410 (12.89)	151 (12.42)	77 (18.33)		
Former	1,254 (22.57)	205 (27.74)	689 (21.66)	251 (20.64)	109 (25.95)		
Now	3,552 (63.93)	422 (57.10)	2082 (65.45)	814 (66.94)	234 (55.71)		
Hyperlipidemia, n (%)						$\chi^2 = 4.195$	0.241
No	1,494 (26.89)	189 (25.58)	840 (26.41)	337 (27.71)	128 (30.48)		
Yes	4,062 (73.11)	550 (74.42)	2,341 (73.59)	879 (72.29)	292 (69.52)		
Hypertension, n (%)						$\chi^2 = 6.521$	0.089
No	3,043 (54.77)	378 (51.15)	1742 (54.76)	694 (57.07)	229 (54.52)		
Yes	2,513 (45.23)	361 (48.85)	1,439 (45.24)	522 (42.93)	191 (45.48)		
BMI, M (Q_1, Q_3)	27.73 (24.24–31.96)	27.66 (24.26–31.95)	27.95 (24.46–32.20)	27.40 (24.00–31.57)	27.15 (23.89–31.71)	$\chi^2 = 7.032$	0.071

Race (1): Non-Hispanic white, Race (2): Non-Hispanic Black, Race (3): Mexican-American, Race (4): Other.
PIR (1):≤1, PIR (2):>1–<4, PIR (3):≥4.

status, drinking status, history of hypertension, dyslipidemia, and diabetes. In the univariate Cox proportional hazards regression model, we identified 12 indicators that were significantly associated with the risk of all-cause mortality. These indicators include age, gender, race, poverty income ratio (PIR), education level, smoking status, drinking status, history of hypertension, history of dyslipidemia, history of diabetes, broccoli consumption frequency, and BMI. The multivariate Cox proportional hazards regression model confirmed that the same

12 indicators identified in the univariate analysis remain significantly associated with the risk of all-cause mortality. Specific details can be seen in Figure 2.

The univariate Cox proportional hazards regression model identified 11 indicators that were significantly associated with the risk of cardiovascular mortality. These indicators include age, gender, race, PIR, education level, smoking status, drinking status, history of hypertension, history of dyslipidemia, history of diabetes, and broccoli consumption frequency. The multivariate Cox proportional hazards regression model confirmed that nine indicators remained significantly associated with the risk of cardiovascular mortality. These indicators include age, gender, race, PIR, education level, smoking status, history of hypertension, history of diabetes, and broccoli consumption frequency. The univariate Cox proportional hazards regression model revealed that 10 indicators were significantly associated with the risk of cancer mortality. These indicators include age, gender, race, PIR, education level, smoking status, drinking status, history of hypertension, history of diabetes, and broccoli consumption frequency. The multivariate Cox proportional hazards regression model demonstrated that eight indicators remained significantly associated with the risk of cancer mortality. These indicators include age, race, PIR, education level, history of hypertension, history of dyslipidemia, broccoli consumption frequency, and BMI. Specific details can be seen in Figures 3, 4.

3.3 Association between broccoli consumption frequency and risks of all-cause and cause-specific mortality after model adjustment

Given the potential confounding effects of covariates on outcomes, we employed adjusted models to reassess the relationship between the frequency of broccoli consumption and the risks of all-cause mortality, as well as specific diseases such as cardiovascular mortality and cancer mortality. We employed three adjustment models to control for potential confounders. Model 1 was adjusted for age, gender, and race; Model 2 was adjusted for age, gender, race, PIR, education level, and BMI; and Model 3 was adjusted for age, gender, race, PIR, education level, BMI, smoking status, drinking status, history of hypertension, history of dyslipidemia, and history of diabetes. In the analysis of model-adjusted results regarding the association between broccoli consumption frequency and the risk of all-cause mortality, the rarely broccoli consumption group ("less than once a week") exhibited a mortality risk hazard ratio (HR) (95% confidence interval [CI]) of 0.700 (0.605–0.809) in Model 1, 0.785 (0.677–0.909) in Model 2, and 0.825 (0.711–0.957) in Model 3, compared to the reference group of individuals who never consume broccoli. For the sometimes broccoli consumption group ("1 to 2 times per week but less than 3 times per week"), the mortality risk HR (95% CI) was 0.577 (0.484–0.689) in Model 1 and 0.680 (0.568–0.815) in Model 2. The mortality risk HR (95% CI) for the often broccoli consumption group ("3 or more times per week") was 0.705 (0.555–0.895) in Model 1 and 0.723 (0.603–0.865) in Model 2 (Supplementary Figure S1).

In the analysis of model-adjusted results regarding the association between broccoli consumption frequency and the risk of cardiovascular mortality, the rarely broccoli consumption group ("less than once a week") exhibited a mortality risk hazard ratio (HR) (95% CI) of 0.688 (0.541–0.874) in Model 1 and 0.779 (0.611–0.995) in Model 2 compared to the reference group of individuals who never consume broccoli. For the sometimes broccoli consumption group ("1 to 2 times per week but less than 3 times per week"), the mortality risk hazard ratio (HR) (95% CI) was 0.522 (0.388–0.702) in Model 1, 0.619 (0.457–0.839) in Model 2, and 0.664 (0.490–0.900) in Model 3 (Supplementary Figure S2).

In the analysis of the model-adjusted results regarding the association between broccoli consumption frequency and cancer mortality risk, compared to the reference group of individuals who never consume broccoli, the rarely broccoli consumption group ("less than once a week") exhibited a mortality risk hazard ratio (HR) (95% CI) of 0.622 (0.461–0.838) in Model 1, 0.697 (0.515–0.944) in Model 2, and 0.716 (0.528–0.970) in Model 3. The sometimes broccoli consumption group ("1 to 2 times per week but less than 3 times per week") had a mortality risk HR (95% CI) of 0.587 (0.411–0.837) in Model 1. The often broccoli consumption group ("3 or more times per week") had a mortality risk HR (95% CI) of 0.599 (0.359–0.998) in Model 1 (Supplementary Figure S3).

3.4 Association between broccoli consumption frequency and all-cause mortality risk after model adjustment stratified by gender

The distribution of broccoli consumption frequency exhibited gender differences, as indicated in Table 1. Thus, we conducted gender-stratified analyses and adjusted for confounding factors to more precisely assess the relationship between broccoli consumption frequency and the risk of all-cause mortality in each gender population. Among men, individuals in the rarely broccoli consumption group ("less than once a week") had a hazard ratio (HR) (95% CI) of 0.650 (0.544–0.776) in Model 1 (adjusted for age, gender, and race), 0.719 (0.599–0.862) in Model 2 (adjusted for variables in Model 1 plus poverty income ratio, education level, and BMI), and 0.743 (0.619–0.892) in Model 3 (adjusted for variables in Models 1 and 2 plus smoking status, drinking status, history of hypertension, history of dyslipidemia, and history of diabetes) compared to those who never consumed broccoli. Among males, individuals who occasionally consumed broccoli ("1 to 2 times per week but less than 3 times per week") had a hazard ratio (HR) (95% CI) of 0.560 (0.445–0.705) in Model 1, 0.651 (0.514–0.825) in Model 2, and 0.657 (0.519–0.832) in Model 3. These findings suggest a more pronounced reduction in the risk of all-cause mortality among males who consume broccoli occasionally.

Among females, individuals in the sometimes broccoli consumption group ("1 to 2 times per week but less than 3 times per week") had a hazard ratio (HR) (95% CI) of 0.634 (0.473–0.849) in Model 1 and 0.742 (0.552–0.997) in Model 2 compared to those who never consumed broccoli. The HR (95% CI) of the often broccoli consumption group ("3 or more times per week") was 0.627 (0.431–0.913) in Model 1 and 0.678 (0.465–0.989) in Model 2. These findings suggest a more pronounced reduction in the risk of all-cause mortality among females who consume broccoli frequently. Additional information can be found in Supplementary Figure S4.

10.3389/fnut.2023.1286658

Subgroup	sample	HR(95% CI)	*p*-Value
Broccoli consumption	5556		
never			
Rarely		0.82(0.71 to 0.96)	0.011
Sometimes		0.72(0.60 to 0.86)	<0.001
Often		0.85(0.67 to 1.08)	0.186
Age	5556		
<65		0.12(0.11 to 0.14)	<0.001
≥65			
Sex	5556		
Male		1.35(1.21 to 1.50)	<0.001
Female			
Race	5556		
Non-Hispanic white		1.47(1.10 to 1.97)	0.009
Non-Hispanic,Black		1.67(1.29 to 2.15)	<0.001
Mexican-American		2.34(1.87 to 2.93)	<0.001
Other			
PIR	5556		
PIR (1)		1.63(1.34 to 1.99)	<0.001
PIR (2)		1.36(1.17 to 1.57)	<0.001
PIR (3)			
EDU	5556		
Middle school or below		1.23(1.07 to 1.42)	0.004
High school		1.03(0.90 to 1.18)	0.694
College or above			
History of smoking	5556		
Yes		1.48(1.21 to 1.81)	<0.001
Quit smoking		1.70(1.45 to 2.00)	<0.001
No			
alchhol history	5556		
Yes		0.76(0.64 to 0.90)	0.001
Quit drinking		1.02(0.86 to 1.21)	0.795
No			
History of diabetes	5556		
Yes		1.79(1.58 to 2.03)	<0.001
Prophase		1.30(1.08 to 1.57)	0.006
No			
Hypertension	5556		
Yes		1.59(1.40 to 1.81)	<0.001
No			
Hyperlipidemia	5556		
Yes		0.76(0.64 to 0.90)	0.001
No			
BMI	5556	0.98(0.97 to 0.99)	<0.001

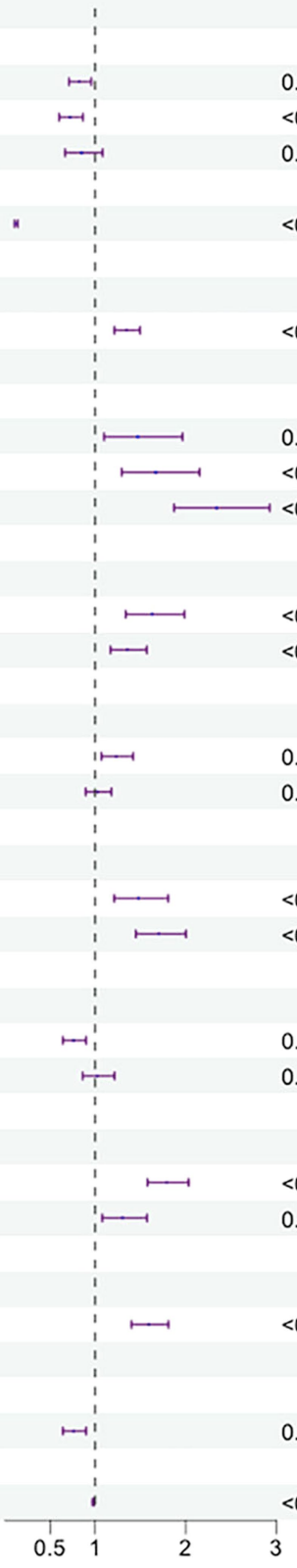

FIGURE 2
Forest plot displaying the hazard ratios of all-cause mortality by multivariate Cox regression analysis (By R 4.2.3).

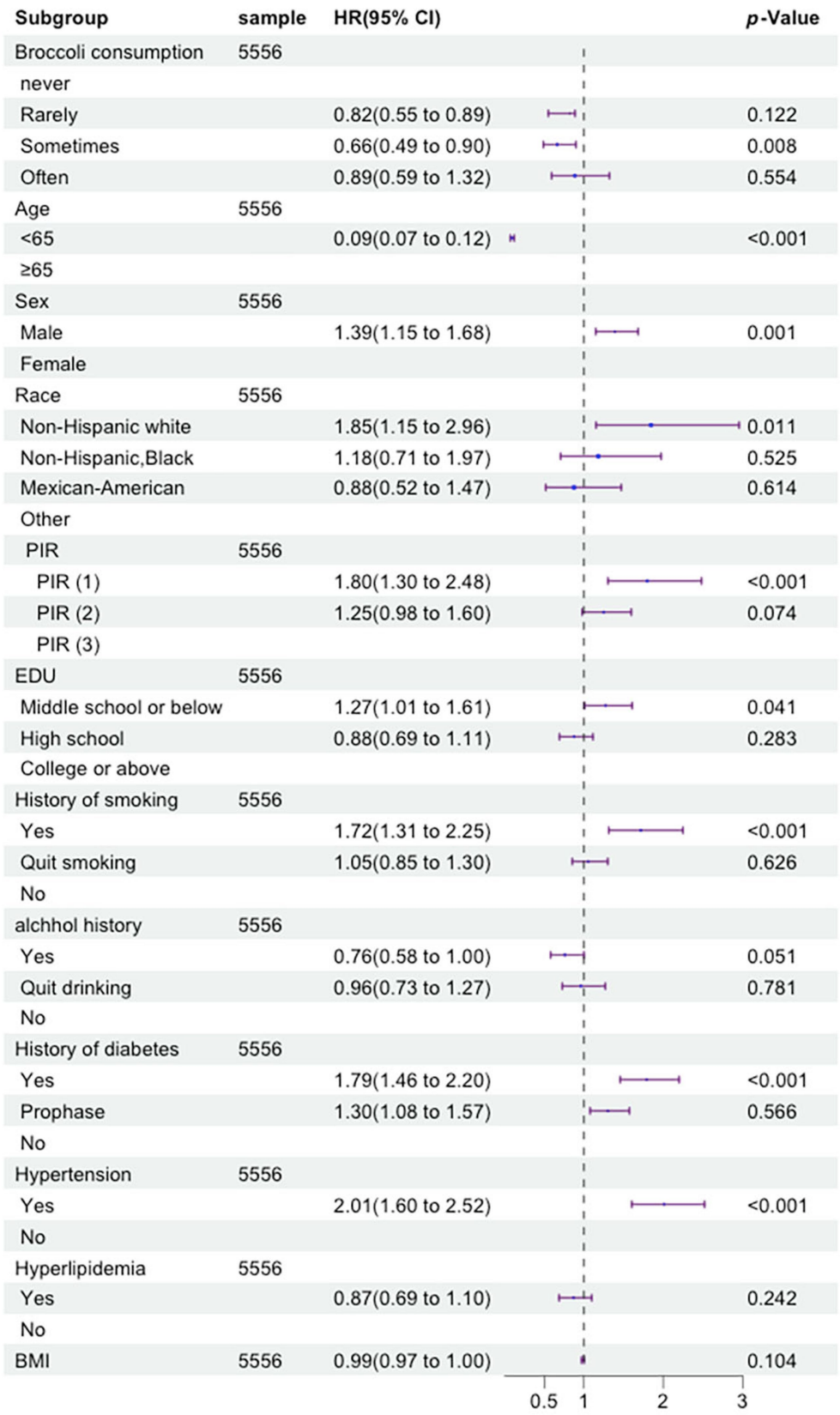

FIGURE 3
Forest plot displaying the hazard ratios of cardiovascular and cerebrovascular disease mortality by multivariate Cox regression analysis (By R 4.2.3).

10.3389/fnut.2023.1286658

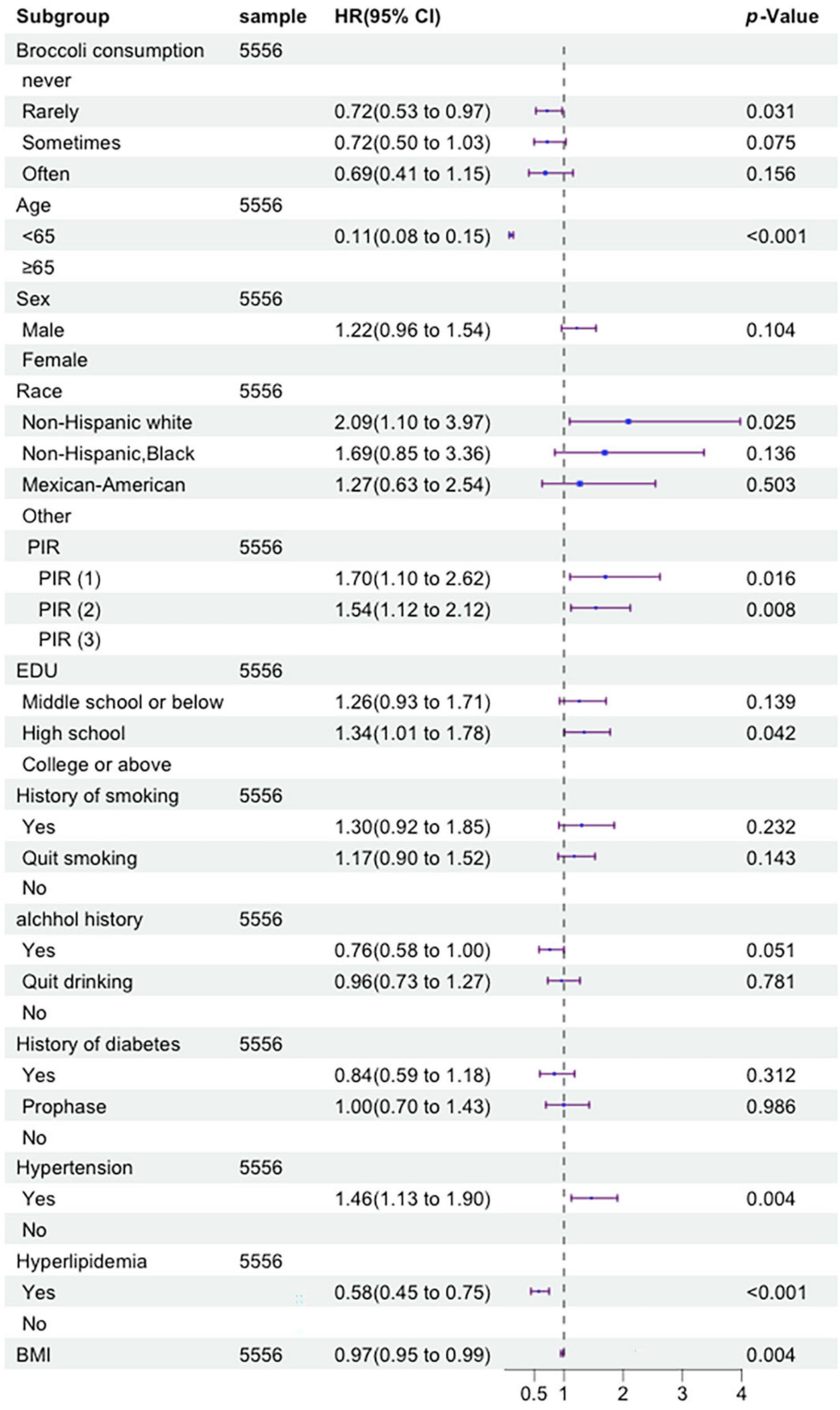

FIGURE 4
Forest plot displaying the hazard ratios of tumor mortality by multivariate Cox regression analysis (By R 4.2.3).

3.5 Association between broccoli consumption frequency and inflammation markers

To investigate the relationship between the frequency of broccoli consumption and inflammation markers, we conducted a correlation analysis using a correlation matrix. The results revealed that the correlation coefficient between broccoli consumption frequency and NLR was −0.032, $p = 0.017$; the correlation coefficient between broccoli consumption frequency and LMR was 0.025, $p = 0.063$; and the correlation coefficient between broccoli consumption frequency and SII was −0.016, $p = 0.248$. These findings suggest a negative correlation between broccoli consumption frequency and NLR. More specific details can be seen in Figure 5.

4 Discussion

The results of this study show that, compared with those who never eat broccoli, participants who consumed broccoli at different frequencies had significantly lower all-cause mortality risks, showing a negative correlation trend, which is consistent with the results of previous meta-analyses on fruit and vegetable intake and mortality risk (16). Specifically, eating broccoli 1–2 times per week can reduce all-cause mortality risk by 32–43%. In addition, broccoli intake frequency was negatively correlated with cardiovascular mortality and cancer mortality. Considering that different genders may respond differently to broccoli intake, we conducted stratified analysis by gender and found that, compared with females, males were more inclined to eat broccoli 1–2 times per week, while females were more inclined to eat broccoli ≥3 times per week to obtain the effect of reducing all-cause mortality. Finally, we found that broccoli intake frequency was negatively correlated with the inflammatory marker NLR. Overall, this study determined a dose–response relationship between broccoli intake frequency and reduced risks of all-cause and cause-specific mortality, providing a basis for developing scientific dietary guidelines.

Our findings are validated by several previous large-scale studies, two of which were conducted in Asia, demonstrating that cruciferous vegetables can enhance cardiovascular health and reduce mortality risk. Several prospective studies have indicated that high fruit and vegetable consumption does not necessarily correlate with reduced cancer incidence. Therefore, we further explored the potential mechanisms through which consuming broccoli may lower the risk of mortality, taking into account its anti-inflammatory and antioxidant properties, its role in modulating lipid metabolism, and its influence on blood glucose homeostasis.

Broccoli contains abundant direct antioxidant nutrients such as vitamin C, carotenoids, and anthocyanins (7), which can eliminate excessive active oxygen-free radicals and inhibit oxidative stress in the body. In addition, sulfur-containing phytochemicals are unique bioactive components in broccoli, such as glucosinolate, which can exert anti-inflammatory effects by inhibiting the production and release of inflammatory factors (17), as well as by protecting the body from inflammatory damage by stimulating the production of antioxidant enzymes (18). Substantial evidence indicates that chronic

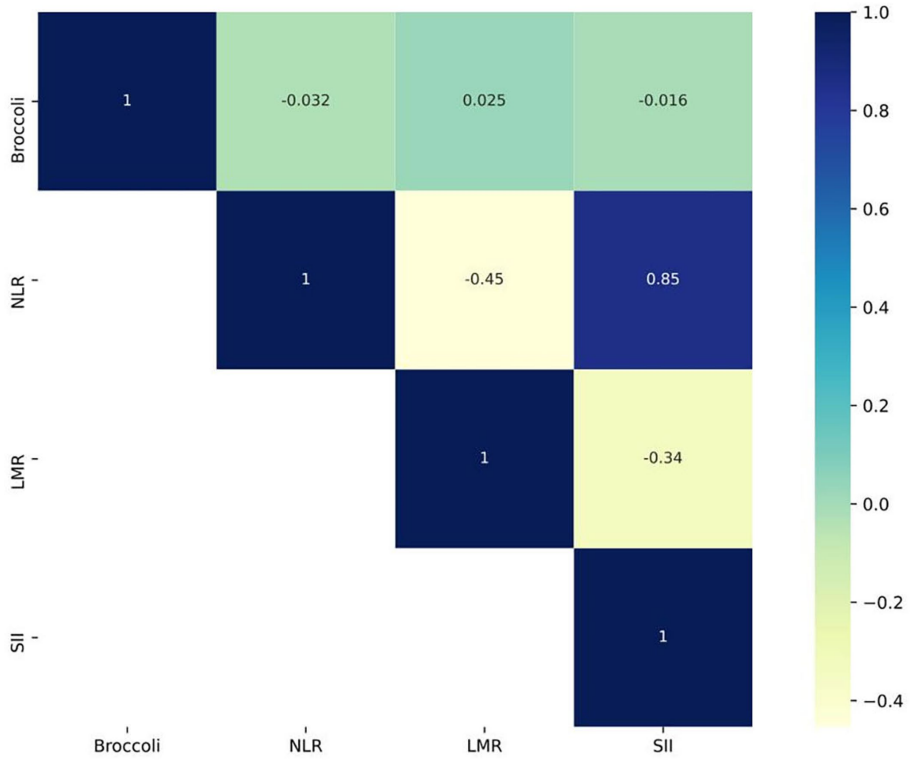

FIGURE 5
Correlation matrix plot describing the frequency of broccoli consumption and inflammatory markers (By R 4.2.3).

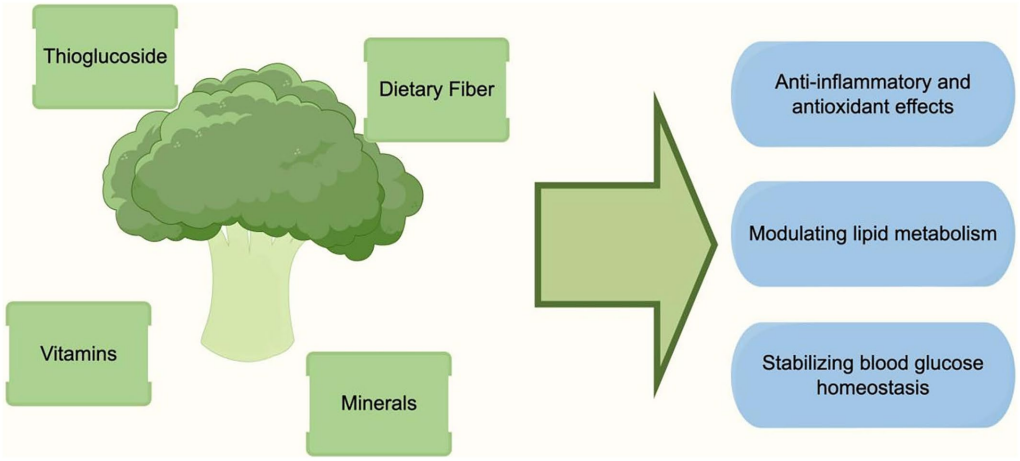

FIGURE 6
Potential mechanisms of broccoli intake in reducing mortality risk (By Figdraw).

inflammation and oxidative stress play important roles in the pathogenesis of various chronic diseases, including cancers, cardiovascular diseases, and type 2 diabetes (19). Chronic inflammation can lead to the release of additional cytokines and growth factors, stimulating angiogenesis and cell proliferation, degrading extracellular matrix enzymes, and providing an advantageous environment for tumor growth (20). Moreover, chronic inflammation can also result in endothelial cell oxidative stress, promote platelet activation, cause endothelial cell damage, and can be considered a key driving factor in the development of cardiovascular diseases (8). Therefore, the abundant anti-inflammatory and antioxidant components in broccoli may be important nutritional mechanisms for its beneficial effects against chronic diseases.

Broccoli contains abundant vitamin K1, which is a fat-soluble vitamin that can promote the generation of clotting factors and inhibit the synthesis and secretion of cholesterol in the liver (21). In addition, minerals in broccoli, such as magnesium, can also reduce cholesterol absorption. The flavonoids abundant in broccoli are believed to have the ability to scavenge free radicals and accelerate cholesterol breakdown (22). The rich dietary fiber, especially the soluble mucilaginous dietary fiber in broccoli, can bind with bile acids to form insoluble complexes, increasing bile acid excretion in feces and thus reducing bile acid reabsorption and decreasing cholesterol synthesis in the body (23). By regulating lipid metabolism, broccoli may reduce the incidence of cardiovascular disease.

The rich dietary fiber, especially water-soluble fiber in broccoli, can prolong the retention time of food in the gastrointestinal tract and slow down the digestion and absorption of carbohydrates, thereby inhibiting drastic fluctuations in postprandial blood glucose and insulin levels (24). In addition, sulforaphane in broccoli can also promote insulin signal transduction in skeletal muscle and liver tissues, enhancing insulin sensitivity in insulin-resistant tissues and thus lowering blood glucose (25). The high content of vitamin C in broccoli is capable of protecting pancreatic beta cells from oxidative stress damage. Adequate intake of broccoli helps maintain the functionality of pancreatic beta cells, preventing insufficient insulin secretion due to pancreatic cell injury and thus stabilizing blood glucose regulation (22). By regulating glucose and lipid metabolism and enhancing insulin sensitivity, broccoli can reduce the risks of metabolic syndrome, type 2 diabetes, and cardiovascular diseases. The mechanism of broccoli intake in reducing mortality risk, as illustrated above, can be seen in Figure 6.

This study found that, compared with females, males were more suitable to eat broccoli 1–2 times per week, while females were more suitable to eat broccoli ≥3 times per week to obtain the effect of reducing all-cause mortality. This may be related to gender differences in dietary patterns and physiological metabolism. On the one hand, the intake of fruits and vegetables is inherently higher in females' diets (26), so they may need to eat broccoli more frequently to produce significant health effects. On the other hand, increased estrogen levels can promote the expression of glutathione peroxidase, enhancing the body's antioxidant capacity (27), which may make females require higher amounts of antioxidant nutrients in broccoli. Overall, there may be some differences in the optimal frequency of broccoli intake between different genders, which should be further clarified in future studies to provide a basis for dietary guidance for both genders.

This study determined the dose–response relationship between broccoli intake frequency and reduced mortality risk in a large sample population, providing an important basis for developing scientific dietary guidelines. However, as an observational study, it cannot demonstrate a direct causal relationship between broccoli and mortality risk reduction. In addition, considering that the participants were all American adults, there may be some differences between different ethnicities, so the research conclusions should be generalized with caution. Finally, FFQ assessments of dietary intake have some subjectivity and may be subject to recall bias. Future rigorous clinical trials are still needed to verify the health effects of broccoli consumption and determine appropriate intake ranges based on different populations in order to provide more rigorous evidence for formulating dietary guidelines.

Data availability statement

The raw data supporting the conclusions of this article will be made available by the authors, without undue reservation.

Ethics statement

The studies involving humans were approved by the National Center for Health Statistics Research Ethics Review Board, duly approved by the ethical review committee (protocol #98-12, #2005-06). The patients/participants provided their written informed consent to participate in this study.

Author contributions

XL: Conceptualization, Data curation, Writing – original draft. YC: Formal analysis, Writing – original draft, Data curation. YL: Data curation, Visualization, Writing – original draft. XZ: Data curation, Writing – original draft. FL: Formal analysis, Investigation, Writing – original draft. JS: Supervision, Visualization, Writing – original draft. HS: Data curation, Writing – original draft. XC: Conceptualization, Supervision, Validation, Writing – review & editing. JC: Conceptualization, Supervision, Validation, Writing – review & editing.

Funding

The author(s) declare that no financial support was received for the research, authorship, and/or publication of this article.

Acknowledgments

The authors are grateful to the NHANES project members for their extensive work in data collection and follow-up.

Conflict of interest

The authors declare that the research was conducted in the absence of any commercial or financial relationships that could be construed as a potential conflict of interest.

Publisher's note

Supplementary material

The Supplementary material for this article can be found online at: https://www.frontiersin.org/articles/10.3389/fnut.2023.1286658/full#supplementary-material

References

1. Stanaway D, Afshin A, Gakidou E. Global, regional, and national comparative risk assessment of 84 behavioural, environmental and occupational, and metabolic risks or clusters of risks for 195 countries and territories, 1990-2017: a systematic analysis for the global burden of disease study 2017. *Lancet (London, England)*. (2018) 392:1923–94. doi: 10.1016/s0140-6736(18)32225-6

2. Cui J, Liu Y, Li F, Zhuo W, Huang L, Xu C, et al. *Evidence-based guideline on immunonutrition in patients with cancer.* (2023) 2:e00031. doi: 10.1097/pn9.0000000000000031

3. Syed RU, Moni SS, Break MKB, Khojali WMA, Jafar M, Alshammari MD, et al. Broccoli: a multi-faceted vegetable for health: an in-depth review of its nutritional attributes, antimicrobial abilities, and anti-inflammatory properties. *Antibiotics*. (2023). 12:1157. doi: 10.3390/antibiotics12071157

4. Barber TM, Kabisch S, Pfeiffer AFH, Weickert MO. The health benefits of dietary fibre. *Nutrients*. (2020) 12:12. doi: 10.3390/nu12103209

5. Hwang JH, Lim SB. Antioxidant and anticancer activities of broccoli by-products from different cultivars and maturity stages at harvest. *Preventive nutrition and food science.* (2015) 20:8–14. doi: 10.3746/pnf.2015.20.1.8

6. Hwang JH, Lim SB. Antioxidant and anti-inflammatory activities of broccoli florets in LPS-stimulated RAW 264.7 cells. *Preventive nutrition and food sci.* (2014) 19:89–97. doi: 10.3746/pnf.2014.19.2.089

7. Bahadoran Z, Mirmiran P, Hosseinpanah F, Rajab A, Asghari G, Azizi F. Broccoli sprouts powder could improve serum triglyceride and oxidized LDL/LDL-cholesterol ratio in type 2 diabetic patients: a randomized double-blind placebo-controlled clinical trial. *Diabetes research and clinical practice.* (2012) 96:348–54. doi: 10.1016/j.diabres.2012.01.009

8. Nijveldt RJ, van Nood E, van Hoorn DE, Boelens PG, van Norren K, van Leeuwen PA. Flavonoids: a review of probable mechanisms of action and potential applications. *Am J clinical nutrition.* (2001) 74:418–25. doi: 10.1093/ajcn/74.4.418

9. Choi S, Lew KL, Xiao H, Herman-Antosiewicz A, Xiao D, Brown CK, et al. D, L-Sulforaphane-induced cell death in human prostate cancer cells is regulated by inhibitor of apoptosis family proteins and Apaf-1. *Carcinogenesis.* (2007) 28:151–62. doi: 10.1093/carcin/bgl144

10. Pham NA, Jacobberger JW, Schimmer AD, Cao P, Gronda M, Hedley DW. The dietary isothiocyanate sulforaphane targets pathways of apoptosis, cell cycle arrest, and oxidative stress in human pancreatic cancer cells and inhibits tumor growth in severe combined immunodeficient mice. *Mol Cancer Ther.* (2004) 3:1239–48. doi: 10.1158/1535-7163.1239.3.10

11. Fimognari C, Nüsse M, Cesari R, Iori R, Cantelli-Forti G, Hrelia P. Growth inhibition, cell-cycle arrest and apoptosis in human T-cell leukemia by the isothiocyanate sulforaphane. *Carcinogenesis.* (2002) 23:581–6. doi: 10.1093/carcin/23.4.581

12. Gamet-Payrastre L, Li P, Lumeau S, Cassar G, Dupont MA, Chevolleau S, et al. Sulforaphane, a naturally occurring isothiocyanate, induces cell cycle arrest and apoptosis in HT29 human colon cancer cells. *Cancer Res*. (2000) 60:1426–33.

13. Zhang X, Shu XO, Xiang YB, Yang G, Li H, Gao J, et al. Cruciferous vegetable consumption is associated with a reduced risk of total and cardiovascular disease mortality. *The American journal of clinical nutrition*. (2011) 94:240–6. doi: 10.3945/ajcn.110.009340

14. Odutayo A, Gill P, Shepherd S, Akingbade A, Hopewell S, Tennankore K, et al. Income disparities in absolute cardiovascular risk and cardiovascular risk factors in the United States, 1999-2014. *JAMA cardiology.* (2017) 2:782–90. doi: 10.1001/jamacardio.2017.1658

15. Nøst TH, Alcala K, Urbarova I, Byrne KS, Guida F, Sandanger TM, et al. Systemic inflammation markers and cancer incidence in the UK biobank. *European journal of epidemiology.* (2021) 36:841–8. doi: 10.1007/s10654-021-00752-6

16. Wang X, Ouyang Y, Liu J, Zhu M, Zhao G, Bao W, et al. Fruit and vegetable consumption and mortality from all causes, cardiovascular disease, and cancer: systematic review and dose-response meta-analysis of prospective cohort studies. *BMJ (Clinical research ed).* (2014) 349:g4490. doi: 10.1136/bmj.g4490

17. Jiang Y, Wu SH, Shu XO, Xiang YB, Ji BT, Milne GL, et al. Cruciferous vegetable intake is inversely correlated with circulating levels of proinflammatory markers in women. *J Acad Nutr Diet*. (2014) 114:700–8.e2. doi: 10.1016/j.jand.2013.12.019

18. Santín-Márquez R, Alarcón-Aguilar A, López-Diazguerrero NE, Chondrogianni N, Königsberg M. Sulforaphane - role in aging and neurodegeneration. *GeroScience.* (2019) 41:655–70. doi: 10.1007/s11357-019-00061-7

19. Reuter S, Gupta SC, Chaturvedi MM, Aggarwal BB. Oxidative stress, inflammation, and cancer: how are they linked? *Free radical biology & medicine.* (2010) 49:1603–16. doi: 10.1016/j.freeradbiomed.2010.09.006

20. López-Chillón MT, Carazo-Díaz C, Prieto-Merino D, Zafrilla P, Moreno DA, Villaño D. Effects of long-term consumption of broccoli sprouts on inflammatory markers in overweight subjects. *Clinical nutrition (Edinburgh, Scotland).* (2019) 38:745–52. doi: 10.1016/j.clnu.2018.03.006

21. Hoffman CJ, Lawson WE, Miller RH, Hultin MB. Correlation of vitamin K-dependent clotting factors with cholesterol and triglycerides in healthy young adults. *Arteriosclerosis and thrombosis: a journal of vascular biology.* (1994) 14:1737–40. doi: 10.1161/01.atv.14.11.1737

22. Bahadoran Z, Mirmiran P, Azizi F. Potential efficacy of broccoli sprouts as a unique supplement for management of type 2 diabetes and its complications. *Journal of medicinal food.* (2013) 16:375–82. doi: 10.1089/jmf.2012.2559

23. Kahlon TS, Chapman MH, Smith GEJFC. In vitro binding of bile acids by spinach, kale, Brussels sprouts, broccoli, mustard greens, green bell pepper, cabbage and collards. *Nutr Res*. (2007) 100:1531–6. doi: 10.1016/j.foodchem.2005.12.020

24. Bahadoran Z, Mirmiran P, Azizi F. Dietary polyphenols as potential nutraceuticals in management of diabetes: a review. *Journal of diabetes and metabolic disorders.* (2013) 12:43. doi: 10.1186/2251-6581-12-43

25. Teng W, Li Y, Du M, Lei X, Xie S, Ren F. Sulforaphane prevents hepatic insulin resistance by blocking serine Palmitoyltransferase 3-mediated ceramide biosynthesis. *Nutrients.* (2019) 11:11. doi: 10.3390/nu11051185

26. Miller V, Yusuf S, Chow CK, Dehghan M, Corsi DJ, Lock K, et al. Availability, affordability, and consumption of fruits and vegetables in 18 countries across income levels: findings from the prospective urban rural epidemiology (PURE) study. *The Lancet Global health.* (2016) 4:e695–703. doi: 10.1016/s2214-109x(16)30186-3

27. Liu H, Wang H, Shenvi S, Hagen TM, Liu RM. Glutathione metabolism during aging and in Alzheimer disease. *Ann N Y Acad Sci*. (2004) 1019:346–9. doi: 10.1196/annals.1297.059

frontiers | Frontiers in Immunology

TYPE Original Research
PUBLISHED 13 May 2024
DOI 10.3389/fimmu.2024.1404086

OPEN ACCESS

EDITED BY
Diego A. Moreno,
Spanish National Research Council (CSIC), Spain

REVIEWED BY
Ilias Kounatidis,
The Open University, United Kingdom
Kwang-Zin Lee,
Fraunhofer Society (FHG), Germany

*CORRESPONDENCE
Christian Zimmermann
christian.a.zimmermann@ernaehrung.uni-giessen.de

RECEIVED 27 March 2024
ACCEPTED 24 April 2024
PUBLISHED 13 May 2024

CITATION
Zimmermann C, Dähn S and Wagner AE (2024) Effect of allyl-isothiocyanate on survival and antimicrobial peptide expression following oral bacterial infections in *Drosophila melanogaster*. *Front. Immunol.* 15:1404086. doi: 10.3389/fimmu.2024.1404086

Effect of allyl-isothiocyanate on survival and antimicrobial peptide expression following oral bacterial infections in *Drosophila melanogaster*

Christian Zimmermann[1]*, Sonja Dähn[1] and Anika E. Wagner[1,2]

[1]Institute of Nutritional Science, Justus Liebig University, Giessen, Germany, [2]Centre for Sustainable Food Systems, Justus Liebig University, Giessen, Germany

Since infections with antibiotic-resistant bacteria cause increasing problems worldwide, the identification of alternative therapies is of great importance. Plant-derived bioactives, including allyl-isothiocyanate (AITC), have received attention for their antimicrobial properties. The present study therefore investigates the impact of AITC on survival and antimicrobial peptide (AMP) levels in *Drosophila melanogaster* challenged with the fly pathogenic bacteria *Pectobacterium carotovorum* subsp. *carotovorum* and *Leuconostoc pseudomesenteroides*. AITC, a sulfur-containing compound derived from glucosinolates, exhibits antimicrobial properties and has been suggested to modulate AMP expression. By using *D. melanogaster*, we demonstrate that AITC treatment resulted in a concentration-dependent decrease of survival rates among female flies, particularly in the presence of the Gram-negative bacterium *Pectobacterium carotovorum* subsp. *carotovorum*, whereas AITC did not affect survival in male flies. Despite the ability of isothiocyanates to induce AMP expression in cell culture, we did not detect significant changes in AMP mRNA levels in infected flies exposed to AITC. Our findings suggest sex-specific differences in response to AITC treatment and bacterial infections, underlining the complexity of host–pathogen interactions and potential limitations of AITC as a preventive or therapeutic compound at least in *D. melanogaster* models of bacterial infections.

KEYWORDS

allyl-isothiocyanate, anti-microbial peptides, *Drosophila melanogaster*, infection, bioactive plant compound, survival, gene expression

1 Introduction

The widespread use of antibiotics in livestock farming and medicine causes increasing problems with antibiotic-resistant pathogenic bacteria (1). In 2019, antibiotic-resistant

bacteria have been made responsible for 1.27 million deaths worldwide (WHO) (2). The identification and the development of alternative therapies and prevention strategies is, therefore, of high importance for the global fight against severe bacterial infections. In this context, bioactive plant compounds may be a promising alternative in the treatment of diseases caused by antibiotic-resistant bacteria (3). Plant bioactives are compounds produced within the secondary metabolism of plants, which are used either as a defense mechanism against environmental stressors such as UV radiation, predators, and pathogenic microorganisms (4) or as coloring agents and odorants to attract pollinators (5, 6). Various plant bioactives have been shown to exhibit several health-promoting properties including anti-inflammatory, anti-infectious, anticancer, and antibacterial effects (7–10). Especially the sulfur-containing compounds such as isothiocyanates have been suggested to mediate antibacterial properties (8). In the presence of a neutral milieu, isothiocyanates are generated through hydrolysis from glucosinolates (GLS) by the enzymatic action of myrosinase, a thioglucohydrolase. While the GLS can be found in the vacuoles of cruciferous plant cells, myrosinase is generally present in separate myrosin cells and only gets in contact with GLS following the destruction of the plant cell by, e.g., chewing or cutting (11).

Allyl-isothiocyanate (AITC), the compound which is responsible for the pungent taste of, e.g., wasabi, radish, and mustard, is formed during the myrosinase-catalyzed conversion of the GLS sinigrin following cell disruption. In humans, several biological and health-promoting effects of AITC have been postulated, including anti-inflammatory and antioxidant effects as well as anticancer properties and antimicrobial activities (12–14). In particular, AITC has been able to inhibit the growth of different strains of *Campylobacter jejuni* (8), *Escherichia coli*, and *Listeria monocytogenes in vitro* (15). In cell culture studies, it has also been demonstrated that isothiocyanates are able to increase the expression levels of antimicrobial peptides (AMPs). In particular, it has been shown that the isothiocyanate sulforaphane induces the expression of human β-defensin-2 in intestinal epithelial cells (16). AMPs are known to play a critical role in the innate immune response and are produced by a variety of organisms including mammalian species, insects, and plants (17). They are mainly positively charged proteins and can act by membrane- or non-membrane-targeting mechanisms, thereby destroying bacteria, fungi, or viruses. Since recently, AMPs have been suggested as an alternative treatment option in the therapy of bacterial infections (1). Therefore, we suggest that AITC exhibits its antibacterial effect via increasing the expression levels of AMPs. To test this hypothesis, we applied the fruit fly *Drosophila melanogaster* as a model organism. *D. melanogaster* is especially known for its use in genetic research but has also been well established as a model to investigate and answer physiological questions (18). Due to its short generation time, the relatively inexpensive and easy maintenance, and the fact that 60% of the genes present have orthologs in mammals, the fruit fly is an ideal model for studying evolutionarily conserved genes and signaling pathways (19, 20). Due to the absence of an adaptive immune response in the fruit fly, processes of the innate immunity can be studied individually (21). In *D. melanogaster*, AMPs are produced in the fat body following systemic infections but also to a certain extent in the gut epithelia. The formation of AMPs in *D. melanogaster* is triggered by the activation of the two NFκB pathways, the toll- and the Imd pathway (22). This is highly similar to humans, where the expression of AMPs is also initiated by an activation of toll-like-receptors (23). To activate these pathways in *D. melanogaster*, we orally applied the two different fly-pathogenic bacterial strains *Pectobacterium carotovorum* subsp. *carotovorum* (ECC) and *Leuconostoc pseudomesenteroides* (LP), which have been shown to induce AMP secretion (24–26). ECC is a Gram-negative bacterium; therefore, it is a potential activator of the Imd pathway. LP is a Gram-positive bacterium, potentially activating the toll pathway (27). To test, whether AITC intervenes in these processes we fed flies AITC-supplemented diets, exposed them to the pathogenic bacteria and checked the flies for health-related parameters including survival and AMP expression.

2 Materials and methods

2.1 Husbandry of w^{1118} *Drosophila melanogaster*

Female and male w^{1118} *D. melanogaster* (Bloomington Drosophila Stock Center, Indiana, USA; #5905) were reared under standard conditions in a climate chamber (Memmert, HPP400, Büchenbach, Germany) at 25°C and 60% humidity with a 12 h/12 h light–dark cycle on Caltech Medium (CT), as described previously (28). For experiments, 3-day-old age-matched flies from synchronized eggs were anesthetized with CO_2 or on ice and separated according to their sex. Then, 25 flies were transferred into vials containing either the control medium or bacterial suspension. The control medium comprises 10% sucrose (Carl Roth, Karlsruhe, Germany), 10% inactive yeast (Genesee via Kisker, Steinfurt, Germany), 2% agar (Apex via Kisker), and as preservatives 0.3% propionic acid (Carl Roth) and 1.5% tegosept (Apex via Kisker) (Linford et al., 2013). A 1-M stock solution of AITC (Sigma-Aldrich, Taufkirchen, Germany) was prepared in ethanol (abs.) (Merck, Darmstadt, Germany). To investigate the effect of AITC and/or bacteria on food intake, survival, and gene expression, different concentrations of AITC (0.250 mM, 0.125 mM) were added to the control medium. For control medium, the same amount of ethanol (abs.) was added to the food.

2.2 Bacterial strains and cultivation

For infection studies, the fly pathogenic bacteria *Pectobacterium carotovorum* subsp. *carotovorum* (ECC) (Leibniz Institute DSMZ – German Collection of Microorganisms and Cell Cultures, Braunschweig, Germany) and *Leuconostoc pseudomesenteroides* (LP) (kind gift from Dr. Kwang-Zin Lee, Fraunhofer Institute for Molecular Biology and Applied Ecology, IME, Giessen, Germany) were grown in LB-Broth (Carl Roth) and MRS-Broth (Carl Roth), respectively. Both bacterial strains used were cultivated in a shaking incubator (B. Braun Biotech International, Melsungen, Germany)

under aerobic conditions at 29°C and grown over night. In experiments, both bacterial strains were applied in their stationary growth phase.

2.3 Oral infection of w^{1118} *Drosophila melanogaster* with *Pectobacterium carotovorum* subsp. *carotovorum* and *Leuconostoc pseudomesenteroides*

For infection experiments, overnight cultures of ECC and LP were adjusted to an OD of 1 with a 100-mM sterile sucrose solution. Subsequently, 1 ml of the bacteria-sucrose suspension or sterile sucrose solution (control solution) was applied to three layers of cellulose paper lining the bottom of the respective vial. Three-day-old age-matched female and male *D. melanogaster* from synchronized eggs were transferred into these vials (25 flies per vial) and maintained under standard conditions for 18 h (see 2.1).

2.4 Gustatory assay

To check for potential effects of AITC on the feeding behavior of *D. melanogaster*, the flies' food intake was determined by applying the gustatory assay according to Deshpande et al. (29). The flies received either a control or an AITC-supplemented diet for 10 days. On day 10, flies were transferred to control medium with and without AITC (0.125 mM and 0.250 mM) supplemented with 0.2% sulforhodamine B sodium salt (Sigma-Aldrich) and kept under standard conditions (see 2.1) for further 8 h. Then, 20 flies per treatment were transferred in 200 µl PBS (pH 7.4) (Thermo Fisher Scientific, Schwerte, Germany) with 1% Triton X-100 (Sigma-Aldrich) and homogenized in a TissueLyser II (Qiagen, Hilden, Germany) at a frequency of 25 s^{-1} for 6 min. Following, the obtained samples were centrifuged (4,000 g, 5 min) and the fluorescence signal (extinction: 535 nm/emission: 590 nm) of the supernatant was detected in a microplate reader SpectraMax iD3 (Molecular Devices, San Jose, USA). Flies fed unstained food served as controls, and the corresponding values were subtracted from the sample readings. Serial dilutions of sulforhodamine B sodium salt were used to generate a standard curve.

2.5 Survival analysis

In order to investigate an effect of both, bacterial infection and AITC supplementation, on the survival rate of *D. melanogaster*, 3-day-old flies from synchronized eggs were separated according to their sex, sorted into different vials, and exposed to the corresponding treatments as depicted in Figure 1. Each experiment was performed two to three times with three vials per sex containing 25 flies each. Every 2–3 days, flies were transferred to new vials with fresh food, whereas dead flies were removed and counted.

2.6 RNA-isolation and real-time PCR

In order to investigate an effect of both, bacterial infection and AITC supplementation, on mRNA expression 3-day-old flies were exposed to the corresponding treatments as depicted in Figure 2. RNA was either isolated by applying TRI Reagent (Ambion, Carlsbad, USA) or the Quick-RNA Tissue/Insect kit (Zymo Research, Freiburg, Germany). In case of RNA isolation with TRI Reagent, five flies were put in a microcentrifuge tube containing 1 ml TRI Reagent and homogenized in a TissueLyser II (Qiagen) at a frequency of 25 s^{-1} for 6 min. After adding 200 µl chloroform, the samples were vortexed and incubated at room temperature for 10 min. Subsequently, the samples were centrifuged at 12,000 g at 4° C for 15 min. Then, the resulting upper, clear phase was transferred

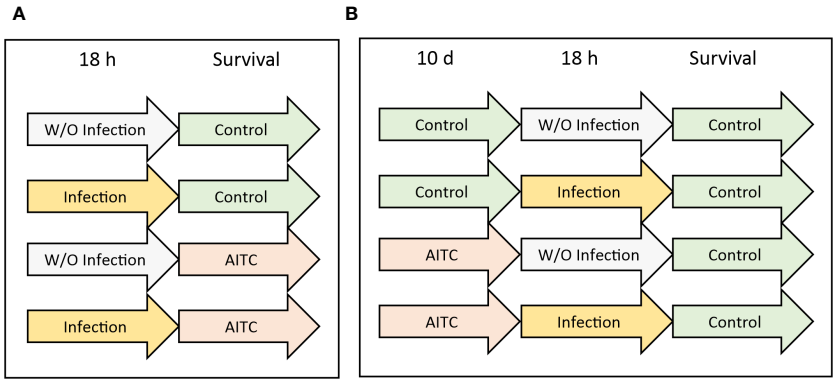

FIGURE 1
Experimental procedure of survival analysis. **(A)** *D. melanogaster* were initially exposed to a 100-mM sucrose solution with or without *L. pseudomesenteroides* or *P. carotovorum* subsp. *carotovorum* for 18 h and were subsequently transferred on either a control or an AITC-supplemented diet (0.125 mM or 0.250 mM) for the rest of their lifetime. **(B)** *D. melanogaster* were initially kept on either a control or an AITC-supplemented diet (0.125 mM or 0.250 mM) for 10 days, followed by an exposure to a 100-mM sucrose solution with or without *L. pseudomesenteroides* or *P. carotovorum* subsp. *carotovorum* for 18 h and were subsequently transferred on a control diet for the rest of their lifetime.

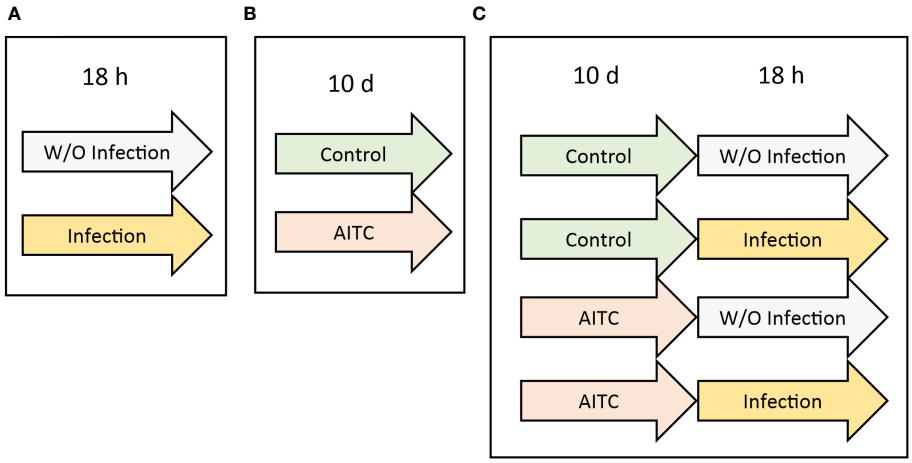

FIGURE 2
Experimental procedure of generating fly samples for subsequent mRNA analysis. **(A)** *D. melanogaster* were initially exposed to a 100-mM sucrose solution with *P. carotovorum* subsp. *carotovorum* or *L. pseudomesenteroides* for 18 h. **(B)** *D. melanogaster* were fed either a control diet or an AITC-supplemented diet (0.125 mM or 0.250 mM) for 10 days. **(C)** *D. melanogaster* were initially kept on either a control or an AITC-supplemented diet (0.125 mM or 0.250 mM) for 10 days and were subsequently transferred to a 100-mM sucrose solution with or without *L. pseudomesenteroides* or *P. carotovorum* subsp. *carotovorum* for 18 h. .

into a fresh microcentrifuge tube, mixed with 500 µl ice cold isopropanol, and left on ice for 10 min. Following, the samples were centrifuged at 12,000 g at 4°C for 15 min. The resulting supernatant was discarded, and the remaining pellet was washed twice with 500 µl ice cold 75% ethanol followed by centrifugation at 12,000 g at 4°C for 10 min. After removing the ethanol in the last washing step, the pellets were air-dried at room temperature for 30 min. Following, the dried pellet was resuspended in 50 µl RNase-free-water (Th. Geyer, Renningen, Germany) and dissolved at 55°C for 10 min. Subsequently, RNA samples were subjected to DNase treatment by applying the DNase kit (Sigma-Aldrich) according to the manufacturer's instructions. In brief, 20 µl of isolated RNA was mixed with 2.5 µl DNase reaction buffer (Sigma-Aldrich) and 2.5 µl DNase I amplification grade (1 U/µl) (Sigma-Aldrich). After 15 min of incubation at room temperature, a 2.5-µl stop solution (Sigma-Aldrich) was added. Then, the samples were heated to 70°C for 10 min. Samples were stored at -80°C until further use.

RNA isolation with the Quick-RNA Tissue/Insect kit (Zymo Research, Freiburg, Germany) was performed according to the manufacturer's instructions. In brief, 10 flies were homogenized in RNA lysis buffer. After that, the homogenate was transferred into a column tube followed by several washing steps and DNase treatment. Finally, RNA was eluted in DNase/RNase-free water. RNA was stored at −80°C until further use.

The purity of the RNA samples was photometrically detected (260/280 nm) in a UVmini-1240 UV-VIS spectrophotometer (Shimadzu, Duisburg, Germany). Samples with a 260/280-nm ratio lower than 1.7 were excluded from further analysis.

For cDNA synthesis, 1 µg RNA was added to DNase/RNase-free-water, resulting in a total volume of 11.5 µl. Then, 1 µl oligo (dt) primers (20 ng/µl) (Promega, Mannheim, Germany), 4 µl M-MLV RT 5× Buffer (Promega), 0.5 µl RNasin RiboLock (40 U/µl) (Sigma-Aldrich), 2 µl dNTP mix (10 mM) (Promega), and 1 µl M-MLW reverse transcriptase (200 U/µl) (Promega) were added. Afterward, the samples were incubated at 42°C for 60 min and subsequently heated in a thermocycler (T-Gradient ThermoBlock, Biometra, Göttingen, Germany) at 70°C for 10 min. The obtained cDNA was stored at −80°C until further use.

For real-time PCR, cDNA was diluted 1:2 in DNase/RNase-free-water. The master mix contained 10 µl PerfeCTa SYBR Green SuperMix, Low ROX (Quantabio, Beverly, MA, USA), 0.25 µl forward/reverse primer (10 pmol/µl), 7.5 µl DNase/RNase-free-water, and 2 µl cDNA.

Semiquantitative real-time PCR was performed in a 7500 Real-Time PCR system (Applied Biosystems, Heidelberg, Germany). *rPl32* (Ribosomal Protein L32), *RpS20* (Ribosomal Protein S20), and *alphaTub84B* (alpha-Tubulin at 84B) were tested as reference genes. *alphaTub84B* showed treatment-dependent effects, why it was excluded as a reference gene. *rPl32* and *RpS20* were used as reference genes (see for *RpS20* in Supplementary Table S1). *Dro* (Drosocin) and *mtk* (Metchnikowin) were measured as target genes (for primer sequences, see Table 1).

2.7 Statistics

Statistical analyses were carried out using GraphPad Prism Software (Version 10.1.2, GraphPad Software, LLC, San Diego, CA, USA). Unless otherwise stated, the experiments were performed in triplicates. Results are presented as mean ± standard deviation (SD) unless otherwise stated. Data were tested for normality of distribution (Shapiro–Wilk) and homogeneity of variances (Brown–Forsythe or Bartlett's). The means of normally distributed data and homogenous variances were compared by one-way ANOVA followed by a *post hoc* test (Tukey's) for multiple comparisons. Data with heterogeneous variances were tested with

TABLE 1 Primer sequences for real-time PCR (*Drosophila melanogaster*).

Gene	Forward primer (5′ → 3′)	Reverse primer (3′ → 5′)	Accession no.	Temp.
dro	GAGGATCACCTGACTCAAGC	ATGACTTCTCCGCGGTATG	NM_001259395.2	56°C
mtk	CCTCATCGTCACCAGGGACC	TTGGACCCGGTCTTGGTTGG	NM_079028.3	55°C
rPl32	GGCAAGCTTCAAGATGACCA	GTTCGATCCGTAACCGATGT	NM_170461.3	55°C
RpS20	TGTGGTGAGGGTTCCAAGAC	GACGATCTCAGAGGGCGAGT	NM_079697.3	58°C
alphaTub84B	TCAGACCTCGAAATCGTAGC	AGCCTGACCAACATGGATAG	NM_057424.4	55°C

dro, Drosocin; mtk, Metchnikowin; rPl32, ribosomal protein L32; RpS20, ribosomal protein S20; alphaTub84B, alpha-tubulin at 84B.

Brown–Forsythe–Welch ANOVA followed by a *post hoc* test (Dunnet's T3) for multiple comparisons. Not normally distributed data were tested with a non-parametric test (Kruskal–Wallis). Survival analysis was performed by the Kaplan–Meier approach and a log-rank test to test for significant differences. Median survival times were calculated and tested for significant differences by the Mann–Whitney test. Significance was accepted at $p < 0.05$.

3 Results

3.1 Effect of AITC on food intake of w^{1118} *Drosophila melanogaster*

To test whether AITC enrichment at different concentrations has an effect on food intake in *D. melanogaster*, a gustatory assay was performed. The application of 0.125 mM AITC for 10 days did not affect the flies' food intake, either in female or in male *D. melanogaster*. In contrast, addition of 0.250 mM AITC significantly reduced the food intake in male flies by approximately 7% but not in female flies (Figures 3A, B).

3.2 Effect of AITC-supplemented diet and bacterial infection on survival of w^{1118} *Drosophila melanogaster*

A survival assay was performed to investigate potential effects of both bacterial infection and AITC supplementation, on the flies' survival rates. *D. melanogaster* initially exposed for 18 h to a 100-mM sucrose solution and subsequently transferred on an AITC-supplemented (Figure 4A) diet led to a significant concentration-dependent decrease of survival time of female flies. In contrast, no effects of AITC on male flies were observed. The medium survival times did not differ between the groups (Figures 4B, C). In female flies, infection with ECC resulted in a decreased survival whereas no significant effect was observed after LP infection. In contrast, LP infection of male flies resulted in an increased survival whereas ECC infection had no effect on the survival of male flies (Figures 4D, E).

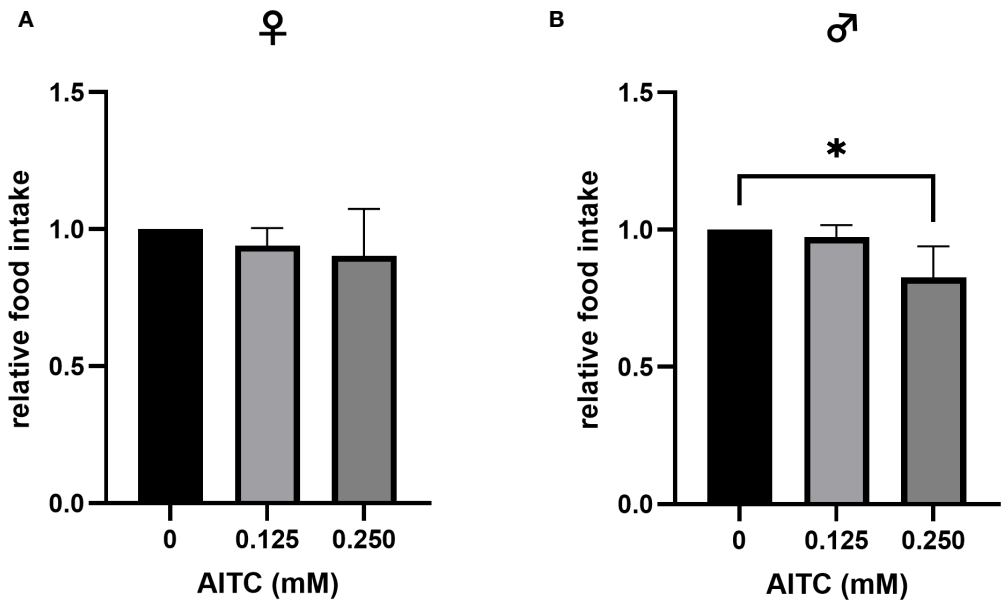

FIGURE 3
Relative food intake of female **(A)** and male **(B)** *D. melanogaster* fed either a control diet or an AITC-supplemented diet (0.125 mM or 0.250 mM), respectively, for 10 days. Bars show the mean ± SD of three independent experiments. Significant differences between groups were tested by applying one-way ANOVA followed by Dunnett's multiple-comparison test. Significance was accepted at $p < 0.05$. *$p < 0.05$.

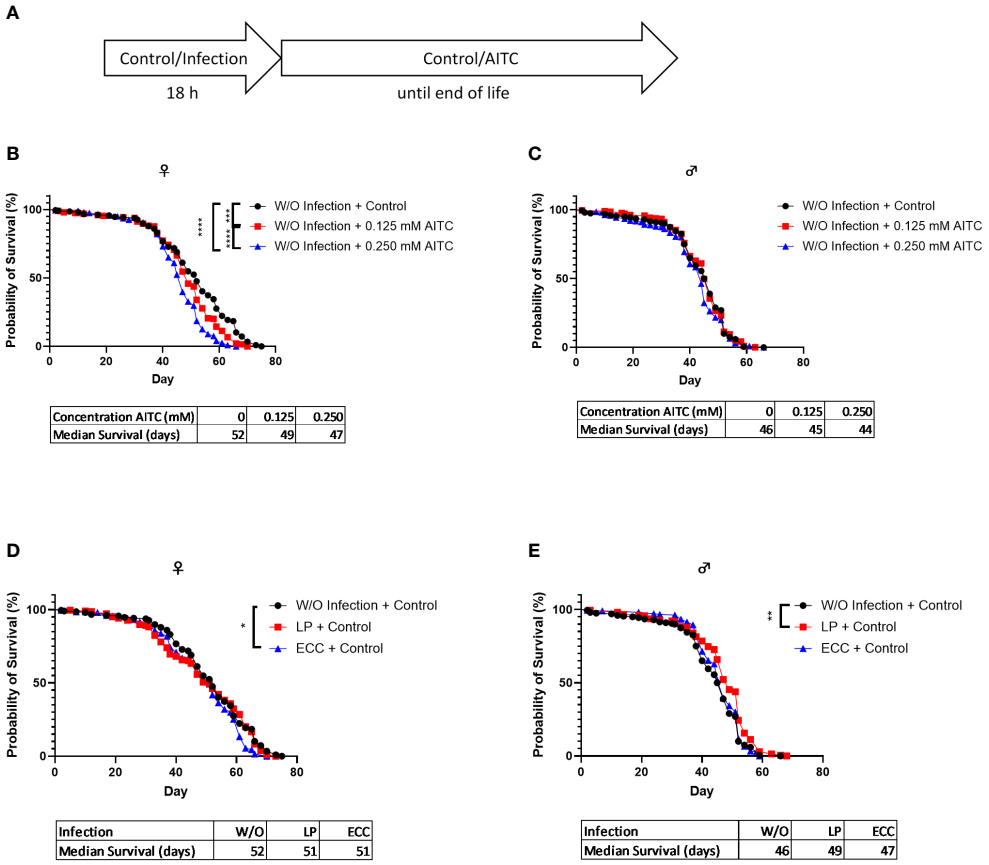

FIGURE 4
Survival curves and median survival time of female **(B, D)** and male **(C, E)** *D. melanogaster* initially exposed to a control solution (W/O Infection) **(B, C)** or a solution with *L. pseudomesenteroides* (LP) or *P. carotovorum* subsp. *carotovorum* (ECC) **(D, E)** for 18 h and subsequently transferred on either a control or an AITC-supplemented diet (0.125 mM or 0.250 mM) for the rest of their lifetime. The experiment procedure is shown in **(A)**. Results show the three independent experiments. Significant differences between treatments were tested by the Kaplan–Meier approach and a log-rank test. Significance was accepted at $p < 0.05$. **p < 0.01, ***p < 0.001, ****p < 0.0001.

In *D. melanogaster* infected with either ECC or LP and subsequent exposure to AITC (Figure 5A), AITC exhibited a significant effect on survival times in ECC-infected female flies only (Figures 5B–E). In this case, the administration of 0.125 mM and 0.250 mM AITC significantly reduced the survival time in a concentration-dependent manner (Figure 5D).

D. melanogaster initially kept on an AITC-supplemented diet for 10 days (Figure 6A) did not show any difference in survival rates compared with flies reared on a control diet (Figures 6B, C). Both ECC and LP infections of female flies reared on a control diet for 10 days also did not have any effect on the survival rates (Figure 6D). In contrast, infection of male flies with ECC resulted in significantly higher survival rates whereas there was no significant difference in the median survival (Figure 6E). A pre-feeding with AITC for 10 days (Figure 7A) resulted in a concentration-dependent decrease in survival rates of ECC-infected female flies (Figure 7D) whereas in ECC-infected male flies, a reduced survival time was observed following exposure of the higher compared with the lower concentration of AITC (Figure 7E). AITC pre-feeding did not exhibit any effects on flies infected with LP (Figures 7B, C).

3.3 Effect of bacterial infections and AITC supplementation on gene expression of antimicrobial peptides in w^{1118} *Drosophila melanogaster*

In order to test for potential changes in the production of AMPs, gene expression levels of *dro* and *mtk* were examined. Neither in flies infected with ECC or LP for 18 h (Figures 8A, B and 9A, B) nor in flies kept on an AITC-supplemented diet for 10 days (Figures 8C, D and 9C, D) effects on either *dro* or *mtk* mRNA expression levels were observed. Flies initially kept on a control diet or an AITC-supplemented diet for 10 days with or without a subsequent bacterial infection did not show any significant changes in *dro* or *mtk* mRNA levels. This applied to infections with both bacterial strains and to both sexes (Figures 10A–H and 11B–H). Only ECC-infected female flies, pre-exposed to an AITC-supplemented diet for 10 days, showed a significant 4.5-fold increase of *mtk* expression levels compared with the uninfected controls (Figure 11A) whereas no significant effect was detected for *dro* expression levels (Figure 10A).

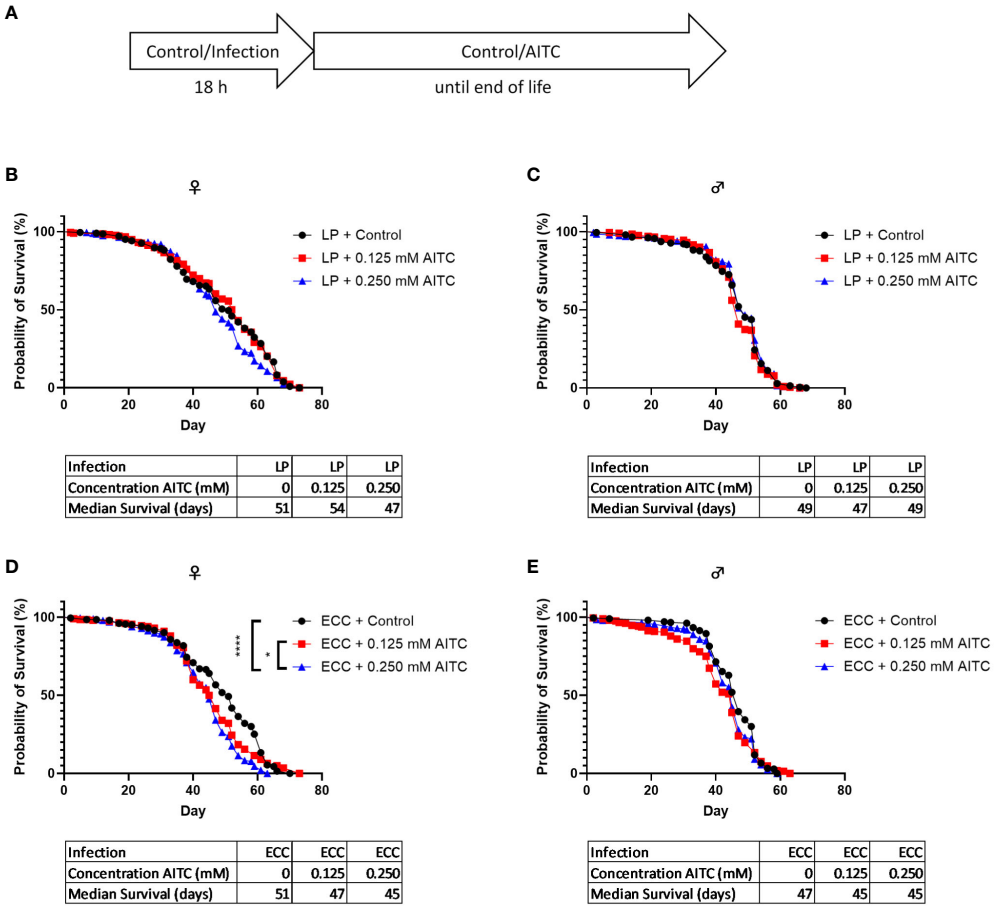

Infection	LP	LP	LP
Concentration AITC (mM)	0	0.125	0.250
Median Survival (days)	51	54	47

Infection	LP	LP	LP
Concentration AITC (mM)	0	0.125	0.250
Median Survival (days)	49	47	49

Infection	ECC	ECC	ECC
Concentration AITC (mM)	0	0.125	0.250
Median Survival (days)	51	47	45

Infection	ECC	ECC	ECC
Concentration AITC (mM)	0	0.125	0.250
Median Survival (days)	47	45	45

FIGURE 5
Survival curves and median survival time of female **(B, D)** and male **(C, E)** *D. melanogaster* initially exposed to a solution with *L. pseudomesenteroides* (LP) **(B, C)** or *P. carotovorum* subsp. *carotovorum* (ECC) **(D, E)** for 18 h and subsequently transferred on either a control or an AITC-supplemented diet (0.125 mM or 0.250 mM) for the rest of their lifetime. The experiment procedure is shown in **(A)**. Results show three independent experiments. Significant differences between treatments were tested by the Kaplan–Meier approach and a log-rank test. Significance was accepted at $p < 0.05$. *$p < 0.05$, ****$p < 0.0001$.

4 Discussion

The rise of bacterial resistance to antibiotics shows a need to identify alternative therapies. Antimicrobial peptides (AMPs) are emerging as promising candidates due to their potent antimicrobial properties (23, 30). Modulating the production of endogenous AMPs, as being already shown for the isothiocyanate sulforaphane *in vitro*, may offer a possibility for preventing bacterial infections (16).

We therefore asked whether AITC may be a potential candidate compound in the treatment of bacterial infections and whether it affects the endogenous production of AMPs. To test health-promoting effects, we initially analyzed the survival of fruit flies exposed to AITC and/or pathogenic bacteria. In male flies, we did not detect any effect of both applied AITC concentrations without the presence of pathogenic bacteria on survival time, neither in a short-term nor in a long-term treatment (Figures 4C, 6C). Intriguingly, we did not detect any effect of AITC on the food intake in female flies but in male flies where 0.250 mM AITC in the diet resulted in a significantly lower food intake (Figure 3B). This may explain the unaltered survival curves following AITC exposure in males compared with females where a long-term treatment with AITC resulted in a significant and dose-dependent decrease of the survival rates (Figure 4B). Due to the lower food intake of male flies, they potentially also consume less AITC, which could explain the difference in mortality compared with female flies. In addition, in male flies, AITC may have induced a kind of caloric restriction, which is well documented to increase lifespan in *D. melanogaster* (31). Interestingly, Merinas-Amo and colleagues (32) tested different cultivars of *Brassica rapa* with a high difference in their individual GLS and consequently isothiocyanate content on effects on the lifespan of *D. melanogaster*. The authors observed a significant dose-dependent increase of the flies' lifespan, which was in contrast to the results of the present study where a significant decrease in the lifespan of female flies (Figure 4B) and no effect on male flies following exposure to AITC (Figure 4C) was detected. These differences may have occurred from the fact that our flies received the isolated isothiocyanate (and not the corresponding precursor sinigrin) via the diet and our results were generated sex-specifically.

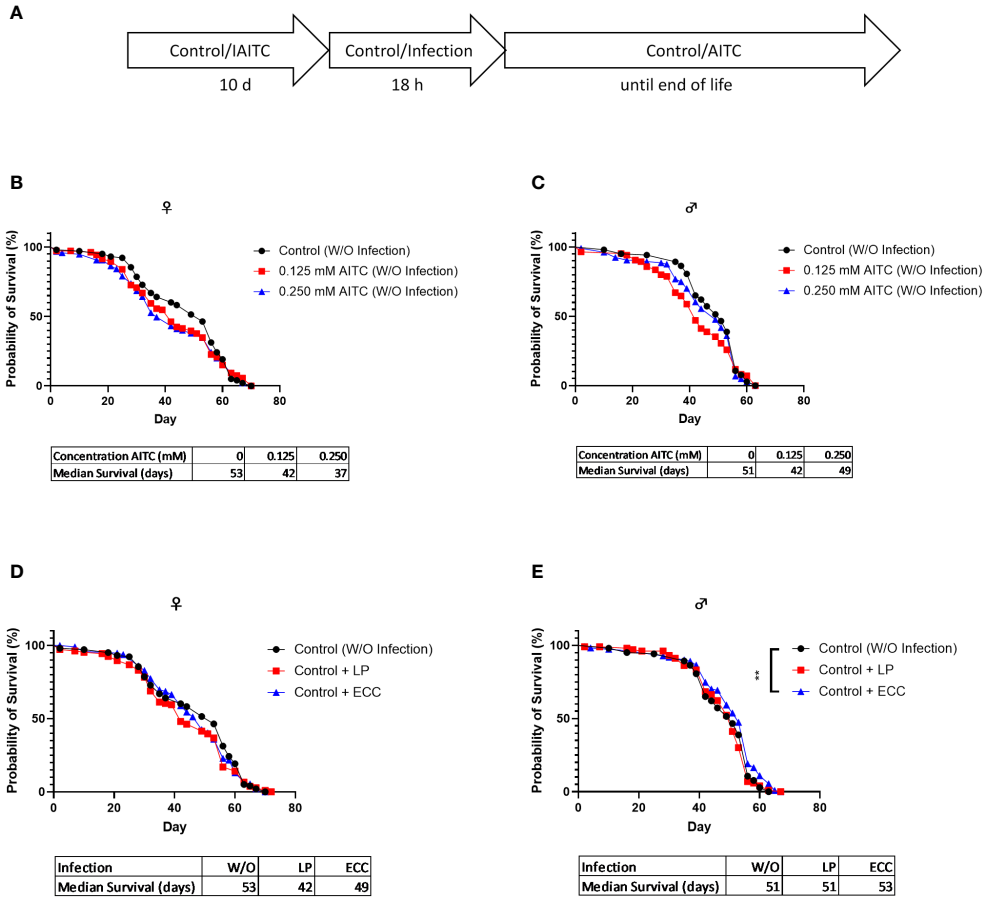

FIGURE 6
Survival curves and median survival time of female **(B, D)** and male **(C, E)** *D. melanogaster* initially kept on either a control or an AITC-supplemented diet (0.125 mM or 0.250 mM) for 10 days then exposed to a control solution (W/O infection) **(B, C)** or a solution with *L. pseudomesenteroides* (LP) or *P. carotovorum* subsp. *carotovorum* (ECC) **(D, E)** for 18 h and subsequently transferred on a control diet for the rest of their lifetime. The experiment procedure is shown in **(A)**. Results show two independent experiments. Significant differences between treatments were tested by the Kaplan–Meier approach and a log-rank test. Significance was accepted at $p < 0.05$. **$p < 0.01$.

One explanation for the detected higher mortality in female flies may have resulted from the applied AITC concentrations that were possibly too high. Insecticidal effects of AITC have been described for other insects but not for *D. melanogaster* (33–36). However, it should be considered that the increased mortality in most studies was caused by AITC applied as a volatile substance. Numerous positive effects were observed in other organisms after an oral ingestion of AITC or AITC-containing extracts possibly due to the intestinal metabolization of AITC (37–42).

However, Mazari et al., 2014 (43) did not detect any weakness or impaired phenotype in wild-type fruit flies exposed to 1 mM AITC in their diet. However, male flies being transgenic for GSTE7, an enzyme important for detoxifying xenobiotics, had a significantly higher mortality when exposed to phenethyl isothiocyanate for 1 week compared with female GSTE7 transgenic flies (43). This may explain the detected differences in the lifespan between male and female flies according to AITC treatment in the present study. Potentially, our male flies had higher GSTE7 levels compared with female flies resulting in an improved detoxification of AITC, which caused the better survival of male compared with female flies.

Although this does not support a potential toxic effect of AITC in our flies, it may be the reason for unchanged *mtk* and *dro* mRNA levels following the exposure to AITC. To examine if AITC exhibited health benefits and affected the mRNA expression of AMPs in pathogen-infected *D. melanogaster*, we orally applied the fly pathogenic bacteria ECC and LP to both female and male *D. melanogaster*. In order to study host–pathogen interactions including the production of AMPs, ECC-infected *D. melanogaster* have already been used (44, 45). Piegholdt et al. (45) showed that ECC induced the mRNA expression levels of the AMPs *mtk*, *dro*, *attB* (attacin B), *attC* (attacin C), and *dpt* (diptericin). In addition, ECC exposure reduced the survival of our *D. melanogaster* under nutrient deficiency (Supplementary Figure S1), as shown for other bacteria (46, 47). For LP-mediated infections, to the best of our knowledge, there is currently only information for bacteriocins produced by LP but no information on a potential effect on AMP expression levels available. However, LP infection also reduced the survival of fruit flies under nutrient deficiency (Supplementary Figure S1), which supports the findings of Hiebert et al. (47). In case of an oral 18-h-infection of 3-day-old female *D. melanogaster* under sufficient nutrient supply, we observed a significant reduction

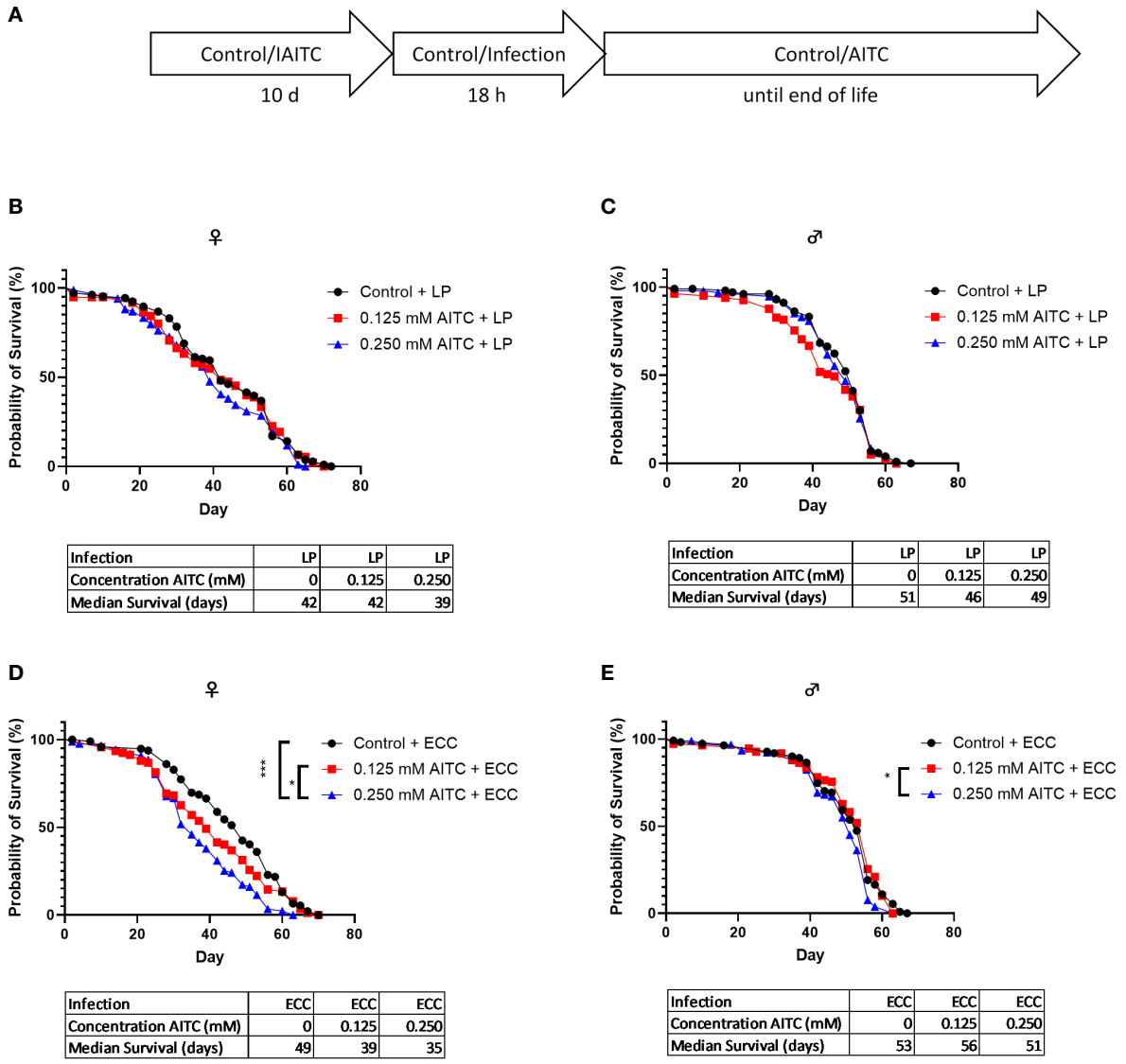

Infection	LP	LP	LP
Concentration AITC (mM)	0	0.125	0.250
Median Survival (days)	42	42	39

Infection	LP	LP	LP
Concentration AITC (mM)	0	0.125	0.250
Median Survival (days)	51	46	49

Infection	ECC	ECC	ECC
Concentration AITC (mM)	0	0.125	0.250
Median Survival (days)	49	39	35

Infection	ECC	ECC	ECC
Concentration AITC (mM)	0	0.125	0.250
Median Survival (days)	53	56	51

FIGURE 7
Survival curves and median survival time of female **(B, D)** and male **(C, E)** *D. melanogaster* initially kept either on a control or an AITC-supplemented diet (0.125 mM or 0.250 mM) for 10 days then exposed to a solution with *L. pseudomesenteroides* (LP) **(B, C)** or *P. carotovorum* subsp. *carotovorum* (ECC) **(D, E)** for 18 h and subsequently transferred on a control diet for the rest of their lifetime. The experiment procedure is shown in **(A)**. Results show two independent experiments. Significant differences between treatments were tested by the Kaplan–Meier approach and a log-rank test. Significance was accepted at $p < 0.05$. *$p < 0.05$, **$p < 0.01$, ***$p < 0.001$.

in survival time following ECC treatment (Figure 4D). In contrast, an infection of 13-day-old female flies had no effect on survival (Figure 6D). In male flies, an infection with LP at the age of 3 days and an infection with ECC at the age of 13 days even resulted in a significant increase in survival time (Figure 4E and Figure 6E). This may be due to a sex-specific response to bacterial infections. It was demonstrated that in general males and females in various species differ in their immunological responses. When challenged with antigens, females generally have a more protective humoral and cell-mediated immune response, whereas for males, more intense inflammatory immune responses were described (48, 49). In *D. melanogaster*, female flies were described to be more likely than male flies to die from infections with several strains of *Beauveria bassiana*, which was postulated to be substantiated from sex-specific differences in the toll and the Imd pathway (50). These pathways are activated by bacteria and fungi consequently inducing the production of AMPs in *D. melanogaster* (27), which only owns an innate immune system (21). The negative effect of AITC on the survival time of female *D. melanogaster* appeared to reinforce the influence of ECC, as an AITC dose-dependent reduction in survival time was observed in both, in an infection followed by long-term treatment with AITC (Figure 5D) and in a 10-days treatment with AITC followed by a subsequent infection (Figure 7D).

When looking at the expression levels of AMPs, no significant differences were detected for *dro* and *mtk* after an 18-h-infection with ECC and LP of 3-day-old female and male flies (Figure 8A and Figure 9A). However, it has to be considered that larger variations between the experimental replicates may have masked a potential

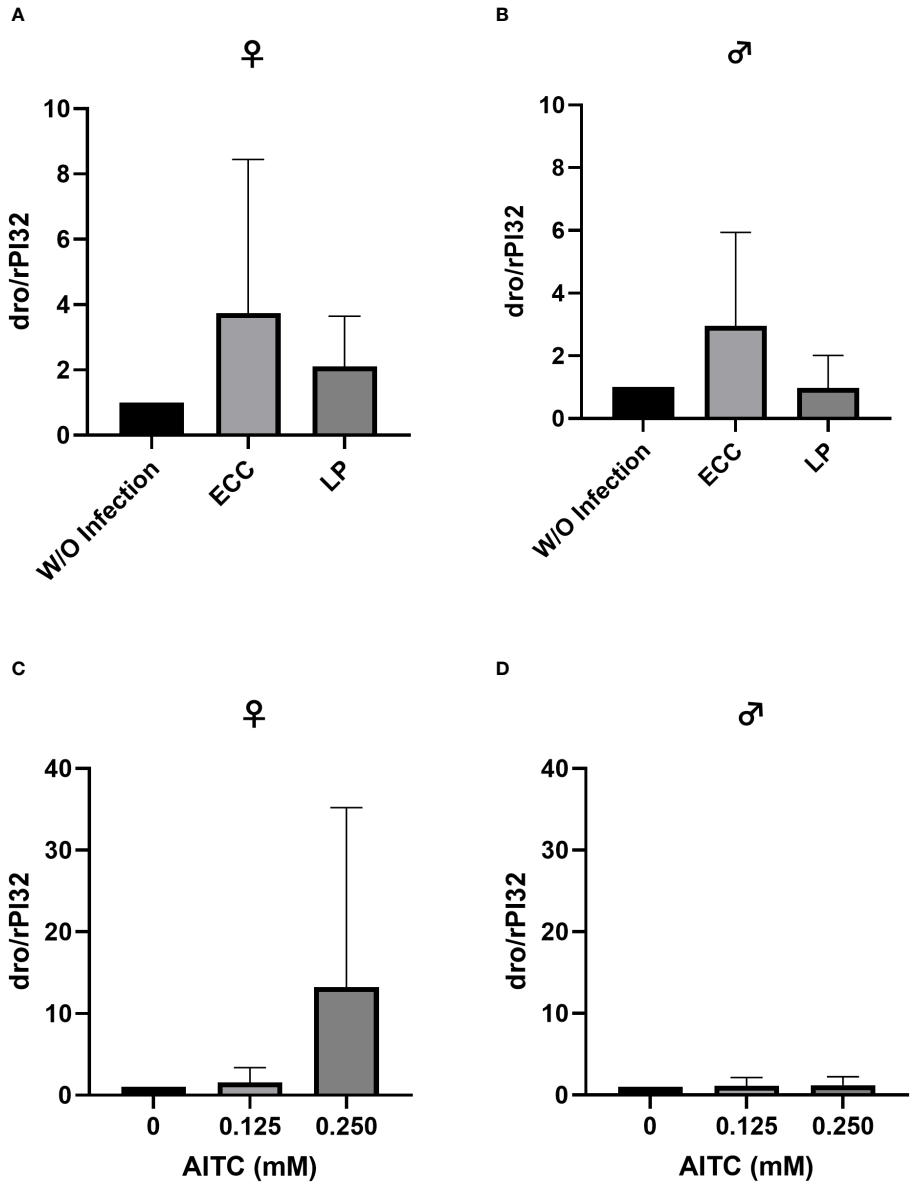

FIGURE 8
Relative mRNA expression levels of *dro* in female **(A, C)** and male **(B, D)** *D. melanogaster* exposed to a 100-mM sucrose solution with *P. carotovorum* subsp. *carotovorum* (ECC) or *L. pseudomesenteroides* (LP) for 18 h **(A, B)** and *D. melanogaster* fed either a control diet or an AITC-supplemented diet (0.125 mM or 0.250 mM) for 10 days **(C, D)**. mRNA levels were determined in fly samples from three independent experiments with three replicates containing 10 flies each. Bars show the mean ± SD. Significant differences between groups were tested by applying one-way ANOVA followed by Dunnett's multiple comparison test. Significance was accepted at $p < 0.05$.

increase in AMP expression levels. Since we analyzed the AMP expression in the whole organism, a detection of AMP levels in individual organs might have reduced the observed variations in our data. In contrast, the infection of 13-day-old females with ECC led to a significant higher expression level of *mtk* (Figure 11A). Rera et al. (51) showed that the expression of AMPs was tightly related to a dysfunction of the intestinal barrier, which increased in the course of life and therefore caused higher AMP levels in older flies (52–54). These adverse effects on the intestinal barrier may be further increased by pathogenic infections. With regard to the AMP expression levels in our flies being exposed to AITC, no effect of both AITC concentrations was observed (Figures 8-11). This was also true for additional bacterial infections, where AITC was applied after oral bacterial infections (Figures 10, 11). Perhaps the larger variations between the experimental replicates, which could be due to differences between the individual flies, masked a potential statistically significant difference between the AMP expression levels.

In female fruit flies, the response to infections also seems to depend on whether they have already mated. If there was only a limited amount of energy available, the fly had to decide where to invest the energy—either in the process of reproduction or in the immune defense. Experiments conducted by Gordon and colleagues (55) support this assumption since infected mated female flies had a

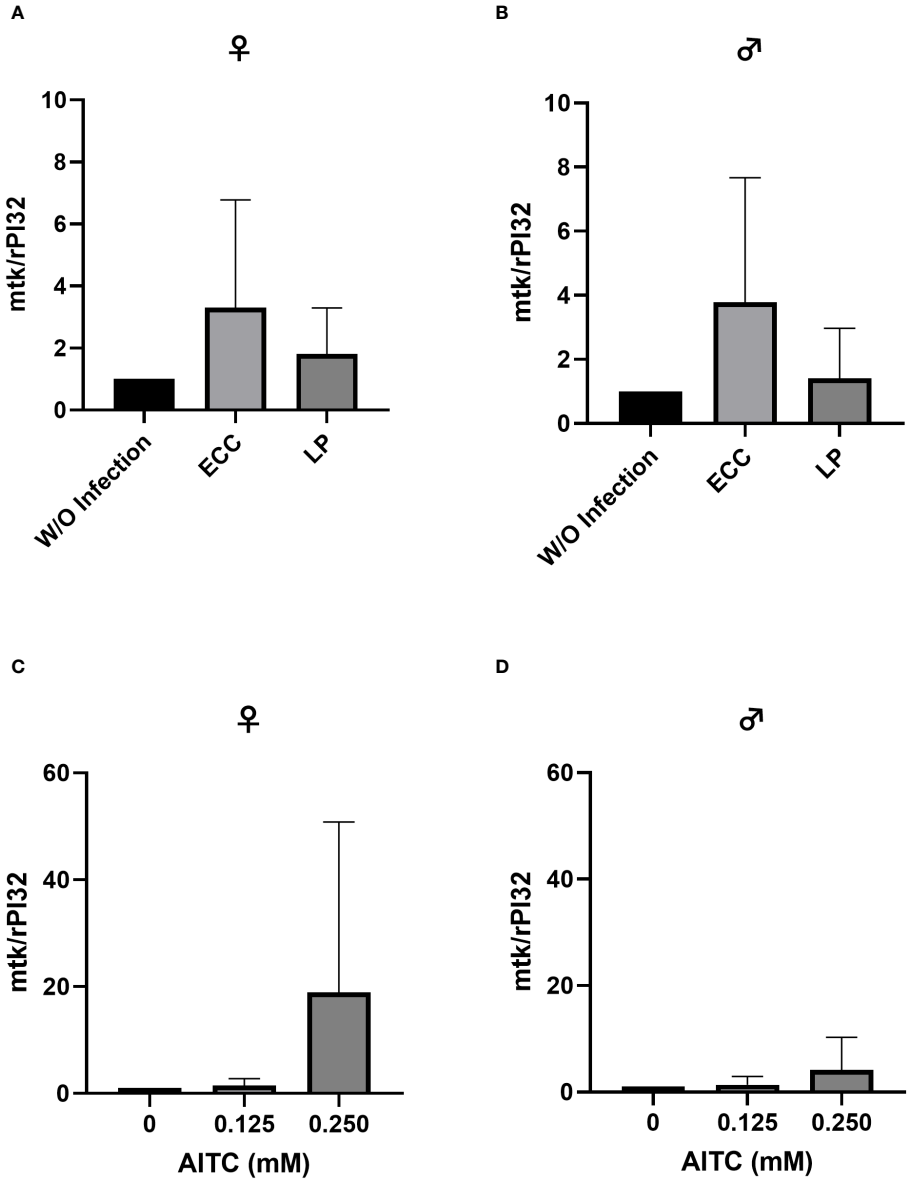

FIGURE 9
Relative mRNA expression levels of *mtk* in female **(A, C)** and male **(B, D)** *D. melanogaster* exposed to a 100-mM sucrose solution with *P. carotovorum* subsp. *carotovorum* (ECC) or *L. pseudomesenteroides* (LP) for 18 h **(A, B)** and *D. melanogaster* fed either a control diet or an AITC-supplemented diet (0.125 mM or 0.250 mM) for 10 days **(C, D)**. mRNA levels were determined in fly samples from three independent experiments with three replicates containing 10 flies each. Bars show the mean ± SD. Significant differences between groups were tested by applying one-way ANOVA followed by Dunnett's multiple-comparison test. Significance was accepted at $p<0.05$.

lower rate of survival, a higher bacterial load, and lower AMP levels in comparison with unmated females. As mated female flies were used in our experiments this could—at least partly—explain why we did not detect many differences in the expression levels of *dro* and *mtk* in the infected flies.

Overall, the results of the present study indicate that AITC treatments caused a significant decrease in survival among females but not males. Furthermore, AITC reduced the survival of females even in the presence of ECC, but not in the presence of LP, whereas no effect of AITC on survival rates were observed in infected male flies. Similarly, AITC did not significantly affect AMP levels in either infected male or infected female flies. The observed differences in survival between female and male flies may depend on sex-specific variations in immune responses as evidenced by the differing outcomes following bacterial infection in males. The high variations in mRNA expression levels of AMPs due to differences between experimental replicates may have obscured significant differences. Therefore, further experiments are needed to investigate the impact of AITC on pathogenic bacterial infections in fruit flies in more depth and with a specific focus on inflammatory signaling pathways.

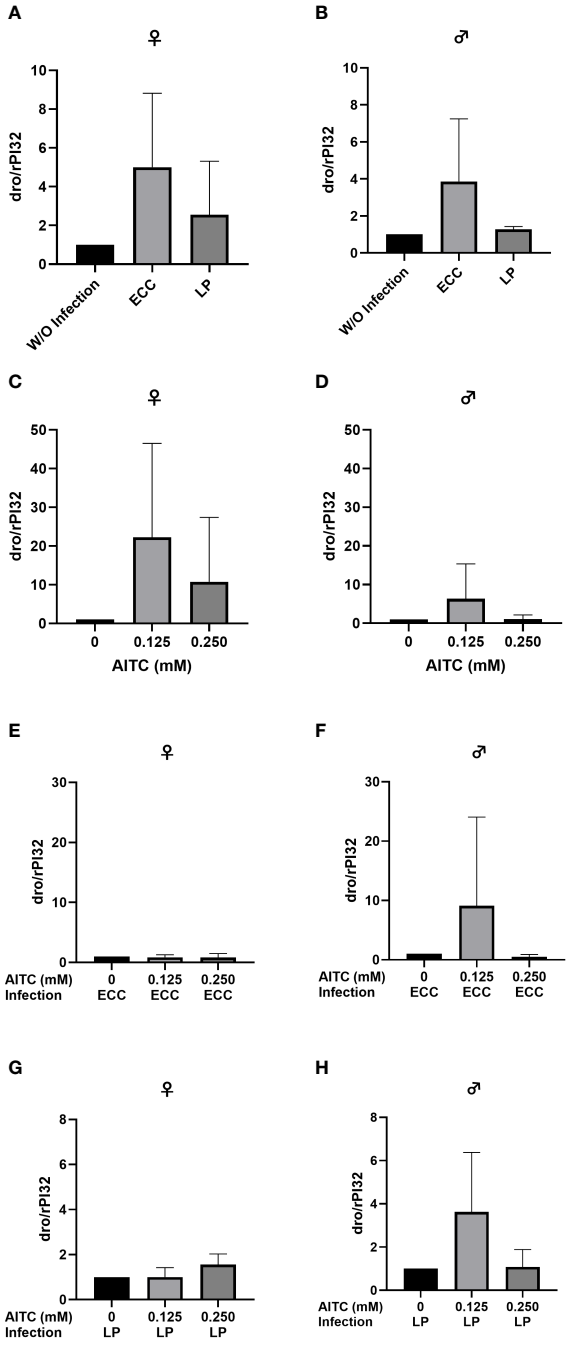

FIGURE 10
Relative mRNA expression levels of *dro* in female **(A, C, E, G)** and male **(B, D, F, H)** *D. melanogaster* initially kept on either a control or an AITC-supplemented diet (0.125 mM or 0.250 mM) for 10 days and subsequently exposed to a 100-mM sucrose solution with or without *L. pseudomesenteroides* (LP) or *P. carotovorum* subsp. *carotovorum* (ECC) for 18 h. mRNA levels were determined in fly samples from three independent experiments with three replicates containing 10 flies each. Bars show the mean ± SD. Significant differences between groups were tested by applying one-way ANOVA followed by Dunnett's multiple-comparison test. Significance was accepted at $p < 0.05$.

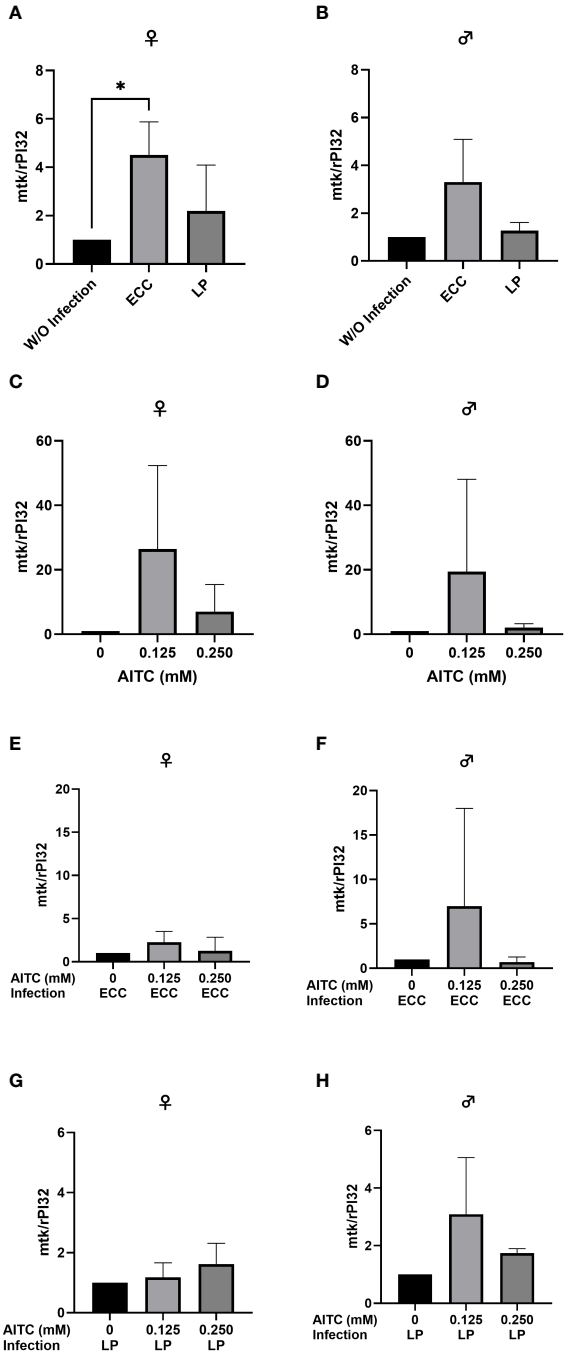

FIGURE 11
Relative mRNA expression levels of *mtk* in female **(A, C, E, G)** and male **(B, D, F, H)** *D. melanogaster* initially kept on either a control or an AITC-supplemented diet (0.125 mM or 0.250 mM) for 10 days and subsequently exposed to a 100-mM sucrose solution with or without *L. pseudomesenteroides* (LP) or *P. carotovorum* subsp. *carotovorum* (ECC) for 18 h. mRNA levels were determined in fly samples from three independent experiments with three replicates containing 10 flies each. Bars show the mean ± SD. Significant differences between groups were tested by applying one-way ANOVA followed by Dunnett's multiple comparison test. Significance was accepted at $p < 0.05$. *$p < 0.05$.

Data availability statement

The original contributions presented in the study are included in the article/Supplementary Material. Further inquiries can be directed to the corresponding author.

Ethics statement

Ethical approval was not required for the study involving animals in accordance with the local legislation and institutional requirements because study included the use of lower invertebrate animals (*Drosophila melanogaster*).

Author contributions

CZ: Conceptualization, Data curation, Formal analysis, Investigation, Methodology, Writing – original draft, Writing – review & editing. SD: Investigation, Methodology, Writing – original draft, Writing – review & editing. AW: Conceptualization, Project administration, Supervision, Writing – original draft, Writing – review & editing.

Funding

The author(s) declare that no financial support was received for the research, authorship, and/or publication of this article.

Acknowledgments

We would like to thank Cordula Becker for excellent technical assistance and Maria Theresia Schminke for experimental support.

Conflict of interest

The authors declare that the research was conducted in the absence of any commercial or financial relationships that could be construed as a potential conflict of interest.

The author(s) declared that they were an editorial board member of Frontiers, at the time of submission. This had no impact on the peer review process and the final decision.

Publisher's note

Supplementary material

The Supplementary Material for this article can be found online at: https://www.frontiersin.org/articles/10.3389/fimmu.2024.1404086/full#supplementary-material

References

1. Huan Y, Kong Q, Mou H, Yi H. Antimicrobial peptides: Classification, design, application and research progress in multiple fields. *Front Microbiol*. (2020) 11:582779. doi: 10.3389/fmicb.2020.582779

2. Murray CJL, Ikuta KS, Sharara F, Swetschinski L, Robles Aguilar G, Gray A, et al. Global burden of bacterial antimicrobial resistance in 2019: a systematic analysis. *Lancet*. (2022) 399:629–55. doi: 10.1016/S0140–6736(21)02724–0

3. Álvarez-Martínez FJ, Barrajón-Catalán E, Micol V. Tackling antibiotic resistance with compounds of natural origin: A comprehensive review. *Biomedicines*. (2020) 8:405. doi: 10.3390/biomedicines8100405

4. Petruk G, Del Giudice R, Rigano MM, Monti DM. Antioxidants from plants protect against skin photoaging. *Oxid Med Cell Longev*. (2018) 2018:1454936. doi: 10.1155/2018/1454936

5. Davies KM, Jibran R, Zhou Y, Albert NW, Brummell DA, Jordan BR, et al. The evolution of flavonoid biosynthesis: A bryophyte perspective. *Front Plant Sci*. (2020) 11:7. doi: 10.3389/fpls.2020.00007

6. Zhang P, Zhu H. Anthocyanins in plant food: current status, genetic modification, and future perspectives. *Molecules*. (2023) 28:866. doi: 10.3390/molecules28020866

7. Zimmermann C, Wagner AE. Impact of food-derived bioactive compounds on intestinal immunity. *Biomolecules*. (2021) 11:1901. doi: 10.3390/biom11121901

8. Dufour V, Alazzam B, Ermel G, Thepaut M, Rossero A, Tresse O, et al. Antimicrobial activities of isothiocyanates against Campylobacter jejuni isolates. *Front Cell Infect Microbiol*. (2012) 2:53. doi: 10.3389/fcimb.2012.00053

9. Keyvani-Ghamsari S, Rahimi M, Khorsandi K. An update on the potential mechanism of gallic acid as an antibacterial and anticancer agent. *Food Sci Nutr*. (2023) 11:5856–72. doi: 10.1002/fsn3.3615

10. Duda-Chodak A, Tarko T, Petka-Poniatowska K. Antimicrobial compounds in food packaging. *Int J Mol Sci*. (2023) 24:2457. doi: 10.3390/ijms24032457

11. Sturm C, Wagner AE. Brassica-derived plant bioactives as modulators of chemopreventive and inflammatory signaling pathways. *Int J Mol Sci*. (2017) 18:1890. doi: 10.3390/ijms18091890

12. Rajakumar T, Pugalendhi P. Allyl isothiocyanate regulates oxidative stress, inflammation, cell proliferation, cell cycle arrest, apoptosis, angiogenesis, invasion and metastasis via interaction with multiple cell signaling pathways. *Histochem Cell Biol*. (2023) 161:211–21. doi: 10.1007/s00418–023-02255–9

13. Tran HT, Stetter R, Herz C, Spöttel J, Krell M, Hanschen FS, et al. Allyl isothiocyanate: A TAS2R38 receptor-dependent immune modulator at the interface between personalized medicine and nutrition. *Front Immunol*. (2021) 12:669005. doi: 10.3389/fimmu.2021.669005

14. Tarar A, Peng S, Cheema S, Peng C-A. Anticancer activity, mechanism, and delivery of allyl isothiocyanate. *Bioengineering (Basel)*. (2022) 9:470. doi: 10.3390/bioengineering9090470

15. Lin CM, Preston JF, Wei CI. Antibacterial mechanism of allyl isothiocyanate. *J Food Prot*. (2000) 63:727–34. doi: 10.4315/0362–028x-63.6.727

16. Schwab M, Reynders V, Loitsch S, Steinhilber D, Schröder O, Stein J. The dietary histone deacetylase inhibitor sulforaphane induces human beta-defensin-2 in intestinal epithelial cells. *Immunology*. (2008) 125:241–51. doi: 10.1111/j.1365-2567.2008.02834.x

17. Mazurkiewicz-Pisarek A, Baran J, Ciach T. Antimicrobial peptides: Challenging journey to the pharmaceutical, biomedical, and cosmeceutical use. *Int J Mol Sci*. (2023) 24:9031. doi: 10.3390/ijms24109031

18. Droujinine IA, Perrimon N. Interorgan communication pathways in physiology: Focus on drosophila. *Annu Rev Genet*. (2016) 50:539–70. doi: 10.1146/annurev-genet-121415–122024

19. Baenas N, Wagner AE. Drosophila melanogaster as an alternative model organism in nutrigenomics. *Genes Nutr*. (2019) 14:14. doi: 10.1186/s12263-019-0641-y

20. Staats S, Lüersen K, Wagner AE, Rimbach G. Drosophila melanogaster as a versatile model organism in food and nutrition research. *J Agric Food Chem*. (2018) 66:3737–53. doi: 10.1021/acs.jafc.7b05900

21. Yu S, Luo F, Xu Y, Zhang Y, Jin LH. Drosophila innate immunity involves multiple signaling pathways and coordinated communication between different tissues. *Front Immunol*. (2022) 13:905370. doi: 10.3389/fimmu.2022.905370

22. Hanson MA, Dostálová A, Ceroni C, Poidevin M, Kondo S, Lemaitre B. Synergy and remarkable specificity of antimicrobial peptides in *vivo* using a systematic knockout approach. *Elife*. (2019) 8:e44341. doi: 10.7554/eLife.44341

23. Campbell Y, Fantacone ML, Gombart AF. Regulation of antimicrobial peptide gene expression by nutrients and by-products of microbial metabolism. *Eur J Nutr*. (2012) 51:899–907. doi: 10.1007/s00394–012-0415–4

24. Gendrin M, Welchman DP, Poidevin M, Hervé M, Lemaitre B. Long-range activation of systemic immunity through peptidoglycan diffusion in Drosophila. *PloS Pathog*. (2009) 5:e1000694. doi: 10.1371/journal.ppat.1000694

25. Sawa N, Okamura K, Zendo T, Himeno K, Nakayama J, Sonomoto K. Identification and characterization of novel multiple bacteriocins produced by Leuconostoc pseudomesenteroides QU 15. *J Appl Microbiol*. (2010) 109:282–91. doi: 10.1111/j.1365-2672.2009.04653.x

26. Makhloufi KM, Carré-Mlouka A, Peduzzi J, Lombard C, van Reenen CA, Dicks LM, et al. Characterization of leucocin B-KM432Bz from Leuconostoc pseudomesenteroides isolated from boza, and comparison of its efficiency to pediocin PA-1. *PloS One*. (2013) 8:e70484. doi: 10.1371/journal.pone.0070484

27. Hanson MA, Lemaitre B. New insights on Drosophila antimicrobial peptide function in host defense and beyond. *Curr Opin Immunol*. (2020) 62:22–30. doi: 10.1016/j.coi.2019.11.008

28. Wagner AE, Piegholdt S, Rabe D, Baenas N, Schloesser A, Eggersdorfer M, et al. Epigallocatechin gallate affects glucose metabolism and increases fitness and lifespan in Drosophila melanogaster. *Oncotarget*. (2015) 6:30568–78. doi: 10.18632/oncotarget.5215

29. Deshpande SA, Carvalho GB, Amador A, Phillips AM, Hoxha S, Lizotte KJ, et al. Quantifying Drosophila food intake: comparative analysis of current methodology. *Nat Methods*. (2014) 11:535–40. doi: 10.1038/nmeth.2899

30. Xuan J, Feng W, Wang J, Wang R, Zhang B, Bo L, et al. Antimicrobial peptides for combating drug-resistant bacterial infections. *Drug Resist Update*. (2023) 68:100954. doi: 10.1016/j.drup.2023.100954

31. Kapahi P, Kaeberlein M, Hansen M. Dietary restriction and lifespan: Lessons from invertebrate models. *Ageing Res Rev*. (2017) 39:3–14. doi: 10.1016/j.arr.2016.12.005

32. Merinas-Amo T, Lozano-Baena M-D, Obregón-Cano S, Alonso-Moraga Á, de Haro-Bailón A. Role of glucosinolates in the nutraceutical potential of selected cultivars of brassica rapa. *Foods*. (2021) 10:2720. doi: 10.3390/foods10112720

33. Wu H, Zhang G-A, Zeng S, Lin K. Extraction of allyl isothiocyanate from horseradish (Armoracia rusticana) and its fumigant insecticidal activity on four stored-product pests of paddy. *Pest Manag Sci*. (2009) 65:1003–8. doi: 10.1002/ps.1786

34. Vilela Ad, Faroni LR, Sousa AH, Pimentel MA, Gomes JL. Toxicological and physiological effects of allyl isothiocyanate upon Callosobruchus maculatus. *J Stored Products Res*. (2020) 87:101625. doi: 10.1016/j.jspr.2020.101625

35. Shi C-H, Hu J-R, Xie W, Yang Y-T, Wang S-L, Zhang Y-J. Control of bradysia odoriphaga (Diptera: sciaridae) with allyl isothiocyanate under field and greenhouse conditions. *J Econ Entomol*. (2017) 110:1127–32. doi: 10.1093/jee/tow303

36. Jabeen A, Zaitoon A, Lim L-T, Scott-Dupree C. Toxicity of five plant volatiles to adult and egg stages of drosophila suzukii matsumura (Diptera: Drosophilidae), the spotted-wing drosophila. *J Agric Food Chem*. (2021) 69:9511–9. doi: 10.1021/acs.jafc.1c01384

37. Hasegawa K, Miwa S, Tsutsumiuchi K, Miwa J. Allyl isothiocyanate that induces GST and UGT expression confers oxidative stress resistance on C. elegans, as demonstrated by nematode biosensor. *PloS One*. (2010) 5:e9267. doi: 10.1371/journal.pone.0009267

38. Yamasaki M, Ogawa T, Wang L, Katsube T, Yamasaki Y, Sun X, et al. Anti-obesity effects of hot water extract from Wasabi (Wasabia japonica Matsum.) leaves in mice fed high-fat diets. *Nutr Res Pract*. (2013) 7:267–72. doi: 10.4162/nrp.2013.7.4.267

39. Ahn J, Lee H, Im SW, Jung CH, Ha TY. Allyl isothiocyanate ameliorates insulin resistance through the regulation of mitochondrial function. *J Nutr Biochem*. (2014) 25:1026–34. doi: 10.1016/j.jnutbio.2014.05.006

40. Thejass P, Kuttan G. Allyl isothiocyanate (AITC) and phenyl isothiocyanate (PITC) inhibit tumour-specific angiogenesis by downregulating nitric oxide (NO) and tumour necrosis factor-alpha (TNF-alpha) production. *Nitric Oxide*. (2007) 16:247–57. doi: 10.1016/j.niox.2006.09.006

41. Rajakumar T, Pugalendhi P, Thilagavathi S. Protective effect of allyl isothiocyanate on glycoprotein components in 7,12-dimethylbenz(a)anthracene induced mammary carcinoma in rats. *Indian J Clin Biochem*. (2018) 33:171–7. doi: 10.1007/s12291–017-0663–4

42. Bhattacharya A, Li Y, Wade KL, Paonessa JD, Fahey JW, Zhang Y. Allyl isothiocyanate-rich mustard seed powder inhibits bladder cancer growth and muscle invasion. *Carcinogenesis*. (2010) 31:2105–10. doi: 10.1093/carcin/bgq202

43. Mazari AM, Dahlberg O, Mannervik B, Mannervik M. Overexpression of glutathione transferase E7 in Drosophila differentially impacts toxicity of organic isothiocyanates in males and females. *PloS One*. (2014) 9:e110103. doi: 10.1371/journal.pone.0110103

44. Basset A, Khush RS, Braun A, Gardan L, Boccard F, Hoffmann JA, et al. The phytopathogenic bacteria Erwinia carotovora infects Drosophila and activates an immune response. *Proc Natl Acad Sci U.S.A*. (2000) 97:3376–81. doi: 10.1073/pnas.97.7.3376

45. Piegholdt S, Rimbach G, Wagner AE. Effects of the isoflavone prunetin on gut health and stress response in male Drosophila melanogaster. *Redox Biol*. (2016) 8:119–26. doi: 10.1016/j.redox.2016.01.001

46. Hiebert N, Carrau T, Bartling M, Vilcinskas A, Lee K-Z. Identification of entomopathogenic bacteria associated with the invasive pest Drosophila suzukii in infested areas of Germany. *J Invertebr Pathol*. (2020) 173:107389. doi: 10.1016/j.jip.2020.107389

47. Hiebert N, Kessel T, Skaljac M, Spohn M, Vilcinskas A, Lee K-Z. The Gram-Positive Bacterium Leuconostoc pseudomesenteroides Shows Insecticidal Activity against Drosophilid and Aphid Pests. *Insects*. (2020) 11:471. doi: 10.3390/insects11080471

48. Marriott I, Huet-Hudson YM. Sexual dimorphism in innate immune responses to infectious organisms. *Immunol Res*. (2006) 34:177–92. doi: 10.1385/IR:34:3:177

49. Klein SL, Flanagan KL. Sex differences in immune responses. *Nat Rev Immunol*. (2016) 16:626–38. doi: 10.1038/nri.2016.90

50. Shahrestani P, Chambers M, Vandenberg J, Garcia K, Malaret G, Chowdhury P, et al. Sexual dimorphism in Drosophila melanogaster survival of Beauveria bassiana infection depends on core immune signaling. *Sci Rep*. (2018) 8:12501. doi: 10.1038/s41598–018-30527–1

51. Rera M, Clark RI, Walker DW. Intestinal barrier dysfunction links metabolic and inflammatory markers of aging to death in Drosophila. *Proc Natl Acad Sci U.S.A*. (2012) 109:21528–33. doi: 10.1073/pnas.1215849110

52. Landis GN, Abdueva D, Skvortsov D, Yang J, Rabin BE, Carrick J, et al. Similar gene expression patterns characterize aging and oxidative stress in Drosophila melanogaster. *Proc Natl Acad Sci U.S.A*. (2004) 101:7663–8. doi: 10.1073/pnas.0307605101

53. Pletcher SD, Macdonald SJ, Marguerie R, Certa U, Stearns SC, Goldstein DB, et al. Genome-wide transcript profiles in aging and calorically restricted Drosophila melanogaster. *Curr Biol*. (2002) 12:712–23. doi: 10.1016/s0960–9822(02)00808–4

54. Zerofsky M, Harel E, Silverman N, Tatar M. Aging of the innate immune response in Drosophila melanogaster. *Aging Cell*. (2005) 4:103–8. doi: 10.1111/j.1474-9728.2005.00147.x

55. Gordon KE, Wolfner MF, Lazzaro BP. A single mating is sufficient to induce persistent reduction of immune defense in mated female Drosophila melanogaster. *J Insect Physiol*. (2022) 140:104414. doi: 10.1016/j.jinsphys.2022.104414

frontiers | Frontiers in Nutrition

TYPE Review
PUBLISHED 11 June 2024
DOI 10.3389/fnut.2024.1386083

OPEN ACCESS

EDITED BY
Diego A. Moreno,
Spanish National Research Council (CSIC), Spain

REVIEWED BY
Iahtisham-Ul-Haq,
Forman Christian College, Pakistan
Mohd Kamil Hussain,
Govt. Raza Post Graduate College, India
Paola Maycotte,
Instituto Mexicano del Seguro Social, Mexico

*CORRESPONDENCE
Qi Wang
✉ q.wang1@uea.ac.uk
Yongping Bao
✉ y.bao@uea.ac.uk

†These authors have contributed equally to this work

RECEIVED 14 February 2024
ACCEPTED 31 May 2024
PUBLISHED 11 June 2024

CITATION
Wang Q, Li D, Liu L, Shan Y and Bao Y (2024) Dietary isothiocyanates and anticancer agents: exploring synergism for improved cancer management.
Front. Nutr. 11:1386083.
doi: 10.3389/fnut.2024.1386083

Dietary isothiocyanates and anticancer agents: exploring synergism for improved cancer management

Qi Wang[1*†], Dan Li[2†], Lihua Liu[3], Yujuan Shan[3] and Yongping Bao[1*]

[1]Norwich Medical School, University of East Anglia, Norwich, United Kingdom, [2]Department of Nutrition, School of Public Health, Sun Yat-Sen University (Northern Campus), Guangzhou, China, [3]Department of Nutrition and Food Hygiene, School of Public Health, Wenzhou Medical University, Wenzhou, China

Human studies have shown the anticancer effects of dietary isothiocyanates (ITCs), but there are some inconsistencies, and more evidence supports that such anticancer effect is from higher doses of ITCs. The inconsistencies found in epidemiological studies may be due to many factors, including the biphasic dose–response (so called hormetic effect) of ITCs, which was found to be more profound under hypoxia conditions. In this comprehensive review, we aim to shed light on the intriguing synergistic interactions between dietary ITCs, focusing on sulforaphane (SFN) and various anticancer drugs. Our exploration is motivated by the potential of these combinations to enhance cancer management strategies. While the anticancer properties of ITCs have been recognized, our review delves deeper into understanding the mechanisms and emphasizing the significance of the hormetic effect of ITCs, characterized by lower doses stimulating both normal cells and cancer cells, whereas higher doses are toxic to cancer cells and inhibit their growth. We have examined a spectrum of studies unraveling the multifaceted interaction and combinational effects of ITCs with anticancer agents. Our analysis reveals the potential of these synergies to augment therapeutic efficacy, mitigate chemoresistance, and minimize toxic effects, thereby opening avenues for therapeutic innovation. The review will provide insights into the underlying mechanisms of action, for example, by spotlighting the pivotal role of Nrf2 and antioxidant enzymes in prevention. Finally, we glimpse ongoing research endeavors and contemplate future directions in this dynamic field. We believe that our work contributes valuable perspectives on nutrition and cancer and holds promise for developing novel and optimized therapeutic strategies.

KEYWORDS

isothiocyanates, sulforaphane, synergistic interactions, anticancer drugs, chemoprevention, cancer management

1 Introduction

Cancer continues to pose a significant global public health challenge, with approximately 20 million new cases and nearly 10 million deaths projected worldwide annually (1). In the United States alone, the 2024 Cancer Statistics report by Siegel et al. estimates 2,001,140 new cases and 611,720 deaths this year. This underscores the ongoing need for advancements in

prevention, early detection, and treatment strategies. Despite some declines in mortality rates due to these improvements, the urgency for continued research and better implementation of cancer control measures remains critical to reduce the disease's overall impact (2).

Within the realm of cancer research, the role of diet, particularly the consumption of dietary isothiocyanates (ITCs) found in cruciferous vegetables, is gaining attention for its potential in cancer chemoprevention and therapy (3, 4). Increasing epidemiological evidence supports an inverse correlation between the consumption of ITC-rich vegetables and cancer risk. Notable studies, such as a prospective analysis in Shanghai, have demonstrated that dietary ITCs are associated with a lowered incidence of lung cancer (5). Similarly, an investigation into cruciferous vegetable intake and mortality in middle-aged adults indicated that higher consumption was linked with lower cancer mortality among men (6). Randomized controlled trials have also suggested that dietary ITCs could be a viable strategy to improve cancer prognosis and survival (7–12). The protective effect of dietary ITCs is particularly pronounced at higher doses or when consumed as part of a cruciferous-rich diet, highlighting the dose-dependent nature of these compounds in cancer prevention (13–15).

Isothiocyanates, such as sulforaphane (SFN), allyl isothiocyanate (AITC), benzyl isothiocyanate (BITC), and phenethyl isothiocyanate (PEITC), are metabolized from glucosinolates and renowned for their potent anticancer properties. Their effectiveness in combating cancer stems from their diverse mechanisms of action, including the modulation of carcinogen metabolism, induction of cell cycle arrest, promotion of apoptotic cell death, activation of cellular defense mechanisms, anti-inflammatory and antioxidant effects, epigenetic regulation, and alteration of various cancer-related signaling pathways (16–21).

Beyond prevention, ITCs show promise in synergizing with conventional anticancer agents, potentially amplifying therapeutic efficacy while minimizing the adverse side effects typically associated with chemotherapy. This synergy is evident through heightened cytotoxic effects on cancer cells, collaborative modulation of drug metabolism and efflux, enhanced drug uptake, and the synergistic induction of apoptotic pathways (17).

One significant impact of isothiocyanates (ITCs) on cancer therapy is their potential to combat chemoresistance, a major obstacle in effective cancer treatment. Chemoresistance, where cancer cells develop mechanisms to resist the effects of chemotherapy, often leads to diminished treatment effectiveness (22, 23). ITCs, notably SFN, have been shown to induce chemosensitization in cancer cells. This is achieved by modulating critical signaling pathways, including MAPK and p53, which can reverse resistance and enhance the efficacy of chemotherapy treatments. Specifically, the activation of the MAPK pathway by ITCs can lead to the upregulation of pro-apoptotic signals. In contrast, the stabilization and activation of p53 by ITCs can halt cell growth and induce apoptosis in chemoresistant cancer cells. These mechanisms highlight the potential of ITCs to serve as valuable adjuncts in cancer therapy, particularly in cases where resistance to conventional chemotherapeutic agents poses a significant challenge (24–28).

Despite their potential, the therapeutic application of ITCs is complex and influenced by their biphasic dose–response (hormetic effect). At low doses, ITCs can promote the growth of both normal and cancer cells, whereas high doses are toxic to cancer cells. Consequently, low doses of ITCs may confer adverse effects on cancer patients, while higher doses lead to beneficial outcomes. This dose-dependent behavior necessitates a nuanced comprehension of ITCs in cancer therapy and the importance of individualized treatment approaches based on specific patient profiles and tumor characteristics (29–31). At low concentrations, ITCs may activate mild oxidative stress, leading to the adaptive activation of protective pathways like Nrf2, enhancing cellular defenses against carcinogens. However, at therapeutic concentrations, ITCs exert pronounced cytotoxic effects on cancer cells, demonstrating their potential as effective anticancer agents. This hormetic behavior underscores the importance of carefully considering dosage in the therapeutic application of ITCs, ensuring that their administration is aligned with an optimal therapeutic window that maximizes anticancer effects while minimizing potential adverse effects.

The selection of SFN as a primary focus in this review is due to its established prominence and effectiveness as a bioactive compound with notable anticancer properties. Extensive research identifies SFN as a potent inhibitor of cancer cell proliferation and an activator of apoptosis in various cancer types. Its distinct mechanisms of action, particularly its inhibition of the nuclear factor kappa B (NF-κB), essential for tumor cell growth and survival, make it a compound of particular interest in cancer chemoprevention studies (32). Furthermore, SFN's ability to target cancer stem cells, thereby addressing a crucial challenge in cancer therapy, underscores its potential as an anticancer stem cell agent (33). The extensive Research Topic of *in vitro* and *in vivo* studies has confirmed SFN's effectiveness in fighting various cancers. Its ability to modulate critical signaling pathways associated with drug resistance makes it a promising candidate in the search for effective cancer treatment strategies (34). This powerful combination of its chemopreventive, therapeutic, and synergistic potential renders SFN a subject of paramount importance in the intricate landscape of cancer research.

This review is dedicated to unraveling the complex interplay between ITCs and anticancer agents, shedding light on the synergistic potentials that could transform cancer therapy. Our exploration encompasses the interactions between SFN and other phytochemicals, the combinational effects between SFN and other ITCs, and the additive or synergistic mechanisms of action between SFN and anticancer drugs. The potential benefits of such combinations are numerous, including enhanced therapeutic efficacy through additive or synergistic effects, the potential to overcome chemoresistance, the ability to administer clinically tolerable lower doses of individual agents, and the capacity to mitigate the hormetic effects often associated with ITCs.

1.1 Dietary isothiocyanates and cancer

Dietary ITCs, derived from glucosinolates found in cruciferous vegetables such as broccoli, Brussels sprouts, cabbage, and kale, transform into their bioactive forms through the action of myrosinase (35, 36). The transformation of these glucosinolate precursors into their active forms, mediated by myrosinase, facilitates various biological effects (14). The anticancer properties of ITCs have been a subject of extensive research, with epidemiological studies suggesting an inverse relationship between the consumption of cruciferous vegetables and the incidence of cancer (31). These findings have been supported by numerous *in vitro* and *in vivo* studies, which have

demonstrated that ITCs can modulate several molecular pathways implicated in carcinogenesis.

One of the crucial mechanisms through which ITCs exert their anticancer effects is by modulating the activity of enzymes involved in the metabolism of carcinogens. Specifically, ITCs inhibit phase I enzymes, such as Cytochrome P450 enzymes (CYP1A1, CYP1A2, and CYP1B1), responsible for pro-carcinogens bioactivation. Concurrently, ITCs induce phase II detoxifying enzymes, including Glutathione S-transferases (GSTs), NAD(P)H Quinone Dehydrogenase 1 (NQO1), and UDP-glucuronosyltransferases (UGTs), which facilitate the excretion of carcinogens, thereby reducing their harmful impact (37).

Sulforaphane (SFN) is an extensively researched ITC with potent anticancer activities demonstrated across various cancer models, including those of the colon, lung, breast, and prostate cancer (14, 34, 36, 38–40). SFN's actions are multifaceted, encompassing the induction of cytoprotective enzymes, modulation of cell proliferation and apoptosis pathways, and regulation of inflammatory responses. SFN's mechanisms of action are diverse, including induction of cytoprotective enzymes, modulation of signaling pathways involved in cell proliferation and death, and regulation of inflammatory responses, underlining its therapeutic potential (32). Notably, SFN has been reported to affect the epigenetic regulation of gene expression and to activate the nuclear factor erythroid 2–related factor 2 (Nrf2) signaling pathway, which leads to the induction of antioxidant response elements and the enhancement of cellular antioxidant capacity (14). Moreover, SFN has been identified as one of the most potent naturally occurring inducers of phase II detoxification enzymes, which are crucial for the elimination of carcinogens from the body (36). By orchestrating a multifaceted approach against cancer, SFN stands out as a promising candidate for further exploration in cancer chemoprevention and therapy.

1.2 Anticancer mechanisms of dietary isothiocyanates

Dietary ITCs have been shown to modulate various cellular and molecular pathways that contribute to their anticancer effects. These mechanisms encompass a broad spectrum of actions, including the inhibition of cell proliferation, induction of cell cycle arrest, promotion of apoptosis, suppression of angiogenesis, alteration of the tumor microenvironment, and modulation of the pharmacokinetics of anticancer drugs (3, 4, 31).

Among the primary mechanisms ITCs exert their anticancer effects is inhibiting cell proliferation. Research indicates that ITCs can decrease the proliferation of various cancer cell lines, thereby restricting tumor growth potential. This antiproliferative effect is often associated with ITCs' ability to induce cell cycle arrest, particularly at the G2/M phase. By inducing cell cycle arrest, ITCs prevent cancer cells from entering mitosis, thereby impeding tumor growth and progression (41, 42).

Significantly, SFN has been identified to downregulate the PI3K/AKT/mTOR signaling pathway and upregulate the expression of PTEN, a tumor suppressor gene. This modulation results in the suppressed growth of cancer cells, indicating a vital mechanism through which SFN exerts its anticancer effects. Furthermore, SFN enhances the production of Bax, a pro-apoptotic protein, thereby promoting apoptosis in cancer cells. These additional layers of SFN's action reinforce its potential as a robust anticancer agent by targeting critical cell survival and death regulators.

Apoptosis, or programmed cell death, is another critical mechanism through which ITCs exert their anticancer effects. ITCs have been shown to induce apoptosis in cancer cells by modulating apoptotic signaling pathways (36, 43). This includes the activation of caspases, which are proteases that play a vital role in the execution phase of cell apoptosis (36).

Angiogenesis, the formation of new blood vessels, is essential for tumor growth and metastasis. ITCs have been reported to exhibit anti-angiogenic properties by inhibiting the formation of new blood vessels in tumors (25, 31). This effect may be mediated by suppressing vascular endothelial growth factor (VEGF) and other angiogenic factors, thereby limiting the supply of nutrients and oxygen to the tumor (31, 44, 45).

The tumor microenvironment, comprising various cell types, extracellular matrix components, and signaling molecules, plays a significant role in cancer progression. ITCs have been shown to modulate the tumor microenvironment, thereby affecting cancer cell behavior (31, 40). For instance, ITCs can modify the inflammatory response within the tumor microenvironment, which may contribute to their anticancer effects (39, 46).

Another important aspect of the anticancer activity of ITCs is their influence on the pharmacokinetics of anticancer drugs. ITCs can affect the metabolism and clearance of drugs, potentially enhancing their efficacy or reducing their toxicity (31, 38). This suggests that ITCs could be used as adjuvants to improve the therapeutic outcomes of conventional anticancer treatments.

Furthermore, ITCs are known to activate the Nrf2 pathway, a crucial regulator of cellular antioxidant responses and detoxification of reactive oxygen species (ROS) (43, 47, 48). This activation leads to the upregulation of antioxidant enzymes and cytoprotective proteins, enhancing cellular defense against oxidative stress, a known contributor to carcinogenesis.

Other key molecular targets or links associated with cancer have been found to be regulated by ITCs, including epithelial-mesenchymal transition (EMT) (49, 50), cancer stem cells and stem cell-like properties (27, 28, 33), microtubule/tubulin polymerization (51–53), mitochondrial biogenesis and dynamics and function (21, 54), autophagy (19, 55, 56), glucolipid metabolism (57, 58), telomerase activity (59, 60) as well as gut microbiota (61, 62).

In short, dietary ITCs exhibit a spectrum of anticancer mechanisms, underscoring their potential as chemopreventive and therapeutic agents. Their multifaceted role in cancer management, including the inhibition of cell proliferation, induction of apoptosis, anti-angiogenic effects, modulation of the tumor microenvironment, impact on the pharmacokinetics of anticancer drugs, and activation of the Nrf2 pathway, highlight their significance.

1.3 Hormetic effect of dietary isothiocyanates

The hormetic effect, a dose–response phenomenon marked by low-dose stimulation and high-dose inhibition, constitutes a crucial element in the biological impact of ITCs on cancer management [48, 49]. At lower concentrations (1–5 μM), SFN has been observed to

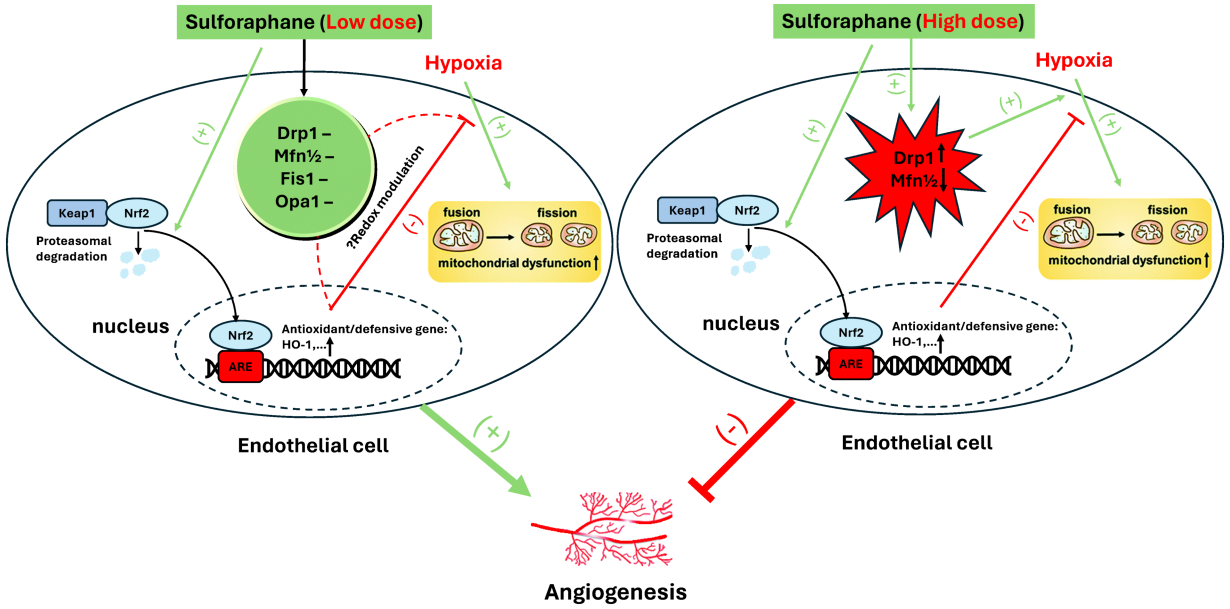

FIGURE 1
Proposed mechanism of biphasic effect of SFN on angiogenesis in hypoxia. Reproduced from Ref. (64) with permission from the Royal Society of Chemistry.

stimulate cell growth in normal cells, potentially aiding in processes such as tissue repair and maintenance. This stimulatory effect on normal cells may render SFN less toxic to normal cells than cancer cells, suggesting a selective action that could benefit therapeutic contexts (30, 63). However, the same compound presents a complex interaction with cancer cells. While low doses of SFN may stimulate certain types of cancer cells, potentially enhancing tumor growth and spread, higher doses ($\geq$ 10 μM) have been shown to inhibit cancer cell proliferation and exert pro-apoptotic effects. This indicates that SFN may either prevent or promote tumor cell growth depending on the dose and the nature of the target cells, underscoring the importance of precise dosing and the consideration of the cellular context in the potential therapeutic use of SFN (30).

The mechanisms underlying the hormetic effects of ITCs are complex and not fully understood. They may entail the modulation of autophagy pathways, as observed by the inhibition of autophagy negating the stimulatory effect of SFN on cell migration. Additionally, the interaction of ITCs with other dietary components, such as selenium, influences their hormetic behavior, with co-treatment enhancing the protective effects of low-dose SFN against free-radical-mediated cell death (30).

Moreover, the hormetic effects of ITCs are influenced by their ability to activate the Nrf2 pathway, which plays a pivotal role in cellular defense against oxidative stress and various carcinogens. The activation of Nrf2 by ITCs can lead to cytoprotective outcomes, and its role in tumor metastasis and growth has also been reported, indicating a dual role of Nrf2 in carcinogenesis, which further complicates the hormetic nature of ITCs (31). In addition, intracellular ROS is altered differentially by low to high doses of ITCs, and its levels ranging from mild to excessive and the time course of ROS production (transient vs. persistent) can differently determine cell fates and carcinogenesis, thus possibly constituting another core mechanism of ITCs' hormesis (30).

Interestingly, angio-hormetic effects of ITCs have also been found in our previous studies, using tumor cells and 3-D human umbilical vein endothelial cells (HUVECs) with pericyte co-culture models in normoxia and hypoxia (64). In particular, under hypoxia, a dose-dependent biphasic angio-regulatory effect of SFN was observed and ascribed to mito-hormetic mechanisms that involve an integrated modulation of Nrf2 and alteration of mitochondrial dynamics by SFN. Specifically, Nrf2 activation by low doses (1–5 μM) of SFN can protect against hypoxia-evoked mitochondrial injury and fission, thus boosting the angiogenic capacity of HUVECs. However, mitochondrial fission induced by high doses ($\geq$ 10 μM) of SFN through the regulation of Drp1 and Mfn1/2, coupled with the aggravated mitochondrial injury, may overwhelm the Nrf2- defense dependent beneficial effect, hence mediating anti-angiogenesis. A schematic diagram of the molecular mechanism is shown in Figure 1.

In summary, the hormetic effects of dietary ITCs present a complex interplay between beneficial and potentially adverse outcomes determined by the specific dose and cellular context. While low doses may stimulate normal cellular functions, they may also promote angiogenesis and tumorigenesis in cancer cells. Therefore, combining ITCs with chemotherapeutic agents offers a promising strategy to enhance their anticancer potential while mitigating the risks associated with hormesis. Further research is essential to understand the mechanisms driving the hormetic effects of ITCs fully and optimizing their application in cancer management.

2 Combinational use of dietary isothiocyanates and anticancer agents

Combinational therapy marks a significant advancement in cancer treatment and prevention by harnessing the synergistic effects of multiple therapeutic agents to boost efficacy, reduce side effects, and

counteract drug resistance (65). The integration of dietary ITCs, especially SFN, with both conventional and non-conventional anticancer agents has paved new pathways for enhancing the effectiveness of cancer management. This section delves into the synergistic potential of SFN when used in conjunction with established chemotherapy drugs and other phytochemicals. Research indicates that SFN can enhance the efficacy of chemotherapeutic agents such as cisplatin and doxorubicin (DOX) (66–68). This enhancement is attributed to its role in modulating drug sensitivity, inducing cell cycle arrest and influencing drug efflux transporters (40, 66). Additionally, SFN's capacity to intensify drug-induced apoptosis and suppress survival pathways in cancer cells contributes to this synergistic effect. This interaction may permit lower dosages of chemotherapeutic drugs, potentially reducing adverse side effects and slowing the development of drug resistance.

The incorporation of ITCs into cancer treatment regimens holds the potential to not only improve therapeutic outcomes but also to mitigate the toxicological impact of chemotherapy. SFN serves a dual role as both a chemosensitizer and a protective agent against drug-induced toxicity, thus paving the way for cancer treatment strategies that are both more tolerable and effective (68). Nevertheless, determining the optimal dosage and the precise combinations of ITCs with anticancer agents is essential to balance therapeutic advantages against potential risks (31). The assessment of combinational effects is often quantified using the combination index (CI) method, where CI values either less than 1, equal to 1, or greater than 1 indicate synergism, additivity, or antagonism, respectively (17, 66, 69). These values provide a quantitative measure of the interaction between compounds, guiding the optimization of combinational treatments for improved efficacy and reduced toxicity.

Since 2006, over 80 published studies on SFN's combination with other anticancer agents have been extensively evaluated in many reviews. In this article, we specifically focus on more recent publications within the past six years.

2.1 Interactions between sulforaphane and other phytochemicals

The combinatorial use of dietary ITCs, such as SFN, with other phytochemicals has garnered significant interest in the field of cancer management. This interest is predicated on the hypothesis that such combinations may exert synergistic effects, thereby enhancing the efficacy of anticancer strategies. This section evaluates recent studies that have tested combinations of SFN with other phytochemicals for enhanced anticancer efficacy. A summary of all relevant studies is presented in Table 1.

Royston et al. uncovered a compelling synergy between Sulforaphane (SFN) and Withaferin A (WA) in combating breast cancer cells (70, 71). WA, from Indian winter cherry, combined with SFN, significantly inhibited cell viability and induced apoptosis in MCF-7 and MDA-MB-231 cells. This combination notably suppressed histone deacetylase (HDAC) expression and influenced DNA methylation transferase (DNMT) activity, tilting gene expression, and favoring pro-apoptotic pathways. The research concluded that even at low concentrations, the WA and SFN duo could effectively hasten cancer cell demise and modulate critical epigenetic modifiers, showcasing a promising pathway for cancer treatment. The integration of SFN with genistein (GEN), another soy-derived DNMT inhibitor, showed a similar impact. The combination treatment showed enhanced efficacy in inducing apoptosis and reducing colony formation in breast cancer cell lines. SFN exhibited strong synergism with GEN (CI < 0.7), especially at specific concentrations (5 μM SFN and 10 μM/15 μM GEN). This synergistic effect extended to promising *in vivo* results, demonstrating potential for mammary cancer prevention and treatment in transgenic mice (72). Furthermore, a tri-combination involving SFN, GEN, and sodium butyrate (NaB) resulted in even more pronounced synergistic inhibition in breast cancer, reaching a minimum CI value of 0.06 in MCF-7 cells (73).

Two other studies have explored the synergy between SFN and complex phytochemical regimens. The first study by Langner et al. (74) investigated a blend (referred to as MIX) of lycopene, SFN, quercetin, and curcumin. It revealed an additive effect in the reduction of colon cancer cell proliferation. The MIX impaired mitochondrial function, instigating cytotoxicity in cancer cells without harming normal cells. Notably, the MIX also enhanced the antiproliferative effects of chemotherapy drugs such as 5-fluorouracil (5-FU) and cisplatin, suggesting its potential as a chemotherapy adjunct. The study highlighted the chemopreventive action of these compounds, particularly when used in combination, and their selective toxicity toward cancer cells, ensuring safety for normal colon epithelial cells and suggesting their suitability for daily dietary inclusion. The second study investigated the synergistic effects of SFN with curcumin and dihydrocaffeic acid (DA) against colon cancer cells (75). Interestingly, the combination of SFN and curcumin showed a relatively high antagonistic effect (CI between 2.5 and 3). At the same time, the SFN + DA (1:1) combination showed significant cytotoxicity and was more selective toward HT-29 colon cancer cells than healthy cells. The CI value of SFN + DA is 0.7, implying a significant synergistic effect. The study suggested that the mechanisms behind the synergistic effects might involve the modulation of oxidative stress, cell cycle arrest, and apoptosis-related pathways.

Moreover, the anti-inflammatory properties of SFN were amplified when combined with luteolin (LUT). The combined treatments led to a more potent inhibition of nitric oxide (NO) production and a reduction in pro-inflammatory protein expression related to the NF-κB pathway and STAT3 activation (76). This synergistic effect not only suppresses pro-inflammatory cytokines but also diminishes oxidative stress, showcasing significant therapeutic promise for inflammatory-related conditions like cancer.

In addition, research by Li et al. on the transgenerational impact of SFN and epigallocatechin-3-gallate (EGCG) from diet on mammary cancer prevention in mice reveals that these compounds can inhibit breast cancer cell growth through epigenetic modifications. The combined consumption of SFN and EGCG demonstrates synergistic advantages in reducing tumor growth and altering tumor-related protein expression in offspring. This suggests that dietary choices can play an important role in cancer prevention through epigenetic pathways (77).

While the evidence for SFN's synergistic effects with other phytochemicals is compelling, it is crucial to recognize the limitations of these findings. Most of the studies are preclinical, and translating these findings to clinical settings requires careful consideration of the pharmacokinetics, bioavailability, and potential interactions of these compounds in humans. Additionally, the optimal doses and ratios for combination treatments need to be determined for each specific type

TABLE 1 Summary of studies on combinational use of SFN and other phytochemicals.

Combination agents	SFN Dosage	Other phytochemicals Dosage	Cancer types	Study models	Combination index (CI) (Chou-Talalay method)	References
SFN + withaferin A (WA)	5.0 μM SFN	1.0 μM WA	Breast cancer	MCF-7 and MDA-MB-231 cells	MCF-7 CI = 0.7 MDA-MB-231 cells CI = 1	(70, 71)
SFN + genistein (GEN)	2–15 μM SFN	5–25 μM GEN	Breast cancer	MCF-7 and MDA-MB-231 cells, C3 (1)-SV40 Tag transgenic mouse model	CI range: >0.1 to <0.7	(72)
SFN + GEN + sodium butyrate (NaB)	0–10 μM SFN	0–25 μM GEN and 0–5 mM NaB	Breast cancer	MCF-7 and MDA-MB-231 cells	CI range: >0.06 to <0.47	(73)
SFN + quercetin + lycopene + curcumin	2.5 μM SFN	2 μM lycopene, 25 μM quercetin, and 10 μM curcumin	Colon cancer	colon epithelial (CCD841 CoTr), and colon cancer (HT-29, LS174T) cells	Not listed	(74)
SFN + curcumin+ Dihydrocaffeic Acid (DA)	5–30 μM SFN	5–35 μM curcumin and 5–80 μM DA	Colon cancer	HT-29, Caco-2 and healthy colon cell	HT-29: CI = 0.7 (SFN: DA 1:1) at 90% cytotoxicity; CI > 1 (SFN + curcumin) Caco-2 CI = 0.9 (5uM SFN + 35uM curcumin+5uM DA)	(75)
SFN + luteolin (LUT)	0.12–0.62 μM SFN	2.5–12.5 μM LUT		Raw 264.7 macrophages	CI < 0.87	(76)
SFN + epigallocatechin-3-gallate (EGCG)	0–15 μM SFN. For *in vivo* study, 26% SFN (w/w) in food	0–30 μM EGCG. For *in vivo* study, 0.5% EGCG (w/v) in drinking water	Breast cancer	MCF-7, MDA-MB-231, MDA-MB-157 and MCF-10A cells, transgenic mice	Not listed	(77)

10.3389/fnut.2024.1386083

of cancer, as the efficacy of these combinations may vary depending on the cancer cell type and the individual's metabolism.

In conclusion, the preclinical evidence suggests that the combination of SFN with other phytochemicals can lead to synergistic effects in cancer management. However, further research is needed to understand the underlying mechanisms of these interactions and establish the clinical relevance of these findings. The use of CI values in these studies provide a quantitative measure of the interactions, with CI values less than 1 indicating synergism. These values are crucial for determining the potential clinical applications of these combinations and for designing future studies to optimize the use of dietary ITCs in combination with other anticancer agents.

2.2 Combinational effect between sulforaphane and other isothiocyanates

The exploration of combinational effects between SFN and other ITCs is a promising area of research, aiming to enhance the efficacy of cancer chemoprevention and therapy. For instance, the combination of SFN with PEITC has been shown to exert synergistic effects in inhibiting inflammation, a process closely linked to carcinogenesis (78). This synergism is likely due to the combined induction of phase II/antioxidant enzymes, including heme-oxygenase1 (HO-1) and NAD(P)H:quinone oxidoreductase 1 (NQO-1), which play a crucial role in the detoxification of carcinogens and protection against oxidative damage (78).

Hutzen et al. (79) explored the effects of SFN and BITC on PANC-1 pancreatic cancer cells and MDA-MB-453 breast cancer cells. Notably, BITC inhibited the phosphorylation of STAT3, a protein implicated in cancer cell growth and survival, whereas SFN's inhibitory effects appeared to be STAT3-independent. Additionally, BITC prevented IL-6-induced STAT3 activation in MDA-MB-453 cells. Combining BITC and SFN proved more effective than either compound alone in reducing cell viability. This combination exhibited an enhanced reduction in pSTAT3 levels and an amplified increase in apoptosis, evident through PARP cleavage.

Furthermore, the combination of SFN with AITC has demonstrated synergistic effects in non-small cell lung carcinoma cells, manifested by increased production of intracellular ROS and concomitant suppression of cancer cell proliferation (17). Moreover, the synergy between AITC and SFN was also observed in cell migration assays, demonstrating the potential of different ITCs used in combination to produce enhanced protective effects against carcinogenesis.

In summary, these findings suggest a potential synergistic relationship between SFN and other ITCs in inhibiting cancer cell growth, migration, and apoptosis. However, the CI values, which quantify the degree of interaction between two agents, are not explicitly discussed in these studies. Furthermore, these investigations are constrained to *in vitro* contexts; thus, translation to *in vivo* models is a requisite for advancing these preliminary findings. Future research should encompass the deployment of suitable models to evaluate and validate these *in vitro* observations.

2.3 Synergisms between sulforaphane and anticancer drugs

The investigation into dietary ITCs, such as SFN, and their combinatorial use with anticancer drugs is at the forefront of oncological research. This focus is driven by the premise that ITCs can amplify the therapeutic effects of standard chemotherapy agents, thereby improving their anticancer properties while potentially diminishing the associated toxicities. This section provides an analysis of recent investigations that have examined the combined use of ITCs with chemotherapeutic agents to enhance anticancer efficacy, focusing specifically on SFN. The assessment considers augmented efficacy, identifies potential limitations, and discusses the significance of Combination Index (CI) values. An overview of these studies is provided in Table 2.

One of the critical challenges in cancer therapy is the development of resistance to chemotherapeutic agents (22, 23). Studies have shown that SFN can sensitize cancer cells to various anticancer drugs, thereby potentially overcoming resistance mechanisms. For example, SFN has been shown to curb the growth of gefitinib-resistant lung cancer cells by altering the sonic hedgehog (SHH) signaling pathway and reducing the expression of markers associated with lung cancer stem cells. The synergistic combination of SFN and gefitinib markedly decreases cell proliferation, presenting a viable treatment option for lung cancer (80). Similarly, studies by Kan et al. (81) revealed that pairing SFN with cisplatin (CIS) significantly curtails tumor growth and progression in ovarian cancer xenograft models, demonstrating dose-dependent inhibition of cell proliferation and synergistic effects in colony formation and cell cycle assays. Additionally, research by Liu et al. (82) found that SFN reverses cisplatin resistance in ovarian carcinoma cells through DNA damage induction and enhanced cisplatin retention, an effect partially mediated by the upregulation of miR-30a-3p. This microRNA typically downregulated in cisplatin-resistant cells, plays a crucial role in modulating cisplatin sensitivity, underscoring the therapeutic potential of SFN in overcoming drug resistance.

In epidermal squamous cell carcinoma, the SFN-cisplatin combination proved more effective than either agent alone in suppressing cell proliferation, invasion, and tumor formation. This combination was particularly effective against cancer stem cells, often resistant to therapy, suggesting a novel approach to targeting these resilient cell populations (42). The efficacy of dietary ITCs, such as SFN, extends beyond ovarian and epidermal cancers. In triple-negative breast cancer (TNBC), the combination of SFN and cisplatin exhibited synergistic antiproliferative effects. CI analysis using MTT cell proliferation assay data revealed that most data points fell into synergism ($CI < 0.8$), indicating a favorable interaction between the two compounds. However, certain concentration combinations exhibited an antagonistic effect ($CI > 1$), signaling potential antagonism at specific concentrations. This highlights the importance of optimizing dosage to achieve the desired synergistic outcome (83).

The synergistic capabilities of SFN extend beyond its combination with cisplatin. When used in conjunction with 5-fluorouracil (5-FU), an increase in effectiveness has been observed in the treatment of triple-negative breast cancer (84). This combination promotes autophagic cell death and premature senescence, potentially mediated by the Nrf2-KEAP1-ARE signaling pathway. Further analysis using the Chou-Talalay method to evaluate SFN and 5-FU across various cancer cell lines, including the colon and prostate, reveals their complex interaction dynamics. In colon cancer cells, synergism was predominantly observed at higher effect levels, whereas in prostate cancer cells, additive effects were prevalent. The LNCaP prostate cancer cell line, however, showed antagonism at all levels, underscoring

TABLE 2 Summary of studies on combinational use of SFN and anticancer drugs.

Combination agents	SFN dosage	Anticancer drug dosage	Cancer types	Study models	Combination index (CI) (Chou-Talalay method)	References
SFN + gefitinib	0–12 μM SFN	0–2 μM gefitinib	Lung cancer	gefitinib-tolerant PC9 cells	Not listed	(80)
SFN + cisplatin (CIS)	0–10 μM SFN	0–20 μM CIS	Ovarian cancer	A2780 and OVcAR cells,	Not listed	(81)
SFN + CIS	0–1.5 μM SFN	30 μM CIS	Ovarian cancer	A2780 and IGROV1 cells and cisplatin resistance A2780/CP70 and IGROV1-R10 cells	Not listed	(82)
SFN + CIS	0.5 or 1 μM SFN	0.5 or 1 μM CIS	Epidermal squamous cell carcinoma	SCC-13 and HaCaT cells	Not listed	(42)
SFN + CIS	0–20 μM SFN	10 or 25 μM CIS	triple-negative breast cancer (TNBC)	MDA-MB-231 and MDA-MB-468 cells	CI < 0.8 (10 μM SFN + 10 μM CIS)	(83)
SFN + 5-fluorouracil (5-FU)	5.4–42.8 μM SFN	6.4–51.5 μM 5-FU	TNBC	MDA-MB-231 cells	0.5 < CI < 0.7	(84)
SFN + 5-FU	5.9–47.3 μM SFN (Caco-2); 6.2–14.4 μM SFN (HT-29)	1.8–14.4 μM 5-FU (Caco-2); 5.3–12.3 μM 5-FU (HT-29)	Colon cancer and Prostate cancer	Caco-2, HT-29, LNCaP, and PC3 cells	Caco-2 CI = 0.7 HT-29 CI = 0.8 PC-3 CI = 1 LNCaP CI = 1.3	(85)
SFN analog, 2-oxohexyl isothiocyanate (2-oxohexyl ITC) + 5-FU	2.6–20.8 μM ITC (Caco-2); 3.5–8.2 μM ITC (HT-29); 2.8–22 μM ITC (PC-3); 7.6–60.8 μM ITC (LNCaP)	1.8–14.4 μM 5-FU (Caco-2); 5.3–12.3 μM 5-FU (HT-29); 2.9–22.8 μM 5-FU (PC-3); 2.0–15.7 μM 5-FU (LNCaP)	Colon cancer and Prostate cancer	Caco-2, HT-29, LNCaP, and PC3 cells	Caco-2 CI < 1 HT-29 CI < 0.5 PC-3 CI = 1 LNCaP CI > 1.1	(69)
SFN analog 4-isoselenocyanato-1-butyl 4-fluorobenzyl sulfoxide (ISC) + 5-FU	2.0–3.0 μM ISC; For *in vivo* study, ISC at the dose of 50 mg/kg	12.9–51.5 μM 5-FU; For *in vivo* study, 5-FU at 100 mg/kg	TNBC	MDA-MB-231 and 4 T1 cells, 4 T1 tumor-bearing female BALB/c mice	0.5 < CI < 0.8	(86)
SFN + 5-FU, folinic acid and oxaliplatin (FOLFOX)	1.25 or 10 μM SFN	0.4 μM 5-FU, 4 μM folinic acid and 0.2 μM oxaliplatin	Colorectal cancer	CX-1 cells	Not listed	(87)
SFN + 5-FU	0.5–30 μM SFN	0.5–30 μM 5-FU	Colon cancer	HCT-15 cells	Not listed	(88)
SFN + Loratadine (LOR)	5 μM SFN;For *in vivo* study, SFN at the dose of 4 mg/kg	0–1,000 μM LOR; For *in vivo* study, LOR at 0.16 mg/kg	Pancreatic cancer	MIA PaCa-2 and Panc-1 cells	Not listed	(89, 90)
SFN + doxorubicin (DOX)	2.2–12.32 μM SFN (MCF-7); 0.37–8.8 μM SFN (MDA-MB-231)	0.14–0.77 μM DOX (MCF-7); 0.007–0.166 μM DOX (MDA-MB-231)	Breast cancer	MCF-7 and MDA-MB-231 cells	MCF-7 CI = 1 MDA-MB-231 CI < 0.76	(67)
SFN + DOX	40 μM SFN; For *in vivo* study, SFN at the dose of 4 mg/kg	50 nM DOX; For *in vivo* study, DOX at 5 mg/kg	Breast cancer	4 T1 cells and 4 T1 tumor-bearing female BALB/c mice	Not listed	(48)
SFN + DOX	0.031–2 μM SFN; For *in vivo* study, SFN at the dose of 1 mg/kg	0.0156–1 μM DOX; For *in vivo* study, DOX at 1.5 mg/ kg	TNBC	MDA-MB-231, and MCF-10A cells, 4 T1 tumor-bearing female BALB/c mice	MDA-MB-231 CI < 0.56 MCF-10A CI > 1	(91)
SFN + DOX	2.5 μM SFN; For *in vivo* study, SFN at a dose of 4 mg/kg	5 μg/mL DOX; For *in vivo* study, DOX at 5 mg/kg	Breast cancer	MCF-7, MDA-MB-231, 13,762 MAT B III and MCF-10A cells; Female Sprague Dawley rats	Not listed	(92)

(Continued)

10.3389/fnut.2024.1386083

TABLE 2 (Continued)

Combination agents	SFN dosage	Anticancer drug dosage	Cancer types	Study models	Combination index (CI) (Chou-Talalay method)	References
SFN metabolites + paclitaxel (PTX)	10 μM SFN metabolites	0–40 nM PTX	Non-small cell lung cancer (NSCLC)	A549 and Taxel-resistant A549 cells	Not listed	(93)
SFN + acetazolamide (AZ)	0–80 μM SFN	0–80 μM AZ	Lung cancer	H727 and H720 cells	Not listed	(94)
SFN + PTX	73 μM SFN	3.08 μM PTX	Prostate cancer	PC3, DU145, and VCaP cells	PC3 CI < 0.41	(95)
SFN + clofarabine (CIF)	10 μM SFN	50 nM or 640 nM CIF	Breast cancer	MCF-7 and MDA-MB-231 cells	MCF-7 CI = 1 MDA-MB-231 CI = 0.9	(96)
SFN + gemcitabine (GEM)	6.8/13.7/27.4 μM SFN (HuCCT-1); 8.5/17.1/34.2 μM SFN (HuH28)	0.14/0.28/0.57 μM GEM (HuCCT-1); 0.17/0.35/0.71 μM GEM (HuH28)	Liver cancer	HuCCT-1 and HuH28 cells; BALB/c mice	HuCCT-1 CI < 0.6 HuH28 CI < 0.7	(97)

the variability in drug combination responses among different cancer types (85).

Additionally, a synergistic effect was observed in colon cancer models with the combination of 2-oxohexyl isothiocyanate (a sulforaphane analog) and 5-FU, particularly enhancing cytotoxic activity and leading to apoptosis in HT-29 cells (69). The combination index (CI) values varied across cell lines, suggesting that the nature of interaction depends on the specific characteristics of each cancer cell line. *In vivo* studies further corroborated these *in vitro* results, with a combination of 5-FU and an SFN analog, 4-isoselenocyanato-1-butyl 4-fluorobenzyl sulfoxide (ISC), showing reduced tumor volume and metastasis in a mammary gland carcinoma animal model, indicating potentiated anticancer activity (86). Moreover, SFN's combination with FOLFOX (5-FU, oxaliplatin, and folinic acid) in highly metastatic human colon carcinoma cells led to a marked decrease in cell viability, enhanced apoptosis, and inhibited spheroid formation while modulating aldehyde dehydrogenase 1 (ALDH1) activity. Interestingly, while SFN alone increased the expression of multidrug resistance protein 2 (MRP2), its combination with FOLFOX normalized ALDH1 activity, suggesting it could counteract FOLFOX-induced resistance mechanisms (87).

Advancements in targeted delivery systems, particularly the co-encapsulation of ITCs and anticancer agents in nanoparticles, have shown promise for enhancing anticancer effects. For instance, nanotechnology-based approaches utilizing lipid-polymer hybrid nanoparticles (LPHNPs) for delivering SFN and chemotherapeutic agents have been explored to improve bioavailability and therapeutic outcomes, highlighting the potential of nanocarriers in optimizing the synergistic effects of SFN and anticancer drugs. Research on EGF-functionalized LPHNPs encapsulating 5-FU and SFN shows potential for improved cancer treatment delivery and outcomes (88). Similarly, the synergy observed between SFN and Loratadine (LOR) in pancreatic cancer chemoprevention, both *in vitro* and *in vivo*, underscores the effectiveness of novel nano formulations (89, 90). Furthermore, the combining SFN with DOX in liposomal nanoparticles enhances cytotoxicity in breast cancer cells, particularly in hormone-resistant types, indicating the nuanced and cancer-specific nature of these synergistic interactions (67).

Another study focused on the immunomodulatory effects of SFN in the context of breast cancer. The co-administration of SFN and DOX was found to attenuate breast cancer growth by preventing the accumulation of myeloid-derived suppressor cells (MDSCs), which are known to inhibit anti-tumor immunity. This combination therapy led to a significant decrease in tumor volume and expansion of MDSCs, alongside an increase in cytotoxic $CD8^+$T cells (48). These findings suggest that SFN can reverse the immunosuppressive microenvironment and enhance the efficacy of DOX. Further research using a TNBC animal model has corroborated the anticancer effects and safety of a liposomal formulation containing DOX and SFN. The combination not only inhibited tumor growth but also exhibited cardioprotective, nephroprotective, and hepatoprotective effects, highlighting the potential for reduced systemic toxicity (91). While SFN has been shown to potentially boost the immune system, some studies indicate it might also be associated with a reduction in T cells. This dual effect suggests a nuanced role for SFN in modulating the immune response within the tumor microenvironment, emphasizing the importance of understanding its comprehensive effects on immune cell populations.

The combination of SFN metabolites and paclitaxel (PTX) shows a synergistic effect in inducing apoptosis in A549/Taxol-resistant lung cancer cells (93). SFN metabolites have been shown to disrupt microtubule dynamics, mechanism of action shared with PTX. This disruption enhances PTX-induced apoptosis in the lung cancer cells, suggesting a potential for reduced drug resistance and lower therapeutic doses. Similar results have been shown by the combination of SFN and acetazolamide (AZ) (94). In another study using prostate cancer cell lines, the co-administration of SFN with PTX resulted in a synergistic effect, reducing the proliferation of both androgen-dependent and independent cancer cells and inducing apoptosis. This synergy was quantified by a CI value of less than 1, indicating a potentiated therapeutic effect when both agents were used together (95).

The synergistic interaction between SFN and anticancer drugs is not only limited to enhancing efficacy but also extends to reducing the toxicity associated with chemotherapy. For example, the combination of SFN with doxorubicin has been shown to potentiate the anticancer effects of doxorubicin while attenuating its cardiotoxicity in a breast cancer model (92). This protective effect is attributed to SFN's ability to activate Nrf2, a key regulator of cellular antioxidant responses, thereby mitigating oxidative stress and inflammation induced by doxorubicin (92). Such findings underscore the potential of SFN to improve the therapeutic index of conventional chemotherapy by enhancing efficacy and reducing adverse effects.

Furthermore, the epigenetic modulation by SFN plays a significant role in its synergistic interactions with anticancer drugs. SFN has proved to induce hypomethylation and upregulation of tumor suppressor genes, thereby sensitizing cancer cells to the effects of chemotherapeutic agents (96). This epigenetic modulation, coupled with SFN's ability to inhibit HDAC activity, presents a novel mechanism through which SFN can enhance the efficacy of anticancer drugs (97).

In conclusion, the preclinical evidence suggests that the combination of SFN with anticancer drugs holds promise for enhancing the efficacy of cancer treatment regimens. The observed synergistic effects, as evidenced by CI values less than 1, indicate the potential for improved therapeutic outcomes. However, it is important to note that the combinational effects of SFN and anticancer drugs are not always synergistic (67, 69, 85, 91). This highlights the complexity of drug interactions and the need for careful consideration of the specific cellular context when evaluating combination therapies. Further research is essential to address current study limitations and establish clinical relevance.

2.4 Mechanisms of anticancer synergy

The combinational use of dietary ITCs with anticancer agents has garnered significant attention due to the potential for enhanced therapeutic efficacy and reduced toxicity. This section delves into the cellular and molecular mechanisms underlying the synergistic interactions between ITCs and various anticancer drugs, which may contribute to improved cancer management (Figure 2).

Apoptosis, a programmed cell death mechanism crucial for removing damaged or unwanted cells, is a common target for ITCs and anticancer drugs. Studies have shown that ITCs, such as SFN and PEITC, can sensitize cancer cells to apoptosis induced by various chemotherapeutic agents (17, 69, 72, 85, 98). This sensitization often involves the upregulation of death receptors (DR), such as DR5, and the activation of both intrinsic and extrinsic apoptotic pathways (32, 66, 81). For instance, the combination of SFN with tumor necrosis factor-related apoptosis-inducing ligand (TRAIL) has been reported to enhance apoptotic signaling in resistant hepatoma cells, suggesting a potential for overcoming drug resistance (81).

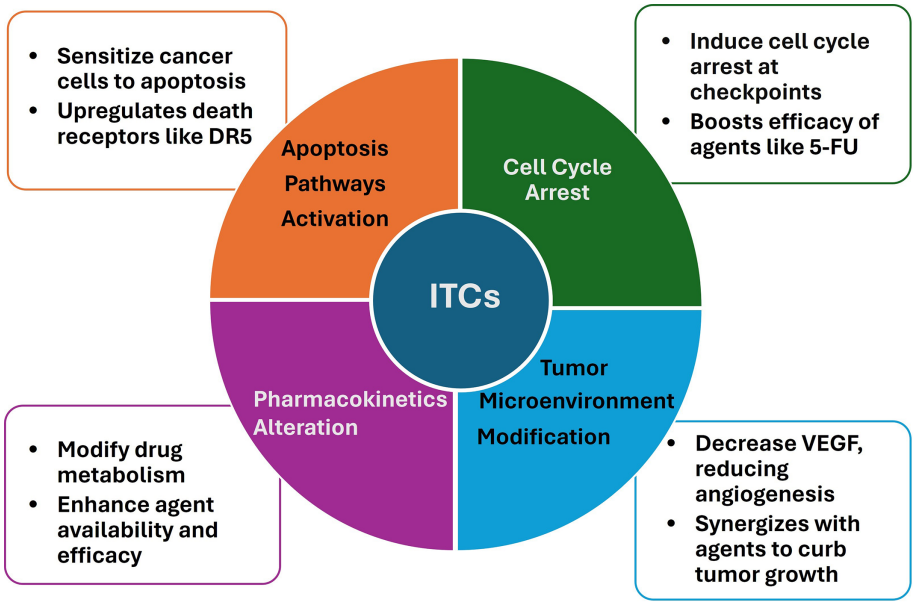

FIGURE 2
Mechanisms involved in the synergistic interactions between ITCs and anticancer agents.

The cell cycle is another critical target for the synergistic action of ITCs and anticancer drugs. ITCs have been documented to induce cell cycle arrest at various checkpoints, thereby halting the proliferation of cancer cells (98–100). When ITCs are combined with chemotherapeutic agents that also disrupt the cell cycle, such as 5-FU, the result can be a more pronounced inhibition of cancer cell growth (69, 85). This effect is likely due to the complementary mechanisms of action, whereby ITCs modulate key cell cycle regulators, such as p21, and enhance the cytostatic effects of the drugs (67, 69).

The tumor microenvironment, which includes the surrounding immune cells and extracellular matrix, plays a significant role in cancer progression and response to therapy. One way ITCs influence the tumor microenvironment is by inhibiting angiogenesis, a crucial process for tumor growth and metastasis. This effect is achieved by reducing VEGF secretion (31, 44, 100, 101). This anti-angiogenic effect, coupled with the anti-metastatic properties of ITCs, can synergize with drugs that target the tumor microenvironment, leading to reduced tumor growth and spread (30, 100).

Pharmacokinetics processes, including drug absorption, distribution, metabolism, and excretion in the body, are also affected by the presence of ITCs. These compounds can alter the metabolism of anticancer drugs, potentially increasing their bioavailability and effectiveness (14, 37). For example, ITCs have been shown to modulate the activity of phase II detoxification enzymes, which can influence the bioavailability and effectiveness of anticancer agents (14, 67).

3 Risks and considerations in dietary isothiocyanates consumption

While extensive research has focused on the chemopreventive properties of ITCs, there is a growing concern regarding potential risks associated with their consumption, particularly in individuals with undetected tumors. This section aims to underscore these risks and considerations, emphasizing the importance of conducting a comprehensive risk assessment to ensure safety and optimize the benefits of ITC intake.

In this review, we define low doses of SFN as 1–5 μM and high doses as above 10 μM, based on concentrations used in cited studies. It is important to note that these ranges can differ depending on the specific treatment and cellular model. The separation of low and high doses is crucial to avoid overlap and to understand the hormetic effects accurately.

The hormetic effects of isothiocyanates (ITCs) have been a subject of recent studies, indicating that their benefits or risks largely depend on the dose and endpoint of interest (30, 31). Despite their capability to induce apoptosis and hinder cell proliferation in cancer cells, the ability of ITCs to stimulate phase II detoxification enzymes and influence cell cycle regulation could inadvertently promote tumor growth under certain circumstances (37, 98). For instance, while the induction of Nrf2 by ITCs plays a critical role in cellular defense against oxidative stress, its prolonged activation has been associated with tumor promotion and chemoresistance (66, 85). This hormetic nature of ITCs necessitates a careful evaluation of the appropriate dosage for cancer prevention and treatment, as well as the timing of intake relative to other cancer therapies (30).

In combination therapy, the hormetic effect of ITCs may be influenced by the presence of other anticancer agents. Therefore, the defined dosage range of ITCs for their hormetic effect may vary due to the complexity of the mechanisms when ITCs and other anticancer agents work simultaneously. For instance, a lower dose of sulforaphane (SFN) at 2.5 μM can protect cardiac cells from the toxicity of doxorubicin, thereby enhancing the therapeutic window (92). Additionally, up to 1.5 μM SFN can enhance cisplatin sensitivity through the accumulation of intracellular cisplatin in ovarian cancer cells (82). Conversely, 10 μM of SFN can reduce cancer cell resistance to conventional anticancer drugs like cisplatin and paclitaxel, working synergistically to enhance the cytotoxic effects on cancer cells (83, 93). This dual capability underscores the potential of SFN to improve overall therapeutic efficacy. Therefore, a nuanced approach to dose selection in combination therapies is essential to maximize anticancer effects while minimizing potential adverse effects.

Moreover, the influence of ITCs on individuals with undetected tumors remains inadequately understood. There is a potential scenario where ITCs could offer protection against the formation of these tumors. Conversely, they could also inadvertently stimulate the growth of pre-existing yet undiagnosed malignancies (30). This highlights the need for comprehensive risk assessment and personalized dietary recommendations, particularly for individuals at high risk of cancer or those with a family history of the disease.

Another consideration is the variability in individual responses to ITCs, which can be influenced by genetic factors such as polymorphisms in genes related to detoxification enzymes (30). These genetic differences can affect the metabolism and bioavailability of ITCs, leading to variations in their chemopreventive efficacy and potential risks. As such, personalized approaches to ITC intake that take into account genetic predispositions may be necessary to ensure safety and maximize the benefits of these compounds.

In light of these considerations, it is imperative to conduct more research to elucidate the mechanisms underlying the hormetic effects of ITCs and their implications in cancer development and treatment. Studies should aim to determine the optimal doses of ITCs for chemoprevention, identify potential interactions with anticancer drugs, and assess the safety of ITC consumption in individuals with undetected tumors. Additionally, research should explore the genetic factors that influence individual responses to ITCs, with the goal of developing personalized dietary guidelines for cancer prevention.

4 Discussion

The comprehensive exploration of ITCs within the context of cancer prevention and therapy showcases a promising avenue in oncology. Particularly, compounds like SFN emerge as potent agents capable of modulating crucial biological processes involved in carcinogenesis, including cell cycle regulation, apoptosis, and anti-angiogenesis. Evidence from epidemiological, *in vitro*, and *in vivo* studies underscores the protective role of ITCs, suggesting their significant contribution to reducing cancer risk and progression. One of the most compelling aspects of ITC research is its potential to synergize with existing chemotherapies. The observed synergistic

interactions, as evidenced by CI values less than 1, could potentially amplify the efficacy of chemotherapeutic agents, mitigate adverse side effects, and overcome drug resistance. However, achieving these synergistic effects necessitates careful consideration of dosage and combination strategies to balance therapeutic benefits against potential risks.

In addition, the synergistic effects of ITCs are not limited to interactions with chemotherapeutic agents. Research has indicated that combinations of multiple ITCs or ITCs with other phytochemicals can exert enhanced antiproliferative effects on various cancer cell lines (17, 74). For example, the combined application of lycopene, SFN, quercetin, and curcumin has shown improved antiproliferative potential in colon cancer cells, suggesting that a cocktail of natural compounds may be an effective strategy against tumor growth. These combinations could leverage multiple dietary components to formulate a more practical approach against cancer. Nevertheless, the translation of these preclinical findings into clinical practice requires meticulous attention to factors like bioavailability, pharmacokinetics, and individual metabolic differences.

The potential for personalized treatment strategies based on the synergistic effects of ITCs and anticancer drugs is an exciting prospect. The variability in response to cancer therapies among individuals underscores the need for personalized medicine approaches considering genetic, environmental, and lifestyle factors. The identification of specific biomarkers that predict the response to ITC-based combination therapies could lead to more tailored and effective treatment regimens. Moreover, ongoing clinical trials are investigating the efficacy and safety of ITCs in combination with established anticancer drugs, which will provide valuable data for developing personalized treatment protocols (31).

Despite these encouraging findings, the path to clinical application is fraught with challenges. The hormetic effects of ITCs, characterized by beneficial or adverse outcomes depending on dosage, underscore the need for precise application in therapeutic contexts. The discussion around their potential risks in individuals with undetected tumors, and the variability in individual responses due to genetic factors introduces a layer of complexity. This highlights the necessity for precise dosing, comprehensive risk assessments, and personalized dietary recommendations to maximize the benefits of ITC intake while minimizing potential adverse effects.

Looking forward, the path to fully harnessing ITCs in cancer management is laden with challenges that demand rigorous investigation. To fully leverage the potential of ITCs, prospective studies should prioritize conducting extensive clinical trials to validate the therapeutic efficacy and safety profile of ITCs, particularly in synergy with existing anticancer therapies. A deeper understanding of the molecular mechanisms driving the synergistic effects of ITCs with anticancer agents is essential for the development of more potent and effective combination treatments. Additionally, exploring the potential of ITCs within the realms of targeted therapy and immunotherapy could unveil groundbreaking approaches to cancer treatment. The advancement of nanotechnology-based delivery systems promises to address the current limitations in the bioavailability and stability of ITCs, setting the stage for enhanced cancer prevention and therapeutic strategies. As the field progresses, it is anticipated that these efforts will lead to more effective and less toxic cancer management options, ultimately improving the quality of life and survival rates for cancer patients.

5 Conclusion

As we advance our understanding of ITCs in cancer management, the journey toward clinical application is filled with promise and challenges. Future research should focus on validating the therapeutic efficacy and safety of ITCs through clinical trials, particularly in combination with anticancer drugs. Unraveling the molecular mechanisms behind the synergistic effects of ITCs will pave the way for more effective combination therapies. Moreover, integrating ITCs into targeted therapy and immunotherapy could revolutionize cancer treatment approaches.

The advancement of nanotechnology offers promising solutions to the limitations of bioavailability and stability of ITCs, potentially enhancing prevention and therapeutic strategies. As research progresses, these efforts are expected to yield more effective and less toxic options for cancer management, ultimately improving patient outcomes.

The potential of dietary ITCs within a multidisciplinary cancer treatment paradigm holds the promise of a future where cancer therapy is more effective and less burdensome for patients. Harnessing this potential will require a concerted effort across the fields of nutrition, pharmacology, oncology, and biotechnology.

Author contributions

QW: Conceptualization, Writing – original draft, Writing – review & editing. DL: Conceptualization, Writing – original draft, Writing – review & editing. LL: Writing – review & editing. YS: Writing – review & editing. YB: Writing – review & editing, Conceptualization, Funding acquisition.

Funding

The author(s) declare that financial support was received for the research, authorship, and/or publication of this article. This work was supported by Cancer Prevention Research Trust, UK.

Acknowledgments

The authors express their gratitude to the Cancer Prevention Research Trust, UK, for their invaluable support. We also extend our thanks to Dr. Rachel Hurst for her meticulous proofreading of the manuscript.

Conflict of interest

The authors declare that the research was conducted in the absence of any commercial or financial relationships that could be construed as a potential conflict of interest.

Publisher's note

References

1. Bray F, Laversanne M, Sung H, Ferlay J, Siegel RL, Soerjomataram I, et al. Globocan estimates of incidence and mortality worldwide for 36 cancers in 185 countries. *CA Cancer J Clin*. (2022) 74:229–63. doi: 10.3322/caac.21834

2. Siegel RL, Giaquinto AN, Jemal A. Cancer statistics, 2024. *CA Cancer J Clin*. (2024) 74:12–49. doi: 10.3322/caac.21820

3. Idrees N, Saquib M, Azmi S, Ahmad I, Hussain MK. (2020). *Anticancer and chemopreventive phytochemicals from cruciferous plants*. Singapore: Springer Singapore. p. 375–385.

4. Idrees N, Tabassum B, Sarah R, Hussain MK. (2019). *Natural compound from genus Brassica and their therapeutic activities*. Singapore: Springer Singapore. p. 477–491.

5. London SJ, Yuan JM, Chung FL, Gao YT, Coetzee GA, Ross RK, et al. Isothiocyanates, glutathione S-transferase M1 and T1 polymorphisms, and lung-Cancer risk: a prospective study of men in Shanghai, China. *Lancet*. (2000) 356:724–9. doi: 10.1016/S0140-6736(00)02631-3

6. Mori N, Shimazu T, Charvat H, Mutoh M, Sawada N, Iwasaki M, et al. Cruciferous vegetable intake and mortality in middle-aged adults: a prospective cohort study. *Clin Nutr*. (2019) 38:631–43. doi: 10.1016/j.clnu.2018.04.012

7. Wang Z, Tu C, Pratt R, Khoury T, Qu J, Fahey JW, et al. A Presurgical-window intervention trial of Isothiocyanate-rich broccoli sprout extract in patients with breast Cancer. *Mol Nutr Food Res*. (2022) 66:e2101094. doi: 10.1002/mnfr.202101094

8. Kaewsit N, Winuprasith T, Trachootham D. Detoxification of heterocyclic aromatic amines from grilled meat using a Peitc-rich vegetable sauce: a randomized crossover controlled trial. *Food Funct*. (2021) 12:10411–22. doi: 10.1039/d1fo01733k

9. Zhang Z, Garzotto M, Davis EW 2nd, Mori M, Stoller WA, Farris PE, et al. Sulforaphane bioavailability and chemopreventive activity in men presenting for biopsy of the prostate gland: a randomized controlled trial. *Nutr Cancer*. (2020) 72:74–87. doi: 10.1080/01635581.2019.1619783

10. Tran H, Schreiner M, Schlotz N, Lamy E. Short-term dietary intervention with cooked but not raw Brassica leafy vegetables increases telomerase activity in Cd8+ lymphocytes in a randomized human trial. *Nutrients*. (2019) 11:786. doi: 10.3390/nu11040786

11. Traka MH, Melchini A, Coode-Bate J, al Kadhi O, Saha S, Defernez M, et al. Transcriptional changes in prostate of men on active surveillance after a 12-Mo glucoraphanin-rich broccoli intervention—results from the effect of Sulforaphane on prostate Cancer prevention (escape) randomized controlled trial. *Am J Clin Nutr*. (2019) 109:1133–44. doi: 10.1093/ajcn/nqz012

12. Chen JG, Johnson J, Egner P, Ng D, Zhu J, Wang JB, et al. Dose-dependent detoxication of the airborne pollutant benzene in a randomized trial of broccoli sprout beverage in Qidong. *China Am J Clin Nutr*. (2019) 110:675–84. doi: 10.1093/ajcn/nqz122

13. Sangkret S, Pongmalai P, Devahastin S, Chiewchan N. Enhanced production of sulforaphane by exogenous glucoraphanin hydrolysis catalyzed by myrosinase extracted from Chinese flowering cabbage (*Brassica Rapa* Var. Parachinensis). *Sci Rep*. (2019) 9:46382. doi: 10.1038/s41598-019-46382-7

14. Vanduchova A, Anzenbacher P, Anzenbacherova E. Isothiocyanate from broccoli, sulforaphane, and its properties. *J Med Food*. (2019) 22:121–6. doi: 10.1089/jmf.2018.0024

15. Li YZ, Yang ZY, Gong TT, Liu YS, Liu FH, Wen ZY, et al. Cruciferous vegetable consumption and multiple health outcomes: an umbrella review of 41 systematic reviews and meta-analyses of 303 observational studies. *Food Funct*. (2022) 13:4247–59. doi: 10.1039/d1fo03094a

16. Mitsiogianni M, Koutsidis G, Mavroudis N, Trafalis D, Botaitis S, Franco R, et al. The role of isothiocyanates as cancer chemo-preventive, chemo-therapeutic and anti-melanoma agents. *Antioxidants*. (2019) 8:106. doi: 10.3390/antiox8040106

17. Rakariyatham K, Yang X, Gao Z, Song M, Han Y, Chen X, et al. Synergistic chemopreventive effect of allyl isothiocyanate and sulforaphane on non-small cell lung carcinoma cells. *Food Funct*. (2019) 10:893–902. doi: 10.1039/c8fo01914b

18. Powolny AA, Bommareddy A, Hahm E-R, Normolle DP, Beumer JH, Nelson JB, et al. Chemopreventative potential of the cruciferous vegetable constituent phenethyl isothiocyanate in a mouse model of prostate cancer. *J Natl Cancer Inst*. (2011) 103:571–84. doi: 10.1093/jnci/djr029

19. Vyas AR, Hahm E-R, Arlotti JA, Watkins S, Stolz DB, Desai D, et al. Chemoprevention of prostate cancer by D,L-sulforaphane is augmented by pharmacological inhibition of autophagy. *Cancer Res*. (2013) 73:5985–95. doi: 10.1158/0008-5472.can-13-0755

20. Singh KB, Kim S-H, Hahm E-R, Pore SK, Jacobs BL, Singh SV. Prostate Cancer chemoprevention by sulforaphane in a preclinical mouse model is associated with inhibition of fatty acid metabolism. *Carcinogenesis*. (2018) 39:826–37. doi: 10.1093/carcin/bgy051

21. Sehrawat A, Roy R, Pore SK, Hahm E-R, Samanta SK, Singh KB, et al. Mitochondrial dysfunction in Cancer chemoprevention by phytochemicals from dietary and medicinal plants. *Semin Cancer Biol*. (2017) 47:147–53. doi: 10.1016/j.semcancer.2016.11.009

22. Alhakamy NA, Saquib M, Sanobar KMF, Khan MF, Ansari WA, Arif DO, et al. Natural product-inspired synthesis of Coumarin–Chalcone hybrids as potential anti-breast Cancer agents. *Front Pharmacol*. (2023) 14:1231450. doi: 10.3389/fphar.2023.1231450

23. Saquib M, Ansari MI, Johnson CR, Khatoon S, Hussain MK, Coop A. Recent advances in the targeting of human DNA ligase I as a potential new strategy for Cancer treatment. *Eur J Med Chem*. (2019) 182:111657. doi: 10.1016/j.ejmech.2019.111657

24. Xie C, Zhu J, Jiang Y, Chen J, Wang X, Geng S, et al. Sulforaphane inhibits the acquisition of Tobacco smoke-induced lung cancer stem cell-like properties via the Il-6/Δnp63α/notch Axis. *Theranostics*. (2019) 9:4827–40. doi: 10.7150/thno.33812

25. Kallifatidis G, Labsch S, Rausch V, Mattern J, Gladkich J, Moldenhauer G, et al. Sulforaphane increases drug-mediated cytotoxicity toward cancer stem-like cells of pancreas and prostate. *Mol Ther*. (2011) 19:188–95. doi: 10.1038/mt.2010.216

26. Gu H, Ren F, Mao X, Du M. Mineralized and Gsh-responsive hyaluronic acid based Nano-carriers for potentiating repressive effects of Sulforaphane on breast Cancer stem cells-like properties. *Carbohydr Polym*. (2021) 269:118294. doi: 10.1016/j.carbpol.2021.118294

27. Wang M, Tang L, Chen S, Wang L, Wu J, Zhong C, et al. Znf217-activated notch signaling mediates Sulforaphane-suppressed stem cell properties in colorectal cancer. *J Nutr Biochem*. (2024) 125:109551. doi: 10.1016/j.jnutbio.2023.109551

28. Chen Y, Wang M, Wu J, Zhu J, Xie C, Li X, et al. Δnp63α mediates Sulforaphane suppressed colorectal Cancer stem cell properties through transcriptional regulation of Nanog/Oct4/Sox2. *J Nutr Biochem*. (2022) 107:109067. doi: 10.1016/j.jnutbio.2022.109067

29. Calabrese V, Cornelius C, Dinkova-Kostova AT, Iavicoli I, di Paola R, Koverech A, et al. Cellular stress responses, Hormetic phytochemicals and Vitagenes in aging and longevity. *Biochim Biophys Acta*. (2012) 1822:753–83. doi: 10.1016/j.bbadis.2011.11.002

30. Bao Y, Wang W, Zhou Z, Sun C. Benefits and risks of the hormetic effects of dietary isothiocyanates on cancer prevention. *PLoS One*. (2014) 9:e114764. doi: 10.1371/journal.pone.0114764

31. Na G, He C, Zhang S, Tian S, Bao Y, Shan Y. Dietary isothiocyanates: novel insights into the potential for cancer prevention and therapy. *Int J Mol Sci*. (2023) 24:1962. doi: 10.3390/ijms24031962

32. Kamal MM, Akter S, Lin C-N, Nazzal S. Sulforaphane as an anticancer molecule: mechanisms of action, synergistic effects, enhancement of drug safety, and delivery systems. *Arch Pharm Res*. (2020) 43:371–84. doi: 10.1007/s12272-020-01225-2

33. Coutinho LDL, Junior TCT, Rangel MC. Sulforaphane: an emergent anti-cancer stem cell agent. *Front Oncol*. (2023) 13:1089115. doi: 10.3389/fonc.2023.1089115

34. Asif Ali M, Khan N, Kaleem N, Ahmad W, Alharethi SH, Alharbi B, et al. Anticancer properties of sulforaphane: current insights at the molecular level. *Front Oncol*. (2023) 13:1168321. doi: 10.3389/fonc.2023.1168321

35. Liu P, Wang W, Tang J, Bowater RP, Bao Y. Antioxidant effects of sulforaphane in human Hepg2 cells and immortalised hepatocytes. *Food Chem Toxicol*. (2019) 128:129–36. doi: 10.1016/j.fct.2019.03.050

36. Yagishita Y, Fahey JW, Dinkova-Kostova AT, Kensler TW. Broccoli or sulforaphane: is it the source or dose that matters? *Molecules*. (2019) 24:3593. doi: 10.3390/molecules24193593

37. Hussain A, Priyani A, Sadrieh L, Brahmbhatt K, Ahmed M, Sharma C. Concurrent sulforaphane and eugenol induces differential effects on human cervical Cancer cells. *Integr Cancer Ther*. (2012) 11:154–65. doi: 10.1177/1534735411400313

38. Wu X, Zhou Q-H, Xu K. Are isothiocyanates potential anti-Cancer drugs? *Acta Pharmacol Sin*. (2009) 30:501–12. doi: 10.1038/aps.2009.50

39. Sharma C, Sadrieh L, Priyani A, Ahmed M, Hassan AH, Hussain A. Anti-carcinogenic effects of sulforaphane in association with its apoptosis-inducing and anti-inflammatory properties in human cervical Cancer cells. *Cancer Epidemiol*. (2011) 35:272–8. doi: 10.1016/j.canep.2010.09.008

40. Rabben H-L, Kodama Y, Nakamura M, Bones AM, Wang TC, Chen D, et al. Chemopreventive effects of dietary isothiocyanates in animal models of gastric Cancer and synergistic anticancer effects with cisplatin in human gastric Cancer cells. *Front Pharmacol*. (2021) 12:613458. doi: 10.3389/fphar.2021.613458

41. Elkashty OA, Tran SD. Broccoli extract increases drug-mediated cytotoxicity towards cancer stem cells of head and neck squamous cell carcinoma. *Br J Cancer*. (2020) 123:1395–403. doi: 10.1038/s41416-020-1025-1

42. Kerr C, Adhikary G, Grun D, George N, Eckert RL. Combination cisplatin and sulforaphane treatment reduces proliferation, invasion, and tumor formation in epidermal squamous cell carcinoma. *Mol Carcinog*. (2018) 57:3–11. doi: 10.1002/mc.22714

43. Otoo RA, Allen AR. Sulforaphane's multifaceted potential: from neuroprotection to anticancer action. *Molecules*. (2023) 28:6902. doi: 10.3390/molecules28196902

44. Strusi G, Suelzu CM, Weldon S, Giffin J, Münsterberg AE, Bao Y. Combination of phenethyl isothiocyanate and dasatinib inhibits hepatocellular carcinoma metastatic potential through Fak/Stat3/cadherin signalling and reduction of Vegf secretion. *Pharmaceutics*. (2023) 15:2390. doi: 10.3390/pharmaceutics15102390

45. Strusi G, Suelzu CM, Horwood N, Münsterberg AE, Bao Y. Phenethyl isothiocyanate and dasatinib combination synergistically reduces hepatocellular carcinoma growth via cell cycle arrest and oxeiptosis. *Front Pharmacol*. (2023) 14:1264032. doi: 10.3389/fphar.2023.1264032

46. Treasure K, Harris J, Williamson G. Exploring the anti-inflammatory activity of sulforaphane. *Immunol Cell Biol*. (2023) 101:805–28. doi: 10.1111/imcb.12686

47. Saw CL, Cintron M, Wu TY, Guo Y, Huang Y, Jeong WS, et al. Pharmacodynamics of dietary phytochemical indoles I3c and dim: induction of Nrf2-mediated phase ii drug metabolizing and antioxidant genes and synergism with isothiocyanates. *Biopharm Drug Dispos*. (2011) 32:289–300. doi: 10.1002/bdd.759

48. Rong Y, Huang L, Yi K, Chen H, Liu S, Zhang W, et al. Co-administration of sulforaphane and doxorubicin attenuates breast cancer growth by preventing the accumulation of myeloid-derived suppressor cells. *Cancer Lett*. (2020) 493:189–96. doi: 10.1016/j.canlet.2020.08.041

49. Wang DX, Zou YJ, Zhuang XB, Chen SX, Lin Y, Li WL, et al. Sulforaphane suppresses EMT and metastasis in human lung cancer through Mir-616-5p-mediated Gsk3β/B-catenin signaling pathways. *Acta Pharmacol Sin*. (2017) 38:241–51. doi: 10.1038/aps.2016.122

50. Chen Y, Chen J-q, Ge M-m, Zhang Q, Wang X-q, Zhu J-y, et al. Sulforaphane inhibits epithelial–mesenchymal transition by activating extracellular signal-regulated kinase 5 in lung cancer cells. *J Nutr Biochem*. (2019) 72:108219. doi: 10.1016/j.jnutbio.2019.108219

51. Zheng Z, Lin K, Hu Y, Zhou Y, Ding X, Wang Y, et al. Sulforaphane metabolites inhibit migration and invasion via microtubule-mediated Claudins dysfunction or inhibition of autolysosome formation in human non-small cell lung cancer cells. *Cell Death Dis*. (2019) 10:259. doi: 10.1038/s41419-019-1489-1

52. Yan Y, Zhou Y, Li J, Zheng Z, Hu Y, Li L, et al. Sulforaphane downregulated fatty acid synthase and inhibited microtubule-mediated mitophagy leading to apoptosis. *Cell Death Dis*. (2021) 12:917. doi: 10.1038/s41419-021-04198-2

53. Byun S, Shin SH, Park J, Lim S, Lee E, Lee C, et al. Sulforaphene suppresses growth of colon cancer-derived tumors via induction of glutathione depletion and microtubule depolymerization. *Mol Nutr Food Res*. (2016) 60:1068–78. doi: 10.1002/mnfr.201501011

54. O'Mealey GB, Berry WL, Plafker SM. Sulforaphane is a Nrf2-independent inhibitor of mitochondrial fission. *Redox Biol*. (2017) 11:103–10. doi: 10.1016/j.redox.2016.11.007

55. Lu Z, Ren Y, Yang L, Jia A, Hu Y, Zhao Y, et al. Inhibiting autophagy enhances sulforaphane-induced apoptosis via targeting NRF2 in esophageal squamous cell carcinoma. *Acta Pharm Sin B*. (2021) 11:1246–60. doi: 10.1016/j.apsb.2020.12.009

56. Li D, Shao R, Wang N, Zhou N, du K, Shi J, et al. Sulforaphane activates a lysosome-dependent transcriptional program to mitigate oxidative stress. *Autophagy*. (2021) 17:872–87. doi: 10.1080/15548627.2020.1739442

57. Xia Y, Kang TW, Jung YD, Zhang C, Lian S. Sulforaphane inhibits nonmuscle invasive bladder cancer cells proliferation through suppression of Hif-1α-mediated glycolysis in hypoxia. *J Agric Food Chem*. (2019) 67:7844–54. doi: 10.1021/acs.jafc.9b03027

58. Huang L, He C, Zheng S, Wu C, Ren M, Shan Y. Akt1/Hk2 Axis-mediated glucose metabolism: a novel therapeutic target of sulforaphane in bladder cancer. *Mol Nutr Food Res*. (2022) 66:e2100738. doi: 10.1002/mnfr.202100738

59. Moon D-O, Kang S-H, Kim K-C, Kim M-O, Choi YH, Kim G-Y. Sulforaphane decreases viability and telomerase activity in hepatocellular carcinoma Hep3b cells through the reactive oxygen species-dependent pathway. *Cancer Lett*. (2010) 295:260–6. doi: 10.1016/j.canlet.2010.03.009

60. Lamy E, Oey D, Eißmann F, Herz C, Münstedt K, Tinneberg H-R, et al. Erucin and benzyl isothiocyanate suppress growth of late stage primary human ovarian carcinoma cells and telomerase activity in vitro. *Phytother Res*. (2013) 27:1036–41. doi: 10.1002/ptr.4798

61. Weir TL, Trikha SRJ, Thompson HJ. Diet and cancer risk reduction: the role of diet-microbiota interactions and microbial metabolites. *Semin Cancer Biol*. (2021) 70:53–60. doi: 10.1016/j.semcancer.2020.06.007

62. He C, Huang L, Lei P, Liu X, Li B, Shan Y. Sulforaphane normalizes intestinal flora and enhances gut barrier in mice with BBN-induced bladder cancer. *Mol Nutr Food Res*. (2018) 62:e1800427. doi: 10.1002/mnfr.201800427

63. Santos PW, Machado ART, de Grandis R, Ribeiro DL, Tuttis K, Morselli M, et al. Effects of Sulforaphane on the oxidative response, apoptosis, and the transcriptional profile of human stomach mucosa cells *in vitro*. *Mutat Res Genet Toxicol Environ Mutagen*. (2020) 854-855:503201. doi: 10.1016/j.mrgentox.2020.503201

64. Wang Y, Chen F, Zhang Y, Zheng X, Liu S, Tang M, et al. Biphasic effect of sulforaphane on angiogenesis in hypoxia via modulation of both Nrf2 and mitochondrial dynamics. *Food Funct*. (2022) 13:2884–98. doi: 10.1039/d1fo04112f

65. Saquib M, Ahamad S, Khan MF, Khan MI, Hussain MK. An ultrasound assisted, ionic liquid-molecular iodine synergy driven efficient green synthesis of pyrrolobenzodiazepine-triazole hybrids as potential anticancer agents. *Front Pharmacol*. (2023) 14:1168566. doi: 10.3389/fphar.2023.1168566

66. Hunakova L, Gronesova P, Horvathova E, Chalupa I, Cholujova D, Duraj J, et al. Modulation of cisplatin sensitivity in human ovarian carcinoma A2780 and Skov3 cell lines by sulforaphane. *Toxicol Lett*. (2014) 230:479–86. doi: 10.1016/j.toxlet.2014.08.018

67. Mielczarek L, Krug P, Mazur M, Milczarek M, Chilmonczyk Z, Wiktorska K. In the triple-negative breast cancer MDA-MB-231 cell line, sulforaphane enhances the intracellular accumulation and anticancer action of doxorubicin encapsulated in liposomes. *Int J Pharm*. (2019) 558:311–8. doi: 10.1016/j.ijpharm.2019.01.008

68. Calcabrini C, Maffei F, Turrini E, Fimognari C. Sulforaphane potentiates anticancer effects of doxorubicin and cisplatin and mitigates their toxic effects. *Front Pharmacol*. (2020) 11:567. doi: 10.3389/fphar.2020.00567

69. Milczarek M, Pogorzelska A, Wiktorska K. Synergistic interaction between 5-Fu and an analog of sulforaphane-2-Oxohexyl isothiocyanate-in an *in vitro* colon cancer model. *Molecules*. (2021) 26:3019. doi: 10.3390/molecules26103019

70. Royston K, Udayakumar N, Lewis K, Tollefsbol T. A novel combination of withaferin a and sulforaphane inhibits epigenetic machinery, cellular viability and induces apoptosis of breast cancer cells. *Int J Mol Sci*. (2017) 18:1092. doi: 10.3390/ijms18051092

71. Royston KJ, Paul B, Nozell S, Rajbhandari R, Tollefsbol TO. Withaferin a and Sulforaphane regulate breast Cancer cell cycle progression through epigenetic mechanisms. *Exp Cell Res*. (2018) 368:67–74. doi: 10.1016/j.yexcr.2018.04.015

72. Paul B, Li YTollefsbol TO. The effects of combinatorial genistein and sulforaphane in breast tumor inhibition: role in epigenetic regulation. *Int J Mol Sci*. (2018) 19:1754. doi: 10.3390/ijms19061754

73. Sharma M, Tollefsbol TO. Combinatorial epigenetic mechanisms of sulforaphane, genistein and sodium butyrate in breast Cancer inhibition. *Exp Cell Res*. (2022) 416:113160. doi: 10.1016/j.yexcr.2022.113160

74. Langner E, Lemieszek MK, Rzeski W. Lycopene, sulforaphane, quercetin, and curcumin applied together show improved antiproliferative potential in colon cancer cells *in vitro*. *J Food Biochem*. (2019) 43:e12802. doi: 10.1111/jfbc.12802

75. Santana-Galvez J, Villela-Castrejon J, Serna-Saldivar SO, Cisneros-Zevallos L, Jacobo-Velazquez DA. Synergistic combinations of curcumin, sulforaphane, and dihydrocaffeic acid against human colon cancer cells. *Int J Mol Sci*. (2020) 21:3108. doi: 10.3390/ijms21093108

76. Rakariyatham K, Wu X, Tang Z, Han Y, Wang Q, Xiao H. Synergism between luteolin and sulforaphane in anti-inflammation. *Food Funct*. (2018) 9:5115–23. doi: 10.1039/c8fo01352g

77. Li S, Wu H, Chen M, Tollefsbol TO. Paternal combined botanicals contribute to the prevention of estrogen receptor–negative mammary Cancer in transgenic mice. *J Nutr*. (2023) 153:1959–73. doi: 10.1016/j.tjnut.2023.05.001

78. Cheung KLKhor TO, Kong A-N. Synergistic effect of combination of phenethyl isothiocyanate and sulforaphane or curcumin and sulforaphane in the inhibition of inflammation. *Pharm Res*. (2009) 26:224–31. doi: 10.1007/s11095-008-9734-9

79. Hutzen B, Willis W, Jones S, Cen L, Deangelis S, Fuh B, et al. Dietary agent, benzyl isothiocyanate inhibits signal transducer and activator of transcription 3 phosphorylation and collaborates with sulforaphane in the growth suppression of PANC-1 cancer cells. *Cancer Cell Int*. (2009) 9:24. doi: 10.1186/1475-2867-9-24

80. Wang F, Wang W, Li J, Zhang J, Wang X, Wang M. Sulforaphane reverses gefitinib tolerance in human lung cancer cells via modulation of sonic hedgehog signaling. *Oncol Lett*. (2018) 15:109–14. doi: 10.3892/ol.2017.7293

81. Kan SF, Wang J, Sun GX. Sulforaphane regulates apoptosis- and proliferation-related signaling pathways and synergizes with cisplatin to suppress human ovarian cancer. *Int J Mol Med*. (2018) 42:2447–58. doi: 10.3892/ijmm.2018.3860

82. Gong TT, Liu XD, Zhan ZP, Wu QJ. Sulforaphane enhances the cisplatin sensitivity through regulating DNA repair and accumulation of intracellular cisplatin in ovarian Cancer cells. *Exp Cell Res*. (2020) 393:112061. doi: 10.1016/j.yexcr.2020.112061

83. Sinha S, Sharma S, Sharma A, Vora J, Shrivastava N. Sulforaphane-cisplatin combination inhibits the stemness and metastatic potential of TNBCS via down regulation of sirtuins-mediated EMT signaling Axis. *Phytomedicine*. (2021) 84:153492. doi: 10.1016/j.phymed.2021.153492

84. Milczarek M, Wiktorska K, Mielczarek L, Koronkiewicz M, Dąbrowska A, Lubelska K, et al. Autophagic cell death and premature senescence: new mechanism of 5-fluorouracil and Sulforaphane synergistic anticancer effect in MDA-MB-231 triple negative breast Cancer cell line. *Food Chem Toxicol*. (2018) 111:1–8. doi: 10.1016/j.fct.2017.10.056

85. Milczarek M, Mielczarek L, Lubelska K, Dąbrowska A, Chilmonczyk Z, Matosiuk D, et al. *In vitro* evaluation of Sulforaphane and a natural analog as potent inducers of 5-fluorouracil anticancer activity. *Molecules*. (2018) 23:3040. doi: 10.3390/molecules 23113040

86. Milczarek M, Cierpiał T, Kiełbasiński P, Małecka-Giełdowska M, Świtalska M, Wietrzyk J, et al. An Organofluorine isoselenocyanate analogue of sulforaphane affects antimetabolite 5-Fluorouracil's anticancer activity: a perspective for new combinatory therapy in triple-negative breast Cancer. *Molecules*. (2023) 28:5808. doi: 10.3390/molecules28155808

87. Čižauskaitė A, Šimčikas D, Schultze D, Kallifatidis G, Bruns H, Čekauskas A, et al. Sulforaphane has an additive anticancer effect to folfox in highly metastatic human colon carcinoma cells. *Oncol Rep*. (2022) 48:205. doi: 10.3892/or.2022.8420

88. Li S, Xu Z, Alrobaian M, Afzal O, Kazmi I, Almalki WH, et al. EGF-functionalized lipid-polymer hybrid nanoparticles of 5-fluorouracil and sulforaphane with enhanced bioavailability and anticancer activity against colon carcinoma. *Biotechnol Appl Biochem*. (2022) 69:2205–21. doi: 10.1002/bab.2279

89. Desai P, Thakkar A, Ann D, Wang J, Prabhu S. Loratadine self-microemulsifying drug delivery systems (Smedds) in combination with sulforaphane for the synergistic chemoprevention of pancreatic cancer. *Drug Deliv Transl Res*. (2019) 9:641–51. doi: 10.1007/s13346-019-00619-0

90. Desai P, Wang KZ, Ann D, Wang J, Prabhu S. Efficacy and pharmacokinetic considerations of loratadine nanoformulations and its combinations for pancreatic Cancer chemoprevention. *Pharm Res*. (2020) 37:21. doi: 10.1007/s11095-019-2737-x

91. Pogorzelska A, Mazur M, Switalska M, Wietrzyk J, Sigorski D, Fronczyk K, et al. Anticancer effect and safety of doxorubicin and nutraceutical sulforaphane liposomal formulation in triple-negative breast Cancer (TNBC) animal model. *Biomed Pharmacother*. (2023) 161:114490. doi: 10.1016/j.biopha.2023.114490

92. Bose C, Awasthi S, Sharma R, Benes H, Hauer-Jensen M, Boerma M, et al. Sulforaphane potentiates anticancer effects of doxorubicin and attenuates its cardiotoxicity in a breast Cancer model. *PLoS One*. (2018) 13:e0193918. doi: 10.1371/journal.pone.0193918

93. Wang Y, Zhou Y, Zheng Z, Li J, Yan Y, Wu W. Sulforaphane metabolites reduce resistance to paclitaxel via microtubule disruption. *Cell Death Dis*. (2018) 9:1134. doi: 10.1038/s41419-018-1174-9

94. Bayat Mokhtari R, Baluch N, Morgatskaya E, Kumar S, Sparaneo A, Muscarella LA, et al. Human bronchial carcinoid tumor initiating cells are targeted by the combination of acetazolamide and sulforaphane. *BMC Cancer*. (2019) 19:864. doi: 10.1186/s12885-019-6018-1

95. Doğan Şiğva ZÖ, Balci Okcanoğlu T, Biray Avci C, Yilmaz Süslüer S, Kayabaşi Ç, Turna B, et al. Investigation of the synergistic effects of paclitaxel and herbal substances and endemic plant extracts on cell cycle and apoptosis signal pathways in prostate Cancer cell lines. *Gene*. (2019) 687:261–71. doi: 10.1016/j.gene.2018.11.049

96. Lubecka K, Kaufman-Szymczyk A, Fabianowska-Majewska K. Inhibition of breast cancer cell growth by the combination of clofarabine and sulforaphane involves epigenetically mediated CDKN2A upregulation. *Nucleosides Nucleotides Nucleic Acids*. (2018) 37:280–9. doi: 10.1080/15257770.2018.1453075

97. Tomooka F, Kaji K, Nishimura N, Kubo T, Iwai S, Shibamoto A, et al. Sulforaphane potentiates gemcitabine-mediated anti-cancer effects against intrahepatic cholangiocarcinoma by inhibiting Hdac activity. *Cells*. (2023) 12:687. doi: 10.3390/cells12050687

98. Wang X, Govind S, Sajankila SP, Mi L, Roy R, Chung FL. Phenethyl isothiocyanate sensitizes human cervical cancer cells to apoptosis induced by cisplatin. *Mol Nutr Food Res*. (2011) 55:1572–81. doi: 10.1002/mnfr.201000560

99. Aumeeruddy MZ, Mahomoodally MF. Combating breast cancer using combination therapy with 3 phytochemicals: piperine, sulforaphane, and thymoquinone. *Cancer*. (2019) 125:1600–11. doi: 10.1002/cncr.32022

100. Núñez-Iglesias MJ, Novío S, García C, Pérez-Muñuzuri E, Soengas P, Cartea E, et al. Glucosinolate-degradation products as co-adjuvant therapy on prostate cancer *in vitro*. *Int J Mol Sci*. (2019) 20:4977. doi: 10.3390/ijms20204977

101. Wang X, Li Y, Dai Y, Liu Q, Ning S, Liu J, et al. Sulforaphane improves chemotherapy efficacy by targeting cancer stem cell-like properties via the MIR-124/Il-6r/Stat3 axis. *Sci Rep*. (2016) 6:36796. doi: 10.1038/srep36796

frontiers | Frontiers in Nutrition

TYPE Review
PUBLISHED 30 September 2024
DOI 10.3389/fnut.2024.1448130

OPEN ACCESS

EDITED BY
Amanda N. Carey,
Simmons University, United States

REVIEWED BY
Jong-Sang Kim,
Kyungpook National University, Republic of Korea
Franziska S. Hanschen,
Leibniz Institute of Vegetable and Ornamental Crops, Germany

*CORRESPONDENCE
Anita A. Panjwani
✉ apanjwan@purdue.edu

RECEIVED 12 June 2024
ACCEPTED 09 September 2024
PUBLISHED 30 September 2024

CITATION
Ramakrishnan M, Fahey JW, Zimmerman AW, Zhou X and Panjwani AA (2024) The role of isothiocyanate-rich plants and supplements in neuropsychiatric disorders: a review and update.
Front. Nutr. 11:1448130.
doi: 10.3389/fnut.2024.1448130

The role of isothiocyanate-rich plants and supplements in neuropsychiatric disorders: a review and update

Monica Ramakrishnan[1], Jed W. Fahey[2,3,4,5], Andrew W. Zimmerman[6], Xinyi Zhou[1,7] and Anita A. Panjwani[1,7]*

[1]Department of Nutrition Science, College of Health and Human Sciences, Purdue University, West Lafayette, IN, United States, [2]Department of Medicine, Johns Hopkins School of Medicine, Baltimore, MD, United States, [3]Department of Pharmacology and Molecular Sciences, Johns Hopkins School of Medicine, Baltimore, MD, United States, [4]Department of Psychiatry, Johns Hopkins School of Medicine, Baltimore, MD, United States, [5]Institute of Medicine, University of Maine, Orono, ME, United States, [6]Department of Pediatrics, UMass Chan Medical School, Worcester, MA, United States, [7]Center on Aging and the Life Course, Purdue University, West Lafayette, IN, United States

Neuroinflammation in response to environmental stressors is an important common pathway in a number of neurological and psychiatric disorders. Responses to immune-mediated stress can lead to epigenetic changes and the development of neuropsychiatric disorders. Isothiocyanates (ITC) have shown promise in combating oxidative stress and inflammation in the nervous system as well as organ systems. While sulforaphane from broccoli is the most widely studied ITC for biomedical applications, ITC and their precursor glucosinolates are found in many species of cruciferous and other vegetables including moringa. In this review, we examine both clinical and pre-clinical studies of ITC on the amelioration of neuropsychiatric disorders (neurodevelopmental, neurodegenerative, and other) from 2018 to the present, including documentation of protocols for several ongoing clinical studies. During this time, there have been 16 clinical studies (9 randomized controlled trials), most of which reported on the effect of sulforaphane on autism spectrum disorder and schizophrenia. We also review over 80 preclinical studies examining ITC treatment of brain-related dysfunctions and disorders. The evidence to date reveals ITC have great potential for treating these conditions with minimal toxicity. The authors call for well-designed clinical trials to further the translation of these potent phytochemicals into therapeutic practice.

KEYWORDS

sulforaphane, glucosinolate, cruciferous, neurodevelopmental, neurodegenerative, neuroinflammation

1 Introduction

Isothiocyanates (ITC) found in cruciferous and related vegetables (e.g., broccoli and cabbage), exhibit diverse properties such as antibacterial, antifungal, antioxidant, and cytoprotective effects. They are produced as a result of enzymatic activity of myrosinase on glucosinolates (ITC precursors) present in plant cell vacuoles (Figure 1). Myrosinase is compartmentalized in cells of the same plant tissues and released upon cell lysis (e.g., chewing or wounding) (1). Additionally, microbiota in the gastrointestinal tracts of animals also

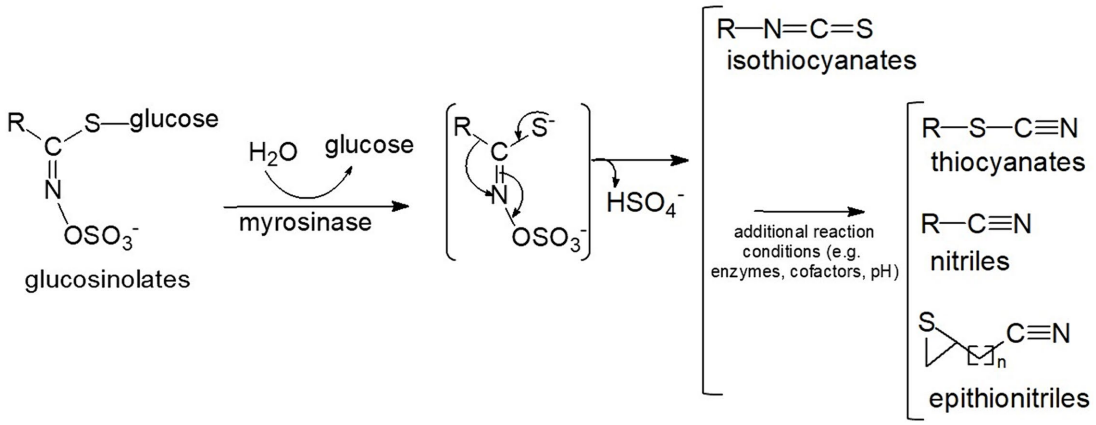

FIGURE 1
Conversion of glucosinolates to isothiocyanates and other reaction products. The myrosinase reaction produces an unstable intermediate which then non-enzymatically rearranges to isothiocyanates, or, in the presence of additional enzymes, cofactors and favorable conditions (e.g., low pH) can form a variety of alternative end-products including thiocyanates, nitriles, and epithionitriles (8).

contribute to this conversion. However, intraindividual differences in microbial conversion vary greatly, resulting in highly variable bioavailability (2). The formation of isothiocyanates from glucosinolates is also influenced by several other factors (3), including pH value, ferrous ions, and specifier proteins such as epithiospecifier protein (ESP), nitrile-specifier protein (NSP), and thiocyanate-forming protein (TFP). ESP, NFP and TFP can lead to the production of epithionitriles or nitriles upon the hydrolysis of glucosinolates in plant tissues (4). Additionally, glucosinolates undergo enzymatic conversion to amines (3, 5). The incomplete or variable conversion of glucosinolates to isothiocyanates may account for differing effects observed in various studies. Additional factors include genetic variability in the glutathione S-transferase M1 gene that could affect the metabolism of SF (6).

Sulforaphane (SF), derived from its glucosinolate precursor, glucoraphanin, is produced in greatest relative abundance in the cruciferous species *Brassica oleracea* var. *italica* (broccoli) as well as in a rangeland weed (*Cardaria draba*), some red cabbage (*B. oleracea var. capitata*) and red kale (*B. oleracea var. capitata*) sprouts. Sulforaphane stands out as a highly studied and promising therapeutic agent currently undergoing preclinical and clinical evaluation of a multitude of diseases and disorders (7). Apart from cruciferous vegetables, which are most familiar to human consumers, 15 other plant families produce over 120 different glucosinolates (8–10). A noteworthy example includes the tropical tree vegetable, *Moringa oleifera*, which is gaining wide recognition for its exceptional nutrient profile along with its cytoprotective properties; these properties are attributable in part to its primary ITC, moringin, derived from the glucosinolate glucomoringin (11). While there are documented toxic effects associated with the overconsumption of cruciferous and related vegetables, such as cabbages rich in indoles and thiocyanates and the presence of plant-derived toxins, they have been safely consumed by many people across the globe as part of a well-balanced diet (12).

Chronic oxidative stress, along with neuroinflammation, plays a central role in the pathogenesis of numerous neuropsychiatric disorders. For instance, in several clinical and preclinical studies, SF counteracts several molecular abnormalities associated with autism spectrum disorder (ASD) that address reduced antioxidant capacity, enhanced oxidative stress, deficient glutathione synthesis, mitochondrial dysfunction, increased lipid peroxidation, and neuroinflammation (2). SF's ability to readily cross the blood–brain barrier likely enables it to exert its clinical neurological effects (1).

A key mechanism of SF involves the activation of the nuclear transcription factor Nrf2 (nuclear factor erythroid 2–related factor 2), which orchestrates a suite of cytoprotective responses. SF binds with Keap1 (Kelch-like ECH-associated protein 1), causing its dissociation from Nrf2. Nrf2 is then free to translocate into the nucleus and induce the transcription of phase 2 detoxification enzyme genes (2). SF also induces anti-inflammatory, heat shock-response (HSR)-inducing, and histone deacetylase (HDAC) inhibiting responses, contributing to its multifaceted cytoprotective effects (2, 13).

Evidence for the effects of ITC from plants other than broccoli, such as *Moringa oleifera* and *Raphanus sativus* (radish), on chronic diseases including cancer, neurologic disorders, and cardiovascular diseases has been reviewed (14–25). We seek herein to review the effects of ITC and ITC-rich plants on brain-related disorders. We include reports on both clinical and pre-clinical studies demonstrating the potential of ITC to ameliorate these disorders. Our focus is on studies published from 2018 to 2023, and serves as an update to our previous review conducted in 2018, though we do reference some studies prior to this period to provide context (26).

2 Neurodevelopmental disorders

Recent clinical and preclinical studies have explored interventions in neurodevelopmental conditions using ITC. These studies mark the initial attempts to address disorders with disparate causes and pathophysiology through targeting potentially common pathways with these phytochemicals.

2.1 Autism spectrum disorder

Autism spectrum disorder (ASD) is a complex and heterogeneous neurodevelopmental disorder characterized by deficits in social communication and restricted, repetitive behaviors (27). The current

prevalence of ASD among 8-year-old children in the US is 1 in 36 (28), with over 600,000 new cases diagnosed annually worldwide (29). Currently, there are no FDA-approved pharmacological treatments for the core features of ASD. In this review, we report 9 clinical studies from 2014 to 2023, including 6 randomized controlled trials (RCTs), 1 non-randomized single arm clinical trial, and 1 case study related to the benefits of ITC on ASD (Table 1). We also report findings of ITC treatment in five preclinical studies, including 4 *in vivo* and 1 *in vitro* models of ASD.

2.1.1 Clinical studies

The first randomized controlled trial conducted in 2014 provided compelling evidence of the therapeutic potential of SF in the management of core features of ASD (NCT01474993) (30). Over an 18-week period, SF treatment (2.2 µmol/kg/day SF) significantly improved social interaction, reduced aberrant behavior, and enhanced verbal communication in autistic males aged 13–27 years. These effects returned to near baseline after a 4-week washout period. Further, responders who continued to consume dietary supplements containing glucoraphanin (GR), the glucosinolate precursor of SF reported sustained benefits for 3 years (31).

Since this first RCT, several clinical studies have attempted to replicate these findings. While the methodology has varied, most studies reported positive results though improvements were not as profound as in the initial study (32–37). The same group conducted another RCT in children aged 3–13 years, using GR plus myrosinase (2.2 µmol/kg/day SF), which showed mixed results (32). While clinical ratings did not significantly differ between the intervention and placebo groups using the clinician-rated Ohio Autism Clinical Impressions Scale (OACIS), there were significant improvements in caregiver-reported measures of aberrant behaviors (ABC-2). In addition, reductions in inflammatory biomarkers (TNF-α, IL-6, IL-1β) and improvements in glutathione redox status and mitochondrial function were apparent in the intervention group compared to the placebo group. Another study tested an adjuvant treatment of SF (50 or 100 µmol of SF/day depending on body weight) with risperidone and found children in the treatment group exhibited greater improvements in irritability and hyperactivity compared to the placebo group (35). A single-arm clinical trial found minimal amelioration in both ASD-related behaviors and fecal microbiome diversity with 2–8 GR plus myrosinase tablets/day depending on body weight (36), and one study found no difference in behavioral measures between treatment and placebo groups with 50 µmol/day (38).

In evaluating the mixed findings, we observed that the two studies that showed greatest improvements delivered SF itself (the plant-derived ITC, not a synthetic version, in a supplement matrix that represented some subset of the original plant extract with its attendant phytochemical diversity) while all other studies relied on the combination of a plant extract rich in GR and co-delivering active plant-derived myrosinase (30, 35). While one of these studies used SF as an adjunctive therapy, we posit that the method of delivery, SF, may be the key to minimizing differences in bioavailability and, consequently, achieving significant behavioral improvements. In the study that did not show any difference in behavior (30), SF (45.1 µmol) may have been inactivated due to high temperatures involved in its preparation. The pharmacokinetics of ITC production from glucosinolates in the gastrointestinal system, vs. delivery of pre-formed SF, are not fully understood, but what is currently known gives credence to this conjecture. The metabolic conversion of GR to SF may vary both developmentally and between individuals. At this writing (spring 2024) there are two ongoing studies using GR + myrosinase that are yet to report their findings on treatment in individuals with ASD (NCT02677051, NCT02909959; Table 1).

2.1.2 Pre-clinical studies

Interventions including oral SF-rich and glucoraphanin-rich preparations, as well as those of the plant maca (*Lepidium meyenii*), have shown promising outcomes in improving autism-associated outcomes. For example, SF treatment (282 µmol/kg/day for 7 days) reduced self-grooming/marble-burying behavior, improved social interaction, decreased T helper 17 (Th17) immune responses and oxidative stress, and increased enzymatic antioxidant defenses in an autism mouse model (39). In another study of a maternal immune activation (MIA) mouse model, GR intake (0.1% GR food pellets) of dams during pregnancy and lactation prevented cognitive and social interaction deficits in juvenile offspring and cognitive deficits in adult offspring (40). Moreover, oral administration of supplements containing GR and active myrosinase (2.2 µmol SF/kg/day for 14 days) increased mRNA levels of cytoprotective enzymes and heat shock proteins while decreasing mRNA levels of pro-inflammatory markers in peripheral blood mononuclear cells (PBMC) of patients with ASD (41). A study focusing on Nrf2 activation demonstrated SF (5 µmol incubated overnight) ameliorated inflammation and nitrative stress in ASD monocytes induced by LPS (lipopolysaccharide) (42). Finally, supplementation with maca (5 g/kg/day for 14 days)—an uncommon vegetable in the US, but one with high levels of glucosinolates—improved social deficits by upregulating oxytocinergic pathways in a valproic acid mouse model of ASD (43).

2.2 Schizophrenia

Schizophrenia is a progressive neurodevelopmental disorder with disruptions in cognitive functions, perceptual understanding, and executive function. Antipsychotic drugs are commonly used in the management of schizophrenia and can have long-term side effects. There have been four clinical studies—1 of which was an RCT—and 2 *in vivo* preclinical studies on schizophrenia and ITC treatment. Early intervention efforts for prodromal symptoms are being explored in patients with schizophrenia, including the incorporation of ITC like SF in the diet (44).

2.2.1 Clinical studies

Several clinical studies have reported on the effects of SF treatment in schizophrenia (Table 2). In an open-phase trial, participants with schizophrenia ($N = 7$) displayed significantly enhanced accuracy in the One Card Learning Task after 8 weeks of GR (68.5 µmol/day) administration (45). Similarly, another open-label study in this patient population ($N = 45$) demonstrated that a higher dose of GR + myrosinase (507.4 µmol SF/day) for 24 weeks resulted in significantly increased superoxide dismutase activity and HsCRP levels and a significant decrease in Positive and Negative Syndrome Scale (PANSS) negative subscale scores (46). Investigators aiming to study schizophrenia first conducted a study in healthy volunteers ($N = 9$) and demonstrated elevated blood glutathione levels after a week of daily SF (100 µmol/day for 7 days) consumption (47). The investigators also measured brain

TABLE 1 Clinical studies reported the effects of sulforaphane or glucoraphanin treatments on behavioral and health outcomes in individuals with ASD.

Author, Year (Study type)	Study population	Compound(s) delivered	Treatment and dose	Duration of intervention	N	Results
Singh et al., 2014 (30) (RCT)	Males (13–27 years old) with moderate to severe ASD	SF	50–150 µmol SF/day dosed by body wt.	18 weeks	44	Significant improvement of behavior scores [$p < 0.001$ (ABC) and $p = 0.017$ (SRS)].
Evans & Fuller, 2016 (37) (Case study)	Males (3–33 years old) enrolled from a public ASD forum	GR + myrosinase	Myrosinase Activated BroccoMax® containing a standardized GR content (the manufacturer claimed an *in vitro* yield of *ca.* 8 mg of SF, but SF delivery was not validated by the study authors)	≤28 weeks	6	Among children: Improvements in 69% of behavioral attributes, with substantial improvement in 29% (ABC and other unknown measures). Among adults: Improvement of 100% of behavioral attributes in the SRS, with substantial improvement in 59% (ABC and other unknown measures).
Bent et al., 2018 (33) (RCT)	Children and young adults (5–22 years old) with ASD and related neurodevelopmental disorders	GR + myrosinase	6–15 Avmacol tablets dosed at 222–555 µmol GR daily depending on body wt.	12 weeks	15	Improvement in mean behavior scores [ABC (ns) and SRS ($p = 0.03$)]. Urinary metabolites correlated with symptom amelioration.
Momtazmanesh et al., 2020 (35) (RCT)	Children (4–12 years old) with ASD	SF	50 µmol of SF/day for body weight lesser than 45 kg and 100 µmol of SF/day for 45–90 kg body wt.	10 weeks	60	Significant improvements in irritability ($p = 0.001$) and hyperactivity ($p = 0.015$), but no improvement in lethargy/social interaction, stereotypy, inappropriate speech (ABC) and frequent adverse events.
Zimmerman et al., 2021 (32) (RCT)	Children (3–12 years old) with ASD	GR + myrosinase	Avmacol equivalent to 2.2 µmol/kg/day SF	36 weeks	60	Significant improvement in scores with a non-randomized analysis of SF exposure duration (ABC $p < 0.001$), but no effects on SRS or OACIS. Significantly lower oxidative stress at 15 weeks ($p < 0.05$ for glutathione redox states). Significantly lower expression of IL-6 ($p = 0.006$) and TNF-α ($p = 0.01$) at 15 weeks but higher IL-1β expression at 7 weeks ($p = 0.03$) and 30 weeks ($p = 0.03$, 0.04). Lower heat shock protein (HSP70) expression correlated with symptom amelioration (ABC; $p < 0.05$) at 15 weeks. Improved mitochondrial function ($p < 0.05$ for increased ATP-Linked Respiration) and improvement correlated with symptom amelioration (ABC).
Ou et al., 2022 (34) (RCT)	Children (3–15 years old) with ASD	GR + myrosinase	Avmacol (2–8 tablets) daily depending on body wt. (4.5–60 kg)	12 weeks	110	Significant improvements of autism features [$p < 0.001$ (CGI-I) and $p < 0.002$ (OARS-4)], but no significant effects on behavior [SRS ($p = 0.885$), ABC ($p = 0.706$) and RBS-R ($p = 0.171$)]. Improvements higher in participants older than 10 years of age and effects spanned range of intelligence.

(Continued)

TABLE 1 (Continued)

Author, Year (Study type)	Study population	Compound(s) delivered	Treatment and dose	Duration of intervention	N	Results
Magner et al., 2023 (38) (RCT)	Children (3–7 years old) with ASD	GR + myrosinase	Laboratory preparation of broccoli and red radish sprout powder mix containing 50 µmol of SF per day	36 weeks	28	No significant improvement in behavior and general level of ASD (ABC, SRS-2 and ADOS-2).
Yang et al., 2023 (36) (Single arm clinical trial)	Boys (4–7 years old) with ASD (n = 6) or healthy controls (n = 11)	GR + myrosinase	Avmacol (2–8 tablets) daily depending on body wt. (4.54–58.97 kg)	12 weeks	17	Significant improvement in verbal or non-verbal communication [$p < 0.05$ (OARS-4)], but not in social interaction and repetitive/ritualistic behaviors. No gut microbial diversity associated with treatment. Correlation of 35 gut microbiome abundance alterations with symptoms of ASD.
Buyske, 2024 (RCT)	Young adults (13–30 years old) with ASD	GR + myrosinase	Avmacol daily; 1.5 µmol GR/kg body wt.	18 weeks	45	None reported yet; NCT02677051
Politte, 2024 (RCT)	Young men (13–30 years old) with ASD	GR + myrosinase	Tablets containing 125 mg broccoli seed extract and 50 mg broccoli sprout extract, equating to *ca.* 15 µmol SF per tablet; dose range: 3–8 tabs/d. based on the participant's wt.	12 weeks	48	None reported yet; NCT02909959

N, Number of participants; RCT, Randomized Clinical Trial; ASD, Autism Spectrum Disorder; SF, Sulforaphane; Wt., Weight; ABC, Aberrant Behavior Checklist; SRS, Social Responsiveness Scale; GR, Glucoraphanin; µmol, Micromole; mg, Milligram; kg, Kilogram; OACIS, Ohio Autism Clinical Impressions Scale; IL-6, Interleukin-6; TNF-α, Tumor Necrosis Factor-alpha; IL-1β, Interleukin-1 beta; ATP, Adenosine Triphosphate; CGI-I, Clinical Global Impression Scale for Improvement; OARS-4, Ohio State University (OSU) Autism Rating Scale-Diagnostic and Statistical Manual of Mental Disorders (DSM)- Fourth edition (IV); RBS-R, Repetitive Behavior Scale-Revised; ADOS-2, Autism Diagnostic Observation Schedule, Second Edition.

metabolites through magnetic resonance spectroscopy (MRS) scanning and reported a significant increase in glutathione concentration in the hippocampus. However, a randomized controlled trial ($N = 58$) found no differences between GR + myrosinase (100 µmol SF per day for 16 weeks) treatment and placebo groups in PANSS scores and cognitive functioning among individuals with schizophrenia (48). An ongoing RCT ($N = 480$) in China is exploring add-on treatments of minocycline (200 mg) and GR (68.5 µmol SF/day for 8 weeks) with antipsychotics to patients with schizophrenia who were non-responsive to the antipsychotic drugs alone (NCT03451734) (49).

2.2.2 Pre-clinical studies

Preclinical studies have provided further insights into the potential benefits of SF in schizophrenia. For example, offspring from pregnant mouse dams subjected to maternal immune activation, fed with a GR-rich diet (~2.3 µmol/kg), showed protection from cognitive defects (50). Similarly, mice repeatedly exposed to phencyclidine demonstrated attenuated cognitive deficits when pretreated with a GR-containing diet (~2.3 µmol/kg) (51).

2.3 Cerebral palsy

Cerebral palsy is a neurological disorder characterized by difficulties in movement, balance, and posture due to weakness or impairment in muscle control and is the most common motor disability in childhood. It is usually associated with pre-or perinatal brain injury or maldevelopment. One *in vivo* study of cerebral palsy with SF treatment has been published. In this preclinical study, rat offspring were exposed to prolonged intrauterine ischemia *in utero*. Offspring born to dams given a diet supplemented with broccoli sprouts (200 mg/day from the beginning of the third trimester to postnatal day 14) had a reduced likelihood of neurocognitive impairment compared to those born to dams that did not receive the treatment (52).

2.4 Fetal alcohol syndrome disorders

Fetal alcohol syndrome disorder (FASD) encompasses a spectrum of conditions resulting from prenatal alcohol exposure, often presenting as a combination of physical, behavioral, and learning difficulties. We have identified two *in vivo* models and one *in vitro* experiment examining the effects of SF on mechanisms involved in FASD, including cell death and oxidative stress. Mouse embryos exposed to ethanol *in vivo* and treated with SF (1 µM for 24 h) displayed reduced apoptosis in neural crest cells compared to untreated exposed mice (53). The reported preventive mechanism of SF against ethanol-induced apoptosis was inhibition of HDAC and the subsequent elevation of histone acetylation in the cells (53).

TABLE 2 Clinical studies reported the effects of sulforaphane or glucoraphanin treatments on behavioral and health outcomes in individuals with schizophrenia.

Author, Year (Study type)	Study population	Compound(s) delivered	Treatment and dose	Duration of intervention	N	Results
Shiina et al., 2015 (38) (Single arm clinical trial)	Outpatients (20–65 years old) with schizophrenia	GR	3 tablets each day equivalent to 68.5 μmol of GR/day	8 weeks	10	Significant improvement in the accuracy component of the OCLT ($p = 0.043$) post-SF treatment. CogState battery scores, PANSS total scores and serum BDNF levels were not different pre-and post-SF treatment
Zeng et al., 2024 (39) (Single arm clinical trial)	Patients (18–50 years old) with schizophrenia	SF	3 Nutramax tablets each day equivalent to 507.4 μmol of SF/day	24 weeks	66	Improvement in PANSS negative subscale ($p < 0.001$) and total scores ($p < 0.001$). No difference in PANSS positive subscale ($p > 0.05$). Increased SOD activity ($p < 0.05$) and HsCRP levels and ($p < 0.05$).
Sedlak et al., 2018 (40) (Single arm clinical trial)	Healthy volunteers (eight of them aged 21–26 years old and 1 participant aged 56 years)	SF	2 gel capsules of standardized broccoli sprout extract containing 100 μmol SF/day	7 days	9	Increased GSH in non-monocytes ($p = 0.02$) and left hippocampus ($p = 0.041$). Blood GSH levels positively correlated GSH in bilateral thalamus brain region ($p = 0.017$). Positive correlations between blood GSH and gamma-aminobutyric acid, glutamine, glutamate, and GSH in the bilateral thalamus were not significant.
Dickerson et al., 2021 (41) (RCT)	Individuals (18–65 years old) diagnosed with scizophrenia	GR + myrosinase	6 Avmacol tablets dosed at 222 μmol GR (equivalent to 100 μmol SF) per day	2 weeks of placebo and 16 weeks of SF	58	No improvement in PANSS scores and cognitive functioning (as measured by MCCB and domain cognitive scores).
Xiao et al., 2021 (42) (RCT)	First-episode schizophrenia patients with less than 25% reduction rate of PANSS score with antipsychotics treatment	GR	3 tablets of GR each day equivalent to 68.5 μmol of GR/day	8 weeks	240	None reported yet; NCT03451734

SF, sulforaphane; mg, milligrams; N, number of participants; OCLT, One Card Learning Task; PANSS, Positive and Negative Syndrome Scale; BDNF, brain-derived neurotrophic factor; SOD, superoxide dismutase; HsCRP, high-sensitivity c-reactive protein; GSH, glutathione; RCT, randomized controlled trial; MCCB, MATRICS Consensus Cognitive Battery.

Inhibition of HDAC causes histone hyperacetylation, resulting in neuroprotective effects (54). Furthermore, pharmacological blockade of catalase or Nrf2 activity intensified ethanol intoxication in mice, and 28.2 μM /kg/day SF (a potent Nrf2 inducer) treatment for 5 days, attenuated these effects (55), leading the study's authors to suggest that Nrf2 activation may serve as a potential therapeutic strategy for preventing acute alcoholism by regulating catalase-mediated ethanol oxidation.

2.5 Fetal hypoxic–ischemic brain injury

Fetal hypoxic–ischemic encephalopathy (HIE) due to placental insufficiency is characterized by low blood and oxygen supply to the fetus. This can result in both intrauterine growth restriction and brain injury. Despite the severity of this condition, research on potential interventions remains limited. One *in vitro* study highlighted the potential efficacy of SF in mitigating the effects of placental insufficiency on neuronal cells (56). In this study, the dose response of SF (0–200 μM) within different brain cell types was examined. A significant protective effect of SF was documented at a concentration of 2.5 μM in astrocytes and co-cultures of multiple cell types but not in neurons alone. Toxicity was not observed until concentrations reached ≥100 μM in astrocytes and ≥50 μM in co-cultures under oxygen/glucose deprived conditions.

3 Neurodegenerative disorders

Since oxidative stress and inflammation play a large role in the pathophysiology of neurodegenerative disorders, the ITC SF and moringin, among other Nrf2 inducers, have garnered attention for their potential to alleviate various symptoms. These disorders include Alzheimer's disease, Parkinson's disease, amyotrophic lateral sclerosis, Huntington's disease, and multiple sclerosis, among others (57). While there are only a couple of clinical studies examining the effects of ITC in neurodegenerative disorders, several preclinical studies support the benefits of these phytochemicals (58).

3.1 Alzheimer's disease

Alzheimer's Disease (AD), the most common form of dementia, is estimated to affect 6.93 million people in the U.S. as of 2024 and is projected to reach 13.85 million by 2060 (59). ITC has shown promise in AD by preventing tau and amyloid-beta (Aβ) accumulation, two notable markers of AD. Abnormal tau builds up in memory-related brain regions, while Aβ forms plaques between neurons (60). To date, there have been 15 *in vivo*, 6 *in vitro*, and 1 *in silico* AD models studied with ITC.

SF has shown promising effects in mitigating AD pathology in several preclinical studies. Both mouse primary cortical neurons (10 or 20 μM for 3 or 6 h) and a triple-transgenic AD mouse model treated with SF (56.4 or 282 μmol/kg/day for 6 days/week for 8 weeks) exhibited enhanced brain-derived neurotropic factor (BDNF) expression, crucial for neuronal survival and synaptic plasticity, suggesting a potential epigenetic mechanism for SF's neuroprotective effects (61). Additionally, SF administered at 28.2 μmol/kg/day for 4 months (62), 141 μmol/kg/day for 80 days (63), or 141 μmol/kg/day for 5 months (64) ameliorated spatial cognitive impairment, reduced Aβ plaques, and regulated specific HDACs, resulting in diminished plaque burden in other AD mouse models (62–64). Changes in memory consolidation and spatial learning were also induced by SF (5 μM) in adult mice (65). A mechanistic study revealed that SF (56.4 or 282 μmol/kg/day for 6 days/week for 8 weeks) cleared Aβ and tau accumulation by increasing levels of a heat shock protein (HSP70) and co-chaperone (CHIP), and mitigated memory deficits in a triple transgenic mouse model of AD (66). SF (141 or 282 μmol/kg/day for 4 months) has also been shown to protect against Aβ-induced neurotoxicity in primary mouse neurons and suppress tau protein phosphorylation in a transgenic AD mouse model (67). Moreover, the prophylactic mechanisms of SF (141 mg/kg/day for 2 weeks) have been shown to protect against LPS-induced prefrontal cortex-related recognition memory impairment in mice by improving recognition memory and reducing neuroinflammation, oxidative stress, neurodegeneration, Aβ accumulation, and microglial activation (68).

Molecular mechanisms underlying the neuroprotective effects of ITC have also been studied *in vitro*. SF (1.25 or 2.5 μM treated for 48 h) upregulated Nrf2 expression and facilitated Nrf2 nuclear translocation by reducing DNA methylation of the Nrf2 promoter in a cellular AD model (69). Furthermore, hydrogen sulfide (H_2S)-releasing hybrids combining rivastigmine with either SF or its metabolite erucin [4-(methylthio) butyl ITC; 5 μmol treated for 24 h] exhibited protective effects against LPS-induced microglia inflammation and increased the expression of antioxidant proteins like glutathione in human neuronal (SH-SY5Y) cells (70). Examining yet another mechanism, SF (0.03 to 3 μM for 60 min) demonstrated six-fold greater potency against β-site amyloid precursor protein cleaving enzyme 1 (BACE1), a rate-limiting enzyme in Aβ production, as compared to resveratrol and quercetin *in silico* (71). Other preclinical investigations demonstrated positive benefits of SF on AD by attenuating Aβ oligomers-mediated reduction of phagocytic activity (5 μM for 24 h) (72), reducing streptozotocin-induced cognitive deficits (141 or 282 μmol/kg/day for 6 weeks) (73), decreasing neuroinflammation and inhibiting tau phosphorylation (1 or 2 μM for 1 h and stimulated with LPS for 23 h) (73), and reducing Aβ production (226 μmol/kg three times a week for 4 weeks) (74) in *in vivo* and *in vitro* AD models.

In addition to SF, other ITC and ITC-rich plants have also demonstrated consistent benefits in ameliorating AD-related pathology. Rats supplemented with *Moringa peregrina* (150 mg/kg/day for 2 months), rich in the ITC moringin, exhibited significant enhancement in short-term and long-term memories, along with increased BDNF, glutathione, and glutathione peroxidase (GPx), and decreased oxidized glutathione in the hippocampus (75). Leaf extracts of the widely consumed *Moringa oleifera* (400 mg/kg/day for 4 months) improved AD-related pathology, reduced Aβ burden, and enhanced synaptic plasticity in mice (76). Similar findings were observed in rats along with reduced homocysteine-induced tau hyperphosphorylation with a *Moringa oleifera* dose of 200 or 400 mg/kg/day for 14 days (77). Additionally, supplementation with *Moringa oleifera* (1, 5% or 10% in diet for 7 or 14 days) in mice mitigated scopolamine-induced spatial memory deficits, restored cholinergic transmission, and maintained neuronal integrity (78). Pretreatment with moringin conjugated with α-cyclodextrin (0.5 μM for 24 h) in an AD cell model reduced gene expression related to autophagy and mitophagy (79). Finally, a study of mice treated with 6-MSITC treatment [6-(methylsulfinyl) hexyl isothiocyanate; 24.3 μmol/kg/day for 10 days] from *Wasabia japonica*, or wasabi, demonstrated attenuated neuroinflammation, memory impairments, inhibited apoptosis, and oxidative stress (80).

3.2 Parkinson's disease

Parkinson's disease (PD), characterized by dopaminergic neuron loss, involves neuroinflammation, oxidative stress, mitochondrial dysfunction, and protein aggregation. One clinical study has been reported on the effects of sulforaphane on PD, while preclinical investigations examining the effects of ITCs on PD include 10 *in vivo* and three *in vitro* studies.

3.2.1 Clinical studies

A self-experimented clinical study was conducted in individuals diagnosed with Parkinson's disease using broccoli seed tea (25–45 μmol SF/day for at least 4 weeks, with weekly administration in the first week and up to twice per week thereafter) rich in SF intended to induce Nrf2 (81). Although statistical significance is uncertain as *p*-values were not provided, the findings revealed the tea reduced non-motor symptoms, including fatigue, constipation, and urinary urgency, while not affecting motor symptoms (Table 3). Currently, there is an ongoing phase 2 placebo-controlled randomized clinical trial (NCT05084365) examining the effect of SF on PD in 100 participants.

3.2.2 Preclinical studies

Several animal studies have also outlined the neuroprotective effects of SF in PD. One study demonstrated that SF treatment (0.05 μM for 24 h) reduced dopamine-induced cell death and restored mitochondrial membrane potential in a knockout mouse model (82). In another PD mouse model, SF (282 μmol/kg once in 2 days for 60 days) inhibited rotenone-induced deficiencies in locomotor activity and dopaminergic neuronal loss (83). Further, in MPTP (1-methyl-4-phenyl-1,2,3,6-tetrahydropyridine)-treated mice, SF treatment (56.4 μmol/kg/day for 10 days) attenuated dopaminergic neurotoxicity by activating BDNF and suppressing methyl CpG-binding protein 2 (MeCP2) (84) and activated Nrf2 (1 μM SF) (85). Sustained activation

TABLE 3 A clinical study reported the effects of glucoraphanin + myrosinase compound on non-motor symptoms in individuals with PD.

Author, Year (Study type)	Study population	Compound(s) delivered	Treatment and dose	Duration of intervention	N	Results
Wright, 2024 (74) (Case study)	Individuals with Parkinson's Disease	GR + myrosinase	30 to 40 mL of broccoli seed tea containing 25–40 μmol SF once per week during the first week with an option to increase to twice per week from the second week	4 weeks	17	Improvement in the non-motor symptoms but no change in motor symptoms

GR, glucoraphanin; SF, sulforaphane; N, number of participants; ml, milliliters; g, grams; μmol, micromoles.

of this transcription factor led to a reduction of abnormal α-synuclein expression (1 μmol SF) and decrease in dopaminergic neuron degeneration in the substantia nigra pars compacta (0.1% GR for 30 days) (78). Further, GR intake (0.1% GR diet for 28 days) protected against the reduction in dopamine transporter density in mice treated with MPTP, indicating its potential in preserving dopaminergic function (86). SF and erucin (from *Eruca sativa* or arugula) at 5 μmol/kg for 4 weeks exhibited neuroprotective effects by protecting against neuronal death and increasing glutathione and Nrf2 levels in a 6-hyzdroxydopamine (6-OHDA) PD mouse model (87). Finally, two synthetic ITC protected dopaminergic neurons and prevented motor deficits associated with PD in mice (88, 89).

Three *in vitro* studies were also identified, providing mechanistic insights into the neuroprotective effects of SF. The first showed that SF treatment (56.4 μmol/kg/day for 10 days) upregulated Nrf2 and BDNF while downregulating MeCP2 in SH-SY5Y cells (84). A second study reported that compared to erucin, SF (5 μmol/kg for 4 weeks) exhibited greater Nrf2 activation, glutathione levels, and resistance to 6-OHDA-induced apoptosis in SH-SY5Y cells (87). The third study revealed that Nrf2 activation by SF (1 μmol SF) suppressed CCAAT/enhancer-binding protein β (C/EBPβ) transcription in SH-SY5Y cells treated with MPP+ (1-methyl-4-phenylpyridinium) (85). SF also reduced α-synuclein aggregation in HEK293-α-Syn-YFP cells treated with preformed fibrils. These findings collectively draw attention to the role of SF in antioxidant defense, neurotrophic support, and neuroprotection.

Additional studies have highlighted the neuroprotective effects of other natural compounds, such as benzyl ITC and indole-3-carbinol (not an ITC, but derived from indole glucosinolates), in preclinical models of PD. Benzyl ITC (67.1 μmol/kg/day for 12 weeks) enhanced the activity and expression of an endogenous antioxidant, GST-π (glutathione S-transferase pi), in Wistar rats with zinc-induced Parkinsonism and ameliorated neurological deficits, neurodegenerative markers, and oxidative stress (90). Similarly, indole-3-carbinol (680 μmol/kg/day) amended striatal dopamine levels and neurodegeneration, and prevented motor dysfunctions in rotenone-induced PD in male albino rats (91).

3.3 Multiple sclerosis

Multiple sclerosis (MS) is an inflammation-mediated demyelinating disease of the human central nervous system, with neurodegeneration being the primary cause of irreversible neurological disability. A total of 5 *in vivo* studies have demonstrated the benefits of ITC in MS.

The experimental mouse models of autoimmune encephalomyelitis (EAE) and cuprizone (a copper-chelator causing demyelination) are the most commonly employed animal models used to study different aspects of MS pathology. In one study using the EAE model, invesigators demonstrated that SF (282 μmol/kg/day for 14 days before EAE induction and 28 days after EAE induction) had anti-inflammatory effects, improved clinical scores in behavioral study, and inhibited demyelination in the spinal cords (92). Four additional studies have reported protective effects of *Moringa oleifera* (or its ITC moringin) in animal models of MS. First, mice receiving moringin pretreatment (16.4 μmol/kg glucomoringin +5 μL myrosinase daily for a week before EAE induction and 28 days after EAE induction) exhibited increased expression of Nrf2, reduced cell apoptosis, and suppressed aberrant Wnt-β-catenin signaling in EAE mice (93). Another study demonstrated that *Moringa oleifera* (1.875 mg/mL for 5 weeks) reversed cuprizone-induced neuropathological deficits by mitigating oxidative stress, memory decline, and cortico-hippocampal neuronal deficits in Wistar rats (94). Moreover, *Moringa oleifera* leaf extract (1.875 mg/mL/day for 5 weeks) ameliorated cuprizone-induced weight loss and histological alterations in the hippocampal CA3 region in female Wistar rats (95). Co-administration of cuprizone with *Moringa oleifera* (1.875 mg/mL/day for 5 weeks) resulted in improved cellular assortment and delineated cytoarchitectural manifestations in cuprizone-treated rats (95). Finally, a topical treatment of 2% moringin cream twice per day alleviated neuropathic pain in the EAE model by attenuating proinflammatory cytokines (interleukin-17 and interferon-γ) while increasing the expression of the anti-inflammatory cytokine interleukin-10 (IL-10) (96).

3.4 Amyotrophic lateral sclerosis

Amyotrophic lateral sclerosis (ALS) is a progressive neurodegenerative disease characterized by the degeneration and death of motor neurons, leading to the inability to control muscle movement. One *in vivo* study has examined the effect of glucomoringin on ALS. In a transgenic rat model, daily treatment with glucomoringin (16.4 μmol/kg) + myrosinase (20 μL/rat) for 2 weeks prior to disease onset demonstrated protective effects, as indicated by measuring inflammatory and apoptotic markers, and it inhibited motor neuron degradation, a key to ALS pathophysiology (97).

3.5 Huntington's disease

Huntington's disease, an autosomal dominant neurodegenerative disorder, involves motor dysfunction, psychiatric issues, and cognitive

decline. Mitochondrial dysfunction is a molecular feature implicated in most neurologic disorders, including Huntington's disease. One *in vivo* study showed that SF (two doses of 28.2 µmol/kg/day) restored mitochondrial function against quinolinic acid-induced damage in an experimental rodent model of Huntington's disease (98).

3.6 Friedreich's ataxia

Friedreich's ataxia (FRDA) is a progressive neurodegenerative disease characterized by oxidative stress and mitochondrial dysfunction with decreased expression of the mitochondrial protein frataxin (FXN). Two preclinical studies, both conducted *in vitro*, have examined the effects of SF in FRDA fibroblasts. First, treatment with SF (5 µM for 24 h) increased frataxin protein expression, promoted axonal re-growth in frataxin-silenced motor neurons and restored Nrf2 transcriptional activity in fibroblasts from patients with FRDA (99). In the second study, there was increased expression of FXN and Nrf2 target genes and increased glutathione concentration in SF (10 µM for 24 h) treated FRDA fibroblasts compared to untreated cells (100).

3.7 Fragile X-associated tremor/ataxia syndrome

Fragile X-Associated Tremor/Ataxia Syndrome (FXTAS), typically caused by a premutation in the FMR1 (fragile X messenger ribonucleoprotein 1) gene, is a nervous system disorder in older adults characterized by tremors, ataxia, memory issues, and mood disorders. One clinical study (Table 4) and one *in vitro* study have demonstrated the effects of SF on FXTAS. The clinical study was a 24-week open-label trial in 11 adults aged 60–88 years with FXTAS (101). SF (100 µmol SF/day) improved spatial working memory but did not improve other clinical outcomes, molecular changes in mitochondria-derived vesicles, or bioenergetics in PBMCs (101). The *in vitro* study was conducted in FRDA fibroblasts in which SF treatment (5 µmol for 72–96 h) that resulted in improvements in deficient pathways associated with FXTAS in both Nrf-2-dependent and independent manners (102). This was observed in primary fibroblasts from FXTAS-affected subjects ranging from stages 2.5 to 5. These improvements included the modulation of oxidative stress, enhancement of mitochondrial function, promotion of DNA repair, and increased clearance of damaged organelles and macromolecules through parkin-ubiquitin proteasomal mechanisms (102).

4 Other brain-related disorders

Neurodevelopmental and neurodegenerative conditions share common pathological mechanisms, encompassing neuronal cell death, microglial activation, neuroinflammation, disrupted redox homeostasis, mitochondrial dysfunction, and synaptic dysfunction. There are other brain-related disorders and conditions that also share these mechanisms, including spinal cord injury, traumatic brain injury, diabetes-induced cognitive decline, depression, and anxiety. There is both clinical and preclinical evidence of amelioration of symptoms with ITC treatment for these conditions.

4.1 Spinal cord injury

Spinal cord injury (SCI) is marked by neurologic dysfunction and neuronal death resulting from inflammatory and oxidative insults. Seven *in vivo* studies with ITC treatment for SCI have been identified.

SF has shown notable effects in mitigating inflammation and oxidative stress associated with SCI in mouse models. SF treatment (56.4 µmol/kg for 11 days) increased the expression of Nrf2 and phase 2 cytoprotective enzymes while inhibiting markers induced by inflammation in two mouse models when inflammatory pain was induced in the spinal cord using complete Freund's adjuvant (103). Beyond its anti-inflammatory effects, SF enhanced the antinociceptive actions of morphine, increasing the effectiveness of pain alleviation compared to morphine alone (103). Similarly, rats subjected to mild thoracic SCI had significantly greater levels of Nrf2 and glutamate-cysteine ligase, decreased levels of inflammatory cytokines and spinal cord lesion volumes, and improved coordination after SCI with an SF dose of 28.2 µmol/kg/day for 3 days (104). SF (28.2 µmol/kg an hour after SCI induction) activation of Nrf2 post-SCI improved locomotor function and reduced inflammatory damage, neuron death, and spinal cord edema, while neurological deficits were more severe and the protective effect of SF was not observed in Nrf2 deficient mice (105). SF (282 µmol/kg at 10 min and 72 h after SCI contusion) in a rat model of contusion SCI upregulated antioxidant responses, reduced inflammatory cytokine mRNA levels, improved hindlimb locomotor function, and increased serotonergic axons caudal to the site of lesion (106). Further, histological examination of spinal cord sections revealed improvements in demyelination and apoptosis, but not inflammation as compared to the vehicle group with SFX-01 (10, 50 or 300 mg/kg twice a day for 3 weeks), a stabilized form of SF, treatment in EAE mice (107).

TABLE 4 A clinical study reported the effects of glucoraphanin + myrosinase compound on cognitive outcomes in individuals with FXTAS.

Author, Year (Study type)	Study population	Compound(s) delivered	Treatment and dose	Duration of intervention	N	Results
Santos et al., 2023 (94) (Single arm clinical trial)	Adults aged 60–88 with FXTAS	GR + myrosinase	Started with 1 Avmacol tablet and increased every other day by 1 tablet to 6 tablets/day (dosed at 222 µmol GR; equivalent to 100 µmol SF) per day; the highest tolerable dose maintained if intolerant to the maximum amount	24 weeks	11	Improvement in spatial working memory score ($p = 0.048$). No improvement in MoCA scores and molecular changes in mitochondria-derived vesicles.

FXTAS, Fragile-X-Associated Tremor and Ataxia Syndrome; GR, glucoraphanin; SF, sulforaphane; N, number of participants; µmol, micromoles; MoCA, Montreal cognitive assessment.

In addition to SF, moringin has shown promising anti-inflammatory and anti-apoptotic effects in the context of SCI. Pretreatment of gingival mesenchymal stem cells (GMSCs) with moringin (0.05 μM 1 h post-SCI) in a mouse model of SCI demonstrated anti-inflammatory and anti-apoptotic effects (108). Moringin-treated GMSCs reduced inflammatory marker levels, restored spinal cord morphology, increased expression of anti-apoptotic marker B-cell lymphoma 2 (Bcl-2) and decreased expressions of apoptotic markers such as Bcl-2-associated X protein (Bax) and caspases 3 and 9 (108). Similarly, post-injury administration of moringin (16.4 μmol glucomoringin/kg + 5 μL myrosinase/day for 7 days before SCI and continued until sacrifice) in mice subjected to SCI through the application of vascular clips showed protective effects against secondary damage by reducing oxidative stress, inflammation, and apoptosis (109).

4.2 Traumatic brain injury

Traumatic brain injury (TBI), often resulting from blunt force, shares pathophysiological similarities with stroke-induced cerebral ischemia, involving cellular damage from excitotoxicity, oxidative stress, apoptosis, and inflammation. Preclinical studies including eight *in vivo* and one *in vitro* experiments have been identified to examine the effects of ITC on traumatic brain injury.

SF has consistently demonstrated protective effects against cerebral ischemia/reperfusion (CIR) injury and associated inflammation in rat models. Two rat studies using a CIR model found SF (28.2 μmol or 56.4 μmol /kg 1 h at the beginning of the injury; 56.4, 112.8 or 225.6 μmol /kg/day for 14 days) had congruent protective effects against CIR-induced damage and inflammation (110, 111). Additionally, SF demonstrated protective effects in rodent models of vascular cognitive impairment induced by ischemia at 56.4 μmol/kg twice a week (112), subarachnoid hemorrhage at 282 μmol/kg every 24 h (113), and intracerebral hemorrhage at 5.64 μmol/kg twice a day (114), with upregulation of Nrf2 and reduced inflammation reported in the latter two.

Moreover, studies have investigated the potential synergistic effects of SF with other compounds in mitigating neuroinflammation and oxidative stress associated with traumatic brain injury. An *in vivo* study in a rat model of traumatic brain injury demonstrated that a combination therapy of N-acetylcysteine and SF yielded modest improvements in motor movement and coordination (115). However, there were no significant effects on composite neuromotor score or cortical lesion area (115). Yet, an *in vitro* combination therapy with N-acetylcysteine and SF (5 and 10 μM) significantly reduced neuroinflammation and nitrite levels while improving neuronal viability (115).

Similarly, moringin treatment (~8 μmol glucomoringin/ml plus 30 μL enzyme 15 min after beginning of ischemia and daily) of rats with CIR injury prevented CIR-induced damage and decreased inflammatory and oxidative mediators that exacerbate disease progression (116). Further, allyl isothiocyanate (AITC; 101 μmol/kg immediately after TBI induction) administered immediately after traumatic brain injury in mice significantly reduced infarct volume and serum IgG extravasation, revealing an improvement in blood–brain barrier permeability (117). AITC also decreased proinflammatory cytokines while increasing Nrf2, neural outgrowth and regeneration marker growth-associated protein 43 (GAP43), and neurogenesis-associated neural cell adhesion molecule levels (117).

4.3 Diabetes-related cognitive decline

Compelling evidence establishes a correlation and potential pathophysiological connection between type 2 diabetes (T2D) and cognitive dysfunction, leading to an increased risk of AD (118). The implicated mechanisms include defects in insulin signaling, neuroinflammation, and mitochondrial metabolism, among others (118). Both SF and moringin have been studied for their potential to attenuate diabetic complications including cognitive decline (119, 120). Eight *in vivo* and two *in vitro* experiments have been identified that demonstrate the effect of these ITC on diabetes-related cognitive decline.

Several studies have investigated the potential neuroprotective effects of SF in various models of diabetes-induced cognitive impairment. In a streptozotocin-induced diabetic rat model, SF (141 μmol/kg/day for 14 days) supplementation yielded preventive effects against learning and memory impairment (121). The rats also showcased attenuated decline in memory, protection against hippocampal neuron apoptosis, decreased caspase-3 expression, and increased expression of an antiapoptotic marker, MCL-1 (myeloid leukemia cell differentiation protein). Similarly, in a type 2 diabetes mellitus mouse model, SF (5.64 μmol/kg/day for 28 days) administration mitigated cognitive decline and reduced pathological hallmarks of AD, such as Aβ-oligomers, Aβ 1–42 plaques, and phospho-tau (122). SF activated Nrf2-regulated antioxidant defenses, enhancing the expression of NrF2 downstream genes HO-1 and NQO1. The study also reported reduced reactive oxygen/nitrogen species in the mice brains and mitigated cognitive decline (122). Additionally, SF (5.64 μmol/kg/day for 15 days) demonstrated therapeutic effects in a rat model induced with nicotinamide and streptozotocin by restoring insulin levels, normalizing motor coordination, improving sensory responses, and ameliorating histopathological changes (123). One study also examined a combination therapy with ulinastatin (10,000 U/kg/day for 26 days) and SF (141 μmol/kg/day for 26 days), which attenuated streptozotocin-induced diabetes and vascular dementia in rats, improving behavioral, endothelial, and biochemical parameters (124).

One *in vitro* study showed that a combination of SF (20 μmoL/L) and vitamin E (200 μg/mL alpha-tocopherol) protected against glucotoxic damages on neuronal structure and function in the nematode *Caenorhabditis elegans*, a model organism used to study the effects of high glucose on neuronal function (125). The duo also prevented reactive oxygen species and methylglyoxal-derived advanced glycation end products formation under hyperglycemic conditions (125). In both *in vitro* (0.5 μM for 24 h) and *in vivo* (141 μmol/kg/day for 14 days) settings, SF mitigated high glucose-induced apoptosis by inhibiting the upregulation of apoptotic markers and the downregulation of antiapoptotic maker Bcl-2 protein in hippocampal neurons exposed to high glucose (126).

Moringa oleifera has also been shown to provide neuroprotection against diabetes-induced cognitive dysfunction. In one study, *Moringa oleifera* leaves added to the diet (0.5 g, 1.0 g and 2.0 g per day for 30 days) reduced brain cholinergic enzymes (AChE, BChE), glycemic index, and lipid profile (TC, TG, LDL-C),

while elevating antioxidant enzymes (SOD, CAT) in rats compared to controls not fed the leaves (127). In another study, the plant's leaves (2.0, 4.0 and 8.0 g/kg/day for 8 weeks) exhibited protective effects on cognitive dysfunction and hippocampal neuron apoptosis in streptozotocin-induced diabetic rats (128). Furthermore, hyperglycemic rats supplemented with *Moringa oleifera* leaves or seeds (2 and 4% of the diet for 14 days) exhibited elevated levels of various antioxidant enzymes and glutathione, concomitantly decreasing biomarkers associated with hyperglycemia-induced cognitive decline (129).

4.4 Anxiety and depression

Mice subjected to acute or chronic stress often exhibit depressive and anxiety-like behaviors, paralleled by immune dysregulation. One RCT and 13 *in vivo* with ITC treatment have been identified for anxiety and depression.

4.4.1 Clinical study

There has been one randomized, double-blind, placebo-controlled clinical trial on the antidepressant effects of SF ($N = 66$) (130). In patients with a history of cardiac interventions, 169.2 µmol/day SF for 6 weeks alleviated mild to moderate depression, leading to greater improvements in the Hamilton Rating Scale for Depression (HAM-D) compared to placebo ($p < 0.001$). Participants on SF demonstrated greater response to treatment rates at the end of the trial compared to those on placebo (30% vs. 6.67%, $p < 0.05$) (Table 5).

4.4.2 Preclinical studies

Preclinical studies have further elucidated the potential mechanisms underlying the antidepressant and anxiolytic effects of SF. SF treatment (56.4 µmol/kg/day for 14 days) significantly reversed anxiety-like behaviors in acutely and chronically stressed mice, reducing serum corticosterone, adrenocorticotropic hormone, interleukin-6, and TNF-α in chronically stressed mice (131). SF (16.92, 56.4 and 169.2 µmol/kg) also combated inflammation-induced depression-like behavior in mice, reducing immobility time and restoring dendritic changes induced by LPS administration (132). Similarly, chronic administration of 56.4 µmol/kg SF for 15 days alleviated anxiety-like behavior and produced antidepressant effects in neuropathic mice, as evidenced by behavioral tests in neuropathic mice (133). Moreover, SF (28.2 µmol/kg/day for 7 days) reversed Aβ-oligomer-induced depressive-like behavior in rats, protecting the serotonergic system and mitigating depressive-like behavior (134).

In one study, GR administration (114.17 µmol/kg) brought about antidepressant effects showcased through reduction in immobility frequency in the forced swimming test (FST) and restoring serotonin (5-HT) levels in soluble Aβ 1–42 (a 42-residue form of Aβ) treated rats (135). Further, treating mice with dietary GR (0.1% GR food pellets) during juvenile and adolescent stages has been shown to prevent LPS-induced depression-like behaviors in adulthood (132, 136).

Moringa oleifera has also demonstrated promising anxiolytic and antidepressant effects in animal models. For example, ITC-rich extracts of *Moringa oleifera* leaf (500 mg/kg administered 30 min prior to tests) induced anxiolytic effects in Swiss mice in light–dark and open field tests (OFT) (137). Additionally, treatment with *Moringa oleifera* seed oil (1 or 2 mL/kg for 23 days) decreased anxiety-and depression-like behaviors, measured using the OFT and FST in the water-immersion restraint stress mouse model. (138). And, pretreatment with *Moringa oleifera* leaf extract (400 mg/kg/day for 14 days) produced anxiolytic effects in both FST and tail suspension test (TST) in the hepatic encephalopathy mouse model (139).

Other ITC-rich plants have also been studied for their antidepressant and anxiolytic properties. Ethanolic and methanolic extracts of *Camelina sativa* var. Madalina (5 g/kg), rich in sinapine, glucosinolates, and flavonol glycosides, brought about anxiolytic and antidepressant effects in stress-induced irritable bowel syndrome mouse models (140). *Isatis tinctoria* leaf extract (50, 100 or 500 mg/kg) reversed stress-induced anxiety-like behavior and regulation of neurooxidative, neuronitrosative, and neuroimmune pathways in mice (141). Further, *Raphanus caudatus* (250 and 500 mg/kg), a radish variety, significantly reduced anxiety-like behavior in mice, comparable to diazepam, a pharmaceutical anxiolytic drug (142). And, indole-3-carbinol (408 µmol/kg for 10 days), an ITC usually found in cabbage, broccoli, and collard greens, prevented chronic social defeat stress (CSDS)-induced behavioral abnormalities associated with depression in mice, though it did not affect behavioral abnormalities related to anxiety (143).

5 Adverse effects

Progoitrin and indole glucosinolates in *Brassica* vegetables can degrade to goitrin in the presence of myrosinase, potentially decreasing thyroid hormone production (144–146). While a clinical study found that a single 25 mg or 50 mg dose of goitrin inhibited thyroid radioiodine uptake, two 10 mg doses did not have this effect (146, 147). Vegetables with low progoitrin levels, such as commercial broccoli and kale, pose minimal risk to iodine uptake. A recent

TABLE 5 A clinical study reported the effects of sulforaphane on depression outcomes in cardiac patients with mild to moderate depression.

Author, Year (Study Type)	Study population	Compound(s) delivered	Treatment and dose	Duration of intervention	N	Results
Ghazizadeh-Hashemi, et al., 2021 (RCT)	Cardiac patients (40–65 years old) with mild to moderate depression	SF	169.2 µmol/day	6 weeks	66	Improvement in the HAM-D in the SF group ($p < 0.001$) Greater response to treatment rates in SF than placebo (30% vs. 6.67%, $p = 0.042$) Remission rate not significantly higher in the SF group than placebo (23.33% vs. 3.33%, $p = 0.052$).

RCT, randomized controlled trial; N, number of participants; mg, milligrams; SF, sulforaphane; mg, milligrams; HAM-D, Hamilton Rating Scale for Depression.

systematic review of 123 studies suggests that regular consumption of Brassica vegetables does not pose a risk of adverse effects, particularly with adequate iodine intake (148).

Some ITCs demonstrate a hormetic effect, offering cytoprotective benefits at low doses and cytotoxic, antitumor properties at higher doses (149, 150). A few studies have shown that SF increases reactive oxygen species (ROS) generation and DNA double-strand breaks (DSB) in cancer cells in a dose-and time-dependent manner (151, 152). While these effects reduce cancer cell survival, normal cells like human dermal fibroblasts and gastric mucosal cells exhibit higher viability and faster DNA repair when exposed to similar doses, suggesting that SF could be an effective cancer therapeutic without harming normal cells (153, 154).

Ingestion of isothiocyanate-containing preparations may cause adverse effects. Higher doses of SF can cause a harsh, burning sensation in the back of the throat, which may deter some from consuming broccoli or sulforaphane preparations (155, 156). Strategies to mask flavors of brocolli extracts and moringa teas have been studied (157, 158). Some individuals may experience gastrointestinal discomfort when consuming SF in large quantities (155). Gradually increasing the dose may help mitigate these effects, allowing the gut to adapt over time (159).

6 Alternative treatments

Bioactive compounds, along with plant sources beyond cruciferous vegetables and dietary nutrients, offer potential alternative approaches for managing neurologic disorders (160–162). Among these, polyphenols (163), flavonoids (164) and certain herbs (165) along with other phytonutrients (166) have demonstrated therapeutic benefits in neurologic disorders. Curcumin is one of the most extensively studied compounds (167, 168), with other common treatments including quercetin (169), resveratrol (170) and luteolin (171). Despite the potential of dietary nutrients like vitamin D and omega-3 fatty acids for neuroprotection (172), findings from studies have yielded mixed results without consistent beneficial effects (173, 174). Exploring the effect of nutraceuticals as treatments for neurologic disorders remains a significant area of interest.

7 Methods

All research articles were retrieved from PubMed and Scopus. The search criteria consisted of the following terms: ("glucosinolate" OR "glucoraphanin" OR "sulforaphane" OR "isothiocyanate" OR "moringin") AND ("brain" OR "mental" OR "cognit*" OR "neuro*" OR "psych*") NOT (FITC OR SITS OR "fluorescein isothiocyanate" OR RITC OR "rhodamine B isothiocyanate" OR "fentanyl isothiocyanate" OR "di-o-tolyl-guanidine-isothiocyanate" OR "isothiocyanate labelled" OR IFN OR "rhodamine isothiocyanate" OR LHRH OR "affinity labeled") for articles published from November 2018 through May 2024. Since this review extends the previous review published in 2018, literature from that review is included along with additional relevant clinical trials that were omitted in the original publication. After 404 duplicates were removed, 1,108 abstracts were screened by two independent reviewers, and 293 full texts were reviewed. A total of 106 articles (clinical and preclinical studies) were included. Criteria for inclusion were original research articles focusing on isothiocyanates derived from natural plant sources and their effects on neuropsychiatric disorders and other brain-related conditions. Studies focusing on other phytochemicals like flavonoids, alkaloids, and polyphenols, and non-brain-related outcomes, were excluded.

8 Conclusion

We illustrate that cruciferous and related vegetables (or supplements rich in glucosinolates or ITC) can contribute to a dietary strategy for combating neuropsychiatric disorders and improving the quality of life. A few studies have also reported their effects as comparable to pharmaceutical treatments with fewer side effects. While these plants contain various phytochemicals, it is the potent and highly bioavailable compounds within the glucosinolate/myrosinase/ITC system that uniquely contribute to the highly potent indirect antioxidant properties of these vegetables. However, other phytochemicals in these plants, including phenols and flavonoids, have also been shown to be beneficial for brain-related outcomes (175). It may therefore be more valuable to consume the vegetable as a whole (or as sprouts) or as water extracted vegetable supplements rather than those containing only a high refined glucosinolate or isothiocyanate.

Through our comprehensive search, we found around 11 preclinical studies on the effects of ITCs from other cruciferous vegetables including maca, radish, and wasabi on neuropsychiatric disorders. A realm of opportunity remains to explore the potential benefits of cabbage, turnips, mustard and other cruciferous vegetables on neuroinflammation and outcomes related to neuropsychiatric disorders.

While this review updates our review published 6 years ago (26), it does not delve into the extensive epidemiological evidence supporting all the benefits of ITC. Furthermore, it is essential to note that there is a plethora of literature highlighting their other properties (155). The comprehensive understanding of the underlying mechanisms now sheds light on why this protection extends across a broad spectrum of chronic conditions, encompassing both neurodevelopmental and neurodegenerative origins. This emphasizes the potential of cruciferous and other ITC-containing vegetables as a safe and effective dietary intervention for enhancing brain health and mitigating the risk and effects of various brain-related disorders. Given the increasing number of *in vitro* and animal studies that show the metabolic and behavioral benefits and safety of ITC, it is now important that clinical trials be expanded to facilitate their application in patients with disorders of the nervous system.

Author contributions

MR: Writing – original draft, Writing – review & editing. JF: Conceptualization, Writing – review & editing. AZ: Conceptualization, Writing – review & editing. XZ: Writing – review & editing. AP: Writing – review & editing, Conceptualization, Resources, Supervision, Writing – original draft.

Funding

The author(s) declare that no financial support was received for the research, authorship, and/or publication of this article.

Conflict of interest

The authors declare that the research was conducted in the absence of any commercial or financial relationships that could be construed as a potential conflict of interest.

One of us (JWF) has consulted for both food and supplement companies in the past year.

Publisher's note

All claims expressed in this article are solely those of the authors and do not necessarily represent those of their affiliated organizations, or those of the publisher, the editors and the reviewers. Any product that may be evaluated in this article, or claim that may be made by its manufacturer, is not guaranteed or endorsed by the publisher.

References

1. Parchem K, Piekarska A, Bartoszek A. Enzymatic activities behind degradation of glucosinolates In: CM Galanakis, editor. Glucosinolates: Properties, recovery, and applications. United Kingdom: Academic Press (2020). 79–106.

2. Liu H, Talalay P, Fahey JW. Biomarker-guided strategy for treatment of autism Spectrum disorder (ASD). *CNS Neurol Disord Drug Targets*. (2016) 15:602–13. doi: 10.2174/1871527315666160413120414

3. Bones AM, Rossiter JT. The enzymic and chemically induced decomposition of glucosinolates. *Phytochemistry*. (2006) 67:1053–67. doi: 10.1016/j.phytochem.2006.02.024

4. Wittstock U, Burow M. Tipping the scales - specifier proteins in Glucosinolate hydrolysis. *IUBMB Life*. (2007) 59:744–51. doi: 10.1080/15216540701736277

5. Ettlinger MG, Lundeen AJ. The structures of sinigrin and sinalbin; an enzymatic rearrangement. *J Am Chem Soc*. (1956) 78:4172–3. doi: 10.1021/ja01597a090

6. Gasper AV, al-janobi A, Smith JA, Bacon JR, Fortun P, Atherton C, et al. Glutathione S-transferase M1 polymorphism and metabolism of sulforaphane from standard and high-glucosinolate broccoli. *Am J Clin Nutr*. (2005) 82:1283–91. doi: 10.1093/ajcn/82.6.1283

7. Fahey JW, Olson ME, Stephenson KK, Wade KL, Chodur GM, Odee D, et al. The diversity of chemoprotective glucosinolates in *Moringaceae* (*Moringa* spp.). *Sci Rep*. (2018) 8:7994. doi: 10.1038/s41598-018-26058-4

8. Fahey JW, Zalcmann AT, Talalay P. The chemical diversity and distribution of glucosinolates and isothiocyanates among plants. *Phytochemistry*. (2001) 56:5–51. doi: 10.1016/S0031-9422(00)00316-2

9. Blažević I, Montaut S, Burčul F, Olsen CE, Burow M, Rollin P, et al. Glucosinolate structural diversity, identification, chemical synthesis and metabolism in plants. *Phytochemistry*. (2020) 169:112100. doi: 10.1016/j.phytochem.2019.112100

10. Agerbirk N, Olsen CE. Glucosinolate structures in evolution. *Phytochemistry*. (2012) 77:16–45. doi: 10.1016/j.phytochem.2012.02.005

11. Fahey JW, Zhang Y, Talalay P. Broccoli sprouts: an exceptionally rich source of inducers of enzymes that protect against chemical carcinogens. *Proc Natl Acad Sci USA*. (1997) 94:10367–72. doi: 10.1073/pnas.94.19.10367

12. Cancer IAfRo. Cruciferous vegetables, isothiocyanates and indoles. Lyon, France: IARC Press (2004).

13. Ho E, Clarke JD, Dashwood RH. Dietary sulforaphane, a histone deacetylase inhibitor for cancer prevention. *J Nutr*. (2009) 139:2393–6. doi: 10.3945/jn.109.113332

14. Li N, Wu X, Zhuang W, Wu C, Rao Z, du L, et al. Cruciferous vegetable and isothiocyanate intake and multiple health outcomes. *Food Chem*. (2022) 375:131816. doi: 10.1016/j.foodchem.2021.131816

15. Kim J. Pre-clinical neuroprotective evidences and plausible mechanisms of sulforaphane in Alzheimer's disease. *Int J Mol Sci*. (2021) 22:2929. doi: 10.3390/ijms22062929

16. Schepici G, Bramanti P, Mazzon E. Efficacy of sulforaphane in neurodegenerative diseases. *Int J Mol Sci*. (2020) 21:8637. doi: 10.3390/ijms21228637

17. Jaafaru MS, Abd Karim NA, Enas ME, Rollin P, Mazzon E, Abdull Razis AF. Protective effect of glucosinolates hydrolytic products in neurodegenerative diseases (NDDs). *Nutrients*. (2018) 10:580. doi: 10.3390/nu10050580

18. Kou X, Li B, Olayanju JB, Drake JM, Chen N. Nutraceutical or pharmacological potential of *Moringa oleifera* lam. *Nutrients*. (2018) 10:343. doi: 10.3390/nu10030343

19. Agrawal S, Yallatikar T, Gurjar P. *Brassica Nigra*: Ethopharmacological review of a routinely used condiment. *Curr Drug Discov Technol*. (2019) 16:40–7. doi: 10.2174/1570163815666180308143400

20. Venditti A, Bianco A. Sulfur-containing secondary metabolites as neuroprotective agents. *Curr Med Chem*. (2020) 27:4421–36. doi: 10.2174/0929867325666180912105036

21. Connolly EL, Sim M, Travica N, Marx W, Beasy G, Lynch GS, et al. Glucosinolates from cruciferous vegetables and their potential role in chronic disease: investigating the preclinical and clinical evidence. *Front Pharmacol*. (2021) 12:767975. doi: 10.3389/fphar.2021.767975

22. Wu YY, Xu YM, Lau ATY. Anti-cancer and medicinal potentials of *Moringa* isothiocyanate. *Molecules*. (2021) 26:7512. doi: 10.3390/molecules26247512

23. Gao Q, Wei Z, Liu Y, Wang F, Zhang S, Serrano C, et al. Characterization, large-scale HSCCC separation and neuroprotective effects of polyphenols from *Moringa oleifera* leaves. *Molecules*. (2022) 27:27. doi: 10.3390/molecules27030678

24. Kamal RM, Abdull Razis AF, Mohd Sukri NS, Perimal EK, Ahmad H, Patrick R, et al. Beneficial health effects of glucosinolates-derived isothiocyanates on cardiovascular and neurodegenerative diseases. *Molecules*. (2022) 27:27. doi: 10.3390/molecules27030624

25. Mundkar M, Bijalwan A, Soni D, Kumar P. Neuroprotective potential of *Moringa oleifera* mediated by NF-kB/Nrf2/HO-1 signaling pathway: a review. *J Food Biochem*. (2022) 46:e14451. doi: 10.1111/jfbc.14451

26. Panjwani AA, Liu H, Fahey JW. Crucifers and related vegetables and supplements for neurologic disorders: what is the evidence? *Curr Opin Clin Nutr Metab Care*. (2018) 21:451–7. doi: 10.1097/MCO.0000000000000511

27. Autism spectrum disorder (ASD). (2024). Centers for disease control and prevention. Available from: https://www.cdc.gov/ncbddd/autism/facts.html#:~:text=people%20without%20ASD.-,Signs%20and%20Symptoms,can%20make%20life%20very%20challenging (Accessed February 04, 2024).

28. CDC. (2023). Autism prevalence higher, according to data from 11 ADDM communities. Available from: https://www.cdc.gov/media/releases/2023/p0323-autism.html (Accessed February 04, 2024).

29. Solmi M, Song M, Yon DK, Lee SW, Fombonne E, Kim MS, et al. Incidence, prevalence, and global burden of autism spectrum disorder from 1990 to 2019 across 204 countries. *Mol Psychiatry*. (2022) 27:4172–80. doi: 10.1038/s41380-022-01630-7

30. Singh K, Connors SL, Macklin EA, Smith KD, Fahey JW, Talalay P, et al. Sulforaphane treatment of autism spectrum disorder (ASD). *Proc Natl Acad Sci USA*. (2014) 111:15550–5. doi: 10.1073/pnas.1416940111

31. Lynch R, Diggins EL, Connors SL, Zimmerman AW, Singh K, Liu H, et al. Sulforaphane from broccoli reduces symptoms of autism: a follow-up case series from a randomized double-blind study. *Glob Adv Health Med*. (2017) 6:2164957X1773582. doi: 10.1177/2164957X17735826

32. Zimmerman AW, Singh K, Connors SL, Liu H, Panjwani AA, Lee LC, et al. Randomized controlled trial of sulforaphane and metabolite discovery in children with autism spectrum disorder. *Mol Autism*. (2021) 12:38. doi: 10.1186/s13229-021-00447-5

33. Bent S, Lawton B, Warren T, Widjaja F, Dang K, Fahey JW, et al. Identification of urinary metabolites that correlate with clinical improvements in children with autism treated with sulforaphane from broccoli. *Mol Autism*. (2018) 9:35. doi: 10.1186/s13229-018-0218-4

34. Ou J, Smith RC, Tobe RH, Lin J, Arriaza J, Fahey JW, et al. Efficacy of sulforaphane in treatment of children with autism spectrum disorder: a randomized double-blind placebo-controlled multi-center trial. *J Autism Dev Disord*. (2022) 54:628–41. doi: 10.1007/s10803-022-05784-9

35. Momtazmanesh S, Amirimoghaddam-Yazdi Z, Moghaddam HS, Mohammadi MR, Akhondzadeh S. Sulforaphane as an adjunctive treatment for irritability in children with autism spectrum disorder: a randomized, double-blind, placebo-controlled clinical trial. *Psychiatry Clin Neurosci*. (2020) 74:398–405. doi: 10.1111/pcn.13016

36. Yang J, He L, Dai S, Zheng H, Cui X, Ou J, et al. Therapeutic efficacy of sulforaphane in autism spectrum disorders and its association with gut microbiota: animal model and human longitudinal studies. *Front Nutr*. (2023) 10:1294057. doi: 10.3389/fnut.2023.1294057

37. Evans S, Fuller DJ. Initial outcomes from an autism treatment demonstration. *Clin Med Invest*. (2016) 1:16–9. doi: 10.15761/CMI.1000103

38. Magner M, Thorová K, Župová V, Houška M, Švandová I, Novotná P, et al. Sulforaphane treatment in children with autism: a prospective randomized double-blind study. *Nutrients*. (2023) 15:718. doi: 10.3390/nu15030718

39. Nadeem A, Ahmad SF, al-Harbi NO, Attia SM, Bakheet SA, Ibrahim KE, et al. Nrf2 activator, sulforaphane ameliorates autism-like symptoms through suppression of Th17 related signaling and rectification of oxidant-antioxidant imbalance in periphery and brain of BTBR T+tf/J mice. *Behav Brain Res*. (2019) 364:213–24. doi: 10.1016/j.bbr.2019.02.031

40. Fujita Y, Fujita A, Ishima T, Hirai A, Suzuki S, Suganuma H, et al. Dietary intake of glucoraphanin during pregnancy and lactation prevents the behavioral abnormalities in the offspring after maternal immune activation. *Neuropsychopharmacol Rep*. (2020) 40:268–74. doi: 10.1002/npr2.12112

41. Liu H, Zimmerman AW, Singh K, Connors SL, Diggins E, Stephenson KK, et al. Biomarker exploration in human peripheral blood mononuclear cells for monitoring sulforaphane treatment responses in autism spectrum disorder. *Sci Rep*. (2020) 10:5822. doi: 10.1038/s41598-020-62714-4

42. Nadeem A, Ahmad SF, al-Ayadhi LY, Attia SM, al-Harbi NO, Alzahrani KS, et al. Differential regulation of Nrf2 is linked to elevated inflammation and nitrative stress in monocytes of children with autism. *Psychoneuroendocrinology*. (2020) 113:104554. doi: 10.1016/j.psyneuen.2019.104554

43. Fu P, Luo S, Liu Z, Furuhara K, Tsuji T, Higashida H, et al. Oral supplementation with maca improves social recognition deficits in the valproic acid animal model of autism spectrum disorder. *Brain Sci*. (2023) 13:316. doi: 10.3390/brainsci13020316

44. Hashimoto K. Recent advances in the early intervention in schizophrenia: future direction from preclinical findings. *Curr Psychiatry Rep*. (2019) 21:75. doi: 10.1007/s11920-019-1063-7

45. Shiina A, Kanahara N, Sasaki T, Oda Y, Hashimoto T, Hasegawa T, et al. An open study of sulforaphane-rich broccoli sprout extract in patients with schizophrenia. *Clin Psychopharmacol Neurosci*. (2015) 13:62–7. doi: 10.9758/cpn.2015.13.1.62

46. Zeng J, Zhang W, Lu X, Zhou H, Huang J, Xu Z, et al. The association of SOD and HsCRP with the efficacy of sulforaphane in schizophrenia patients with residual negative symptoms. *Eur Arch Psychiatry Clin Neurosci*. (2023) 274:1083–92. doi: 10.1007/s00406-023-01679-7

47. Sedlak TW, Nucifora LG, Koga M, Shaffer LS, Higgs C, Tanaka T, et al. Sulforaphane augments glutathione and influences brain metabolites in human subjects: a clinical pilot study. *Mol Neuropsychiatry*. (2018) 3:214–22. doi: 10.1159/000487639

48. Dickerson F, Origoni A, Katsafanas E, Squire A, Newman T, Fahey J, et al. Randomized controlled trial of an adjunctive sulforaphane nutraceutical in schizophrenia. *Schizophr Res*. (2021) 231:142–4. doi: 10.1016/j.schres.2021.03.018

49. Xiao J, Huang J, Long Y, Wang X, Wang Y, Yang Y, et al. Optimizing and individualizing the pharmacological treatment of first-episode schizophrenic patients: study protocol for a multicenter clinical trial. *Front Psychol*. (2021) 12:611070. doi: 10.3389/fpsyt.2021.611070

50. Matsuura A, Ishima T, Fujita Y, Iwayama Y, Hasegawa S, Kawahara-Miki R, et al. Dietary glucoraphanin prevents the onset of psychosis in the adult offspring after maternal immune activation. *Sci Rep*. (2018) 8:2158. doi: 10.1038/s41598-018-20538-3

51. Shirai Y, Fujita Y, Hashimoto R, Ohi K, Yamamori H, Yasuda Y, et al. Dietary intake of sulforaphane-rich broccoli sprout extracts during juvenile and adolescence can prevent phencyclidine-induced cognitive deficits at adulthood. *PLoS One*. (2015) 10:e0127244. doi: 10.1371/journal.pone.0127244

52. Black AM, Armstrong EA, Scott O, Juurlink BJH, Yager JY. Broccoli sprout supplementation during pregnancy prevents brain injury in the newborn rat following placental insufficiency. *Behav Brain Res*. (2015) 291:289–98. doi: 10.1016/j.bbr.2015.05.033

53. Yuan F, Chen X, Liu J, Feng W, Cai L, Wu X, et al. Sulforaphane restores acetyl-histone H3 binding to Bcl-2 promoter and prevents apoptosis in ethanol-exposed neural crest cells and mouse embryos. *Exp Neurol*. (2018) 300:60–6. doi: 10.1016/j.expneurol.2017.10.020

54. Shukla S, Tekwani BL. Histone deacetylases inhibitors in neurodegenerative diseases, neuroprotection and neuronal differentiation. *Front Pharmacol*. (2020) 11:537. doi: 10.3389/fphar.2020.00537

55. Xu JF, Lu JJ, Cao Y, Wang W, Li HH, Chen JG, et al. Sulforaphane alleviates ethanol-mediated central inhibition and reverses chronic stress-induced aggravation of acute alcoholism via targeting Nrf2-regulated catalase expression. *Neuropharmacology*. (2020) 176:108235. doi: 10.1016/j.neuropharm.2020.108235

56. Ladak Z, Garcia E, Yoon J, Landry T, Armstrong EA, Yager JY, et al. Sulforaphane (SFA) protects neuronal cells from oxygen & glucose deprivation (OGD). *PLoS One*. (2021) 16:e0248777. doi: 10.1371/journal.pone.0248777

57. Liddell JR. Are astrocytes the predominant cell type for activation of nrf2 in aging and neurodegeneration? *Antioxidants (Basel)*. (2017) 6:65. doi: 10.3390/antiox6030065

58. Giacoppo S, Galuppo M, Montaut S, Iori R, Rollin P, Bramanti P, et al. An overview on neuroprotective effects of isothiocyanates for the treatment of neurodegenerative diseases. *Fitoterapia*. (2015) 106:12–21. doi: 10.1016/j.fitote.2015.08.001

59. Rajan KB, Weuve J, Barnes LL, McAninch EA, Wilson RS, Evans DA. Population estimate of people with clinical Alzheimer's disease and mild cognitive impairment in the United States (2020-2060). *Alzheimers Dement*. (2021) 17:1966–75. doi: 10.1002/alz.12362

60. Rajmohan R, Reddy PH. Amyloid-beta and phosphorylated tau accumulations cause abnormalities at synapses of Alzheimer's disease neurons. *J Alzheimers Dis*. (2017) 57:975–99. doi: 10.3233/JAD-160612

61. Kim J, Lee S, Choi BR, Yang H, Hwang Y, Park JH, et al. Sulforaphane epigenetically enhances neuronal BDNF expression and TrkB signaling pathways. *Mol Nutr Food Res*. (2017) 61:1600194. doi: 10.1002/mnfr.201600194

62. Hou TT, Yang HY, Wang W, Wu QQ, Tian YR, Jia JP. Sulforaphane inhibits the generation of amyloid-β oligomer and promotes spatial learning and memory in Alzheimer's disease (ps1v97l) transgenic mice. *J Alzheimers Dis*. (2018) 62:1803–13. doi: 10.3233/JAD-171110

63. Zhang R, Miao QW, Zhu CX, Zhao Y, Liu L, Yang J, et al. Sulforaphane ameliorates neurobehavioral deficits and protects the brain from amyloid β deposits and peroxidation in mice with Alzheimer-like lesions. *Am J Alzheimers Dis Other Dement*. (2015) 30:183–91. doi: 10.1177/1533317514542645

64. Zhang J, Zhang R, Zhan Z, Li X, Zhou F, Xing A, et al. Beneficial effects of sulforaphane treatment in Alzheimer's disease may be mediated through reduced HDAC 1/3 and increased P75NTR expression. *Front Aging Neurosci*. (2017) 9:121. doi: 10.3389/fnagi.2017.00121

65. Sunkaria A, Bhardwaj S, Yadav A, Halder A, Sandhir R. Sulforaphane attenuates postnatal proteasome inhibition and improves spatial learning in adult mice. *J Nutr Biochem*. (2017) 51:69–79. doi: 10.1016/j.jnutbio.2017.09.016

66. Lee S, Choi BR, Kim J, LaFerla FM, Park JHY, Han JS, et al. Sulforaphane upregulates the heat shock protein co-chaperone chip and clears amyloid-β and tau in a mouse model of Alzheimer's disease. *Mol Nutr Food Res*. (2018) 62:e1800240. doi: 10.1002/mnfr.201800240

67. Yang W, Xu QQ, Yuan Q, Xian YF, Lin ZX. Sulforaphene, a CDK5 inhibitor, attenuates cognitive deficits in a transgenic mouse model of Alzheimer's disease via reducing Aβ deposition, tau hyperphosphorylation and synaptic dysfunction. *Int Immunopharmacol*. (2023) 114:109504. doi: 10.1016/j.intimp.2022.109504

68. Alzahrani NA, Bahaidrah KA, Mansouri RA, Aldhahri RS, Abd El-Aziz GS, Alghamdi BS. Possible prophylactic effects of sulforaphane on LPS-induced recognition memory impairment mediated by regulating oxidative stress and neuroinflammatory proteins in the prefrontal cortex region of the brain. *Biomedicine*. (2024) 12:1107. doi: 10.3390/biomedicines12051107

69. Zhao F, Zhang J, Chang N. Epigenetic modification of Nrf2 by sulforaphane increases the antioxidative and anti-inflammatory capacity in a cellular model of Alzheimer's disease. *Eur J Pharmacol*. (2018) 824:1–10. doi: 10.1016/j.ejphar.2018.01.046

70. Sestito S, Pruccoli L, Runfola M, Citi V, Martelli A, Saccomanni G, et al. Design and synthesis of H(2) S-donor hybrids: a new treatment for Alzheimer's disease? *Eur J Med Chem*. (2019) 184:111745. doi: 10.1016/j.ejmech.2019.111745

71. Youn K, Yoon JH, Lee N, Lim G, Lee J, Sang S, et al. Discovery of sulforaphane as a potent BACE1 inhibitor based on kinetics and computational studies. *Nutrients*. (2020) 12:3026. doi: 10.3390/nu12103026

72. Chilakala RR, Manchikalapudi AL, Kumar A, Sunkaria A. Sulforaphane attenuates Aβ oligomers mediated decrease in phagocytic activity of microglial cells. *Neuroscience*. (2020) 429:225–34. doi: 10.1016/j.neuroscience.2020.01.002

73. Yang W, Liu Y, Xu QQ, Xian YF, Lin ZX. Sulforaphene ameliorates neuroinflammation and hyperphosphorylated tau protein via regulating the PI3K/akt/GSK-3β pathway in experimental models of Alzheimer's disease. *Oxidative Med Cell Longev*. (2020) 2020:1–17. doi: 10.1155/2020/4754195

74. Zhang S, Zhao J, Bai Z, Luo L, Wu F, Li B, et al. Sulforaphane inhibits the production of Aβ partially through the activation of Nrf2-regulated oxidative stress. *Food Funct*. (2021) 12:11482–90. doi: 10.1039/D1FO02651H

75. Alzoubi KH, Rawashdeh NQ, Khabour OFEl-Elimat T, Albataineh H, Al-Zghool HM. Evaluation of the effect of *Moringa peregrina* extract on learning and memory: role of oxidative stress. *J Mol Neurosci*. (2017) 63:355–63. doi: 10.1007/s12031-017-0986-x

76. Mahaman YAR, Feng J, Huang F, Salissou MTM, Wang J, Liu R, et al. *Moringa oleifera* alleviates Aβ burden and improves synaptic plasticity and cognitive impairments in APP/PS1 mice. *Nutrients*. (2022) 14:4284. doi: 10.3390/nu14204284

77. Mahaman YAR, Huang F, Wu M, Wang Y, Wei Z, Bao J, et al. *Moringa oleifera* alleviates homocysteine-induced alzheimer's disease-like pathology and cognitive impairments. *J Alzheimers Dis*. (2018) 63:1141–59. doi: 10.3233/JAD-180091

78. Onasanwo SA, Adamaigbo VO, Adebayo OG, Eleazer SE. *Moringa oleifera*-supplemented diet protect against cortico-hippocampal neuronal degeneration in scopolamine-induced spatial memory deficit in mice: role of oxido-inflammatory and cholinergic neurotransmission pathway. *Metab Brain Dis*. (2021) 36:2445–60. doi: 10.1007/s11011-021-00855-9

79. Silvestro S, Chiricosta L, Gugliandolo A, Iori R, Rollin P, Perenzoni D, et al. The moringin/α-CD pretreatment induces neuroprotection in an in vitro model of Alzheimer's disease: a transcriptomic study. *Curr Issues Mol Biol*. (2021) 43:197–214. doi: 10.3390/cimb43010017

80. Morroni F, Sita G, Graziosi A, Turrini E, Fimognari C, Tarozzi A, et al. Protective effects of 6-(methylsulfinyl)hexyl isothiocyanate on Aβ(1-42)-induced cognitive deficit, oxidative stress, inflammation, and apoptosis in mice. *Int J Mol Sci*. (2018) 19:2083. doi: 10.3390/ijms19072083

81. Wright AF. The redox stress test: a novel technique reveals oxidative stress in Parkinson's disease. *Medical Research Archives*. (2024) 12. doi: 10.18103/mra.v12i1.4955

82. Dinkova-Kostova AT, Baird L, Holmström KM, Meyer CJ, Abramov AY. The spatiotemporal regulation of the Keap1-Nrf2 pathway and its importance in cellular bioenergetics. *Biochem Soc Trans*. (2015) 43:602–10. doi: 10.1042/BST20150003

83. Zhou Q, Chen B, Wang X, Wu L, Yang Y, Cheng X, et al. Sulforaphane protects against rotenone-induced neurotoxicity in vivo: involvement of the mTOR, Nrf2, and autophagy pathways. *Sci Rep*. (2016) 6:32206. doi: 10.1038/srep32206

84. Cao Q, Zou Q, Zhao X, Zhang Y, Qu Y, Wang N, et al. Regulation of BDNF transcription by Nrf2 and MeCP2 ameliorates MPTP-induced neurotoxicity. *Cell Death Dis*. (2022) 8:267. doi: 10.1038/s41420-022-01063-9

85. Lin Z, Huang L, Cao Q, Luo H, Yao W, Zhang JC. Inhibition of abnormal C/EBPβ/α-Syn signaling pathway through activation of Nrf2 ameliorates Parkinson's disease-like pathology. *Aging Cell*. (2023) 22:e13958. doi: 10.1111/acel.13958

86. Pu Y, Qu Y, Chang L, Wang SM, Zhang K, Ushida Y, et al. Dietary intake of glucoraphanin prevents the reduction of dopamine transporter in the mouse striatum after repeated administration of MPTP. *Neuropsychopharmacol Rep*. (2019) 39:247–51. doi: 10.1002/npr2.12060

87. Morroni F, Sita G, Djemil A, D'Amico M, Pruccoli L, Cantelli-Forti G, et al. Comparison of adaptive neuroprotective mechanisms of sulforaphane and its interconversion product erucin in *in vitro* and *in vivo* models of Parkinson's disease. *J Agric Food Chem*. (2018) 66:856–65. doi: 10.1021/acs.jafc.7b04641

88. Lee JA, Son HJ, Kim JH, Park KD, Shin N, Kim HR, et al. A novel synthetic isothiocyanate ITC-57 displays antioxidant, anti-inflammatory, and neuroprotective properties in a mouse Parkinson's disease model. *Free Radic Res*. (2016) 50:1188–99. doi: 10.1080/10715762.2016.1223293

89. Lee JA, Son HJ, Park KD, Han SH, Shin N, Kim JH, et al. A novel compound ITC-3 activates the Nrf2 signaling and provides neuroprotection in parkinson's disease models. *Neurotox Res*. (2015) 28:332–45. doi: 10.1007/s12640-015-9550-z

90. Chauhan AK, Mittra N, Singh BK, Singh C. Inhibition of glutathione S-transferase-pi triggers c-Jun N-terminal kinase-dependent neuronal death in Zn-induced parkinsonism. *Mol Cell Biochem*. (2019) 452:95–104. doi: 10.1007/s11010-018-3415-8

91. Mohamad KA, El-Naga RN, Wahdan SA. Neuroprotective effects of indole-3-carbinol on the rotenone rat model of Parkinson's disease: impact of the SIRT1-AMPK signaling pathway. *Toxicol Appl Pharmacol*. (2022) 435:115853. doi: 10.1016/j.taap.2021.115853

92. Yoo IH, Kim MJ, Kim J, Sung JJ, Park ST, Ahn SW. The anti-inflammatory effect of sulforaphane in mice with experimental autoimmune encephalomyelitis. *J Korean Med Sci*. (2019) 34:e197. doi: 10.3346/jkms.2019.34.e197

93. Giacoppo S, Soundara Rajan T, De Nicola GR, Iori R, Bramanti P, Mazzon E. Moringin activates Wnt canonical pathway by inhibiting GSK3β in a mouse model of experimental autoimmune encephalomyelitis. *Drug Des Devel Ther*. (2016) 10:3291–304. doi: 10.2147/DDDT.S110514

94. Omotoso GO, Gbadamosi IT, Afolabi TT, Abdulwahab AB, Akinlolu AA. Ameliorative effects of *Moringa* on cuprizone-induced memory decline in rat model of multiple sclerosis. *Anat Cell Biol*. (2018) 51:119–27. doi: 10.5115/acb.2018.51.2.119

95. Omotoso GO, Kolo RM, Afolabi T, Jaji-Sulaimon R, Gbadamosi IT. *Moringa oleifera* ameliorates histomorphological changes associated with cuprizone neurotoxicity in the hippocampal cornu ammonis (CA) 3 region. *Niger J Physiol Sci*. (2018) 33:95–9.

96. Giacoppo S, Iori R, Bramanti P, Mazzon E. Topical moringin-cream relieves neuropathic pain by suppression of inflammatory pathway and voltage-gated ion channels in murine model of multiple sclerosis. *Mol Pain*. (2017) 13:174480691772431. doi: 10.1177/1744806917724318

97. Galuppo M, Giacoppo S, Iori R, De Nicola GR, Bramanti P, Mazzon E. Administration of 4-(α-L-rhamnosyloxy)-benzyl isothiocyanate delays disease phenotype in SOD1(G93A) rats: a transgenic model of amyotrophic lateral sclerosis. *Biomed Res Int*. (2015) 2015:259417:1–12. doi: 10.1155/2015/259417

98. Luis-García ER, Limón-Pacheco JH, Serrano-García N, Hernández-Pérez AD, Pedraza-Chaverri J, Orozco-Ibarra M. Sulforaphane prevents quinolinic acid-induced mitochondrial dysfunction in rat striatum. *J Biochem Mol Toxicol*. (2017) 31. doi: 10.1002/jbt.21837

99. Petrillo S, Piermarini E, Pastore A, Vasco G, Schirinzi T, Carrozzo R, et al. Nrf2-inducers counteract neurodegeneration in Frataxin-silenced motor neurons: disclosing new therapeutic targets for Friedreich's Ataxia. *Int J Mol Sci*. (2017) 18:2173. doi: 10.3390/ijms18102173

100. Petrillo S, D'Amico J, La Rosa P, Bertini ES, Piemonte F. Targeting Nrf2 for the treatment of Friedreich's Ataxia: a comparison among drugs. *Int J Mol Sci*. (2019) 20:5211. doi: 10.3390/ijms20205211

101. Santos E, Clark C, Biag HMB, Tang SJ, Kim K, Ponzini MD, et al. Open-label sulforaphane trial in FMR1 premutation carriers with fragile-x-associated tremor and ataxia syndrome (FXTAS). *Cells*. (2023) 12:2773. doi: 10.3390/cells12242773

102. Napoli E, Flores A, Mansuri Y, Hagerman RJ, Giulivi C. Sulforaphane improves mitochondrial metabolism in fibroblasts from patients with fragile X-associated tremor and ataxia syndrome. *Neurobiol Dis*. (2021) 157:105427. doi: 10.1016/j.nbd.2021.105427

103. Redondo A, Chamorro PAF, Riego G, Leánez S, Pol O. Treatment with sulforaphane produces antinociception and improves morphine effects during inflammatory pain in mice. *J Pharmacol Exp Ther*. (2017) 363:293–302. doi: 10.1124/jpet.117.244376

104. Wang X, de Rivero Vaccari JP, Wang H, Diaz P, German R, Marcillo AE, et al. Activation of the nuclear factor E2-related factor 2/antioxidant response element pathway is neuroprotective after spinal cord injury. *J Neurotrauma*. (2012) 29:936–45. doi: 10.1089/neu.2011.1922

105. Mao L, Wang H, Wang X, Liao H, Zhao X. Transcription factor Nrf2 protects the spinal cord from inflammation produced by spinal cord injury. *J Surg Res*. (2011) 170:e105–15. doi: 10.1016/j.jss.2011.05.049

106. Benedict AL, Mountney A, Hurtado A, Bryan KE, Schnaar RL, Dinkova-Kostova AT, et al. Neuroprotective effects of sulforaphane after contusive spinal cord injury. *J Neurotrauma*. (2012) 29:2576–86. doi: 10.1089/neu.2012.2474

107. Galea I, Copple IM, Howat DW, Franklin S. SFX-01 reduces residual disability after experimental autoimmune encephalomyelitis. *Mult Scler Relat Disord*. (2019) 30:257–61. doi: 10.1016/j.msard.2019.02.027

108. Mammana S, Gugliandolo A, Cavalli E, Diomede F, Iori R, Zappacosta R, et al. Human gingival mesenchymal stem cells pretreated with vesicular moringin nanostructures as a new therapeutic approach in a mouse model of spinal cord injury. *J Tissue Eng Regen Med*. (2019) 13:1109–21. doi: 10.1002/term.2857

109. Giacoppo S, Galuppo M, De Nicola GR, Iori R, Bramanti P, Mazzon E. 4(α-l-rhamnosyloxy)-benzyl isothiocyanate, a bioactive phytochemical that attenuates secondary damage in an experimental model of spinal cord injury. *Bioorg Med Chem*. (2015) 23:80–8. doi: 10.1016/j.bmc.2014.11.022

110. Yu C, He Q, Zheng J, Li LY, Hou YH, Song FZ. Sulforaphane improves outcomes and slows cerebral ischemic/reperfusion injury via inhibition of NLRP3 inflammasome activation in rats. *Int Immunopharmacol*. (2017) 45:74–8. doi: 10.1016/j.intimp.2017.01.034

111. Ma LL, Xing GP, Yu Y, Liang H, Yu TX, Zheng WH, et al. Sulforaphane exerts neuroprotective effects via suppression of the inflammatory response in a rat model of focal cerebral ischemia. *Int J Clin Exp Med*. (2015) 8:17811–7.

112. Mao L, Yang T, Li X, Lei X, Sun Y, Zhao Y, et al. Protective effects of sulforaphane in experimental vascular cognitive impairment: contribution of the Nrf2 pathway. *J Cereb Blood Flow Metab*. (2019) 39:352–66. doi: 10.1177/0271678X18764083

113. Zhao X, Wen L, Dong M, Lu X. Sulforaphane activates the cerebral vascular Nrf2-ARE pathway and suppresses inflammation to attenuate cerebral vasospasm in rat with subarachnoid hemorrhage. *Brain Res*. (2016) 1653:1–7. doi: 10.1016/j.brainres.2016.09.035

114. Yin XP, Chen ZY, Zhou J, Wu D, Bao B. Mechanisms underlying the perifocal neuroprotective effect of the Nrf2-ARE signaling pathway after intracranial hemorrhage. *Drug Des Devel Ther*. (2015) 9:5973–86. doi: 10.2147/DDDT.S79399

115. Kyyriäinen J, Kajevu N, Bañuelos I, Lara L, Lipponen A, Balosso S, et al. Targeting oxidative stress with antioxidant duotherapy after experimental traumatic brain injury. *Int J Mol Sci*. (2021) 22:10555. doi: 10.3390/ijms221910555

116. Galuppo M, Giacoppo S, Iori R, De Nicola GR, Milardi D, Bramanti P, et al. 4(α-l-rhamnosyloxy)-benzyl isothiocyanate, a bioactive phytochemical that defends cerebral tissue and prevents severe damage induced by focal ischemia/reperfusion. *J Biol Regul Homeost Agents*. (2015) 29:343–56.

117. Caglayan B, Kilic E, Dalay A, Altunay S, Tuzcu M, Erten F, et al. Allyl isothiocyanate attenuates oxidative stress and inflammation by modulating Nrf2/HO-1 and NF-κB pathways in traumatic brain injury in mice. *Mol Biol Rep*. (2019) 46:241–50. doi: 10.1007/s11033-018-4465-4

118. Riederer P, Korczyn AD, Ali SS, Bajenaru O, Choi MS, Chopp M, et al. The diabetic brain and cognition. *J Neural Transm (Vienna)*. (2017) 124:1431–54. doi: 10.1007/s00702-017-1763-2

119. Sajja RK, Prasad S, Tang S, Kaisar MA, Cucullo L. Blood-brain barrier disruption in diabetic mice is linked to Nrf2 signaling deficits: role of ABCB10? *Neurosci Lett*. (2017) 653:152–8. doi: 10.1016/j.neulet.2017.05.059

120. Jiménez-Osorio AS, González-Reyes S, Pedraza-Chaverri J. Natural Nrf2 activators in diabetes. *Clin Chim Acta*. (2015) 448:182–92. doi: 10.1016/j.cca.2015.07.009

121. Wang G, Fang H, Zhen Y, Xu G, Tian J, Zhang Y, et al. Sulforaphane prevents neuronal apoptosis and memory impairment in diabetic rats. *Cell Physiol Biochem*. (2016) 39:901–7. doi: 10.1159/000447799

122. Pu D, Zhao Y, Chen J, sun Y, Lv A, Zhu S, et al. Protective effects of sulforaphane on cognitive impairments and ad-like lesions in diabetic mice are associated with the upregulation of Nrf2 transcription activity. *Neuroscience*. (2018) 381:35–45. doi: 10.1016/j.neuroscience.2018.04.017

123. Moustafa PE, Abdelkader NF, El Awdan SA, El-Shabrawy OA, Zaki HF. Extracellular matrix remodeling and modulation of inflammation and oxidative stress by sulforaphane in experimental diabetic peripheral neuropathy. *Inflammation*. (2018) 41:1460–76. doi: 10.1007/s10753-018-0792-9

124. Sharma P, Kaushik P, Jain S, Sharma BM, Awasthi R, Kulkarni GT, et al. Efficacy of ulinastatin and sulforaphane alone or in combination in rat model of streptozotocin diabetes induced vascular dementia. *Clin Psychopharmacol Neurosci*. (2021) 19:470–89. doi: 10.9758/cpn.2021.19.3.470

125. Schlotterer A, Masri B, Humpert M, Krämer BK, Hammes HP, Morcos M. Sulforaphane and vitamin E protect from glucotoxic neurodegeneration and lifespan reduction in *C. elegans*. *Exp Clin Endocrinol Diabetes*. (2021) 129:887–94. doi: 10.1055/a-1158-9248

126. Tang L, Ren X, Han Y, Chen L, Meng X, Zhang C, et al. Sulforaphane attenuates apoptosis of hippocampal neurons induced by high glucose via regulating endoplasmic reticulum. *Neurochem Int*. (2020) 136:104728. doi: 10.1016/j.neuint.2020.104728

127. Ademosun AO, Oboh G, Ajeigbe OF. Influence of *Moringa* (*Moringa oleifera*) enriched ice creams on rats' brain: exploring the redox and cholinergic systems. *Curr Res Food Sci*. (2022) 5:366–73. doi: 10.1016/j.crfs.2022.01.021

128. Sun Y, Zhao C, Liu YY, Sui YL, Zhu JZ. Effects of spicy leaves on cognitive function and apoptosis of hippocampal neurons in diabetic rats. *Zhongguo Ying Yong Sheng Li Xue Za Zhi*. (2021) 37:638–43. doi: 10.12047/j.cjap.6123.2021.070

129. Oboh G, Oyeleye SI, Akintemi OA, Olasehinde TA. *Moringa oleifera* supplemented diet modulates nootropic-related biomolecules in the brain of STZ-induced diabetic rats treated with acarbose. *Metab Brain Dis*. (2018) 33:457–66. doi: 10.1007/s11011-018-0198-2

130. Ghazizadeh-Hashemi F, Bagheri S, Ashraf-Ganjouei A, Moradi K, Shahmansouri N, Mehrpooya M, et al. Efficacy and safety of sulforaphane for treatment of mild to moderate depression in patients with history of cardiac interventions: a randomized, double-blind, placebo-controlled clinical trial. *Psychiatry Clin Neurosci*. (2021) 75:250–5. doi: 10.1111/pcn.13276

131. Wu S, Gao Q, Zhao P, Gao Y, Xi Y, Wang X, et al. Sulforaphane produces antidepressant-and anxiolytic-like effects in adult mice. *Behav Brain Res*. (2016) 301:55–62. doi: 10.1016/j.bbr.2015.12.030

132. Zhang JC, Yao W, Dong C, Yang C, Ren Q, Ma M, et al. Prophylactic effects of sulforaphane on depression-like behavior and dendritic changes in mice after inflammation. *J Nutr Biochem*. (2017) 39:134–44. doi: 10.1016/j.jnutbio.2016.10.004

133. Ferreira-Chamorro P, Redondo A, Riego G, Leánez S, Pol O. Sulforaphane inhibited the nociceptive responses, anxiety-and depressive-like behaviors associated with neuropathic pain and improved the anti-allodynic effects of morphine in mice. *Front Pharmacol*. (2018) 9:1332. doi: 10.3389/fphar.2018.01332

134. Wang W, Wei C, Quan M, Li T, Jia J. Sulforaphane reverses the amyloid-β oligomers induced depressive-like behavior. *J Alzheimers Dis*. (2020) 78:127–37. doi: 10.3233/JAD-200397

135. Tucci P, Bove M, Sikora V, Dimonte S, Morgese MG, Schiavone S, et al. Glucoraphanin triggers rapid antidepressant responses in a rat model of beta amyloid-induced depressive-like behaviour. *Pharmaceuticals (Basel)*. (2022) 15:1054. doi: 10.3390/ph15091054

136. Yao W, Zhang JC, Ishima T, Dong C, Yang C, Ren Q, et al. Role of Keap1-Nrf2 signaling in depression and dietary intake of glucoraphanin confers stress resilience in mice. *Sci Rep*. (2016) 6:30659. doi: 10.1038/srep30659

137. Islam MT, Martins N, Imran M, Hameed A, Ali SW, Salehi B, et al. Anxiolytic-like effects of *Moringa oleifera* in Swiss mice. *Cell Mol Biol (Noisy-le-Grand)*. (2020) 66:73–7. doi: 10.14715/cmb/2020.66.4.12

138. Purwoningsih E, Arozal W, Lee HJ, Barinda AJ, Sani Y, Munim A. The oil formulation derived from *Moringa oleifera* seeds ameliorates behavioral abnormalities in water-immersion restraint stress mouse model. *J Exp Pharmacol*. (2022) 14:395–407. doi: 10.2147/JEP.S386745

139. Mahmoud MS, El-Kott AF, AlGwaiz HIM, Fathy SM. Protective effect of *Moringa oleifera* lam. Leaf extract against oxidative stress, inflammation, depression, and apoptosis in a mouse model of hepatic encephalopathy. *Environ Sci Pollut Res Int*. (2022) 29:83783–96. doi: 10.1007/s11356-022-21453-x

140. Cojocariu RO, Balmus IM, Lefter R, Hritcu L, Ababei DC, Ciobica A, et al. *Camelina sativa* methanolic and ethanolic extract potential in alleviating oxidative stress, memory deficits, and affective impairments in stress exposure-based irritable bowel syndrome mouse models. *Oxidative Med Cell Longev*. (2020) 2020:1–20. doi: 10.1155/2020/9510305

141. Nicosia N, Kwiecień I, Mazurek J, Mika K, Bednarski M, Miceli N, et al. Hydroalcoholic leaf extract of *Isatis tinctoria* L. *via* antioxidative and anti-inflammatory effects reduces stress-induced behavioral and cellular disorders in mice. *Oxidative Med Cell Longev*. (2022) 2022:1–18. doi: 10.1155/2022/3567879

142. Siddiq A, Younus I. The radish, *Raphanus sativus* L. Var. caudatus reduces anxiety-like behavior in mice. *Metab Brain Dis*. (2018) 33:1255–60. doi: 10.1007/s11011-018-0240-4

143. Pan S, Ma Y, Yang R, Lu X, You Q, Ye T, et al. Indole-3-carbinol selectively prevents chronic stress-induced depression-but not anxiety-like behaviors via suppressing pro-inflammatory cytokine production and oxido-nitrosative stress in the brain. *Front Pharmacol*. (2022) 13:829966. doi: 10.3389/fphar.2022.829966

144. Latté KP, Appel KE, Lampen A. Health benefits and possible risks of broccoli - an overview. *Food Chem Toxicol*. (2011) 49:3287–309. doi: 10.1016/j.fct.2011.08.019

145. Vanderpas J. Nutritional epidemiology and thyroid hormone metabolism. *Annu Rev Nutr*. (2006) 26:293–322. doi: 10.1146/annurev.nutr.26.010506.103810

146. Felker P, Bunch R, Leung AM. Concentrations of thiocyanate and goitrin in human plasma, their precursor concentrations in *Brassica* vegetables, and associated potential risk for hypothyroidism. *Nutr Rev*. (2016) 74:248–58. doi: 10.1093/nutrit/nuv110

147. Langer P, Michajlovskij N, Sedlák J, Kutka M. Studies on the antithyroid activity of naturally occurring L-5-vinyl-2-thiooxazolidone in man. *Endokrinologie*. (1971) 57:225–9.

148. Galanty A, Grudzińska M, Paździora W, Służały P, Paśko P. Do *Brassica* vegetables affect thyroid function?- a comprehensive systematic review. *Int J Mol Sci*. (2024) 25:3988. doi: 10.3390/ijms25073988

149. Zanichelli F, Capasso S, Cipollaro M, Pagnotta E, Cartenì M, Casale F, et al. Dose-dependent effects of R-sulforaphane isothiocyanate on the biology of human mesenchymal stem cells, at dietary amounts, it promotes cell proliferation and reduces senescence and apoptosis, while at anti-cancer drug doses, it has a cytotoxic effect. *Age (Dordr)*. (2012) 34:281–93. doi: 10.1007/s11357-011-9231-7

150. Zanichelli F, Capasso S, di Bernardo G, Cipollaro M, Pagnotta E, Cartenì M, et al. Low concentrations of isothiocyanates protect mesenchymal stem cells from oxidative injuries, while high concentrations exacerbate DNA damage. *Apoptosis*. (2012) 17:964–74. doi: 10.1007/s10495-012-0740-3

151. Sestili P, Paolillo M, Lenzi M, Colombo E, Vallorani L, Casadei L, et al. Sulforaphane induces DNA single strand breaks in cultured human cells. *Mutat Res*. (2010) 689:65–73. doi: 10.1016/j.mrfmmm.2010.05.003

152. Sekine-Suzuki E, Yu D, Kubota N, Okayasu R, Anzai K. Sulforaphane induces DNA double strand breaks predominantly repaired by homologous recombination pathway in human cancer cells. *Biochem Biophys Res Commun*. (2008) 377:341–5. doi: 10.1016/j.bbrc.2008.09.150

153. Xie J, Yang MR, Hu X, Hong ZS, Bai YY, Sheng J, et al. Isothiocyanate quinazolinone derivatives inhibit U251 glioma cell proliferation through cell cycle regulation and apoptosis induction. *Int J Mol Sci*. (2023) 24:11376. doi: 10.3390/ijms241411376

154. Hać A, Brokowska J, Rintz E, Bartkowski M, Węgrzyn G, Herman-Antosiewicz A. Mechanism of selective anticancer activity of isothiocyanates relies on differences in DNA damage repair between cancer and healthy cells. *Eur J Nutr*. (2020) 59:1421–32. doi: 10.1007/s00394-019-01995-6

155. Yagishita Y, Fahey JW, Dinkova-Kostova AT, Kensler TW. Broccoli or sulforaphane: is it the source or dose that matters? *Molecules*. (2019) 24:3593. doi: 10.3390/molecules24193593

156. Lüthy B, Matile P. The mustard oil bomb: rectified analysis of the subcellular organisation of the myrosinase system. *Biochem Physiol Pflanz*. (1984) 179:5–12. doi: 10.1016/S0015-3796(84)80059-1

157. Bierwirth JE, Oftedal KN, Civille GV, Fahey JW. Flavor misattribution: a novel approach to improving compliance and blinding in food-based clinical interventions. *NFS J*. (2015) 1:24–30. doi: 10.1016/j.nfs.2015.07.001

158. Fahey JWWK, Stephenson KK, Shi Y, Liu H, Panjwani AA, Warrick CR, et al. A strategy to deliver precise oral doses of the glucosinolates or isothiocyanates from *moringa oleifera* leaves for use in clinical studies. *Nutrients*. (2019) 11:1547. doi: 10.3390/nu11071547

159. Houghton CA. The rationale for sulforaphane favourably influencing gut homeostasis and gut-organ dysfunction: a clinician's hypothesis. *Int J Mol Sci*. (2023) 24:13448. doi: 10.3390/ijms241713448

160. Grosso C, Santos M, Barroso MF. From plants to psycho-neurology: unravelling the therapeutic benefits of bioactive compounds in brain disorders. *Antioxidants (Basel)*. (2023) 12:1603. doi: 10.3390/antiox12081603

161. Amro MS, Teoh SL, Norzana AG, Srijit D. The potential role of herbal products in the treatment of Parkinson's disease. *Clin Ter*. (2018) 169:e23–33. doi: 10.7417/T.2018.2050

162. Makkar R, Behl T, Bungau S, Zengin G, Mehta V, Kumar A, et al. Nutraceuticals in neurological disorders. *Int J Mol Sci*. (2020) 21:4424. doi: 10.3390/ijms21124424

163. Arias-Sánchez RA, Torner L, Fenton NB. Polyphenols and neurodegenerative diseases: potential effects and mechanisms of neuroprotection. *Molecules*. (2023) 28:5415. doi: 10.3390/molecules28145415

164. Minocha T, Birla H, Obaid AA, Rai V, Sushma P, Shivamallu C, et al. Flavonoids as promising neuroprotectants and their therapeutic potential against Alzheimer's disease. *Oxidative Med Cell Longev*. (2022) 2022:1–13. doi: 10.1155/2022/6038996

165. Iriti M, Vitalini S, Fico G, Faoro F. Neuroprotective herbs and foods from different traditional medicines and diets. *Molecules*. (2010) 15:3517–55. doi: 10.3390/molecules15053517

166. Murugesan V, Govindraj R, Amarnath Satheesh M, Rajagopal S. Phytonutrients in neurological disorders In: S Rajagopal, S Ramachandran, G Sundararaman and S Gadde Venkata, editors. Role of nutrients in neurological disorders. Singapore: springer Singapore (2022). 3–15.

167. Garodia P, Hegde M, Kunnumakkara AB, Aggarwal BB. Curcumin, inflammation, and neurological disorders: how are they linked? *Integr Med Res*. (2023) 12:100968. doi: 10.1016/j.imr.2023.100968

168. Joshi P, Bisht A, Joshi S, Semwal D, Nema NK, Dwivedi J, et al. Ameliorating potential of curcumin and its analogue in central nervous system disorders and related conditions: a review of molecular pathways. *Phytother Res*. (2022) 36:3143–80. doi: 10.1002/ptr.7522

169. Chiang MC, Tsai TY, Wang CJ. The potential benefits of quercetin for brain health: a review of anti-inflammatory and neuroprotective mechanisms. *Int J Mol Sci*. (2023) 24:6328. doi: 10.3390/ijms24076328

170. Yadav E, Yadav P, Khan MMU, Singh H, Verma A. Resveratrol: a potential therapeutic natural polyphenol for neurodegenerative diseases associated with mitochondrial dysfunction. *Front Pharmacol*. (2022) 13:922232. doi: 10.3389/fphar.2022.922232

171. Kempuraj D, Thangavel R, Kempuraj DD, Ahmed ME, Selvakumar GP, Raikwar SP, et al. Neuroprotective effects of flavone luteolin in neuroinflammation and neurotrauma. *Biofactors*. (2021) 47:190–7. doi: 10.1002/biof.1687

172. Patrick RP, Ames BN. Vitamin D and the omega-3 fatty acids control serotonin synthesis and action, part 2: relevance for ADHD, bipolar disorder, schizophrenia, and impulsive behavior. *FASEB J*. (2015) 29:2207–22. doi: 10.1096/fj.14-268342

173. Okereke OI, Vyas CM, Mischoulon D, Chang G, Cook NR, Weinberg A, et al. Effect of long-term supplementation with marine omega-3 fatty acids vs placebo on risk of depression or clinically relevant depressive symptoms and on change in mood scores: a randomized clinical trial. *JAMA*. (2021) 326:2385–94. doi: 10.1001/jama.2021.21187

174. Kang JH, Vyas CM, Okereke OI, Ogata S, Albert M, Lee IM, et al. Effect of vitamin D on cognitive decline: results from two ancillary studies of the VITAL randomized trial. *Sci Rep*. (2021) 11:23253. doi: 10.1038/s41598-021-02485-8

175. Kakarla R, Karuturi P, Siakabinga Q, Kasi Viswanath M, Dumala N, Guntupalli C, et al. Current understanding and future directions of cruciferous vegetables and their phytochemicals to combat neurological diseases. *Phytother Res*. (2024) 38:1381–99. doi: 10.1002/ptr.8122

frontiers | Frontiers in Nutrition

TYPE Brief Research Report
PUBLISHED 30 October 2024
DOI 10.3389/fnut.2024.1357906

OPEN ACCESS

EDITED BY
Paul Licciardi,
Murdoch Childrens Research Institute, Royal Children's Hospital, Australia

REVIEWED BY
Anita Panjwani,
Purdue University, United States
Lawrence Cheskin,
George Mason University, United States

*CORRESPONDENCE
Johannah Katz
✉ johannahKatzRD@gmail.com

RECEIVED 19 December 2023
ACCEPTED 25 September 2024
PUBLISHED 30 October 2024

CITATION
Giron J, Smiarowski L and Katz J (2024) The effect of sulforaphane on markers of inflammation and metabolism in virally suppressed HIV patients.
Front. Nutr. 11:1357906.
doi: 10.3389/fnut.2024.1357906

The effect of sulforaphane on markers of inflammation and metabolism in virally suppressed HIV patients

Jose Giron[1,2,3], Lauren Smiarowski[2,4] and Johannah Katz[5]*

[1]Sunshine Specialty Health Care, Orlando, FL, United States, [2]Department of Medicine, Florida State University, College of Medicine, Tallahassee, FL, United States, [3]Department of Medicine, University of Central Florida College of Medicine, Orlando, FL, United States, [4]OrlandoHealth- Arnold Palmer Hospital for Children, Orlando, FL, United States, [5]Florida Center for Hormones and Wellness, Orlando, FL, United States

There are currently 1.2 million people living with HIV (Human Immunodeficiency Virus) in the United States. Virally suppressed HIV patients commonly experience chronic inflammation which increases the risk for other chronic conditions. This inflammation can be quantified with a variety of biomarkers. Some current antiretroviral compounds bring about metabolic abnormalities and promote weight gain often associated with increases in visceral adipose tissue (VAT) and an increase in the risk of diabetes mellitus and cardiovascular disease. Sulforaphane, an isothiocyanate found in cruciferous vegetables, has shown efficacy in animal models by reducing lipid levels, lowering inflammatory markers, and decreasing fat mass. A double-blind randomized controlled pilot study with 14 virally suppressed HIV patients was conducted to evaluate the effects of 40 mg (225 μmol) of sulforaphane, once daily, over 12 weeks, followed by a 4-week washout period. There was a significant decrease in C-reactive protein compared to the control group ($p = 0.019$). Sulforaphane has been studied in a multitude of conditions and diseases, but this is the first study in a human population of patients living with HIV.

KEYWORDS

human immunodeficiency virus, sulforaphane (cruciferous antioxidants), antioxidant — phytochemical studies, metabolic syndome, acquired immunodeficiency syndrome, highly active antiretroviral therapy

Introduction

There are currently 1.2 million people living with HIV (Human Immunodeficiency Virus) in the United States (1). Therapeutic advances in HIV care have dramatically altered the natural history of HIV disease allowing patients to live normal lives. Although life expectancy has significantly increased, it remains slightly less than the general population- one theory for this is related to chronic inflammation. Patients living with virally suppressed HIV exist in a state of chronic inflammation, quantifiable by inflammatory markers such as Interleukin-6 (IL-6) and C-reactive protein (CRP) (2). Living in a state of chronic inflammation increases the risk for other chronic conditions in these patients. A commonly experienced side effect of highly active antiretroviral therapies (HAART) is metabolic abnormalities such as increases in lipids, triglycerides, and weight (3). These changes are associated with increases in visceral adipose tissue (VAT), which in turn increase the risk of diabetes and cardiovascular disease (CVD) (3–5).

Sulforaphane, a phytochemical, or phytonutrient, and the most potent natural activator of the transcription factor nuclear factor erythroid 2 (Nrf2)- an isothiocyanate produced from the precursor glucoraphanin (GR). It is commonly found in cruciferous vegetables, primarily broccoli, and has been shown to reduce lipid levels, inflammatory markers, and weight in animal models (6). Human studies of sulforaphane have shown improvement in inflammatory markers, and decreasing adipose mass, with an excellent safety profile (7–13).

Sulforaphane has been studied in a variety of clinical settings, both in healthy subjects and in studies of people living with chronic diseases such as hypertension, schizophrenia, type 2 diabetes, fatty liver, sickle cell disease, and asthma (14). Sulforaphane is a bioactive phytochemical, a constituent of plants that in human beings is an activator of cellular defense mechanisms (15). A tremendous body of evidence has now been built around the multiple molecular mediators of these effects, and interventions with glucoraphanin-rich or sulforaphane-rich broccoli preparations in humans lead to diverse beneficial effects (16). Sulforaphane has been shown to reduce inflammatory biomarkers and fat mass in humans and has been shown to ameliorate obesity in animal studies as well (6). Shehatou and Suddek (17), they found sulforaphane supplementation attenuated the development of artherosclerosis and prevented CRP elevation in high cholesterol diets in animal studies. An often-monitored inflammatory marker in these studies is high sensitivity C-reactive protein (HsCRP). CRP is secreted by the liver in response to inflammation in the body in response to inflammatory cytokines. CRP levels rise steeply with acute insult in response to trauma, inflammation, or infection (18). Sulforaphane has not yet been studied in humans living with HIV.

Previous studies investigating Antiretroviral Therapies (ART) has well characterized adverse effects of these disease altering medications. Frequently used medications in the treatment of HIV are Biktarvy, Genvoya, Descovy, Odefsey, and Symtuza all of which are combination medications of two or more antiretrovirals. A meta-analysis examining side effect profiles of ART in 8 randomized clinical trials showed significant weight gain after initiation of Antiretroviral Therapy (ART), in patients living with HIV, particularly with medications including tenofovir alafenamide (TAF) (5). A switch study by Mallon et al. (19) consisting of 6,908 people showed an association with early pronounced weight gain when switching from tenofovir disoproxil fumarate (TDF) to TAF, regardless of which medication was used, which then slowed down approximately 9 months after switching to TAF (19). Along with weight gain, Visceral Adipose Tissue (VAT) accumulation is a major correlate of diabetogenic, atherogenic, prothrombotic, and proinflammatory metabolic abnormalities referred to as metabolic syndrome (20, 23). According to the World Health Organization, 70% of all deaths globally can be attributed to chronic inflammatory diseases. Chronic inflammation has a significant impact on quality of life and increased risk of diseases, as cited in a review by Mazarakis et al. (21), who also described the positive effects of sulforaphane on inflammation.

The aim of the present study was to assess the effects of sulforaphane on inflammatory and lipid biomarkers in a virally suppressed HIV population.

Abbreviations: AST, Aspartate Aminotransferase; ALT, Alanine Aminotransferase; CD4, Cluster of Differentiation 4 (infection-fighting white blood cells); CD8, Cluster of Differentiation 8 (infection-fighting white blood cells); CRP, C-Reactive Protein; CT, Computed Tomography; DEXA, Dual Emission X-Ray Absorptiometry; GR, Precursor glucoraphanin; HIV, Human Immunodeficiency Virus; IL-6, Interleukin-6 (inflammatory cytokine); ITC, Isothiocyanate; LDL-C, Low Density Lipoprotein Cholesterol; Nrf2, Nuclear factor erythroid 2; TAF, Tenofovir alafenamide; TDF, Tenofovir disoproxil fumarate; Total-C, Total Cholesterol; VAT, Visceral Adipose Tissue.

Methods

Sampling

This study was approved by the Institutional Review Board of the Florida State University (STUDY00002532). This study was registered with the Food and Drug Administration (FDA) as a clinical trial (NCT05224492) with sulforaphane registered as a new drug (IND: 157470). All 14 participants were virally suppressed HIV patients from a private infectious disease practice directed by one of the authors (JG) in the greater Orlando area. Eligability criteria for this study included: a patient of the JG, living with virally suppressed HIV, demonstrating previous laboratory evidence of metabolic disease. All participants were provided written informed consent to participate in the study. The body mass index (BMI) of all participants had increased by 10% or more since initiation of HIV treatment, and at initiation of study the mean BMI was ≥30. Additional demographic information is available in Table 1.

Participants were randomly assigned to either a control group who received a placebo sachet filled with mustard seed powder and maltodextrin or an experimental group who received a dietary supplement consisting of powdered, concentrated glucoraphanin-rich broccoli seed extract and mustard seed powder containing active myrosinase, which react together to produce sulforaphane (hereinafter referred to as "sulforaphane"). Both participants and investigators were blinded to the contents of the product used. Participants received treatment (supplement) or control for 12 weeks. Participants were assigned a participant number, and numbers were randomized via an online random number generator.

TABLE 1 Enrolled patient demographics – total 9 patients.

Baseline characteristic	Sulforaphane		Placebo	
	n = 4	%	*n* = 5	%
Age				
31–50 years	1	25	3	60
51–70 years	3	75	2	40
Gender				
Female	0	0	1	20
Male	4	100	4	80
Self-identified race/ethnicity				
Hispanic	2	50	3	60
African American	1	25	1	20
Caucasian	1	25	1	20
Sexual behaviors				
MSM	4	100	4	80
No MSM	0	0	1	20

After study initiation, investigators measured clinical parameters and recorded any adverse events at intervals of 6, 12, and at 16 weeks after a 4-week washout period.

Supplementation

The supplements were provided in individual powder sachets for the patient to open and mix into their choice of food or beverage once daily. Both the sulforaphane and the placebo powders were provided by Brassica Protection Products, LLC (Baltimore, MD, United States). Each subject in the experimental group received 1,516 mg of the GR-rich extract (TrueBroc®) plus 601 mg of myrosinase-containing mustard seed powder, calculated to yield approximately 40 mg (225 μmol) of sulforaphane, daily. The placebo group did not receive any sulforaphane as their powder lacked glucoraphanin, the precursor for sulforaphane (14). The TrueBroc compound mixed with mustard seed powder was a beige-yellow color. The mustard seed powder only sachet was the same beige-yellow in color with no discernable difference between the experimental supplement and placebo. Patients in both groups were advised to continue their regular diet throughout the study period. The intervention period was 12 weeks followed by a 4-week washout period.

Parameters measured

Parameters tested at initiation of the supplement (listed below) provided a baseline for all levels measured throughout the study. HIV viral load was measured to ensure there was no unexpected drug interaction with patients' existing antiretroviral regimen. Additional safety parameters were measured, including AST, ALT, CBC, CMP, creatinine, CD4 and CD8 to monitor for adverse events related to supplementation. A table of all laboratory tests collected is found in Table 2. Blood specimens for all parameters except for IL-6 were processed through Quest Laboratories or Labcorp. IL-6 samples were processed by an academic lab. During transportation and storage, IL-6 samples became hemolyzed and developed fibrin clots. These samples were deemed unreliable due to sample quality and are thus not included in our results. Adherence to the study was self-reported by participants weekly during a weekly phone check in with one of the investigators. During these calls, participants were asked about if they missed any doses and any side effects they may have experienced. Participants were additionally asked about any changes to their health during the study time period including acute infections and changes to medications.

Statistical analysis

Data were analyzed using T-test assuming unequal variances using percentage change. Data collection and analysis was conducted using Excel (Microsoft V. 16.75) and the alpha was set at 0.05% for determination of significance. Difference in difference value was also calculated for CRP data using the mean CRP at week 0 and mean CRP at week 12. Data are presented in the subsequent tables.

TABLE 2 List of parameters measured for patients enrolled in the study.

1. White cell count
2. Hemoglobin
3. Platelet count
4. Creatinine
5. AST
6. ALT
7. CD4
8. CD8
9. HIV viral load
10. CRP
11. IL-6
12. Triglycerides
13. Total Cholesterol
14. Low density lipoprotein (LDL) Cholesterol
15. Pregnancy test (for women of childbearing age)

Results

A total of 9 participants completed this study. A breakdown of their demographic data can be found in Table 1.

C-reactive protein

Both groups had a reduction in mean C-Reactive Protein (CRP) at the end of 12 weeks, however the sulforaphane group had a significantly greater reduction. Subjects in the sulforaphane group experienced a mean reduction in CRP of 40% at the end of 12 weeks (Table 3), whereas subjects in the placebo group experienced a 12% reduction in CRP at the end of the study intervention. The difference in difference estimate between the two groups at the end of the 12 weeks was −0.61 ($p = 0.32$). Between cessation of sulforaphane treatment at 12 weeks, and the 16-week follow-up visits, the intervention group's CRP levels increased by 13%. While a 13% increase was seen following cessation of sulforaphane, a non-significant decrease of approximately 21% was observed as compared to baseline. At the 16-week mark, a decrease of 6% was observed in the control group.

Total cholesterol

At 12 weeks, a reduction in total cholesterol (Total-C; Table 3) of 12% was observed in the sulforaphane group while the placebo group experienced no change.

Low density lipoprotein-C

After 6 weeks of intervention, the low-density lipoprotein-C (LDL-C) levels of the sulforaphane group dropped 12% from baseline levels, and the placebo group dropped only 3% (Table 3). At the end of the intervention period (12 weeks), the intervention group's LDL-C had dropped by 24%, a differential that was maintained throughout the washout period. Control group LDL-C

10.3389/fnut.2024.1357906

TABLE 3 Average change in biomarkers with 12-week supplementation of sulforaphane vs. placebo among adult patients with HIV ($N = 9$).

Parameters (change from baseline)	Treatment ($n = 4$)	Placebo ($n = 5$)	p-value ($\alpha = 0.05$)*
CRP			
6 weeks	8.6%	3.6%	
12 weeks	−40%	−11.6%	0.02
16 weeks	−27%	−13%	
Total Cholesterol			
6 weeks	2.0%	0%	
12 weeks	−12%	0%	0.17
16 weeks	−10%	0%	
LDL-C			
6 weeks	−12.8%	−3%	
12 weeks	−18%	−3%	0.24
16 weeks	−24.4%	14%	
Triglycerides			
6 weeks	−15%	−1.9%	
12 weeks	−11%	6.3%	0.21
16 weeks	25.6%	−9.7%	

*p-values calculated from t-test.

TABLE 4 Average change from baseline in physical measurements with 12-week supplementation of sulforaphane vs. placebo among adult patients with HIV ($N = 9$).

Parameters (change from baseline)	Treatment ($n = 3$)	Placebo ($n = 5$)	p- value ($\alpha = 0.05$)
Weight			
12 weeks	−2%	−1%	0.29
Abdominal circumference			
12 weeks	1%	−3.7%	0.84

dropped only 3% by the end of the intervention, though after the washout period, they had a 14% reduction in LDL-C compared to baseline.

Triglycerides

The average change in triglycerides from baseline to conclusion of the intervention at 12 weeks for the treatment group was −11% (Table 3). The average percent change per patient from baseline to 12 weeks in the placebo group was 6.3% increase.

Body mass and abdominal circumference

Neither the control nor the experimental group experienced a significant change in weight. Additionally, there was no significant change in abdominal circumference between study groups as demonstrated in Table 4. One waist circumference value is missing from the data.

Adverse effects

Patients were contacted weekly via phone to follow up, ensure adherence with the study protocol, and to record any adverse events reported by patients. There were no serious adverse events experienced by patients. Overall, the sulforaphane supplement was well tolerated among study participants. The most frequent reported event was mild nausea ($n = 2$). Two patients reported an episode of emesis. One of the participants chose to drop out of the study due to unrelated health issues. Consistent with the literature, among the patients who did experience nausea, it was brief and subsided over time with continued use. No adverse drug interactions were found with the HIV medications. All side effects and patient experiences were reported to the FDA. Side effects can be found in Appendix A.

Discussion

This small pilot study shows promise for the efficacy of sulforaphane, a natural and safe compound, in reducing CRP, a key

biomarker of chronic inflammation, in patients living with virally suppressed HIV. As chronic inflammation has been well-described as a major contributor to the development of many chronic diseases, we believe interventions to reduce inflammatory stimuli result in beneficial effects in virally suppressed HIV patients (21). No serious adverse events were observed during the course of study. Adverse effects were recorded in Appendix A.

In animal models and in human studies, sulforaphane has shown efficacy in reducing decreasing inflammatory markers through reported decreased activation of NF-kB regulated inflammatory pathways (6–8, 22). Human studies using sulforaphane have demonstrated significant reductions in inflammation in various disease states (eg. Obesity) and in healthy volunteers (11, 12). To the researchers' knowledge, this is the first study to assess the effect of sulforaphane in humans living with virally suppressed HIV. Patients receiving sulforaphane supplementation in this study demonstrated a significant decrease of 40% in the inflammatory marker C-reactive protein (CRP) from onset of the study (week 0) to conclusion of the supplementation (week 12) ($p = 0.02$). A difference in difference calculation for CRP, found compared to the control group, the sulforaphane group had a decrease of 0.611 mg/dL. During the study period, patients did not report any acute infections that may have otherwise influenced a change in CRP. Patients were monitored throughout the duration of the study for changes in their health including acute infection and changes in medications through weekly phone calls with one of the investigators. With CRP being the only statistically significant change appreciated during the study period as well as the only biomarker measured, unreported changes to a patient's health could significantly impact the findings of this study. Our findings are consistent with previous research in humans on the use of sulforaphane's effects on human biomarkers of systemic inflammation.

Virally suppressed HIV patients are commonly in a chronic inflammatory state, which can be quantified by inflammatory markers (2), increasing risks for other chronic conditions. Some of the new antiretroviral compounds bring about metabolic abnormalities (changes in lipids and triglycerides) and promote weight gain often associated with an increase in visceral adipose tissue (3, 5, 24), increasing the risk of diabetes and cardiovascular disease (4). Although a greater decrease in LDL-C was observed in the group supplemented with sulforaphane, this result was non-significant ($p = 0.24$). This decrease in lipids observed in the intervention group is consistent with an effect previously observed in other human studies (7, 8). A decrease in triglycerides was also appreciated during our study, suggesting sulforaphane may induce a moderate, though non-significant ($p = 0.21$) reduction of triglycerides. Further studies with greater study power are warranted to further explore the relationship between sulforaphane, LDL-C, and triglycerides in patients living with HIV.

While our results suggest an improvement in biomarkers in patients living with HIV, our study found little effect on the patient's body habitus- both weight and abdominal circumference. The sulforaphane group experienced a −2% change in weight from baseline to 12 weeks, while the placebo group experienced a −1% change. Additionally, there was no significant change in abdominal circumference between study groups ($p = 0.84$). Studies using larger sample sizes and/or longer interventions are warranted to increase the power of the study, allowing significant trends to be more easily elucidated.

We believe that further, larger studies evaluating the effects of sulforaphane in the HIV population are warranted for sulforaphane as a complement to standard of care for antiretroviral therapy, given the observed significant reduction in CRP, a key biomarker of chronic inflammation, and positive trends for lipid parameters in this small pilot study. We would encourage future studies to include other well-established inflammatory markers to further demonstrate the efficacy of sulforaphane as an effective means of improving inflammation. Longer interventions would also indicate safety profile, effect, and compliance of long-term use.

A limitation to this study is the small sample size as it is a pilot study. As the two arms of this study each contain fewer than 5 participants, the weight of each participant greatly affected the statistical analysis. For this reason, results should be interpreted with caution. Furthermore, with further studies, additional demographic information including education level should be collected by investigators as a proxy for socioeconomic status. A validated measure to collect demographic data should be used in future studies to better characterize patient race and ethnic information. Future studies should incorporate participants keeping a food log to evaluate for any confounding variables in the participants diet such as consuming large quantities of GR rich foods. This study lacked access to a DEXA scan, Tanita technology, or CT slice for most accurate description of body fat mass to better characterize patient body composition. Alternatively, waist circumference was measured as an indicator of visceral adipose tissue, but due to the relatively short timeframe of the intervention it may have been unrealistic to expect changes in this parameter. Furthermore, the presence of mustard seed powder in the placebo (used for taste/smell masking, as well as to ensure greatest fidelity to the active intervention), will invariably contain the isothiocyanates(s) (ITC) specific to mustard seed, almost exclusively allyl-ITC, which is much less active in most pathways investigated, but by-and-large does have similar targets to sulforaphane. Of great importance, the only available biomarker in this study was CRP as the blood samples for IL-8 were hemolyzed during transit. Further studies should incorporate additional biomarkers such as IL-8 to better understand other biomarkers affected in the inflammatory pathway.

Conclusion

In summary, this pilot study underscores the evidence for the therapeutic effects of sulforaphane in attenuating inflammation and indicates a trend for improving lipid parameters in HIV patients. The intricate interplay between chronic inflammation and metabolic disease in this population emphasizes the need for novel and holistic approaches to management of HIV drug-related side effects. Larger randomized controlled trials are warranted to validate sulforaphane as an adjunctive therapy in the comprehensive care of individuals with HIV. To our knowledge, this is the first study to investigate the effects of sulforaphane on chronic inflammation in HIV patients. Despite the small sample size of this pilot study, $n = 9$, we observed a 40% reduction in CRP over the 12 weeks of the study period, indicating sulforaphane has the potential to be a useful tool in modulating the negative effects of inflammation in virally suppressed HIV patients and potentially in other populations experiencing chronic inflammation.

Data availability statement

The raw data supporting the conclusions of this article will be made available by the authors, without undue reservation.

Ethics statement

The studies involving humans were approved by Florida State University College of Medicine. The studies were conducted in accordance with the local legislation and institutional requirements. The participants provided their written informed consent to participate in this study.

Author contributions

JG: Conceptualization, Funding acquisition, Investigation, Methodology, Project administration, Resources, Supervision, Visualization, Writing – original draft. LS: Formal analysis, Writing – original draft, Writing – review & editing. JK: Conceptualization, Data curation, Investigation, Methodology, Project administration, Visualization, Writing – original draft, Writing – review & editing.

Funding

The author(s) declare that financial support was received for the research, authorship, and/or publication of this article. All funding was through the medical practice of one of the investigators (JG). Additionally, sulforaphane and the placebo powders were provided free of charge by Brassica Protection Products, LLC.

Acknowledgments

The researchers would like to acknowledge Jed Fahey and Angela Mastaloudis who assisted in obtaining study supplies, commenting on study design, and providing helpful critiques of the manuscript. The researchers also acknowledge Rosemont Pharmacy for their assistance in creating the individual sulforaphane and placebo sachets. Lastly, the researchers want to thank the patient participants and research technicians.

Conflict of interest

The authors declare that the research was conducted in the absence of any commercial or financial relationships that could be construed as a potential conflict of interest.

Publisher's note

All claims expressed in this article are solely those of the authors and do not necessarily represent those of their affiliated organizations, or those of the publisher, the editors and the reviewers. Any product that may be evaluated in this article, or claim that may be made by its manufacturer, is not guaranteed or endorsed by the publisher.

References

1. CDC. *Basic Statistics HIV Basics HIV/AIDS*. CDC. (2023). Avaiable at: https://www.cdc.gov/hiv/basics/statistics.html.

2. Slim J, Saling CF. A review of management of inflammation in the HIV population. *Biomed Res Int*. (2016) 2016:1–12. doi: 10.1155/2016/3420638

3. Bailin SS, Gabriel CL, Wanjalla CN, Koethe JR. Obesity and weight gain in persons with HIV. *Curr HIV/AIDS Rep*. (2020) 17:138–50. doi: 10.1007/s11904-020-00483-5

4. Kumar S, Samaras K. The impact of weight gain during HIV treatment on risk of pre-diabetes, diabetes mellitus, cardiovascular disease, and mortality. *Front Endocrinol*. (2018) 9. doi: 10.3389/fendo.2018.00705

5. Sax PE, Erlandson KM, Lake JE, McComsey GA, Orkin C, Esser S, et al. Weight gain following initiation of antiretroviral therapy: risk factors in randomized comparative clinical trials. *Clin Infect Dis*. (2019) 71:1379–89. doi: 10.1093/cid/ciz999

6. Du K, Fan Y, Li D. Sulforaphane ameliorates lipid profile in rodents: an updated systematic review and meta-analysis. *Sci Rep*. (2021) 11:7804. doi: 10.1038/s41598-021-87367-9

7. Armah CN, Derdemezis C, Traka MH, Dainty JR, Doleman JF, Saha S, et al. Diet rich in high glucoraphanin broccoli reduces plasma LDL cholesterol: evidence from randomised controlled trials. *Mol Nutr Food Res*. (2015) 59:918–26. doi: 10.1002/mnfr.201400863

8. Bahadoran Z, Mirmiran P, Hosseinpanah F, Rajab A, Asghari G, Azizi F. Broccoli sprouts powder could improve serum triglyceride and oxidized LDL/LDL-cholesterol ratio in type 2 diabetic patients: a randomized double-blind placebo-controlled clinical trial. *Diabetes Res Clin Pract*. (2012) 96:348–54. doi: 10.1016/j.diabres.2012.01.009

9. Houghton CA. Sulforaphane: its "coming of age" as a clinically relevant nutraceutical in the prevention and treatment of chronic disease. *Oxidative Med Cell Longev*. (2019) 2019:2716870. doi: 10.1155/2019/2716870

10. Lei P, Tian S, Teng C, Huang L, Liu X, Wang J, et al. Sulforaphane improves lipid metabolism by enhancing mitochondrial function and biogenesis in vivo and in vitro. *Mol Nutr Food Res*. (2019) 63:e1800795. doi: 10.1002/mnfr.201800795

11. López-Chillón MT, Carazo-Díaz C, Prieto-Merino D, Zafrilla P, Moreno DA, Villaño D. Effects of long-term consumption of broccoli sprouts on inflammatory markers in overweight subjects. *Clin Nutr (Edinburgh, Scotland)*. (2019) 38:745–52. doi: 10.1016/j.clnu.2018.03.006

12. Medina S, Domínguez-Perles R, Moreno DA, García-Viguera C, Ferreres F, Gil JI, et al. The intake of broccoli sprouts modulates the inflammatory and vascular prostanoids but not the oxidative stress-related isoprostanes in healthy humans. *Food Chem*. (2015) 173:1187–94. doi: 10.1016/j.foodchem.2014.10.152

13. Xu L, Nagata N, Ota T. Glucoraphanin: a broccoli sprout extract that ameliorates obesity-induced inflammation and insulin resistance. *Adipocytes*. (2018) 7:218–25. doi: 10.1080/21623945.2018.1474669

14. Fahey JW, Kensler TW. The challenges of designing and implementing clinical trials with broccoli sprouts… and turning evidence into public health action. *Front Nutr*. (2021) 8. doi: 10.3389/fnut.2021.648788

15. Lee JM, Johnson JA. An important role of Nrf2-ARE pathway in the cellular defense mechanism. *BMB Rep*. (2004) 37:139–43. doi: 10.5483/BMBRep.2004.37.2.139

16. Yagishita Y, Fahey JW, Dinkova-Kostova AT, Kensler TW. Broccoli or sulforaphane: is it the source or dose that matters? *Molecules*. (2019) 24:3593. doi: 10.3390/molecules24193593

17. Shehatou GS, Suddek GM. Sulforaphane attenuates the development of atherosclerosis and improves endothelial dysfunction in hypercholesterolemic rabbits. *Exp Biol Med (Maywood)*. (2016) 241:426–36. doi: 10.1177/1535370215609695

18. Du Clos TW. Function of C-reactive protein. *Ann Med*. (2000) 32:274–8. doi: 10.3109/07853890009011772

19. Mallon PW, Brunet L, Hsu RK, Fusco JS, Mounzer KC, Prajapati G, et al. Weight gain before and after switch from TDF to TAF in a U.S. cohort study. *J Int AIDS Soc*. (2021) 24:e25702. doi: 10.1002/jia2.25702

20. Després JP. Is visceral obesity the cause of the metabolic syndrome? *Ann Med*. (2006) 38:52–63. doi: 10.1080/07853890500383895

21. Mazarakis N, Snibson K, Licciardi PV, Karagiannis TC. The potential use of l- sulforaphane for the treatment of chronic inflammatory diseases: a review

of the clinical evidence. *Clin Nutr*. (2020) 39:664–75. doi: 10.1016/j.clnu.2019.03.022

22. Rodríguez-Cantú LN, Gutiérrez-Uribe JA, Arriola-Vucovich J, Díaz-De La Garza RI, Fahey JW, Serna-Saldivar SO. Broccoli (*Brassica oleracea* var. *italica*) sprouts and extracts rich in glucosinolates and isothiocyanates affect cholesterol metabolism and genes involved in lipid homeostasis in hamsters. *J Agric Food Chem*. (2011) 59:1095–103. doi: 10.1021/jf103513w

23. Cunha JD. Impact of antiretroviral therapy on lipid metabolism of human immunodeficiency virus-infected patients: old and new drugs. *World J Virol*. (2015) 4:56–77. doi: 10.5501/wjv.v4.i2.56

24. Ellulu MS, Patimah I, Khaza'ai H, Rahmat A, Abed Y. Obesity and inflammation: the linking mechanism and the complications. *Arch Med Sci*. (2017) 4:851–63. doi: 10.5114/aoms.2016.58928

10.3389/fnut.2024.1357906

Appendix A

TABLE A1 Summary of adverse events reported by patients.

Symptom experienced	Number of patients reporting symptom	Week of study reported	Study arm	Comments
Nausea	2	Weeks 1, 2, and 7	Sulforaphane	
Vomiting	1	Week 1	Sulforaphane	Patient withdrew from the study
Kidney stones	1	Week 3	Control	Patient withdrew from the study

frontiers | Frontiers in Nutrition

TYPE Original Research
PUBLISHED 06 January 2025
DOI 10.3389/fnut.2024.1485466

OPEN ACCESS

EDITED BY
Mireille Sthijns,
Maastricht University, Netherlands

REVIEWED BY
Antje R. Weseler,
Medical School Hamburg, Germany
Alie De Boer,
Maastricht University, Netherlands

*CORRESPONDENCE
Scott M. Plafker
✉ Scott-Plafker@omrf.org

RECEIVED 23 August 2024
ACCEPTED 11 December 2024
PUBLISHED 06 January 2025

CITATION
Plafker KS, Georgescu C, Pezant N, Pranay A and Plafker SM (2025) Sulforaphane acutely activates multiple starvation response pathways.
Front. Nutr. 11:1485466.
doi: 10.3389/fnut.2024.1485466

Sulforaphane acutely activates multiple starvation response pathways

Kendra S. Plafker[1], Constantin Georgescu[2], Nathan Pezant[3], Atul Pranay[1] and Scott M. Plafker[1]*

[1]Aging and Metabolism Research Program, Oklahoma City, OK, United States, [2]Genes and Human Disease Research Program, Oklahoma City, OK, United States, [3]Center for Biomedical Data Sciences, Oklahoma Medical Research Foundation, Oklahoma City, OK, United States

Sulforaphane (SFN) is an isothiocyanate derived from cruciferous vegetables that has demonstrated anti-cancer, anti-microbial and anti-oxidant properties. SFN ameliorates various disease models in rodents (e.g., cancer, diabetes, seizures) that are likewise mitigated by dietary restrictions leading us to test the hypothesis that this compound elicits cellular responses consistent with being a fasting/caloric restriction mimetic. Using immortalized human retinal pigment epithelial cells, we report that SFN impacted multiple nutrient-sensing pathways consistent with a fasted state. SFN treatment (i) increased mitochondrial mass and resistance to oxidative stress, (ii) acutely suppressed markers of mTORC1/2 activity via inhibition of insulin signaling, (iii) upregulated autophagy and further amplified autophagic flux induced by rapamycin or nutrient deprivation while concomitantly promoting lysosomal biogenesis, and (iv) acutely decreased glucose uptake and lactate secretion followed by an adaptive rebound that coincided with suppressed protein levels of thioredoxin-interacting protein (TXNIP) due to early transcriptional down-regulation. This early suppression of TXNIP mRNA expression could be overcome with exogenous glucosamine consistent with SFN inhibiting glutamine F6P amidotransferase, the rate limiting enzyme of the hexosamine biosynthetic pathway. SFN also altered levels of multiple glycolytic and tricarboxylic acid (TCA) cycle intermediates while reducing the inhibitory phosphorylation on pyruvate dehydrogenase, indicative of an adaptive cellular starvation response directing pyruvate into acetyl coenzyme A for uptake by the TCA cycle. RNA-seq of cells treated for 4 h with SFN confirmed the activation of signature starvation-responsive transcriptional programs. Collectively, these data support that the fasting-mimetic properties of SFN could underlie both the therapeutic efficacy and potential toxicity of this phytochemical.

KEYWORDS

sulforaphane, starvation, autophagy, mTOR, Txnip, Sestrin 2

Introduction

Sulforaphane (SFN) is an organosulfur compound derived from vegetables belonging to the *Brassicaceae* family (e.g., kale, broccoli, Brussels sprouts). Studies over the past three decades have established the therapeutic potential of SFN, determined a clinical history and safety profile for the compound, and demonstrated that SFN can be readily combined with other interventions (1, 2).

The pharmacological efficacy of SFN has largely been characterized in the context of stabilizing and activating NF-E2-related factor 2 (Nrf2), a master anti-stress and anti-oxidant transcription factor. SFN-mediated activation of Nrf2 induces the expression of a battery of

genes encoding proteins that maintain and restore redox and proteome homeostasis (reviewed in (3, 4)). Nrf2 activation additionally shunts glucose into anti-oxidant pathways by inducing the expression of the rate limiting enzymes for the pentose phosphate pathway, the glucuronidation pathway, and nucleotide biosynthesis. This redirection of glucose into anabolic pathways generates molecules for neutralizing oxidative stress and eliminating xenobiotics, for replacing damaged proteins and DNA, and for restoring homeostasis (4).

Nrf2 activation by SFN has been studied intensively in the context of mitochondrial impacts including a body of work related to the capacity of the phytochemical to counter neurodegeneration [e.g., (5)]. SFN can preserve mitochondrial membrane potential by increasing the resistance of mitochondria to the deleterious consequences of redox imbalances stemming from unchecked reactive oxygen species (ROS) [e.g., (6)] and dopamine toxicity [e.g., (7)]. Moreover, SFN preserved mitochondrial function, induced mitochondrial biogenesis [e.g., (8–11)] and mitigated pathologies in rodent models of brain injury, spinal cord injury, stroke, Alzheimer's disease, Parkinson's disease, Huntington's disease, depression, and multiple sclerosis [reviewed in (12)].

In the work presented here, we investigated the hypothesis that SFN is a fasting mimetic at the cellular level. Our rationale was twofold. First, evidence from both animal and human studies have shown that caloric restriction, fasting regimens, timed feeding, and low carbohydrate diets can extend lifespan, slow age-related declines in muscle loss and cognitive function, and prevent or mitigate a variety of chronic diseases (13). The *in vivo* efficacy of these dietary strategies includes improvements in fasting blood glucose, fasting insulin, triglycerides, C-reactive protein (CRP), fibroblast growth factor 21 (FGF21), circulating branched chain amino acids, adiposity, and blood pressure, concomitant with increased stress resistance, altered redox metabolism, reduced inflammation, and reduced numbers of auto-reactive immune cells (13). At the organismal and cellular level, these nutritional approaches converge to modulate proliferation cascades, proteome homeostasis, stress responses, and central metabolic nodes (13). Importantly, SFN elicits many of these same responses *in vivo* [e.g., (11, 14–19)]. Second, we previously demonstrated that SFN induces a protective mitochondrial hyperfusion phenotype (20) similar to what was observed in cells challenged with complete nutrient deprivation (21). Together, these *in vitro* and *in vivo* observations led to us to test if SFN phenocopied other aspects of cellular starvation involving mTOR signaling, autophagy, lysosomal and mitochondrial biogenesis, and signature transcriptional responses to starvation.

To extend our previous work with SFN and Nrf2 in cultured cells (20, 22–24) the studies of this report were done in telomerase-immortalized human retinal pigment epithelial cells (RPE-1 cells), which we have shown rapidly and robustly respond to SFN treatment in both Nrf2-dependent (20) and Nrf2-independent ways (24). The use of RPE-1 cells additionally enabled us to take advantage of several stably-transfected RPE-1 reporter cell lines we previously generated and characterized for tracking dynamic changes in mitochondrial redox status, mitophagy, and autophagy (20, 25). In the current work, we characterized the impacts of SFN on nutrient-sensing pathways using 25 μ M SFN, a concentration within the range detected in the serum of numerous human and animal studies studying the compound [e.g., (26)]. Our assays use early time points (e.g., 1, 4, and 8 h) to interrogate acute direct effects of the phytochemical on different cellular pathways and later time points (i.e., 16 and 24 h) to detect cellular adaptations to these acute impacts. The data presented here test whether SFN induces a fasted cellular state, in the presence of sufficient nutrients, characterized by reduced pro-proliferative signaling, increased autophagic flux, increased lysosomal biogenesis, as well as altered glucose and pyruvate metabolism.

Materials and methods

Chemical, reagents, antibodies

A comprehensive list of the chemicals, reagents, and antibodies used, along with the companies these were acquired from, the catalog numbers, and the concentrations/dilutions used are provided in Supplementary Table S1.

Cell culture

Telomerase-immortalized, human retinal pigment epithelium cells (RPE-1, ATCC CRL-4000) were cultured as described (20). Briefly, cells (passage ~8–24) were plated to ~70% confluency in complete DMEM (1 g/L glucose supplemented with 1X non-essential amino acids and 10% (v/v) heat-inactivated fetal calf serum (FCS)) 1 day before experimental treatments. RPE-1 cells stably expressing GFP-LC3, mtKeima and mito-roGFP have been described previously (25). Starvation media was as follows: no glucose (Corning cat#17-207-CV no glucose DMEM supplemented with pyruvate, glutamine, non-essential amino acids, and 10% (v/v) dialyzed-heat-inactivated fetal calf serum (dFCS)), no serum (Corning, 17-207-CV supplemented with 1 g/L glucose, pyruvate, glutamine and non-essential amino acids), no amino acids or Ringer's (Alfa Aesar Kreb's-Ringer bicarbonate-buffered solution cat# J67591 with or without 10% (v/v) dFCS). siRNA transfection was performed as previously described (24). 25 μM SFN treatment was used exclusively throughout this manuscript for the indicated incubation times.

Flow cytometry

GFP-LC3, mito-RoGFP, mtKeima, LTR, and MTG/TMRE flow cytometry were done as described (25), and FlowJo 10.3 software was used for gating analysis and quantification for all flow cytometry studies.

Mitochondrial membrane potential was determined in RPE-1 cells treated with vehicle (DMSO), SFN, or different nutrient deprivations for 4 or 24 h and co-labeled during the final 30 min of treatment with 5 nM tetramethylrhodamine ethyl ester (TMRE) and 200 nM MitoTracker Green™ (MTG). Cells were trypsinized, resuspended in complete media lacking Phenol Red, filtered through 100 µm mesh and subjected to flow cytometry. MTG was visualized with a 488 nm laser and a 510/21 nm filter. TMRE was visualized with the 561 nm laser and a 582/15 nm filter. Membrane potential changes were calculated using the ratio between the TMRE (red) and MTG (green) signals. Mitochondrial mass of RPE-1 cells treated for 24 h with either vehicle (DMSO), SFN, or

different nutrient deprivations was measured by incubating cells in 200 nM MTG for the final 30 min of the 24 h treatments. Cells were processed for flow cytometry and mitochondrial mass was calculated by median fluorescence intensity (MFI) and graphed as fraction of control.

To assess mitochondrial redox stress, RPE-1 cells stably expressing mito-roGFP were treated for 4 h with SFN, FCCP, or different nutrient deprivations and then processed for flow cytometry using the 405 nm laser with 525/50 nm filter to visualize oxidized mito-GFP and the 488 nm laser with 530/30 nm filter to visualize reduced mito-GFP.

To quantify mitophagy, RPE-1 cells stably expressing mitochondria-targeted (mt)-mKeima and YFP-parkin were treated for 4 h at 37°C with vehicle, SFN, different nutrient deprivations or FCCP. Cells were then trypsinized, resuspended in 10% fetal calf serum (FCS) and 0.5 mM EDTA in PBS, passed through 100 µm mesh, and subjected to flow cytometry. YFP-Parkin positive cells were detected with 488 nm excitation and a 530/30 nm emission filter. Mt-mKeima was detected with a 488 nm excitation laser and a 695/40 nm emission filter for mitochondrial localization, and a 561 nm laser with 670/30 nm filter for lysosomal localization. YFP-Parkin-positive cells were plotted in FlowJo as acidic against neutral and two gates defined the cells exhibiting predominately lysosomal or mitochondrial mt-mKeima localization.

For autophagy assays, RPE-1 cells stably expressing GFP-LC3 were treated with SFN, the indicated pharmacological treatments, or starved of various nutrients for 24 h. Cells were then trypsinized, resuspended in 0.05% (v/v) Saponin/PBS to leak out soluble GFP-LCS not associated with autophagolysosomes, pelleted at 500 × g for 5 min, resuspended in PBS, filtered and subjected to flow cytometry.

Lysosomal mass was quantified by LysoTracker Red (LTR) uptake in RPE-1 cells treated with vehicle, SFN, Rapa, or different nutrient deprivations for 16 h. Cells were incubated with 50 nM LTR for the final 30 min of the 16 h. Cells were resuspended in PBS + 2% FCS and subjected to flow cytometry using the 561 nm laser and 582/15 nm filter.

Western blotting

Western blotting was performed as previously described (22, 23, 25) with the antibodies listed in Supplementary Table S1. Samples were solubilized in 2-times concentrated Laemmli buffer (100 mM Tris,pH 6.7; 2% (w/v) SDS; 25% (v/v) glycerol; 0.001% (w/v) Pyrinin Y; 0.008% (w/v) Bromophenol Blue; 285 mM b-mercaptoethanol) and heated in a boiling water bath for 5 min prior to being loaded onto gels for reducing, denaturing SDS-PAGE. All depicted Western blots are representative of at least 3 independent experiments and the migration of molecular weight markers (kDa) are indicated to left side of blots.

qPCR

RNA was isolated using the *Zymo Direct-zol microRNA Isolation Kit and cDNA* was produced using the Quanta qScript cDNA Supermix, both per manufacturers' instructions. qPCR was performed with PowerUp SYBR Green (Applied Biosystems, Inc.) using the primers listed in Supplementary Table S2.

Lysosome labeling

Lysosomes were visualized in live cells by incubating in 50 nM LysoTracker Red for 30 min.

Unincorporated dye was removed by replacing the media and images were captured on a Nikon TE2000 inverted microscope as described (25).

Immunofluorescence

RPE-1 cells were plated in 12-well dishes containing sterile glass coverslips. After the indicated treatments, cells were fixed in 4% (w/v) paraformaldehyde/PBS for 20 min, permeabilized in 0.2% (v/v) Triton X-100/PBS for 5 min, blocked in 3% (w/v) bovine serum albumin/PBS and probed overnight with anti-pPDH1 diluted 1:250. The following day, cells were washed in PBS and incubated in $Alexa_{488}$-conjugated donkey anti-rabbit IgG and Hoechst 33342, mounted and sealed on microscope slides, and imaged as described (22, 23, 25).

Glucose uptake and lactate secretion assays

Following treatment with DMSO, 25 μM SFN or 5 mM 2-deoxy-d-glucose (2-DG) for the indicated times, RPE-1 cells were washed with warm media lacking both serum and glucose, incubated with Glucose Uptake Probe-Green (Dojindo,Inc. catalog# UP02) diluted 1:500 in glucose-and serum-free media for 15 min, washed with ice cold 1X WI buffer (Dojindo, Inc.), scraped into 1X WI buffer, filtered through 70 μm mesh, and subjected to flow cytometry on a BD FacsCelesta cell sorter equipped with a 488 nm laser and processed with Flowjo software.

For assessing lactate secretion per 10,000 cells, RPE-1 cells were plated in 24 well plates and incubated with 25 μM SFN or DMSO vehicle for 8 h after which media was removed for analysis (initial 8 h measurement) and replaced with fresh media containing 25 μM SFN or DMSO vehicle for an additional 16 h (for a total of 24 h treatment). Media was again removed for analyses (final 16 h measurement). Both the initial 8 h and final 16 h media collections were subjected to centrifugation at 4°C (500xg for 5 min) to remove cellular debris. Clarified supernatants were then snap frozen in liquid nitrogen. To determine cell number, remaining adherent cells were fixed and stained with 0.5% (w/v) crystal violet in 25% (v/v) methanol for 20 min, and then washed, air-dried, dissolved in methanol and the OD_{570} was read and compared against a standard curve made using known numbers of cells. The lactate concentration in the previously snap frozen media was assayed using the L-Lactate Assay Kit I (Eton Biosciences, Inc.) and normalized to cell number.

Metabolomics

RPE-1 cells (1.5×10^6 for LC/MS and 0.5×10^6 for GC/MS, 5 replicates/treatment/analysis) in complete DMEM were treated with vehicle or 25 μM SFN for 4 h. Cells were then washed with ice cold PBS before being snap frozen in liquid nitrogen. LC–MS analysis was performed as previously published (27) on an Agilent 6,546

LC/Q-TOF coupled to an Agilent 1,290 Infinity II LC. Chromatographic separation was performed on an Agilent InfinityLab Poroshell 120 HILIC-Z, 2.1 × 150 mm, 2.7 µm column, coupled with a UHPLC Guard, HILIC-Z, 2.1 mm × 5 mm, 2.7 µm, at 15°C, with a total run time of 29 min. GC/MS was performed as previously described (28).

Co-immunoprecipitation assay

RPE-1 cells were treated with vehicle or 25 μM SFN for 4 h before being lysed on ice in TPER (Thermo Scientific, Inc. catalog# 78510) supplemented with a proteinase inhibitor cocktail containing AEBSF hydrochloride, aprotinin, bestatin, E-64, leupeptin hemisulfate, and pepstatin A (EZBlock™, Biovision, Inc). Insoluble cellular debris was removed by centrifugation at 4°C (16,000 x g for 15 min) and soluble, extracted MondoA/MLX was captured by overnight incubation at 4°C with an anti-MLX antibody. Immunoprecipitates were washed, solubilized, and resolved by denaturing, reducing SDS-PAGE. MondoA was visualized with anti-MondoA antibody.

Chromatin immunoprecipitation assay

CHIP was performed as described in (29). 1×10^7 RPE-1 cells were treated with vehicle or 25 μM SFN for 4 h, trypsinized, washed and fixed in 1% (w/v) formaldehyde in PBS at room temp for 5 min before the reaction was stopped by the addition of 125 mM glycine. Cells were washed and DNA was sheared using a Covaris E220. Chromatin DNA (chDNA) was mixed with anti-MondoA (MLXIP) antibody and Protein G magnetic beads overnight at 4°C. Bound chDNA was eluted, cleaned up with Zymo CHIP DNA Clean and Concentrator and used for CHIP qPCR with the following primers: TXNIP-CHIP7: 5'-CTC GCG TGG CTC TTC TG-3′ and TXNIP-CHIP8: 5'-GCA GGA GGC GGA AAC GT-3′. ΔCt was calculated by normalizing to input chDNA.

RNA-seq

RPE-1 cells (50,000 cells/replicate, 5 replicates/treatment) in complete DMEM were treated with vehicle or 25 μM SFN for 4 h. RNA was isolated as described above and sequenced in the OMRF Clinical Genomics Center. The Lexogen QuantSeq sequencing data was aligned using a pipeline established by Bluebee, the Lexogen associated data analysis tool. Ensemble gene IDs were annotated using the biomart library in R for the GRCh38 (human) build. Read-count normalization and differentially expressed analyses were performed using the edgeR package from Bioconductor. Expression values quantile normalized with the voomWithDreamWeights function were analyzed for differential expression, accounting for repeated measure dependencies, using the standard functions of the limma package. Moderate t-test *p*-values were adjusted for multiple testing using the false discovery rate (FDR) method and FDR (q.value) <0.05 was used to filter significant differences. For a comparative look at fasting effect, raw fastq files and count data on HeLa cells under nutrient starvation protocol were downloaded from GEO repository, (accession code GSE211066), processed and analyzed alongside our sequencing data. Differentially expressed genes (DEGs) were defined by having an adjusted *p*-value (*q*- value) < 0.05 and a log2FC < −1 or log2FC > 1. Using the ggVennDiagram" package in R, DEGs from both analyses were compared via Venn diagram and the percentage of Starvation DEGs found to be in common with SFN DEGs was calculated.

Statistics

Statistical differences were measured with unpaired Student's t-test or Analysis of Variance (ANOVA) that was appropriate for each data set and analysis. Normal distribution was verified by Shapiro–Wilk test and a Mann–Whitney nonparametric test was used when normal distribution was not present. Error bars represent standard deviations, and all experimental data derived from at least 3 independent replicates.

Results

We previously reported that treating RPE-1 cells with SFN rapidly induced mitochondrial fusion and elongation (24), a phenotype similar to complete nutrient starvation (21). Deprivation of amino acids (AAs) or just glutamine was sufficient to induce fusion but removal of just serum or glucose caused mitochondrial fragmentation whereas coupling these reductions with AA deprivation exacerbated mitochondrial fusion (21). Functionally, the fused mitochondria were protected from starvation-induced degradation by autophagolysosomes (21). This shared mitochondrial fusion between SFN and nutrient deprivation prompted us to test the hypothesis that SFN phenocopies additional cellular responses to starvation.

Effects of SFN on mitochondrial membrane potential, mass, matrix redox status, and mitophagy

We first compared the impacts of SFN versus different nutrient deprivations on mitochondrial mass and membrane potential. RPE-1 cells were labeled with MitoTracker Green (MTG) to mark total mitochondria and with tetramethylrhodamine ethyl ester (TMRE) to label mitochondria with intact membrane potential. Flow cytometry was used to quantify the uptake of both dyes, and FCCP treatment served as a positive control to show that the loss of mitochondrial membrane potential was readily detectable in this assay (Figure 1A, left graphs top and bottom). Membrane potential was measured at 4 h and 24 h post-treatment but mitochondrial mass was measured only at 24 h to provide sufficient time for mitochondrial biogenesis. SFN treatment caused a very modest but statistically significant loss of membrane potential at the 4 h time point but preserved mitochondrial membrane potential and increased mitochondrial mass after 24 h, most closely reflecting the mitochondrial response to AA deprivation (Figure 1A). In contrast, cells incubated in media lacking glucose showed reduced mitochondrial membrane potential, and serum deprivation increased mitochondrial mass but reduced mitochondrial membrane potential (Figure 1A).

In complementary experiments, we compared SFN treatment to nutrient deprivations to assess the extent of mitochondrial matrix oxidation, a proxy of mitochondrial redox status. These assays used

10.3389/fnut.2024.1485466

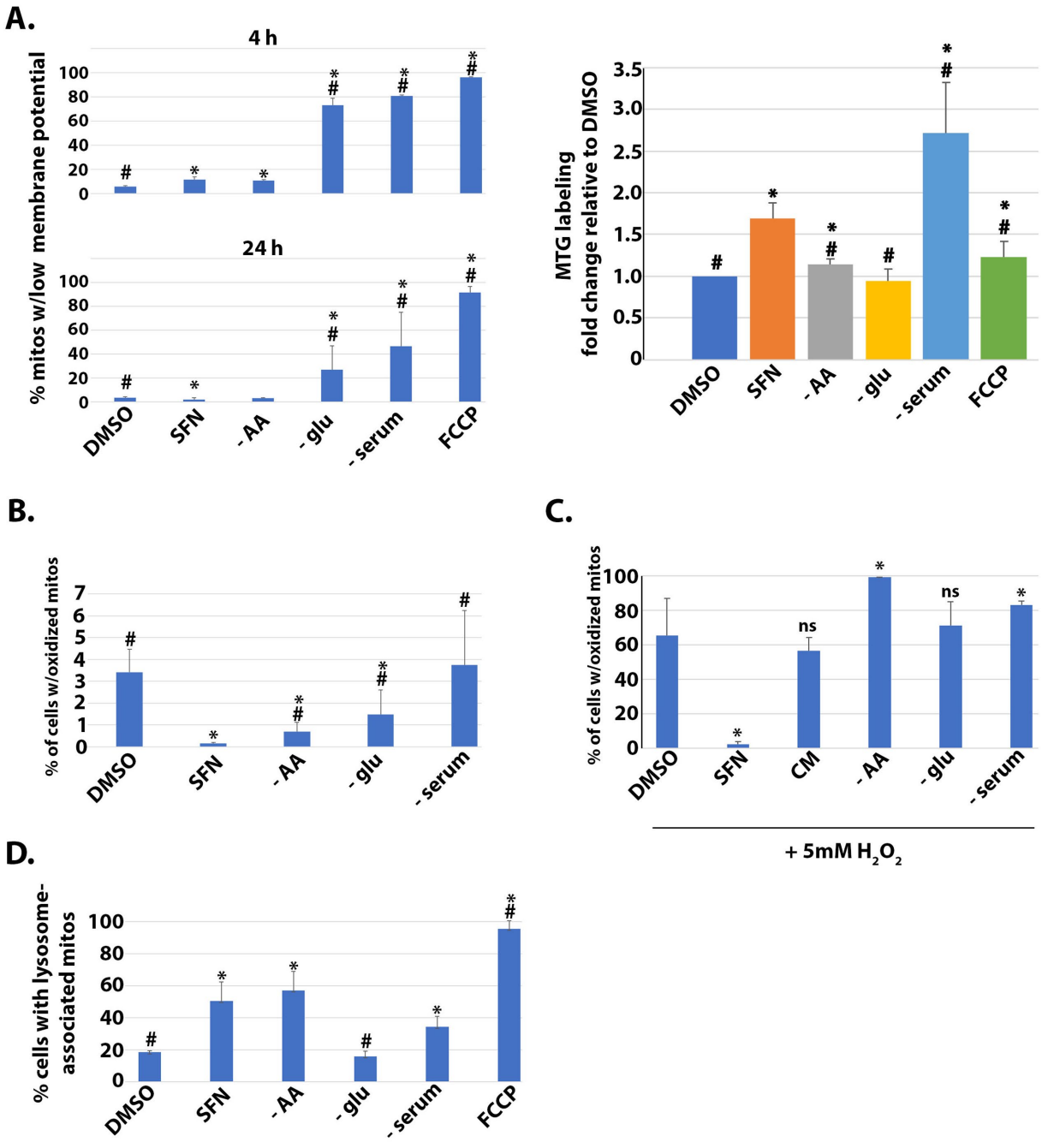

FIGURE 1
SFN promotes a reductive mitochondrial matrix environment, increased mitochondrial mass, mitophagy, and resistance to oxidative stress. **(A)** RPE-1 cells were treated with vehicle (DMSO), SFN, or culture media lacking AA (– AA), glucose (– glu), or serum (– serum) or with 5 μM FCCP for 4 (top graph) or 24 h (bottom and right graphs). Mitochondria were labeled with 200 nM MitoTracker Green (MTG) and 5 nM tetramethylrhodamine ethyl ester (TMRE) for 30 min. Cells were washed, trypsinized, analyzed by flow cytometry and graphed as the fraction of mitochondria with membrane potential loss or normalized to mitochondrial mass of DMSO-treated cells (right graph). **(B)** RPE-1 cells stably expressing mito-roGFP were treated as described for **(A)** for 4 h and then harvested for analysis by flow cytometry. Graph shows the fraction of cells containing mitochondria with oxidized matrices. **(C)** Mito-roGFP RPE-1 cells were treated as described for (B) with the addition of a complete media (CM) treatment before a 1 h challenge with 5 mM H_2O_2. Mitochondrial matrix oxidation was determined as for **(B)**. **(D)** RPE-1 cells stably expressing mtKeima and the E3 ligase parkin were treated as described for **(B)** and then analyzed by flow cytometry to determine the fraction of cells with lysosome-associated mitochondria. For **A**,**B**, and **D**, * indicates $p < 0.05$ compared to DMSO and # indicates $p < 0.05$ compared to SFN. For C, SFN is compared to DMSO whereas each nutrient deprivation is compared to CM. * indicates $p < 0.05$ for both comparisons and 'ns' = not significant.

RPE-1 cells stably expressing mito-roGFP, a mitochondrially-targeted GFP variant that harbors two redox-sensing cysteines (30). These cysteines modulate the excitation profile of the GFP, thereby allowing the redox state of the mitochondrial matrix to be quantified by measuring fluorescence intensity at the oxidizing and reducing excitation wavelengths (20). Four hour of SFN suppressed the

fraction of mitochondria with an oxidized matrix (Figure 1B). Compared to DMSO-treated cells without starvation, both AA and glucose starvation also significantly decreased the percent of mitochondria with oxidized matrices but to a lesser extent than SFN. AA starvation looked most similar to SFN in this assay although all starvation conditions tested had statistically significant increases in oxidized mitochondrial matrices compared to SFN (Figure 1B).

This resistance to an oxidized mitochondrial matrix by SFN led us to test the hypothesis that the isothiocyanate could protect against mitochondrial oxidation induced by an exogenous oxidative challenge. Mito-roGFP RPE-1 cells were pre-treated for 4 h with SFN or DMSO followed by a 1 h exposure to 5 mM H_2O_2 to induce mitochondrial oxidation. Cells subjected to various nutrient starvations were likewise challenged with H_2O_2 (Figure 1C). In contrast to cells deprived of nutrients, versus complete media (CM), SFN prevented mitochondrial oxidation induced by H_2O_2 (Figure 1C). We next examined if SFN impacted homeostatic levels of mitochondria being targeted to lysosomes for mitophagy using RPE-1 cells stably expressing mitochondria-targeted Keima (mtKeima) and the parkin E3 ligase. mtKeima is a pH-dependent fluorescent protein containing the mitochondrial targeting sequence from COX VIII. mtKeima excites at 440 nm when mitochondria are in the cytoplasm and at 586 nm when mitochondria have been engulfed by lysosomes. The emission wavelength for mtKeima is ~620 nm and is independent of pH (31). As homeostatic mitophagy is minimal in unchallenged RPE-1 cells, stable over-expression of parkin accelerates mitophagy (31) to enable the evaluation and comparison of acute treatments (i.e., 4 h). FCCP treatment validated the sensitivity of the assay for tracking mitochondrial turnover by mitophagy in the time frame tested (Figure 1D). SFN, AA starvation, and serum deprivation all individually increased the percent of cells undergoing mitophagy whereas glucose deprivation was comparable to unstarved, DMSO-treated cells (Figure 1D). Together, these data show that SFN preserves mitochondrial membrane potential, limits mitochondrial matrix oxidation, and promotes homeostatic mitophagic flux (i.e., mitophagy and biogenesis), thereby mirroring aspects of nutrient deprivation, with the most similarities to AA starvation.

Impacts of SFN on signaling through mTOR

Nutrient signaling through the mechanistic target of rapamycin (mTOR) involves two integrated kinase hubs, mTORC1 and mTORC2. These complexes function as primary sensors of amino acids (mTORC1) and growth factors (mTORC2) (reviewed in (32)). In time-course experiments analyzing the acute effects of SFN on nutrient sensing, we tracked the phosphorylation of multiple proteins in the insulin signaling cascade with a focus on phosphatidylinositol 3-kinase (PI-3 K), Akt, and downstream substrates and effectors. These experiments compared SFN to the pharmacological inhibitors of insulin signaling GSK2334470 (GSK233), AZD8055 (AZD), and copanlisib (Cop). Targets of each inhibitor are diagrammed in Figure 2A. GSK233 inhibits phosphoinositide-dependent kinase-1 (PDK1), the kinase that activates Akt via phosphorylation of threonine 308 (T308), whereas AZD inhibits both mTORC1 and mTORC2, and Cop inhibits PI-3 K.

Compared to DMSO, phosphorylation of T308 on Akt was decreased by SFN, GSK233, and AZD (Figure 2B, lanes 1–4). To facilitate visualizing T308 phosphorylation, the signal was amplified by co-treating cells for the last 60 min of the 90 min incubation with GDC-0068 (GDC), an agent that blocks phosphatase access to T308 (33). This signal enhancement confirmed that SFN reduced T308 phosphorylation (Figure 2B, lane 5 versus 6) albeit to a lesser extent than the PDK1 inhibitor, GSK233 (Figure 2B, lane 6 versus 7), and that AZD altered the pattern of Akt phosphorylation (Figure 2B, lane 5 versus 8). T308 phosphorylation primes Akt to phosphorylate threonine 86 (T86) of Sin, an activating subunit of mTORC2. In turn, activated mTORC2 feeds back to phosphorylate Akt on serine 473 (S473) to generate fully activated Akt, which then phosphorylates and inhibits the downstream effectors PRAS and TSC2 (34, 35) (Figure 2A). In kinetic studies with homeostatic phosphorylation levels represented by time point '0', the reduction by SFN of the priming T308 phosphorylation on Akt (Figure 2B) led to reduced phosphorylation of T86 on Sin and S473 on Akt by mTORC2 (Figure 2C, lanes 1–5). Consistent with dampening Akt activation, SFN reduced phosphorylation of the downstream substrates PRAS and TSC2 over the course of 60 min (Figure 2C, lanes 1–5). Notably, TSC2 is part of a complex that inhibits mTORC1, and is a phosphorylation substrate of AMPK (36). When compared to pharmacological inhibitors, the kinetics and specificity of phosphorylation loss mediated by SFN for each protein analyzed most closely approximated those observed when PDK1 was pharmacologically inhibited by GSK233 (Figure 2C, lanes 1–5 compared to 6–10). PI-3 K is the kinase directly upstream of PDK1 and Cop inhibits PI-3 K as well as the generation of PIP_3, which activates mTORC2 through direct binding to the PH-domain of Sin (37). Therefore, in cells treated with Cop, the loss of pSin T86 and pAKT S473 occurred within 5 min (Figure 2C, lanes a-e). Likewise, because AZD inhibits mTORC2, pSin T86 is largely preserved while loss of pAKT S473 also occurs within the first 5 min and pS6 decreased by 1 h (Figure 2C, lanes f-j). Together, these data show that SFN elicits a temporal phosphorylation pattern resembling the PDK1 inhibitor, GSK233. In contrast to the relatively rapid inhibition of mTORC2 signaling by SFN, phosphorylation of S6 (pS6) downstream of mTORC1 was unchanged during the first 60 min of treatment (Figure 2C, lanes 1 and 5). However, 8 h of SFN markedly reduced pS6 levels with a concomitant increase in the mTORC1 inhibitor, Sestrin 2. (Figure 2D, lane 4). The elevation of Sestrin 2 by SFN is mediated in part by stability/turnover. Sestrin 2 is stabilized by SFN (Figure 2E, lane 1 versus 3) and by MG132 in the absence of SFN (Figure 2E, lane 1 versus 2) but inhibition of the proteasome in the presence of SFN did not further increase Sestrin 2 levels (Figure 2E, lane 3 versus 4), indicating that the phytochemical limits the proteasomal degradation of Sestrin 2. Elevated Sestrin 2 is also mediated at the transcriptional level as SFN increased *Sestrin 2* mRNA by ~10-fold (Figure 2F).

Effects of SFN on autophagic flux and lysosomes

We next tested the hypothesis that SFN would activate autophagy since suppression of mTORC1/2 relieves autophagy inhibition to promote the salvaging of cellular bioenergetic substrates and building blocks (38). In addition, SFN has been reported to both activate [e.g.,

10.3389/fnut.2024.1485466

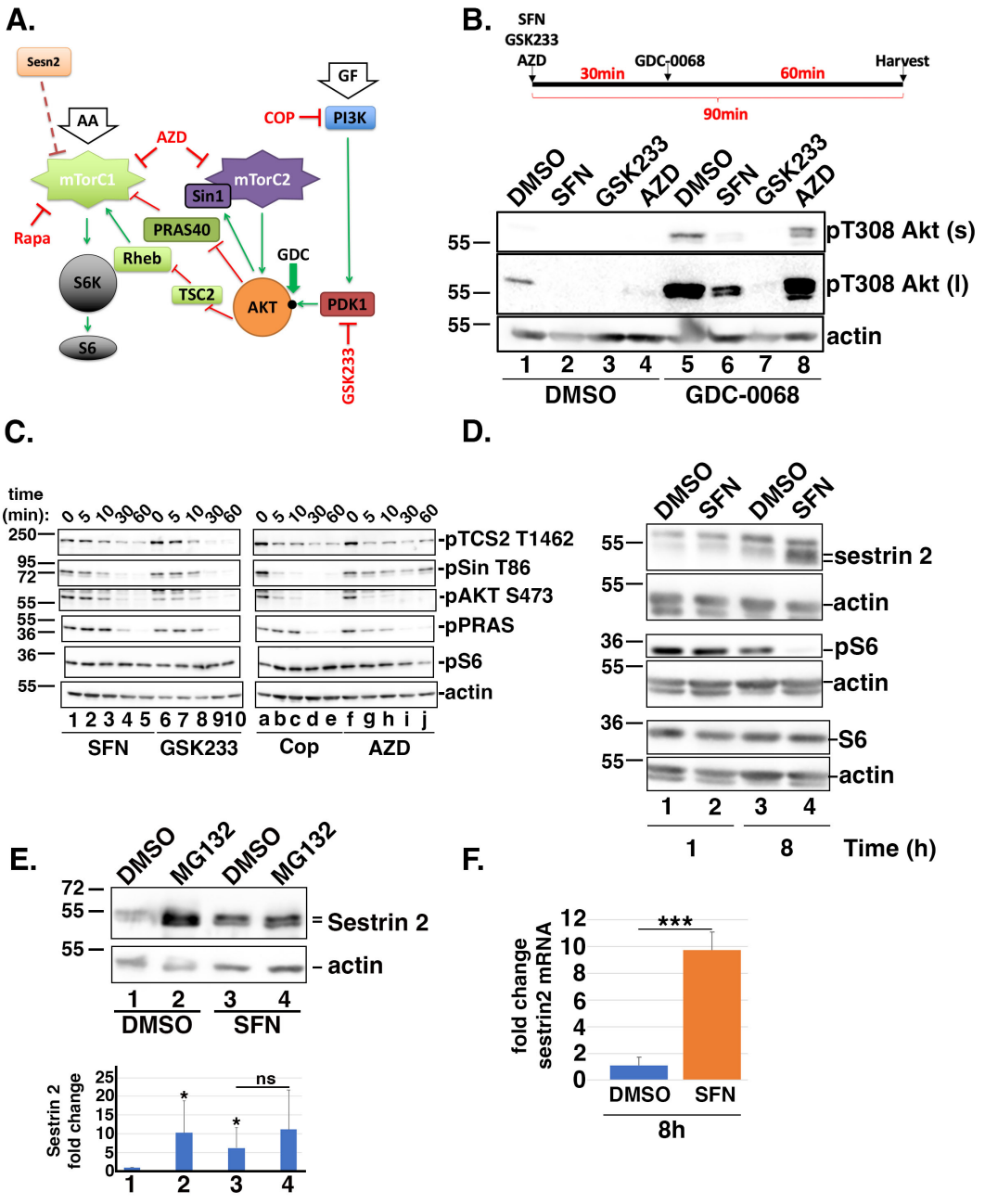

FIGURE 2
SFN disrupts insulin and mTORC1/2 signaling. **(A)** Cartoon highlighting the proteins and phosphorylation events analyzed within the insulin and mTORC1/2 signaling cascades. Green arrows indicate activation and red 'T' symbols indicate inhibition. Pharmacological inhibitors are denoted in red text. Black dot on AKT marks the threonine 308 (T308) phosphoacceptor. AA = amino acids; GF = growth factors; Sesn2 = Sestrin 2; S6K = S6 kinase. **(B)** Schematic of the experimental design. RPE-1 cells were treated for 90 min with DMSO, SFN, 1 μM GSK233 or 250 nM AZD and co-treated with DMSO (lanes 1–4) or with 5 μM GDC-0068 (lanes 5–8) for the last 60 min of the 90 min incubation. Lysates were analyzed by Western blotting with antibodies against phosphorylated Akt on T308 (top and middle blots) and actin (bottom blot). 's' and 'l' denote short and long exposures, respectively. * indicates $p < 0.05$ compared to DMSO/DMSO (lane 1) and 'ns' on graph indicates no significance between lanes 3 and 4. **(C)** RPE-1 cells were treated with SFN, GSK233, Cop, or AZD for the indicated times. Lysates were probed with antibodies specific for the phosphorylated forms of TSC2 on threonine 1,462 (pTSC2 T1462), Sin on threonine 86 (pSin T86), Akt on serine 473 (pAKT S473), PRAS on threonine 246 (pPRAS), and S6 on serines 235/236 (pS6) as well as actin. **(D)** RPE-1 cells were treated with DMSO or SFN for 1 or 8 h and harvested for Western blot analysis with the indicated antibodies. **(E)** RPE-1 cells were treated with DMSO or SFN with or without 5 μM MG132 for 8 h. Sestrin 2 protein expression was analyzed by Western blotting and graph shows quantification of Sestrin 2 protein levels from 5 independent experiments. Numbers below graph correspond to lane numbers from a representative Western blot. **(F)** qPCR of *sestrin 2* mRNA expression levels following 8 h of DMSO or SFN. For all western blots, the migration of molecular weight markers (in kDa) is indicated to the left of each blot. Blots in B-D are representative of 3–5 independent experiments, and all graphed data were compiled from ≥3 independent experiments with DMSO set to a value of 1.0. *** indicates $p < 0.001$.

(39, 40)] and inhibit [e.g., (41)] autophagy based on Western blotting for microtubule-associated protein 1A/1B-light chain 3 (LC3) to measure the lipidated and unlipidated forms (LC3-I and LC3-II, respectively). Increased LC3-II levels are typically interpreted as a proxy of elevated autophagic flux. However, because LC3-II accumulation can occur through either an increase in autophagic flux or conversely, a block in autophagy progression downstream of autophagosome formation, we used RPE-1 cells stably expressing GFP-tagged LC3 (GFP-LC3) (25) in combination with bafilomycin A1 (Baf) and flow cytometry to determine the consequences of SFN on autophagic flux. Baf is a macrolide antibiotic that blocks the autophagy pathway by preventing fusion of autophagosomes to lysosomes and by inhibiting the vacuolar H^+ ATPase to prevent the acidification of lysosomes and protein degradation (42). Eight hours of SFN treatment led to increased GFP-LC3 puncta as well as increased LysoTracker Red™ (LTR)-positive puncta, a marker of lysosomes (Figure 3A). To further analyze autophagic flux, RPE-1 cells stably expressing GFP-LC3 were treated with SFN, the indicated pharmacological treatments, or deprived of different nutrients for 24 h. Parallel wells of cells were co-treated with Baf during the final 6 h of the 24 h incubation. Prior to quantifying GFP-LC3 levels by flow cytometry, cells were permeabilized with saponin to leak out soluble GFP-LC3 not incorporated into autophagic vesicles. As Baf inhibits the degradation of autophagic cargoes, the amount of GFP-LC3 in cells incubated with Baf represents the "total" amount of autophagic traffic that entered the system during the final 6 h of the experiment. GFP-LC3 levels in cells not treated with Baf represent "residual" traffic actively transiting through the autophagy system, and the difference (i.e., total – residual) represents the amount of "cleared" autophagic traffic. Compared to established inducers of autophagy including rapamycin (Rapa), inhibitors of insulin signaling (GSK233, AZD, Cop), and nutrient deprivations, SFN treatment yielded greater amounts of total and residual GFP-LC3 autophagic vesicles (Figure 3B). With the exception of serum deprivation (− serum), SFN induced greater clearance of autophagic vesicles compared to the other treatments (Figure 3B).

The amplification of autophagic flux by SFN was further corroborated by testing whether combining the phytochemical with pharmacological inducers of autophagy (Figure 3C) or with nutrient deprivations that induce autophagy (Figure 3D) would further augment vesicular GFP-LC3 beyond the levels reached by each individual treatment. RPE-1 cells stably expressing GFP-LC3 were incubated for 24 h with inducers of autophagy and compared to the same treatments combined with SFN. Remarkably, co-treatment with SFN and pharmacological inducers of autophagy elevated GFP-LC3 levels with the exception of Cop, which approached significance ($p = 0.092$; Figure 3C). Moreover, depriving cells of serum and/or AA induced autophagy and SFN also amplified these inductions (Figure 3D).

We next tested if the increased autophagic flux induced by SFN was accompanied by increased cellular lysosomal content, as indicated by fluorescence microscopy of LTR-labeled cells (Figure 3A). We quantified lysosomal content by LTR uptake using flow cytometry, comparing SFN to nutrient deprivations and to Rapa (Figure 3E). Cells were treated with SFN, Rapa, or starved of specific nutrients overnight and then stained with LTR. Notably, neither Rapa nor AA starvation increased lysosomal content (Figure 3E gray and green bars, respectively) indicating that lysosomal biogenesis was responsive to the inhibition of insulin signaling but not inhibition of mTORC1 by Rapa or AA deprivation in this assay. SFN robustly increased lysosomal content, consistent with the phytochemical inducing the transcription factor EB (TFEB)-directed CLEAR transcriptional program downstream of mTOR, as recently reported (43). Using qPCR, we confirmed that 24 h of treatment with SFN induced the expression of canonical CLEAR target genes (*ATP6V*, *LAMP1*, *TFEB*, *CTSA*, and *MCOLN1*) by 1.5-to 4.5-fold over vehicle treatment (Figure 3F).

Impacts of SFN on glycolysis, the TCA cycle, and the hexosamine biosynthetic pathway

We next interrogated the time-dependent impacts of SFN on glucose uptake and metabolism based on work showing SFN, through its induction of Nrf2 transcriptional activity, induces genes encoding the rate limiting enzymes of pathways that shunt glucose out of glycolysis (44). We quantified glucose uptake using flow cytometry to measure the intracellular accumulation of a fluorescent glucose analog added to the media. Glucose uptake was reduced by SFN at 1 h, 4 h, and 8 h post-treatment similarly to 2-deoxy-glucose (2-DG), an established inhibitor of glucose uptake (Figure 4A). This reduced glucose uptake correlated with decreased extracellular lactate levels during the initial 8 h of SFN exposure (Figure 4B). However, glucose uptake recovered within 24 h of SFN treatment, with levels comparable to DMSO-treated cells (Figure 4A), and lactate secretion rebounded accordingly (Figure 4B, final 16 h). Complementary metabolomic analysis of glycolytic and tricarboxylic acid (TCA) cycle intermediates showed that 4 h of SFN led to the accumulation of intracellular glucose and the two downstream glycolytic intermediates, glucose-6-phosphate (G6P) and fructose-6-phosphate (F6P) (Figure 4C). Other assayed glycolytic intermediates were unchanged. TCA metabolite analysis revealed increased citrate and aconitate whereas a-ketoglutarate, succinate, fumarate and malate were all decreased (Figure 4D).

Concomitant with these effects on glycolysis and the TCA cycle, SFN reduced phosphorylation of PDH (Figure 4E), the mitochondrial enzyme that converts pyruvate to acetyl-CoA for the TCA cycle. Phosphorylation of PDH (pPDH) inactivates the enzyme and dephosphorylation converts PDH to an active form (45, 46). Immunofluorescence assays with an antibody recognizing Ser293 phosphorylation of PDH (pPDH), a proxy of PDH activity (47, 48), revealed that 4 h of SFN treatment robustly reduced the percentage of cells with mitochondria-associated pPDH (Figure 4E). AA deprivation or serum starvation both increased pPDH whereas glucose starvation reduced pPDH (Figure 4E). Thus, SFN most closely mimicked glucose starvation in this assay.

The accumulation of G6P, the first oxidation product of glycolysis, can elevate the expression of thioredoxin (TXN)-interacting protein (TXNIP), a central regulator of glucose entry into cells (49–53). By modulating glucose transporter (GLUT) endocytosis, increased levels of TXNIP reduce cellular glucose uptake whereas decreased TXNIP abundance promotes glucose uptake into cells [e.g., (49, 52)]. Based on SFN treatment acutely reducing glucose uptake but then restoring it by 24 h (Figure 4A), we tested the hypothesis that this restoration was mediated by reducing TXNIP despite increased G6P levels. After confirming that *TXNIP* mRNA and protein expression are glucose-responsive and dependent in RPE-1 cells (Supplementary Figure S1A), we examined TXNIP levels by Western blotting lysates from RPE-1 cells treated with the phytochemical for different lengths of time. Compared

10.3389/fnut.2024.1485466

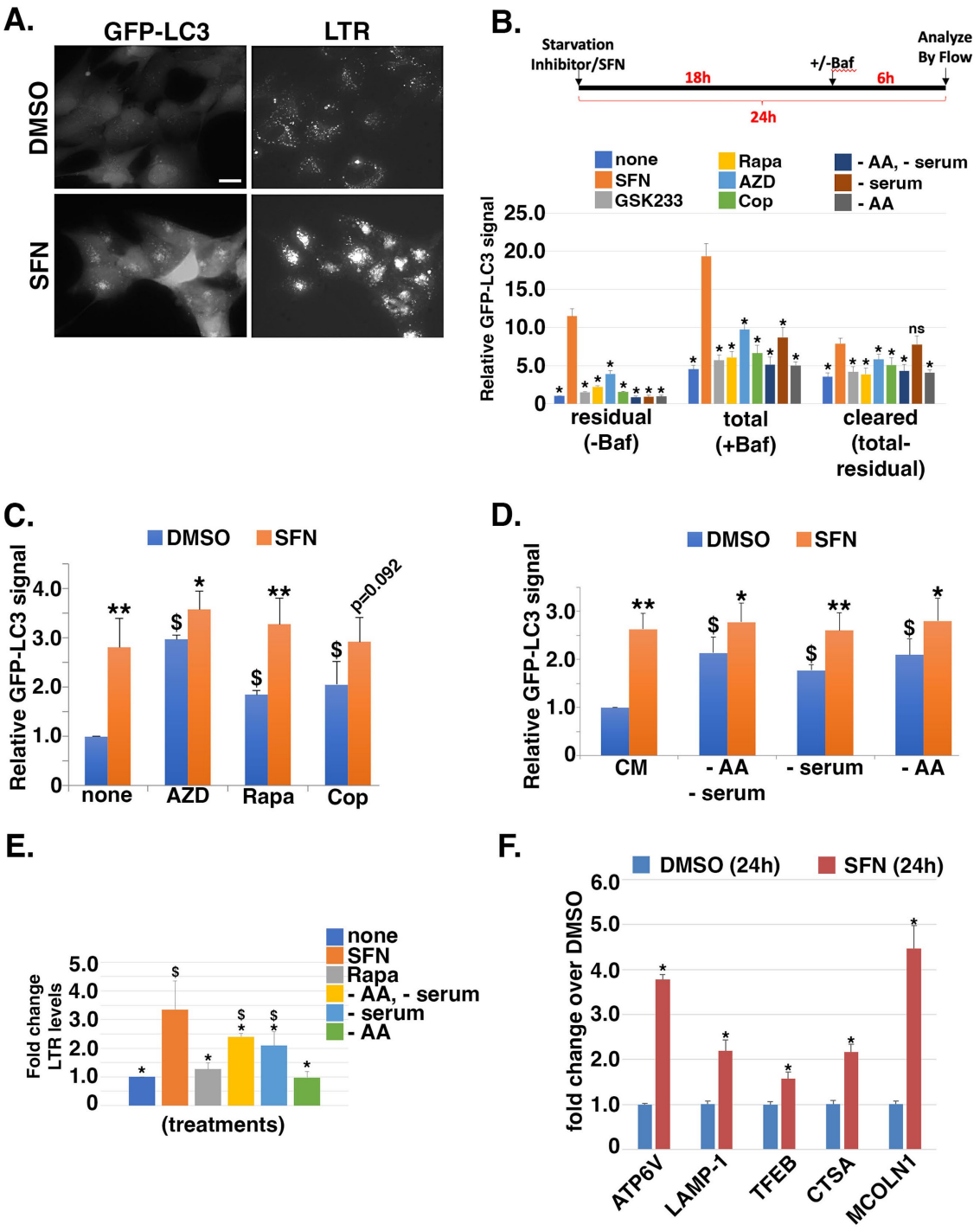

FIGURE 3
SFN is a potent inducer of autophagy and increases lysosomal mass. **(A)** RPE-1 cells stably expressing GFP-LC3 were treated with DMSO or SFN for 8 h and 50 nM LysoTracker Red™ (LTR) was added during the final 30 min. Figure shows representative live-cell photomicrographs. Size bar = 10 microns. **(B)** Schematic of the experimental design. RPE-1 cells stably expressing GFP-LC3 were treated with vehicle (none), SFN, GSK233, Rapa, AZD, Cop or media lacking amino acids and serum (–AA/–serum), lacking just serum (– serum), or lacking just AA (– AA) for 24 h. Vehicle (-Baf) or 160 μM Bafilomycin (+Baf) were added for the final 6 h of the 24 h incubation. Cells were trypsinized, resuspended in 0.05% (w/v) saponin/PBS, washed, and GFP-LC3 fluorescence intensity was analyzed by flow cytometry. Data graphed as GFP-LC3 fluorescence intensity relative to vehicle for residual (–Baf), total (+Baf) and cleared (total-residual). * indicates $p \leq 0.05$ for comparison versus SFN (orange bars). **(C,D)** GFP-LC3-expressing RPE-1 cells were co-treated with the indicated autophagy inducers **(C)** or nutrient deprivations **(D)** plus DMSO (blue bars) or SFN (orange bars) for 24 h. Cells were processed and analyzed by flow cytometry as described for **(B)**. Data graphed as GFP-LC3 fluorescence intensity relative to none + DMSO **(C)** or CM + DMSO **(D)**. **(E)** RPE-1 cells were treated with SFN, 10 nM Rapa, or media lacking the indicated nutrients (as in B) for 16 h, stained with 50 nM LTR for 30 min, trypsinized, and analyzed by flow cytometry. Data graphed as fold change in fluorescence intensity compared to no treatment (none). **(F)** RPE-1 cells were treated with DMSO or SFN for 24 h before RNA isolation and qPCR using primers against the indicated CLEAR network gene products. Results graphed as fold change in mRNA levels compared to DMSO. For **(C,D)**, asterisks indicate significance between each paired set of blue and orange bars, respectively; *$p \leq 0.05$, ** $p \leq 0.01$, and $ indicates significance compared to 'none' + DMSO for **(C)** or CM + DMSO for **(D)**; $p \leq 0.05$.

to vehicle-treated cells, 8 h and 24 h of SFN treatment dramatically reduced TXNIP protein expression (Figure 5A, lanes 3 versus 4 and 5 versus 6). Notably, the elevation of TXNIP at 8 and 24 h in the DMSO samples compared to the 1 h time point is consistent with glucose being taken up by the RPE-1 cells initially after replating into fresh media followed by an increase in TXNIP to restrict further uptake at the later time points (Figure 5A, lanes 3 and 5). Co-treatment with the proteasome inhibitor, MG132, stabilized TXNIP indicating that proteasome-mediated degradation of this protein was not adversely impacted by SFN (Figure 5B, lanes 3 versus 4) (49, 51). In contrast, co-administration of SFN with the global transcription inhibitor, actinomycin D (Act D), normalized TXNIP expression between DMSO and SFN in the presence and absence of MG132 (Figure 5B, lanes 5 versus 7 and lanes 6 versus 8), indicating that the SFN-mediated decrease in TXNIP occurs at the transcriptional level. qPCR analysis confirmed that 4 h of SFN robustly decreased *TXNIP* mRNA expression as well as the mRNA levels of the TXNIP paralogue, *ARRDC4* (Figure 5C).

After ruling out that SFN was not accelerating the degradation of *TXNIP* mRNA (Supplementary Figure S1B), we examined the glucose-dependent transcription complex MondoA/Mlx. This heterodimeric transcription factor mediates *TXNIP* and *ARRDC4* mRNA expression by binding a carbohydrate response element within their respective promoters (52). 1, 8, or 24 h of SFN treatment did not statistically significantly decrease MondoA or Mlx protein levels (Figure 5A blots and graph). Endogenous protein co-immunoprecipitations showed that SFN also does not disrupt complex formation between MondoA and Mlx (Supplementary Figure S1C). Chromatin immunoprecipitation (CHIP) assays however revealed that SFN reduced MondoA residency on the *TXNIP* promoter by ~30% (Figure 5D).

As Nrf2 can bind to the *TXNIP* promoter (54), we next tested the hypothesis that SFN-mediated suppression of *TXNIP* mRNA and protein levels is Nrf2 dependent. After confirming the efficiency of *Nrf2* mRNA knockdown by siRNA using qPCR (Supplementary Figure S1D), we found that *TXNIP* mRNA and protein suppression by SFN were comparable between control (siCON) and Nrf2 (siNrf2) knockdown cells (Figures 5E, F, respectively). Additionally, stabilization of Nrf2 by other activators had only a very modest or no effect on *TXNIP* mRNA

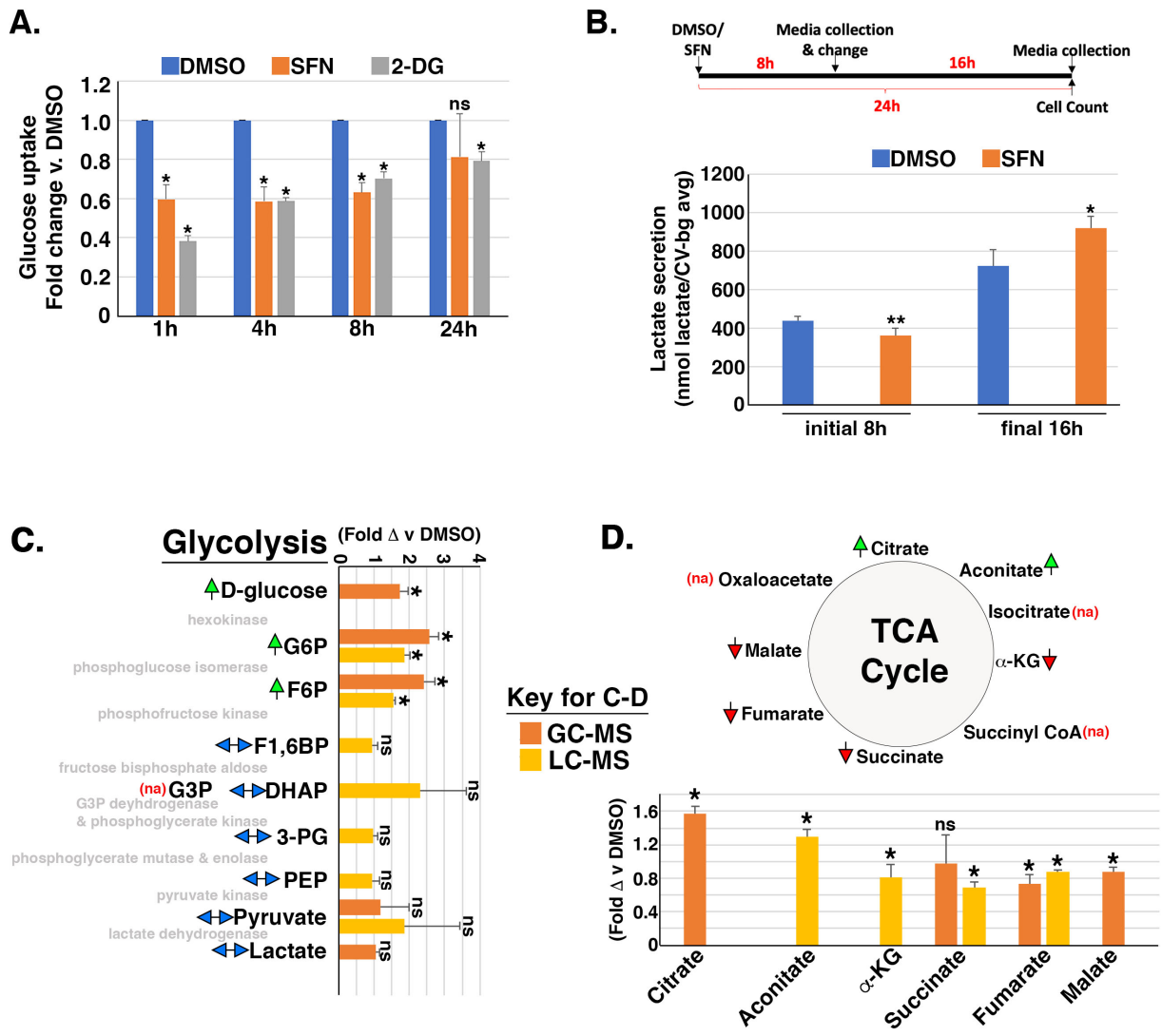

FIGURE 4 (Continued)

10.3389/fnut.2024.1485466

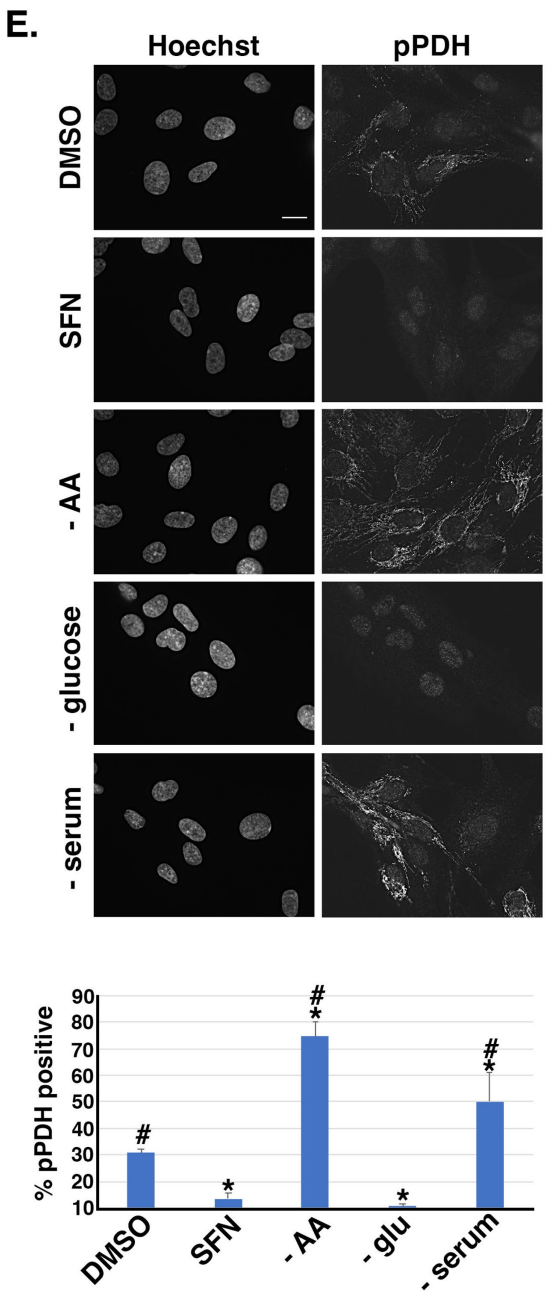

FIGURE 4
SFN impacts flux through glycolysis and the TCA cycle. **(A)** RPE-1 cells were treated with DMSO, SFN or 5 mM 2-DG for the indicated times followed by glucose uptake measurements using the Dojindo Green Probe per manufacturer's instructions. Glucose uptake was graphed as fold change versus DMSO treatment. **(B)** Schematic of the experimental design. RPE-1 cells were treated with DMSO or SFN for 8 h after which media was collected (initial 8 h measurement) and replaced with fresh media containing DMSO or SFN for an additional 16 h (for a total of 24 h treatment). Media was again collected for the final 16 h measurement. Media from the initial 8 h incubation and from the final 16 h incubation were separately analyzed with the L-Lactate Assay Kit I (Eton Biosciences, Inc.) and normalized to cell number with data graphed as lactate secretion per normalized cell number. **(C,D)** RPE-1 cells were treated with DMSO or SFN for 4 h and then analyzed by GC–MS (orange bars) and/or LC–MS (yellow bars) for glycolytic intermediates **(C)** or TCA metabolites **(D)**. Green arrows indicate elevation of the metabolite by SFN, red arrows indicate suppression of the metabolite by SFN, and two-headed blue arrows indicate no change in the metabolite. 'na' denotes that the metabolite was not assayed. The enzymes that mediate each step of glycolysis are shown in light gray text for reference **(C)**. Abbreviations: Glucose-6-phosphate (G6P), fructose-6-phosphate (F6P), fructose-1,6-bisphosphate (F1,6P), Glyceraldehyde-3-phosphate (G3P), dihydroacetone-phosphate (DHAP), 3-phosphoglycerate (3PG), Phosphoenolpyruvate (PEP), α-ketoglutarate (α-KG). **(E)** RPE-1 cells were treated as indicated for 4 h and labeled with the DNA counterstain Hoechst and an antibody to phosphorylated pyruvate dehydrogenase (pPDH). Size bar represents 10 microns. Graph of the fraction of pPDH-positive cells counted as a function of treatment with DMSO, SFN, or the indicated nutrient deprivations. All graphs compiled from ≥3 independent experiments. For **(A,C,D)**, asterisks indicate statistical significance ($p < 0.05$) versus DMSO for each time point; 'ns' denotes not significant. For B, comparisons are between DMSO and SFN for each time point with * indicating $p \leq 0.01$ and ** indicating $p \leq 0.001$. For **E**, asterisks indicate statistical significance ($p < 0.05$) compared to DMSO, # indicates statistical significance ($p < 0.05$) compared to SFN, and 'ns' denotes not significant.

(Continued)

FIGURE 4 (Continued)

levels despite robustly inducing the Nrf2 target gene, heme-oxygenase 1 (*HO-1*) (Figure 5G). These data show that the suppression of TXNIP mRNA and protein expression by SFN is independent of Nrf2 induction.

Ayer and colleagues demonstrated that 2-DG induces the Mondo/Mlx transcriptional activation of *TXNIP* (52). This glucose derivative is phosphorylated by hexokinase to produce 2-DG-6-phosphate, a product that cannot be further processed for glucose oxidation and is a relatively poor substrate for glucose-6-phosphate dehydrogenase (G6PDH) (55). We therefore tested the hypothesis that SFN could suppress 2-DG-mediated TXNIP induction. Four hours of 2-DG followed by 4 h of DMSO elevated *TXNIP* mRNA expression ~8-fold but 4 h of SFN treatment suppressed this *TXNIP* induction (Figure 5H). Likewise, *TXNIP* transcription is also increased by treatment with Trichostatin A (TSA) (Figure 5I), a Class I/II histone deacetylase inhibitor (56). Pretreatment for 4 h with SFN prevented the TSA-induced transcriptional increase of *TXNIP* (Figure 5I). These data demonstrate that SFN suppresses TXNIP mRNA induction and does so independently of Nrf2 activation.

The hexosamine biosynthetic pathway (HBP) diverts F6P from glycolysis into an anabolic pathway for *de novo* generation of uridine diphosphate-N-acetyl glucosamine (UDP-GlcNAc), the substrate transferred to recipient proteins for N-and O-linked glycosylation reactions (reviewed in (57)). Notably, HBP activation can increase TXNIP mRNA expression (58). Because SFN treatment increased F6P levels (Figure 4C), we tested the hypothesis that the phytochemical inhibits glutamine F6P amidotransferase (GFAT), the first and rate-limiting enzyme of the HBP that converts F6P to glucosamine-6-phosphate. Consistent with this hypothesis, the suppression of *TXNIP* mRNA expression by SFN was reversed by supplying cells with exogenous glucosamine and this rescue was dose-dependent (Figure 6A). Glucosamine is phosphorylated by hexokinase to produce glucosamine-6-phosphate, the product produced by GFAT from F6P and glutamine. Thus, providing glucosamine to cells bypasses GFAT inhibition and increases *TXNIP* mRNA expression. This interpretation was independently confirmed using two GFAT pharmacological inhibitors, 6-diazo-5-oxo-L-norleucine (Don) and azaserine (Aza). Inhibiting GFAT with Don or Aza suppressed *TXNIP* mRNA expression ~ 80% (Figure 6B), and exogenous glucosamine likewise overcame this GFAT block leading to elevated *TXNIP* (Figure 6C). Consistent with the HBP

10.3389/fnut.2024.1485466

being integrated with the unfolded protein response (UPR) and ER stress (59), 4 h of SFN upregulated the mRNA expression of the UPR-and ER stress responsive transcription factors XBP1 and ATF4 (Figure 6D). In contrast, inhibition of GFAT with either Don or Aza failed to increase *XBP1* mRNA expression and only modestly increased *ATF4* mRNA expression. These data demonstrate that the suppression of TXNIP mRNA expression by SFN likely results from inhibiting GFAT.

Acute effects of SFN on the transcriptional landscape

We further interrogated the transcriptional starvation responses elicited using RNA-seq analysis of RPE-1 cells treated with SFN for 4 h (raw data file accessible via GEO number GSE275316). Ingenuity Pathway Analysis (IPA) showed that the top canonical pathways impacted were general transcription machinery, iron uptake and transport, signaling by insulin receptor, unfolded protein response, and chaperone-mediated autophagy signaling (Figure 7A). Gene ontology (GO) enrichment analysis of canonical starvation pathways showed that SFN reduced mRNA expression of many components of general transcription, but selectively activated a number of transcriptionally-modulated stress and starvation-related response pathways including the UPR, ER stress, autophagy, and amino acid regulation of mTORC1 (Figure 7B). Highly induced genes included chaperones (i.e., heat shock proteins A1A, A1B, and A6), numerous ATG genes of the autophagy pathway as well as *XBP1* (see Supplementary Table S3 – list of differentially expressed

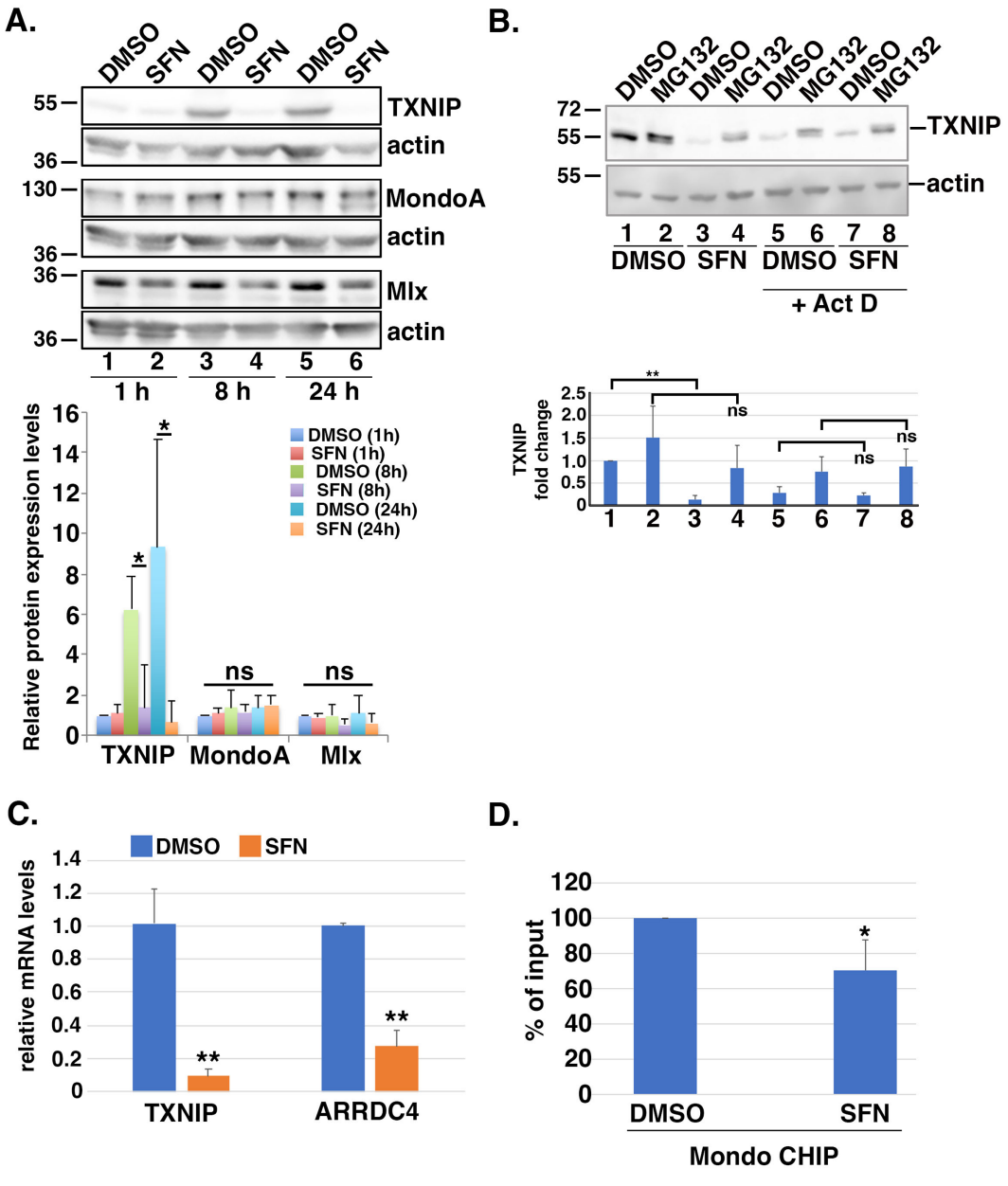

FIGURE 5 (Continued)

10.3389/fnut.2024.1485466

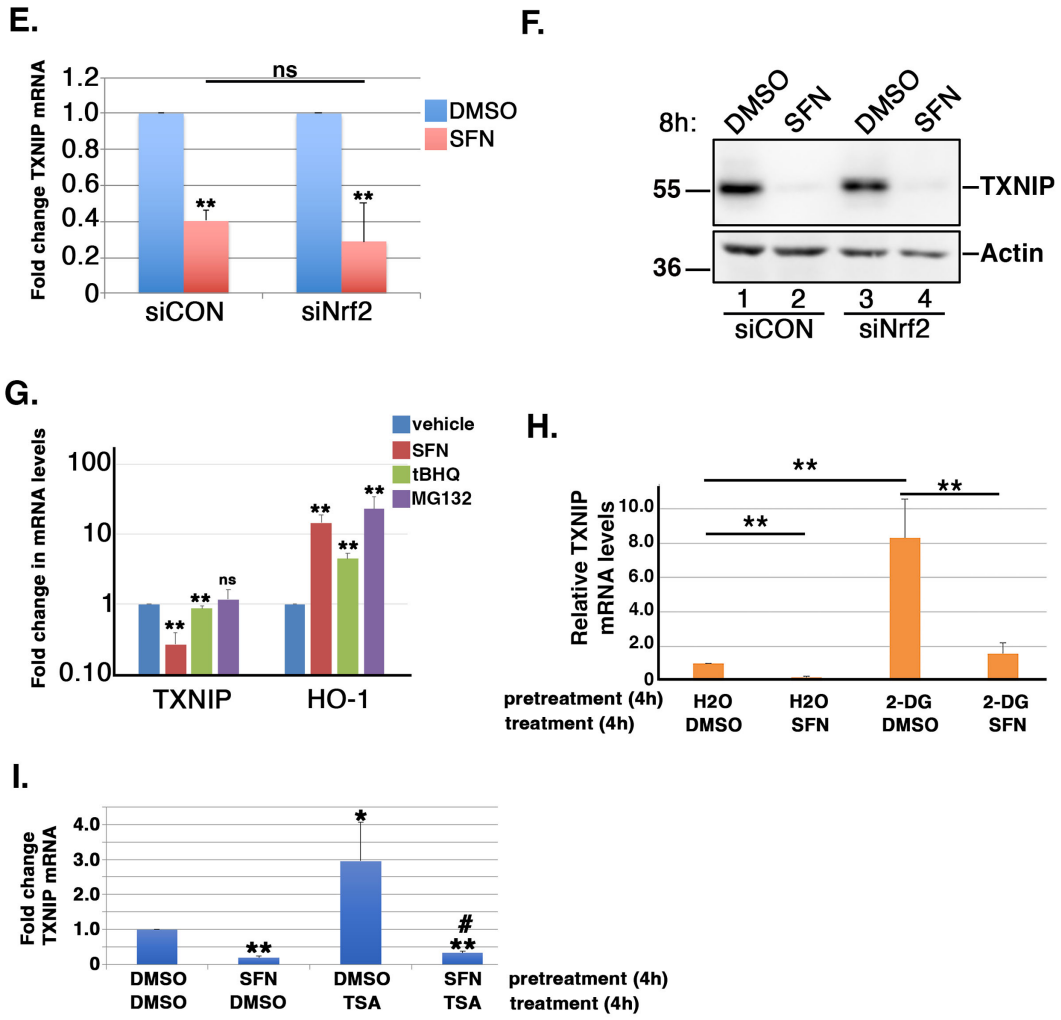

FIGURE 5
SFN suppresses TXNIP expression. **(A)** RPE-1 cells were treated with DMSO or SFN for the indicated times and lysates were run in triplicate for analysis by Western blotting with antibodies against TXNIP, MondoA, Mlx, and actin. Graph below blots shows quantified levels of TXNIP, MondoA, and Mlx (relative to 1 h of DMSO treatment) from >3 independent experiments. **(B)** RPE-1 cells were treated with DMSO or SFN with or without 5 μM MG132 for 8 h. Cells in lanes 5–8 were also treated with 1 μM Act D. TXNIP protein expression was analyzed by Western blotting and graph shows quantification of TXNIP protein levels. Numbers below graph correspond to lane numbers from Western blot. **(C)** RPE-1 cells treated with DMSO or SFN for 4 h were analyzed for *TXNIP* and *ARRDC4* mRNA levels by qPCR. Graph of qPCR data shows change relative to DMSO treatment. **(D)** Chromatin from RPE-1 cells treated with DMSO or SFN for 4 h was analyzed by CHIP with primers specific to the promoter of TXNIP and graphed as fraction of DMSO treatment. **(E,F)** RPE-1 cells were treated for 2 days with control siRNA (siCON) or siRNA targeting Nrf2 (siNrf2) and then exposed to DMSO or SFN for 8 h. Cells were then harvested to measure *TXNIP* mRNA levels by qPCR **(E)** and TXNIP protein expression by Western blotting **(F)**. The migration of molecular weight markers (in kDa) is indicated to the left of the blots. **(G)** RPE-1 cells treated with DMSO, SFN, 5 μM tBHQ or 5 μM MG132 for 8 h were harvested to measure mRNA levels of *TXNIP* and *HO-1* relative to vehicle treatment. **(H)** RPE-1 cells were pre-treated for 4 h with either vehicle (H_2O) or 5 mM 2-DG followed by an additional 4 h with either DMSO or SFN and then were harvested to measure *TXNIP* mRNA levels by qPCR. Graph of *TXNIP* mRNA expression levels relative to H_2O + DMSO. **(I)** RPE-1 cells were pre-treated for 4 h with either DMSO or SFN followed by an additional 4 h with either DMSO or 100 nM TSA prior to being harvested for qPCR to measure *TXNIP* mRNA levels. Asterisks indicate statistical significance compared to DMSO/DMSO and # indicates statistical significance ($p < 0.05$) compared to DMSO/TSA. All graphed data compiled from ≥3 independent experiments. * indicates $p < 0.05$, ** indicates $p < 0.01$ and 'ns' denotes not significant.

genes (DEGs) ranked by *p*-value). In addition to playing a central role for the UPR, XBP1 is a nexus for directing responses to starvation (60).

Four hours of SFN treatment decreased mitochondrial biogenesis pathway as identified by IPA (Figure 7B), although there was robust induction of GA binding protein transcription factor (*GABPB1*) (Figure 7C), an inducer of gene targets that promote mitochondrial biogenesis (61). The CLEAR signaling pathway was also suppressed at 4 h, based on decreased mRNA expression of the CLEAR inducing transcription factors, TFEB and MITF. Yet, 24 h of SFN increased *TFEB* mRNA expression along with a set of CLEAR genes (Figure 3E). Notably, Cesana et al. observed that it took 6 h for *TFEB* to be transcriptionally upregulated in starved HeLa cells and that the early growth response 1 (EGR1) protein promotes TFEB transcriptional activity (62). *EGR1* mRNA was robustly increased (> 16-fold) by 4 h of SFN (Figure 7C). Additional changes consistent with a nutrient deprivation response were upregulation of several inhibitors of mTOR including DNA damage-inducible transcript 4 protein

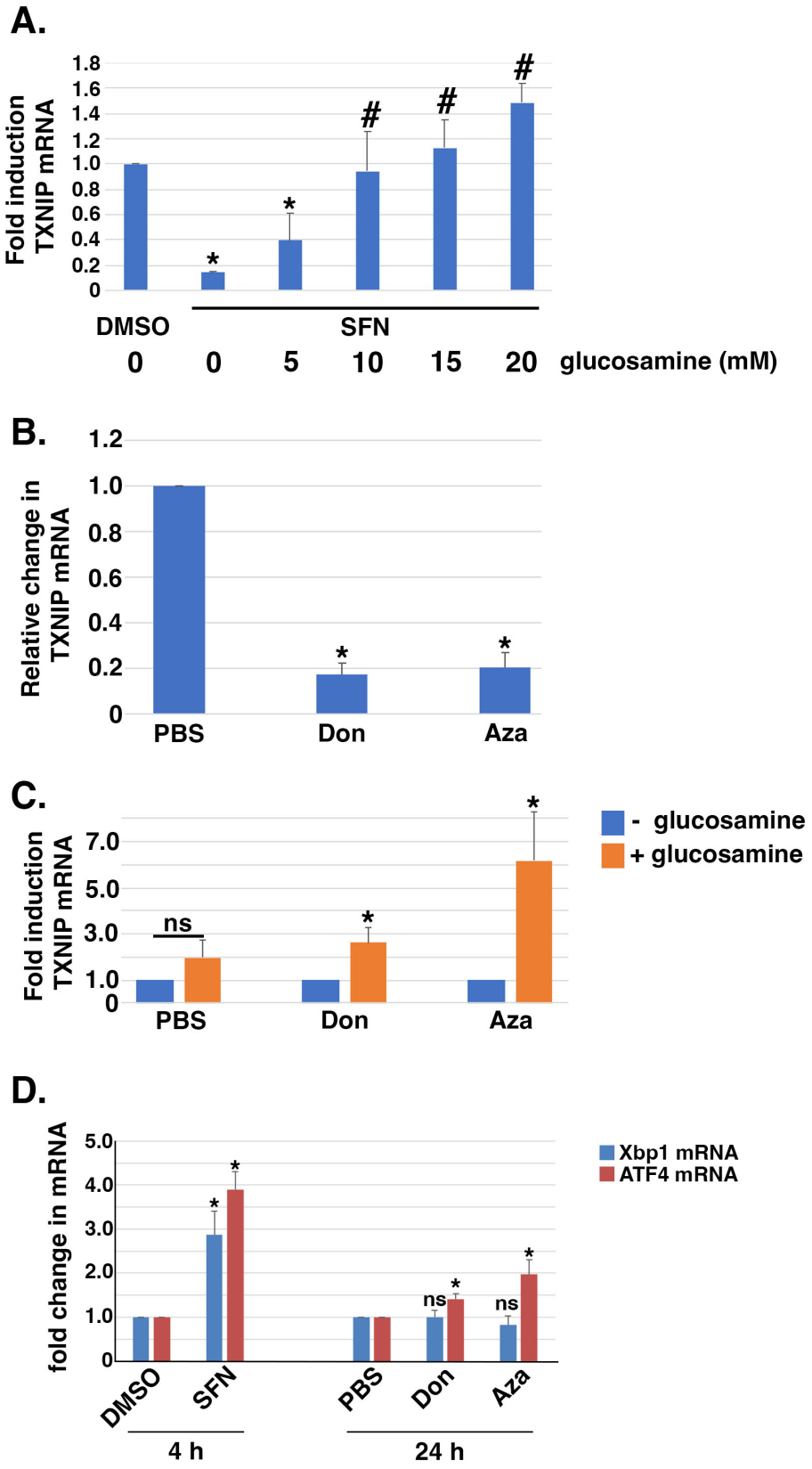

FIGURE 6
Exogneous glucosamine rescues SFN-mediated suppression of *TXNIP* mRNA expression. **(A)** RPE-1 cells treated with DMSO or SFN +/– increasing amounts of glucosamine for 4 h were harvested to measure *TXNIP* mRNA levels by qPCR. **(B)** RPE-1 cells were incubated with PBS or 100 μM 6-diazo-5-oxo-L-norleucine (Don) or 2.5 μM azaserine (Aza) for 24 h and then harvested for qPCR to measure *TXNIP* mRNA expression levels. **(C)** RPE-1 cells were incubated with either vehicle (PBS), Don, or Aza in the absence (blue bars) or presence (orange bars) of 15 mM glucosamine for 24 h prior to

(Continued)

FIGURE 6 (Continued)

being harvested for qPCR to quantify *TXNIP* mRNA levels. **(D)** RPE-1 cells were treated for 4 h with DMSO or SFN or with PBS, Don, or Aza for 24 h and then harvested to measure mRNA expression of *Xbp1* (blue bars) or *ATF4* (red bars) by qPCR. All graphs compiled from 3 independent experiments with asterisks indicating statistical significance ($p < 0.05$) and 'ns' denoting not significant. For **(A)**, asterisks denote statistical significance compared to DMSO and # denotes significance compared to SFN without glucosamine supplementation. For **(D)**, statistical significance was determined by comparing SFN to DMSO and by comparing Don and Aza to PBS.

(*DDIT4* (aka REDD1); >16-fold increase) and *sestrin 2* (> 8-fold increase) (Figure 7C), confirming the reduced mTOR signaling and elevated sestrin 2 detected by Western blotting and qPCR (Figure 2). Both of these mTORC1 inhibitors are downstream targets of the ATF4 transcription factor (63), which was likewise elevated (Figures 6D, 7C). These RNA-seq data show that acute SFN treatment induces numerous transcriptional responses elicited by fasting.

Discussion

Across species, caloric restriction (CR) without malnourishment extends lifespan and healthspan by activating pathways that collectively improve organismal resilience at the cellular level. These include autophagy, DNA repair and maintenance, mitochondrial and lysosomal biogenesis, and stress neutralization (e.g., glutathione synthesis, xenobiotic detoxification) (64). Numerous approaches to achieving CR have been tested, albeit with mixed results. These approaches work well in laboratory environments in which experimentalists control animal adherence to dietary restrictions and eating patterns/timing, but compliance among humans is more challenging and represents a major confounding factor in clinical trials [e.g., (65, 66)].

Alternative strategies to CR include fasting mimetics that elicit therapeutic benefits without necessarily reducing caloric or macronutrient consumption. Natural compounds and derivatives characterized as CR mimetics include rapamycin (mTOR inhibitor), metformin (AMPK activator), 2-DG (glycolysis inhibitor), resveratrol and nicotinamide (activators of sirtuins), spermidine (regulator of proteome acetylation), curcumin (anti-oxidant), and fungal polysaccharides, among others [reviewed in (64)]. Our data show that SFN treatment acutely elicits hallmarks of a CR mimetic (see Figure 8 model), mirroring aspects of AA, glucose, and growth factors deprivation. Because SFN modifies susceptible cysteine residues on multiple proteins, the effects of the phytochemical represent the sum of the pathways directly modified plus any accompanying downstream cellular adaptations. As such, SFN activates *select* responses rather than the full repertoire of cellular starvation responses. We observed that SFN: (1) preserves mitochondrial membrane potential, limits mitochondrial matrix oxidation, promotes homeostatic mitophagy, and adaptively induces mitochondrial biogenesis to increase mitochondrial mass; (2) acutely suppresses insulin and mTORC2 signaling and adaptively decreases mTORC1 signaling, (3) amplifies autophagic flux and cargo clearance, (4) activates programs to increase lysosome abundance, (5) adaptively increases glucose uptake and a proxy of PDH activity to increase acetyl-CoA entering the TCA cycle, and (6) activates signature starvation-responsive transcriptional programs. Notably absent was a sustained activation of AMPK (data not shown), a mechanism invoked during an energy crisis arising from a deficiency of ATP (67, 68).

We identified novel mechanisms by which SFN functions as a CR mimetic in the context of TXNIP-regulated glucose uptake. TXNIP increases GLUT endocytosis from the plasma membrane to restrict extracellular glucose uptake (49, 51). In the absence of insulin signaling, such as during starvation or exercise, TXNIP protein levels increase (69, 70). Yet, if these scenarios lead to ATP shortages, AMPK phosphorylates TXNIP to mark it for degradation allowing increased cellular glucose uptake to restore bioenergetic homeostasis (49). At the transcriptional level, *TXNIP* mRNA expression is induced when levels of the glycolytic intermediates G6P (52) or glyceraldehyde-3-phosphate (71) or adenine nucleotides (72) accumulate above a threshold. Glucosamine-6-phosphate produced by the HBP can also induce *TXNIP* gene expression (58).

In RPE-1 cells, SFN initially decreased glucose uptake (Figure 4A), likely due to the rapid but acute disruption of Akt signaling (Akt pThr308, pSer473) (Figures 2B,C), followed by a compensatory decrease in TXNIP to restore glucose uptake (Figures 5A,C, respectively). This reduction of *TXNIP* at the mRNA level was partially attributable to blocking the MondoA/Mlx heterodimer from occupying the *TXNIP* promoter (Figure 5D), although this was not a consequence of SFN preventing MondoA and Mlx heterodimer formation (Supplementary Figure S1C) or altering levels of MondoA or Mlx protein amounts (Figure 5A). Notably, in a mouse photoreceptor-derived cell culture line challenged with advanced glycation end products that elevated *TXNIP* mRNA, SFN suppressed this induction through the AMPK pathway (73). We did not observe AMPK activation but did find that supplementing cells with exogenous glucosamine reversed *TXNIP* mRNA suppression by SFN (Figure 6A), consistent with the isothiocyanate inhibiting GFAT of the HBP. Additional evidence supporting this interpretation is that pharmacological inhibition of GFAT reduced *TXNIP* mRNA similarly to SFN (Figure 6B) and this reduction was likewise reversed by glucosamine supplementation (Figure 6C). Further evidence consistent with GFAT inhibition by the phytochemical stems from SFN elevating levels of F6P (Figure 4C), the substrate for GFAT.

SFN also inhibited insulin-PI3K-PDK1-Akt signaling in RPE-1 cells within minutes (Figure 2), but this inhibition resolved and Akt signaling recovered by 8 h and was sustained at 24 h, as indicated by phosphorylation of PRAS (pPRAS), a substrate and functional readout of active Akt (Supplementary Figure S1E). This restored Akt activity was coincident with a dramatic suppression of TXNIP protein expression at 8 and 24 h (Figure 5A and (51)) leading to increased glucose uptake as an adaptive response at 24 h (Figure 4A). Thus, SFN initially reduces glucose uptake but this transient effect resolves, and the cellular uptake of glucose recovers over time coincident with the suppressed expression of *de novo* TXNIP. Notably, circulating free fatty acids such as those resulting from consuming a Western diet or having diabetes, induce mitochondrial ROS in muscle, which leads to over-expression of TXNIP, reduced glucose uptake, and hyperglycemia (74). These findings along with our work indicate that the

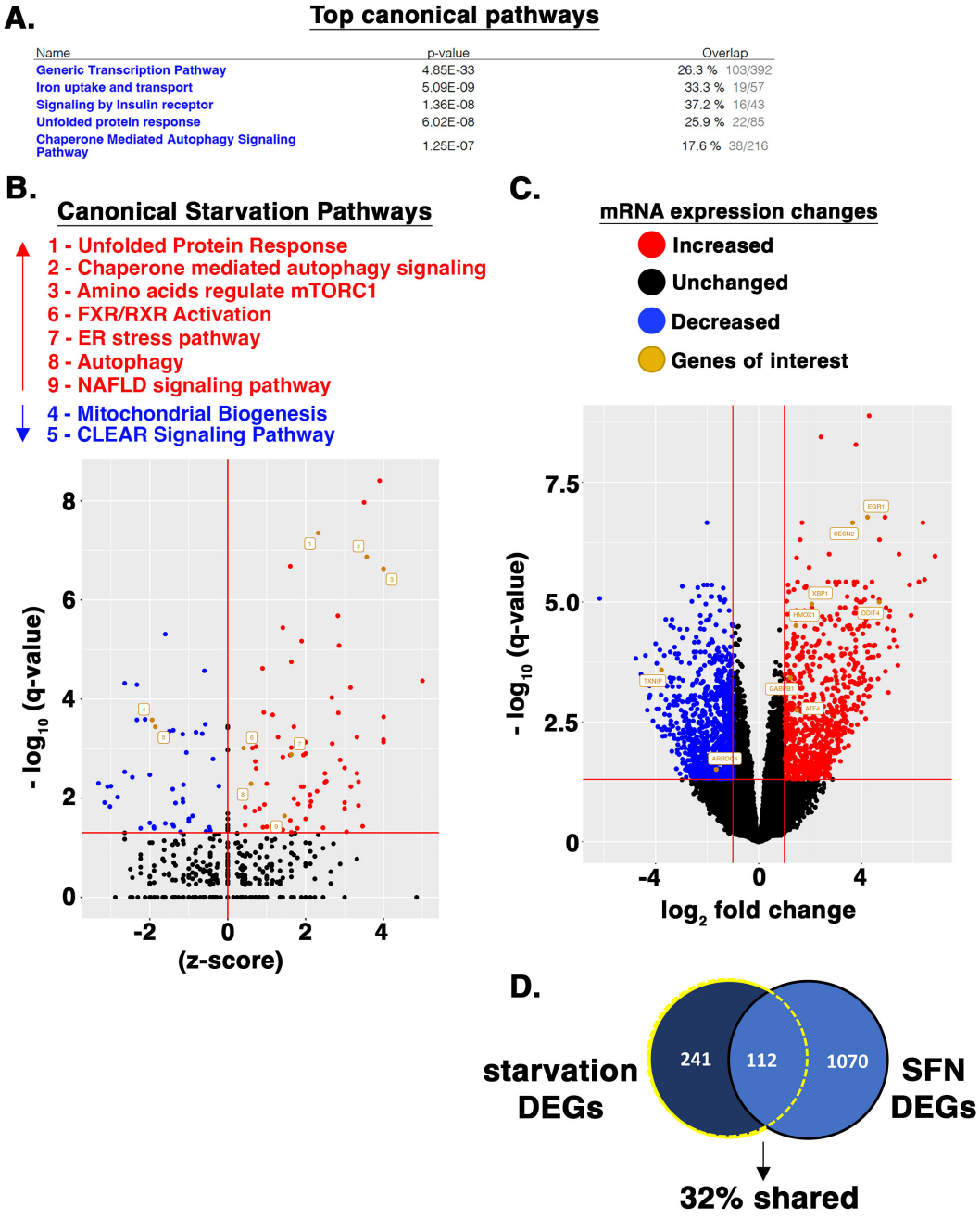

FIGURE 7
SFN induces starvation-responsive transcriptional programs. **(A)** RPE-1 cells were treated with DMSO or SFN for 4 h after which RNA was isolated and subjected to RNA-seq analysis. Listed are the top canonical pathways impacted according to IPA along with *p*-values and the fraction of pathway genes changed for each pathway. **(B)** Volcano plot showing elevated (red dots and text) and suppressed (blue dots and text) canonical pathways associated with starvation as identified by IPA. **(C)** Volcano plot highlighting expression changes in specific genes that were analyzed in various other assays or discussed throughout the manuscript. Red dots represent increased mRNA expression, blue dots represent decreased mRNA expression, and black dots represent unchanged. Orange dots and name tags denote genes of interest. **(D)** SFN and HeLa cell starvation RNA-seq datasets were filtered to DEGs as defined by having an adjusted p-value (i.e., q-value) < 0.05 and a log2FC < −1 or log2FC > 1. 353 DEGs (242 + 112) from the starved HeLa cells and 1,182 DEGs (1,070 + 112) from the SFN treated RPE-1 cells met these criteria. The DEG list from both analyses were compared via Venn diagram and the number and percentage of DEGs shared between the two data sets is displayed.

anti-hyperglycemic efficacy of SFN (75) likely stems from a combination of suppressing ROS (via Nrf2 activation) and suppressing TXNIP (Nrf2-independent). Consistent with our RPE-1 cell culture data, human studies have shown anti-hyperglycemic effects and reduced HbA1c elicited by SFN in obese patients with poorly-managed type 2 diabetes [e.g., (19)]. Increased turnover of intracellular components by autophagy is a hallmark of CR and CR mimetics [e.g., (76)] and SFN promoted autophagic flux (Figures 3B–D) accompanied by the induction of CLEAR genes (Figure 3F), increased lysosomal mass (Figures 3A,E), and increased mitophagy (Figure 1D). These data support a model in which SFN inhibits mTORC1 (Figure 2D), leading to activation of the EGR1 and TFEB transcription factors to

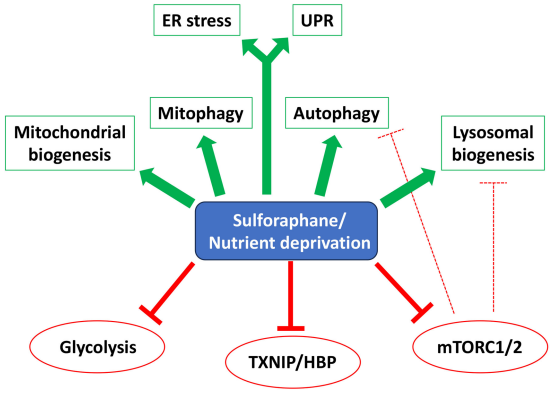

FIGURE 8
SFN is a starvation/CR mimetic. Model showing overlapping pathways affected by SFN and starvation/Caloric Restriction (CR). Green arrows indicate activation and red 'T' symbols (solid and hashed) indicate inhibition. Abbreviations: Endoplasmic Reticulum (ER) Stress, Unfolded Protein Response (UPR), Hexosamine Biosynthetic Pathway (HBP).

induce autophagy and the CLEAR transcriptional program for lysosome biogenesis (Figure 3), extending previous studies of SFN-promoted autophagic flux (40) and induction of the CLEAR network in HeLa, Hep2G, and 1,321 N1 human astrocytoma cells (43).

Akin to the challenges currently facing the therapeutic applications of caloric restriction and fasting (13), identifying the dose, dosing frequency, and route of administration for SFN in each particular disease setting and patient population constitutes a primary challenge in demonstrating consistent and reliable efficacy (26). Resolving these dosing questions may be facilitated by our finding that SFN augmented autophagy beyond the robust induction achieved by rapamycin and nutrient deprivation (Figure 3C). The maximal responses elicited by SFN support the consideration of employing pulsatile dosing regimens to remove and replace damaged macromolecules and organelles while retaining cellular health and survival through periods of SFN holidays (77). In alignment with this notion, we previously showed that administering SFN three times a week (Monday, Wednesday, and Friday) for 3 months recovered cone function in mice undergoing RPE oxidative stress (78).

A comparison of RNA-seq from HeLa cells starved of all nutrients for 4 h by Galves et al. (79) versus our RNA-seq data from 4 h of SFN treatment revealed that 32% of the DEGs changed 2-fold or greater by starvation were likewise changed by SFN (Figure 7D). Notably, SFN and complete starvation both induced responses related to ER stress, the UPR, autophagy, as well as inhibition of mTOR signaling. Galves et al. highlighted a list of 17 activated genes they termed known 'starvation-genes' and SFN induced 10 of these (*ATF3*, *ZFP36*, *EIF2AK3*, *ZFYVE1*, *ASNS*, *DDIT3*, *GABARAPL1*, *NFE2L2*, *XBP1*, and *ATF4*), decreased none, and did not statistically significantly alter the expression of 7 (*RRAGC*, *MTMR3*, *FNIP1*, ATG14, SIRT1, ULK1, and *KLF10*) (Supplementary Table S3). Because this comparison uses two distinct human epithelial cell lines, the robust overlap between starvation-associated DEGs in the two data sets highlights the conservation of responses to starvation between cell types within a species, consistent with the evolutionary conservation of nutrient deprivation responses across species [e.g., (80)].

The cultured RPE-1 cells used for these studies enabled mechanistic pathway analyses to be done, which were further facilitated by leveraging RPE-1 reporter cell lines for mitochondrial redox status, mitophagy, and autophagy (20, 25). The cultured cells additionally allowed for the application of pharmacological inhibitors to rapidly inhibit insulin signaling and HBP, circumventing *in vivo* challenges including metabolism by the liver (i.e., first pass effect) and determining the most efficient routes of administration to reach target cells or tissues. Caveats of using cultured cells in these studies include not addressing tissue context, age, sex, health, or morbidities. An additional consideration is that the effects of SFN *in vivo* could vary depending on the specific cell type being studied (e.g., adipocytes versus RPE) and the local metabolic milieu. Consistent with our autophagy and mitophagy findings, SFN increased the autophagy of lipids (aka, lipophagy) in 3 T3-L1 adipocytes by inhibiting mTOR (81) and induced adipocyte browning and glucose uptake (82). The phytochemical also inhibited adipogenesis and reduced obesity through AMPK pathway activation *in vivo* in mice fed a high-fat, obesogenic diet (11). Importantly, the reported physiological outcomes of SFN *in vivo* are largely consistent with the cellular impacts of the phytochemical that we report here.

Although we did not definitively identifying any new substrates directly modified by the phytochemical, the findings of this study advance our understanding of SFN by implicating potential new candidate targets including PDK1 (Figure 2C), phosphofructose kinase (Figure 4C), PDH kinase (Figure 4E), MondoA/Mlx (Figure 5D), and GFAT (Figure 6A). Moreover, the recognition of SFN as a fasting mimetic provides a plausible mechanistic explanation for many of the physiological effects of the compound (e.g., reduced hyperglycemia and resistance to mitochondrial dysfunction) and could be useful for informing dosing strategies to circumvent starvation-associated toxicities.

Data availability statement

The datasets presented in this study can be found in online repositories. The names of the repository/repositories and accession number(s) can be found in the article/Supplementary material.

Ethics statement

Ethical approval was not required for the studies on humans in accordance with the local legislation and institutional requirements because only commercially available established cell lines were used.

Author contributions

KP: Conceptualization, Formal analysis, Methodology, Writing – original draft, Writing – review & editing. CG: Data curation, Formal analysis, Methodology, Writing – review & editing. NP: Data curation, Formal analysis, Writing – review & editing. AP: Data curation, Formal analysis, Methodology, Writing – review & editing. SP: Conceptualization, Data curation, Funding acquisition, Supervision, Writing – original draft, Writing – review & editing.

Funding

The author(s) declare that financial support was received for the research, authorship, and/or publication of this article. This work was supported by National Institutes of Health grant no. R01EY024944 (to SMP), monies from The Oklahoma Center for the Advancement of Science and Technology (grant no. HR16-068 to SMP), and monies from a Presbyterian Health Foundation grant (to SMP). Metabolomic data was generated by the OMRF Metabolic Phenotyping Core, supported by P20GM139763.

Acknowledgments

We are grateful to Jocelyn McCoy-Washington for technical support and to Kenneth Humphries and Jake Kirkland for helpful discussions.

Conflict of interest

The authors declare that the research was conducted in the absence of any commercial or financial relationships that could be construed as a potential conflict of interest.

Publisher's note

All claims expressed in this article are solely those of the authors and do not necessarily represent those of their affiliated organizations, or those of the publisher, the editors and the reviewers. Any product that may be evaluated in this article, or claim that may be made by its manufacturer, is not guaranteed or endorsed by the publisher.

Supplementary material

The Supplementary material for this article can be found online at: https://www.frontiersin.org/articles/10.3389/fnut.2024.1485466/full#supplementary-material

SUPPLEMENTARY FIGURE S1
(A) RPE-1 cells were starved of glucose for the indicated times. Representative graph of the fold change response of TXNIP mRNA levels (detected by qPCR). RPE-1 cells were incubated for 8 h in the indicated concentrations of glucose. Protein lysates were analyzed by anti-TXNIP Western blotting. (B) RPE-1 cells were treated with DMSO (blue trace) or SFN (red trace) as well as with 1 μM Actinomycin D to block de novo TXNIP mRNA synthesis for the time indicated. TXNIP mRNA levels were analyzed by qPCR. (C) MondoA Western blots of RPE-1 cell lysates (Inputs) and co-immunoprecipitation (IPs) with an antibody to Mlx. Cells were treated for 0, 4, or 8 h with SFN. MondoA expression is shown in both a short and longer exposure to facilitate visualization of the Inputs. (D) RPE-1 cells were treated with siCON or siNrf2 for 2 days and then harvested to quantify Nrf2 mRNA levels by qPCR. (E) Samples from Figure 5A were probed for pPRAS and actin. ****indicates statistical significance ($p = 0.0002$). The migration of molecular weight markers (kDa) is shown to the left of blots (A, C, and E).

SUPPLEMENTARY TABLE S1
List of chemicals, reagents, and antibodies, companies, catalog numbers, and concentrations/dilutions used in these studies.

SUPPLEMENTARY TABLE S2
List of qPCR primers used in these studies.

SUPPLEMENTARY TABLE S3
List of DEGs (ranked by *p*- value) with a p-value ≤ 0.05 derived from RNA-seq of RPE-1 cells treated with either DMSO (vehicle) or SFN for 4 h ($n = 5$ samples/treatment). Yellow highlighting of gene symbols (Column H) marks individual DEGs discussed in the text.

References

1. Shapiro TA, Fahey JW, Dinkova-Kostova AT, Holtzclaw WD, Stephenson KK, Wade KL, et al. Safety, tolerance, and metabolism of broccoli sprout glucosinolates and isothiocyanates: a clinical phase I study. *Nutr Cancer*. (2006) 55:53–62. doi: 10.1207/s15327914nc5501_7

2. Yang L, Palliyaguru DL, Kensler TW. Frugal chemoprevention: targeting Nrf 2 with foods rich in sulforaphane. *Semin Oncol*. (2016) 43:146–53. doi: 10.1053/j.seminoncol.2015.09.013

3. Dinkova-Kostova AT, Copple IM. Advances and challenges in therapeutic targeting of NRF2. *Trends Pharmacol Sci*. (2023) 44:137–49. doi: 10.1016/j.tips.2022.12.003

4. Luchkova A, Mata A, Cadenas S. Nrf 2 as a regulator of energy metabolism and mitochondrial function. *FEBS Lett*. (2024) 598:2092–105. doi: 10.1002/1873-3468.14993

5. Goodfellow MJ, Borcar A, Proctor JL, Greco T, Rosenthal RE, Fiskum G. Transcriptional activation of antioxidant gene expression by Nrf 2 protects against mitochondrial dysfunction and neuronal death associated with acute and chronic neurodegeneration. *Exp Neurol*. (2020) 328:113247. doi: 10.1016/j.expneurol.2020.113247

6. Greco T, Shafer J, Fiskum G. Sulforaphane inhibits mitochondrial permeability transition and oxidative stress. *Free Radic Biol Med*. (2011) 51:2164–71. doi: 10.1016/j.freeradbiomed.2011.09.017

7. Dinkova-Kostova AT, Baird L, Holmstrom KM, Meyer CJ, Abramov AY. The spatiotemporal regulation of the Keap 1-Nrf 2 pathway and its importance in cellular bioenergetics. *Biochem Soc Trans*. (2015) 43:602–10. doi: 10.1042/BST20150003

8. Alattar A, Alshaman R, Al-Gayyar MMH. Therapeutic effects of sulforaphane in ulcerative colitis: effect on antioxidant activity, mitochondrial biogenesis and DNA polymerization. *Redox Rep*. (2022) 27:128–38. doi: 10.1080/13510002.2022.2092378

9. Briones-Herrera A, Ramirez-Camacho I, Zazueta C, Tapia E, Pedraza-Chaverri J. Altered proximal tubule fatty acid utilization, mitophagy, fission and supercomplexes arrangement in experimental Fanconi syndrome are ameliorated by sulforaphane-induced mitochondrial biogenesis. *Free Radic Biol Med*. (2020) 153:54–70. doi: 10.1016/j.freeradbiomed.2020.04.010

10. Lei P, Tian S, Teng C, Huang L, Liu X, Wang J, et al. Sulforaphane improves lipid metabolism by enhancing mitochondrial function and biogenesis in vivo and in vitro. *Mol Nutr Food Res*. (2021) 65:e2170023. doi: 10.1002/mnfr.202170023

11. Choi KM, Lee YS, Kim W, Kim SJ, Shin KO, Yu JY, et al. Sulforaphane attenuates obesity by inhibiting adipogenesis and activating the AMPK pathway in obese mice. *J Nutr Biochem*. (2014) 25:201–7. doi: 10.1016/j.jnutbio.2013.10.007

12. Holmstrom KM, Kostov RV, Dinkova-Kostova AT. The multifaceted role of Nrf 2 in mitochondrial function. *Curr Opin Toxicol*. (2016) 1:80–91. doi: 10.1016/j.cotox.2016.10.002

13. Longo VD, Anderson RM. Nutrition, longevity and disease: from molecular mechanisms to interventions. *Cell*. (2022) 185:1455–70. doi: 10.1016/j.cell.2022.04.002

14. Zhang Y, Wu Q, Liu J, Zhang Z, Ma X, Zhang Y, et al. Sulforaphane alleviates high fat diet-induced insulin resistance via AMPK/Nrf 2/GPx4 axis. *Biomed Pharmacother*. (2022) 152:113273. doi: 10.1016/j.biopha.2022.113273

15. Tian S, Wang Y, Li X, Liu J, Wang J, Lu Y. Sulforaphane regulates glucose and lipid metabolisms in obese mice by restraining JNK and activating insulin and FGF21 signal pathways. *J Agric Food Chem*. (2021) 69:13066–79. doi: 10.1021/acs.jafc.1c04933

16. Shehatou GS, Suddek GM. Sulforaphane attenuates the development of atherosclerosis and improves endothelial dysfunction in hypercholesterolemic rabbits. *Exp Biol Med (Maywood)*. (2016) 241:426–36. doi: 10.1177/1535370215609695

17. Senanayake GV, Banigesh A, Wu L, Lee P, Juurlink BH. The dietary phase 2 protein inducer sulforaphane can normalize the kidney epigenome and improve blood pressure in hypertensive rats. *Am J Hypertens*. (2012) 25:229–35. doi: 10.1038/ajh.2011.200

18. Bai Y, Cui W, Xin Y, Miao X, Barati MT, Zhang C, et al. Prevention by sulforaphane of diabetic cardiomyopathy is associated with up-regulation of Nrf 2 expression and transcription activation. *J Mol Cell Cardiol*. (2013) 57:82–95. doi: 10.1016/j.yjmcc.2013.01.008

19. Axelsson AS, Tubbs E, Mecham B, Chacko S, Nenonen HA, Tang Y, et al. Sulforaphane reduces hepatic glucose production and improves glucose control in

patients with type 2 diabetes. *Sci Transl Med*. (2017) 9:477. doi: 10.1126/scitranslmed.aah4477

20. O'Mealey GB, Plafker KS, Berry WL, Janknecht R, Chan JY, Plafker SM. A PGAM5-KEAP1-Nrf 2 complex is required for stress-induced mitochondrial retrograde trafficking. *J Cell Sci*. (2017) 130:3467–80. doi: 10.1242/jcs.203216

21. Rambold AS, Lippincott-Schwartz J. Mechanisms of mitochondria and autophagy crosstalk. *Cell Cycle*. (2011) 10:4032–8. doi: 10.4161/cc.10.23.18384

22. Plafker KS, Plafker SM. The ubiquitin-conjugating enzyme UBE2E3 and its import receptor importin-11 regulate the localization and activity of the antioxidant transcription factor NRF2. *Mol Biol Cell*. (2015) 26:327–38. doi: 10.1091/mbc.E14-06-1057

23. Plafker KS, Nguyen L, Barneche M, Mirza S, Crawford D, Plafker SM. The ubiquitin-conjugating enzyme Ubc M2 can regulate the stability and activity of the antioxidant transcription factor Nrf 2. *J Biol Chem*. (2010) 285:23064–74. doi: 10.1074/jbc.M110.121913

24. O'Mealey GB, Berry WL, Plafker SM. Sulforaphane is a Nrf 2-independent inhibitor of mitochondrial fission. *Redox Biol*. (2017) 11:103–10. doi: 10.1016/j.redox.2016.11.007

25. Plafker KS, Zyla K, Berry W, Plafker SM. Loss of the ubiquitin conjugating enzyme UBE2E3 induces cellular senescence. *Redox Biol*. (2018) 17:411–22. doi: 10.1016/j.redox.2018.05.008

26. Yagishita Y, Fahey JW, Dinkova-Kostova AT, Kensler TW. Broccoli or Sulforaphane: is it the source or dose that matters? *Molecules*. (2019) 24:593. doi: 10.3390/molecules24193593

27. Harold KM, Matsuzaki S, Pranay A, Loveland BL, Batushansky A, Mendez Garcia MF, et al. Loss of cardiac PFKFB2 drives metabolic, functional, and electrophysiological remodeling in the heart. *J Am Heart Assoc*. (2024) 13:e033676. doi: 10.1161/JAHA.123.033676

28. Batushansky A, Matsuzaki S, Newhardt MF, West MS, Griffin TM, Humphries KM. GC-MS metabolic profiling reveals fructose-2, 6-bisphosphate regulates branched chain amino acid metabolism in the heart during fasting. *Metabolomics*. (2019) 15:18. doi: 10.1007/s11306-019-1478-5

29. Braun SMG, Kirkland JG, Chory EJ, Husmann D, Calarco JP, Crabtree GR. Rapid and reversible epigenome editing by endogenous chromatin regulators. *Nat Commun*. (2017) 8:560. doi: 10.1038/s41467-017-00644-y

30. Hanson GT, Aggeler R, Oglesbee D, Cannon M, Capaldi RA, Tsien RY, et al. Investigating mitochondrial redox potential with redox-sensitive green fluorescent protein indicators. *J Biol Chem*. (2004) 279:13044–53. doi: 10.1074/jbc.M312846200

31. Katayama H, Kogure T, Mizushima N, Yoshimori T, Miyawaki A. A sensitive and quantitative technique for detecting autophagic events based on lysosomal delivery. *Chem Biol*. (2011) 18:1042–52. doi: 10.1016/j.chembiol.2011.05.013

32. Liu GY, Sabatini DM. mTOR at the nexus of nutrition, growth, ageing and disease. *Nat Rev Mol Cell Biol*. (2020) 21:183–203. doi: 10.1038/s41580-019-0199-y

33. Lin K, Lin J, Wu WI, Ballard J, Lee BB, Gloor SL, et al. An ATP-site on-off switch that restricts phosphatase accessibility of Akt. *Sci Signal*. (2012) 5:ra 37. doi: 10.1126/scisignal.2002618

34. Nascimento EB, Snel M, Guigas B, van der Zon GC, Kriek J, Maassen JA, et al. Phosphorylation of PRAS40 on Thr 246 by PKB/AKT facilitates efficient phosphorylation of Ser 183 by mTORC1. *Cell Signal*. (2010) 22:961–7. doi: 10.1016/j.cellsig.2010.02.002

35. Inoki K, Li Y, Zhu T, Wu J, Guan KL. TSC2 is phosphorylated and inhibited by Akt and suppresses mTOR signalling. *Nat Cell Biol*. (2002) 4:648–57. doi: 10.1038/ncb839

36. Inoki K, Zhu T, Guan KL. TSC2 mediates cellular energy response to control cell growth and survival. *Cell*. (2003) 115:577–90. doi: 10.1016/S0092-8674(03)00929-2

37. Liu P, Gan W, Chin YR, Ogura K, Guo J, Zhang J, et al. Ptd ins (3, 4, 5) P 3-dependent activation of the mTORC2 kinase complex. *Cancer Discov*. (2015) 5:1194–209. doi: 10.1158/2159-8290.CD-15-0460

38. He C. Balancing nutrient and energy demand and supply via autophagy. *Curr Biol*. (2022) 32:R684–96. doi: 10.1016/j.cub.2022.04.071

39. Liu Y, Hettinger CL, Zhang D, Rezvani K, Wang X, Wang H. Sulforaphane enhances proteasomal and autophagic activities in mice and is a potential therapeutic reagent for Huntington's disease. *J Neurochem*. (2014) 129:539–47. doi: 10.1111/jnc.12647

40. Lee JH, Jeong JK, Park SY. Sulforaphane-induced autophagy flux prevents prion protein-mediated neurotoxicity through AMPK pathway. *Neuroscience*. (2014) 278:31–9. doi: 10.1016/j.neuroscience.2014.07.072

41. Peng ZT, Gu P. Sulforaphane suppresses autophagy during the malignant progression of gastric carcinoma via activating mi R-4521/PIK3R3 pathway. *Hum Exp Toxicol*. (2021) 40:S711–20. doi: 10.1177/09603271211054437

42. Yamamoto A, Tagawa Y, Yoshimori T, Moriyama Y, Masaki R, Tashiro Y. Bafilomycin A1 prevents maturation of autophagic vacuoles by inhibiting fusion between autophagosomes and lysosomes in rat hepatoma cell line, H-4-II-E cells. *Cell Struct Funct*. (1998) 23:33–42. doi: 10.1247/csf.23.33

43. Li D, Shao R, Wang N, Zhou N, Du K, Shi J, et al. Sulforaphane activates a lysosome-dependent transcriptional program to mitigate oxidative stress. *Autophagy*. (2021) 17:872–87. doi: 10.1080/15548627.2020.1739442

44. Heiss EH, Schachner D, Zimmermann K, Dirsch VM. Glucose availability is a decisive factor for Nrf 2-mediated gene expression. *Redox Biol*. (2013) 1:359–65. doi: 10.1016/j.redox.2013.06.001

45. Linn TC, Pettit FH, Reed LJ. Alpha-keto acid dehydrogenase complexes. X. Regulation of the activity of the pyruvate dehydrogenase complex from beef kidney mitochondria by phosphorylation and dephosphorylation. *Proc Natl Acad Sci U S A*. (1969) 62:234–41. doi: 10.1073/pnas.62.1.234

46. Baudry M, Kessler M, Smith EK, Lynch G. The regulation of pyruvate dehydrogenase activity in rat hippocampal slices: effect of dichloroacetate. *Neurosci Lett*. (1982) 31:41–6. doi: 10.1016/0304-3940(82)90051-9

47. Korotchkina LG, Patel MS. Mutagenesis studies of the phosphorylation sites of recombinant human pyruvate dehydrogenase. Site-specific regulation. *J Biol Chem*. (1995) 270:14297–304.

48. Rardin MJ, Wiley SE, Naviaux RK, Murphy AN, Dixon JE. Monitoring phosphorylation of the pyruvate dehydrogenase complex. *Anal Biochem*. (2009) 389:157–64. doi: 10.1016/j.ab.2009.03.040

49. Wu N, Zheng B, Shaywitz A, Dagon Y, Tower C, Bellinger G, et al. AMPK-dependent degradation of TXNIP upon energy stress leads to enhanced glucose uptake via GLUT1. *Mol Cell*. (2013) 49:1167–75. doi: 10.1016/j.molcel.2013.01.035

50. Wilde BR, Kaadige MR, Guillen KP, Butterfield A, Welm BE, Ayer DE. Protein synthesis inhibitors stimulate Mondo a transcriptional activity by driving an accumulation of glucose 6-phosphate. *Cancer Metab*. (2020) 8:27. doi: 10.1186/s40170-020-00233-6

51. Waldhart AN, Dykstra H, Peck AS, Boguslawski EA, Madaj ZB, Wen J, et al. Phosphorylation of TXNIP by AKT mediates acute influx of glucose in response to insulin. *Cell Rep*. (2017) 19:2005–13. doi: 10.1016/j.celrep.2017.05.041

52. Stoltzman CA, Peterson CW, Breen KT, Muoio DM, Billin AN, Ayer DE. Glucose sensing by Mondo a: mlx complexes: a role for hexokinases and direct regulation of thioredoxin-interacting protein expression. *Proc Natl Acad Sci U S A*. (2008) 105:6912–7. doi: 10.1073/pnas.0712199105

53. Kaadige MR, Yang J, Wilde BR, Ayer DE. Mondo A-mlx transcriptional activity is limited by mTOR-Mondo a interaction. *Mol Cell Biol*. (2015) 35:101–10. doi: 10.1128/MCB.00636-14

54. He X, Ma Q. Redox regulation by nuclear factor erythroid 2-related factor 2: gatekeeping for the basal and diabetes-induced expression of thioredoxin-interacting protein. *Mol Pharmacol*. (2012) 82:887–97. doi: 10.1124/mol.112.081133

55. Chi MM, Pusateri ME, Carter JG, Norris BJ, McDougal DB, Lowry OH. Enzymatic assays for 2-deoxyglucose and 2-deoxyglucose 6-phosphate. *Anal Biochem*. (1987) 161:508–13. doi: 10.1016/0003-2697(87)90481-7

56. Cha-Molstad H, Saxena G, Chen J, Shalev A. Glucose-stimulated expression of Txnip is mediated by carbohydrate response element-binding protein, p 300, and histone H4 acetylation in pancreatic beta cells. *J Biol Chem*. (2009) 284:16898–905. doi: 10.1074/jbc.M109.010504

57. Paneque A, Fortus H, Zheng J, Werlen G, Jacinto E. The Hexosamine biosynthesis pathway: regulation and function. *Genes (Basel)*. (2023) 14:933. doi: 10.3390/genes14040933

58. Stoltzman CA, Kaadige MR, Peterson CW, Ayer DE. Mondo a senses non-glucose sugars: regulation of thioredoxin-interacting protein (TXNIP) and the hexose transport curb. *J Biol Chem*. (2011) 286:38027–34. doi: 10.1074/jbc.M111.275503

59. Wang ZV, Deng Y, Gao N, Pedrozo Z, Li DL, Morales CR, et al. Spliced X-box binding protein 1 couples the unfolded protein response to hexosamine biosynthetic pathway. *Cell*. (2014) 156:1179–92. doi: 10.1016/j.cell.2014.01.014

60. Shao M, Shan B, Liu Y, Deng Y, Yan C, Wu Y, et al. Hepatic IRE1alpha regulates fasting-induced metabolic adaptive programs through the XBP1s-PPARalpha axis signalling. *Nat Commun*. (2014) 5:3528. doi: 10.1038/ncomms4528

61. Sun T, Song C, Zhao G, Feng S, Wei J, Zhang L, et al. HOMER3 promotes non-small cell lung cancer growth and metastasis primarily through GABPB1-mediated mitochondrial metabolism. *Cell Death Dis*. (2023) 14:814. doi: 10.1038/s41419-023-06335-5

62. Cesana M, Tufano G, Panariello F, Zampelli N, Ambrosio S, De Cegli R, et al. EGR1 drives cell proliferation by directly stimulating TFEB transcription in response to starvation. *PLoS Biol*. (2023) 21:e3002034. doi: 10.1371/journal.pbio.3002034

63. Xu C, Shen G, Chen C, Gelinas C, Kong AN. Suppression of NF-kappa B and NF-kappa B-regulated gene expression by sulforaphane and PEITC through Ikappa Balpha, IKK pathway in human prostate cancer PC-3 cells. *Oncogene*. (2005) 24:4486–95. doi: 10.1038/sj.onc.1208656

64. Martel J, Chang SH, Wu CY, Peng HH, Hwang TL, Ko YF, et al. Recent advances in the field of caloric restriction mimetics and anti-aging molecules. *Ageing Res Rev*. (2021) 66:101240. doi: 10.1016/j.arr.2020.101240

65. Pannen ST, Maldonado SG, Nonnenmacher T, Sowah SA, Gruner LF, Watzinger C, et al. Adherence and dietary composition during intermittent vs. continuous calorie restriction: follow-up data from a randomized controlled trial in adults with overweight or obesity. *Nutrients*. (2021) 13:1195. doi: 10.3390/nu13041195

66. Martin CK, Hochsmann C, Dorling JL, Bhapkar M, Pieper CF, Racette SB, et al. Challenges in defining successful adherence to calorie restriction goals in humans: results from CALERIE 2. *Exp Gerontol*. (2022) 162:111757. doi: 10.1016/j.exger.2022.111757

67. Hardie DG, Carling D, Halford N. Roles of the Snf 1/Rkin 1/AMP-activated protein kinase family in the response to environmental and nutritional stress. *Semin Cell Biol*. (1994) 5:409–16. doi: 10.1006/scel.1994.1048

68. Hardie DG. Sensing of energy and nutrients by AMP-activated protein kinase. *Am J Clin Nutr*. (2011) 93:891S–6S. doi: 10.3945/ajcn.110.001925

69. Sheth SS, Castellani LW, Chari S, Wagg C, Thipphavong CK, Bodnar JS, et al. Thioredoxin-interacting protein deficiency disrupts the fasting-feeding metabolic transition. *J Lipid Res*. (2005) 46:123–34. doi: 10.1194/jlr.M400341-JLR200

70. Hui ST, Andres AM, Miller AK, Spann NJ, Potter DW, Post NM, et al. Txnip balances metabolic and growth signaling via PTEN disulfide reduction. *Proc Natl Acad Sci U S A*. (2008) 105:3921–6. doi: 10.1073/pnas.0800293105

71. Kanari Y, Sato Y, Aoyama S, Muta T. Thioredoxin-interacting protein gene expression via Mondo a is rapidly and transiently suppressed during inflammatory responses. *PLoS One*. (2013) 8:e59026. doi: 10.1371/journal.pone.0059026

72. Han KS, Ayer DE. Mondo a senses adenine nucleotides: transcriptional induction of thioredoxin-interacting protein. *Biochem J*. (2013) 453:209–18. doi: 10.1042/BJ20121126

73. Lv J, Bao S, Liu T, Wei L, Wang D, Ye W, et al. Sulforaphane delays diabetes-induced retinal photoreceptor cell degeneration. *Cell Tissue Res*. (2020) 382:477–86. doi: 10.1007/s00441-020-03267-w

74. Mandala A, Das N, Bhattacharjee S, Mukherjee B, Mukhopadhyay S, Roy SS. Thioredoxin interacting protein mediates lipid-induced impairment of glucose uptake in skeletal muscle. *Biochem Biophys Res Commun*. (2016) 479:933–9. doi: 10.1016/j.bbrc.2016.09.168

75. Xu Y, Fu JF, Chen JH, Zhang ZW, Zou ZQ, Han LY, et al. Sulforaphane ameliorates glucose intolerance in obese mice via the upregulation of the insulin signaling pathway. *Food Funct*. (2018) 9:4695–701. doi: 10.1039/C8FO00763B

76. Marino G, Pietrocola F, Madeo F, Kroemer G. Caloric restriction mimetics: natural/physiological pharmacological autophagy inducers. *Autophagy*. (2014) 10:1879–82. doi: 10.4161/auto.36413

77. Brandhorst S, Choi IY, Wei M, Cheng CW, Sedrakyan S, Navarrete G, et al. A periodic diet that mimics fasting promotes multi-system regeneration, enhanced cognitive performance, and Healthspan. *Cell Metab*. (2015) 22:86–99. doi: 10.1016/j.cmet.2015.05.012

78. Qi X, Walton DA, Plafker KS, Boulton ME, Plafker SM. Sulforaphane recovers cone function in an Nrf 2-dependent manner in middle-aged mice undergoing RPE oxidative stress. *Mol Vis*. (2022) 28:378–93.

79. Galves M, Sperber M, Amer-Sarsour F, Elkon R, Ashkenazi A. Transcriptional profiling of the response to starvation and fattening reveals differential regulation of autophagy genes in mammals. *Proc Biol Sci*. (1995) 290:20230407. doi: 10.1098/rspb.2023.0407

80. Dwyer DS, Horton RY, Aamodt EJ. Role of the evolutionarily conserved starvation response in anorexia nervosa. *Mol Psychiatry*. (2011) 16:595–603. doi: 10.1038/mp.2010.95

81. Masuda M, Yoshida-Shimizu R, Mori Y, Ohnishi K, Adachi Y, Sakai M, et al. Sulforaphane induces lipophagy through the activation of AMPK-mTOR-ULK1 pathway signaling in adipocytes. *J Nutr Biochem*. (2022) 106:109017. doi: 10.1016/j.jnutbio.2022.109017

82. Zhang HQ, Chen SY, Wang AS, Yao AJ, Fu JF, Zhao JS, et al. Sulforaphane induces adipocyte browning and promotes glucose and lipid utilization. *Mol Nutr Food Res*. (2016) 60:2185–97. doi: 10.1002/mnfr.201500915

Frontiers in Nutrition

Explores what and how we eat in the context of health, sustainability and 21st century food science

A multidisciplinary journal that integrates research on dietary behavior, agronomy and 21st century food science with a focus on human health.

Discover the latest Research Topics

See more →

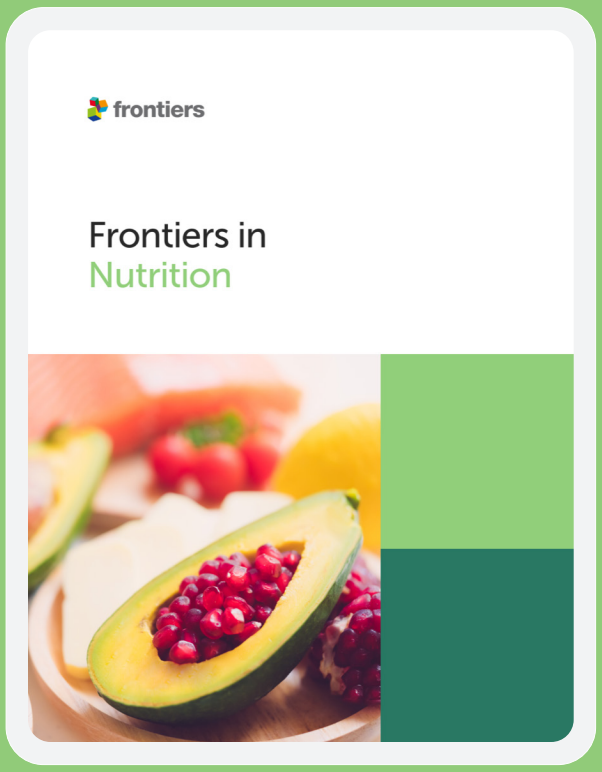

Frontiers

Avenue du Tribunal-Fédéral 34
1005 Lausanne, Switzerland
frontiersin.org

Contact us

+41 (0)21 510 17 00
frontiersin.org/about/contact